universität wien

DISSERTATION

Titel der Dissertation

A microscopic screen for mutations affecting synaptonemal complex formation in Budding yeast

Mag. Jean Mbogning

Angestrebter akademischer Grad

Doktor der Naturwissenschaften (Dr.rer.nat.)

Wien, 2011

Studienkennzahl lt. Studienblatt: A 091 441

Dissertationsgebiet lt.Studienblatt: Genetik-Mikrobiologie (Stzw)

Betreuerin / Betreuer: Uni.-Prof.Dr. Franz Klein

Table of contents

1 Introduction

1.1 Meiosis – an overview

Sexual reproduction requires the formation of specialized germ cells by meiosis. Meiosis consists of two consecutive rounds of chromosome segregation, preceded by a single phase of DNA replication (Figure 1). Central to meiosis is a process of recombination between paternal and maternal chromosomes, which increases the genetic diversity of progeny and ensures proper homologous chromosome segregation (Szekvolgyi and Nicolas, 2010).

The first meiotic division (MI) is preceded by a special and prolonged prophase, during which homologous chromosomes align and pair. Pairing of homologs is initiated during leptotene, progresses during zygotene and is complete in pachytene nuclei. Subsequently, synapsis between the chromosomal axes of the paired homologous chromosomes is achieved by the formation of the synaptonemal complex (SC). During the initial phase of chromosome pairing in both yeast and mammals, all telomeres cluster on the nuclear membrane, while the chromosomal arms loop towards the center of the nucleus, forming the transient bouquet stage. The formation of this configuration and the associated chromosomal movements are required for correct chromosome synapsis (Kosaka et al., 2008; Koszul et al., 2008; Koszul and Kleckner, 2009).

In many species, including yeast and mammals, homologous chromosome pairing requires formation and repair of meiosis-specific DNA double-strand breaks (DSBs) catalyzed by the topoisomerase II-like enzyme Spo11 (Keeney et al., 1997a; Keeney and Neale, 2006; Pan et al., 2011). But homolog pairing occurs normally in *Caenorhabditis elegans* and in *Drosophila melanogaster* females in the complete absence of DSBs (Dernburg et al., 1998; McKim et al., 1998; MacQueen et al., 2002b).

In yeast and mouse, the formation and repair of meiotic DSBs, leading to the formation of crossovers, is directly required for proper pairing, synapsis and the segregation of homologous chromosomes during the first meiotic division.

In addition to a physical linkage established between homologs (named chiasmata) and sister chromatids arms cohesion, proper reductional segregation of the homologs in meiosis I requires that the homologous kinetochores capture microtubules from opposite poles of the spindle, reviewed in (Bardhan et al., 2010).

During the second or equational meiotic division (MII) the sister chromatids are then segregated into haploid gametes (Figure 1). In somatic cells, DSBs may arise due to exogenous and endogenous DNA damage. In contrast to meiosis, a single round of DNA replication is followed by only one round of chromosome segregation, resulting in the transfer of the complete genetic information into two genetically identical daughter cells during vegetative growth (Petronczki et al., 2003).

In yeast, gametogenesis is referred to as sporulation and the four final meiotic products which are packed into an ascus are termed spores. In this form yeast is highly resistant to a wide range of environmental conditions and upon favorable conditions spores will germinate and eventually fuse to form diploid cells.

1.2 Commitment to meiosis and the pre-meiotic S-phase

Unicellular organisms such as the budding yeast *Saccharomyces cerevisiae* have evolved to survive constant variations in their external environments by adapting their internal systems to meet the challenges of each new environment. The hemi-ascomycete *S.cerevisiae* exists in both diploid and haploid states of the chromosome complement.

Two different developmental pathways control the onset of meiosis. Two haploid cells of the corresponding opposite mating type (Mata and Matα) must fuse to form a diploid zygote; which, upon nutrient deprivation (especially glucose and nitrogen starvation) and in the presence of a non-fermentable carbon source, usually acetate; resumes the developmental program of meiosis or sporulation (Lee and Amon, 2001; Jambhekar and Amon, 2008).

Nutritional signaling cascade result in the transcription of two master regulators of meiosis: Ime1 and Ime2. Ime1 is a transcription factor that activates the transcription of early meiotic genes and is therefore required for entry into meiosis (Honigberg and Purnapatre, 2003; Jambhekar and Amon, 2008). One important target of Ime1 is Ime2, which is a meiosis-specific kinase with multiple functions in regulating entry into meiosis. Ime2 regulates entry into meiosis by stimulating the degradation of the S-phase CDK inhibitor Sic1 and stabilisation of B-type cyclins through the inhibition of the anaphase-promoting complex/ cyclosome (APC/C) (Guttmann-Raviv et al., 2001; Bolte et al., 2002).

Although, meiotic and mitotic DNA replication share many components and characteristics; such as a common evolutionary origin of replication (Collins and Newlon, 1994; Murakami and Nurse, 2001; Ofir et al., 2004), the same S-phase B-type cyclins: Clb5 and Clb6 (Dirick et al., 1998; Stuart and Wittenberg, 1998); there are some differences in regulation as demonstrated by the identification of meiosis-specific S-phase factors such as : *CSM1* and *MUM2* (Davis et al., 2001; Wysocka et al., 2004). But also, pre-meiotic S-phase is significantly longer compared to mitotic S-phase in all organisms analysed so far, taking up to 3

times longer than normal mitotic DNA replication in budding yeast (Cha et al., 2000). Importantly, the length of the pre-meiotic S-phase is modulated by recombination factors such as Spo11, Mer2 and the cohesion complex subunit Rec8 (Jiao et al., 1999; Cha et al., 2000), indicating a function of these proteins already at the time of DNA replication.

It has been shown that pre-meiotic DNA replication is required for the establishment of interhomologue interactions such as pairing, DSB formation and SC assembly (Borde et al., 2000a; Smith et al., 2001b; Matos et al., 2008; Wan et al., 2008a). Replication-deficient meiotic cells are defective in chromosome morphology. This defect in chromosome synapsis can partially be explained by reduced levels of chromatin-bound cohesion, which in turn causes improper chromosomes axes formation (Smith and Nicolas, 1998; Klein et al., 1999).

All together, available data to date strongly support the idea that pre-meiotic DNA replication is required to establish a chromatin conformation, which allows the promotion of homologous recombination during meiosis I and the completion of the meiotic program.

Commitment to meiosis is a stepwise process, yeast cells undergoing sporulation are fully committed to meiosis when they can no longer return to the vegetative growth (once they are unable to divide mitotically when inoculated in rich medium), this corresponds to the end of prophase I, prior to the first meiotic division (Simchen, 2009).

1.3 Chromosomal morphogenesis during the meiotic prophase I

The chromatin of meiotic chromosomes is organized in a series of loops emanating from meiotic axis (Kleckner, 2006; Novak et al., 2008). Chromosomal morphogenesis during meiotic prophaseI culminates by the formation of a peptidic scaffold termed synaptonemal complex (SC), which holds homologs together until meiotic recombination and genetic exchange have taken place. Chromosome dynamics during meiotic prohase I involves several processes (Figure 2) such as:

A physical linkage established between sister chromatids during pre-meiotic S phase;

Homologous chromosomes recognition and pairing;

Programmed variations in molecular composition and compaction of bulk chromatin.

In eukaryotic cells, cohesion between sister chromatids is mediated by a highly conserved multisubunit complex called cohesin (Guacci et al., 1997). In *Saccharomyces cerevisiae*, the cohesin complex comprises at least four core subunits: two Smc (Structural Maintenance of Chromosomes) proteins, Smc1 and Smc3, and two non-Smc proteins, Scc1/Mcd1 (replaced by Rec8 in meiosis) and Scc3 (= Irr1). An accessory protein termed Pds5 binds loosely to the cohesin complex and is required for the maintenance of functional cohesion (Panizza et al., 2000).

A separate complex containing the Scc2 and Scc4 proteins plays an essential role in cohesin´s association with chromosomes. Like Scc2 and Scc4, an acetyl transferase named Eco1 is also required to establish cohesion during S-phase (Nasmyth and Haering, 2009).

In additon to these proteins, essential for sister chromatid cohesion many other factors merely necessary to improve the efficiency of sister chromatid

cohesion have been identified. In budding yeast these proteins include a factor known as Ctf4 which forms a complex with various DNA-replication proteins such as Cdc45, Mrc1, Csm3 (Gambus et al., 2006) but with also a Replication Factor C (RFC) complex containing the Ctf1-like protein Ctf18 and the additional subunits Dcc1 and Ctf8 (Mayer et al., 2001).

First demonstrated to be involved in meiosis in *C.elegans* (Hagstrom et al., 2002), another Smc complex namely the condensin complex is also involved in chromosome compaction and resolution. Interestingly, this complex has been implicated in the recruitment of meiosis-specific axial element (AE) proteins Hop1 and Red1, thereby promoting the assembly of SC in yeast (Yu and Koshland, 2003a). In budding yeast, large scale chromosome movements accompagny the individual steps of meiotic recombination.

Prior to DSB formation, chromosomes undergo a series of homology-independent interactions that are thought to reduce the search space required for homology identification. These interactions include non-homologous centromeres pairing mediated by Zip1 which is progressively replaced by homologous interactions upon DSBs formation (Falk et al., 2010a; Obeso and Dawson, 2010). As DSB repair progresses, namely at zygotene, telomeres cluster in one area of the spindle pole body (SPB) forming the so called chromosomal bouquet configuration also thought to promote chromosome synapsis (Zickler and Kleckner, 1998; Scherthan and Schonborn, 2001).

But as the bouquet formation occurs very late in the pairing process (that is at zygotene), it is likely not the primary mediator of homology search. Recently it was shown that the *csm4* null mutation is not completely defective in chromosome synapsis. Cells lacking *CSM4* showed zygotene-like nuclei with fragments of SC on chromosome spreads (Kosaka et al., 2008; Koszul and Kleckner, 2009). Csm4 is a meiosis-specific protein required for telomere clustering, *csm4* mutant is deficient in bouquet formation. However, it has been proposed that telomere-led movement of meiotic chromosome (including the bouquet stage) produces in combination with compaction and expansion of

chromatin, an overall dynamic whose primary role is regularization of topological relationships among pairing chromosomes (Koszul et al., 2008).

Chromatin structure modifications (epigenome modifications) occuring during the meiotic prophase I also contribute to the synaptonemal complex formation (SC). These modifications include a post-translational histone covalent modifications (acetylation, phosphorylation, methylation, ubiquitination) as well as ATP-dependent chromatin remodeling.

Chromosomes likely begin a search for their homologous counterpart during pre-meiotic S phase, this early homology search could be mediated by DNA transcription as evidenced by EM (electron microscopy) observations, showing the presence of lampbrush (chromatin loops associated with ribonucleo particles) structures which progressively associate between them in guinea pig spermatogonia during pre-meiotic S phase (Vazquez-Nin et al., 2003).

Chromatin is diffuse during pre-meiotic S phase. This relaxed chromatin status is associated with specific epigenetic marks such as histone H4 acetylation, histone H3 lysine 9 acetylation (H3K9ac) which are considered to as open chromatin marks (euchromatic marks) (Webster et al., 2005). But repressive chromatin marks such as (H4K20 trimethylation, H3K9 trimethylation) are present in centromeres, telomeres and nearby chromatin throughout pre-meiotic S phase and remained until late pachytene in mammals (Peters et al., 2001). These repressive histone marks are thought to be required for regulating incorporation and preservation of telomeric and centromeric chromatin in the synaptonemal complex. Chromatin dynamics during pre-leptotene is further manisfested by histone H3 serine10 phosphorylation (H3S10P), a histone mark associated with chromosome relaxation and compaction. H3S10P first appears during pre-leptotene, decreases during leptotene and is diffusely detected at zygotene, indicating that this histone mark is needed for prophase progression (Kleckner et al., 2004). It was shown that partial histone replacement such as H2A exchanged by H2AX that occurs during the pre-leptotene stage in mouse

and rat, is required for further chromatin modification (Baarends and Grootegoed, 2003).

The monoubiquitination of histone H2B at lysine 123 by Rad6-Bre1 allows allows histone H3 lysine 4 and 79 trimethylation by COMPASS (Set1) and Dot1 respectively, this crosstalk between histones is thought to promote chromatin remodeling and DSBs formation (Yamashita et al., 2004; Rousseaux et al., 2005; Dehe and Geli, 2006). Furthermore, the histone variant H2A.X (H2A in budding yeast) is phosphorylated upon DSBs formation by ATR/ATM (Mec1/Tel1). This epigenetic mark is thought to promote the recruitment of recombination enzymes to the DSB sites (Baarends and Grootegoed, 2003; Fink et al., 2007).

During branch migration, the ATP-dependent chromatin remodeling activity of Rad54 is required to unwind duplex DNA, thereby promoting DSB repair (Baarends and Grootegoed, 2003).

1.4 Meiotic recombination: DSB formation and repair

Meiotic recombination is initiated by a self-inflicting introduction of programmed DSBs during the early stage of meiotic prophaseI in budding yeast (Figure 3). The distribution of DSB across chromosomes is not a random event, as some regions are more susceptible to DSB formation than others; respectively termed hospots and coldspots (Baudat and Nicolas, 1997; Wahls, 1998; Pan et al., 2011).

In *S.cerevisiae*, at least ten proteins are absolutely required for DSBs formation during meiosis.

Rec102, Rec104, Ski8 and Spo11 subcomplex

Spo11 is a highly conserved catalytic subunit of the DSB forming machinery (Keeney et al., 1997a; Neale et al., 2005) and is structurally related to the Top6A subunit of the archeal type-IIB topoisomerase, TopoVI. This structural relationship provides key insights into Spo11 biochemical properties (Diaz et al., 2002) and evidence suggests that Spo11-dependent cleavage of both strands occurs by a transesterification mechanism analogous to type-II topoisomerases. Though Spo11 is likely incapable of catalyzing a classical two-gate DNA-passage mechanism (Corbett and Berger, 2003).

It was shown by Immunofluorescence studies that, the localization of Spo11 to meiotic chromosomes required two other proteins essential for DSB formation: Rec102, Rec104 and probably Ski8/Rec103 (Storlazzi et al., 2003; Prieler et al., 2005). The Spo11 subcomplex (Spo11. Rec102, Rec104 and Ski8) likely interacts with other subcomplexes of the DSB forming machinery (Mei4-Mer2-Rec114, Mre11-Rad50-Xrs2), as a strong interaction between Rec104 and Rec114 has been reported (Arora et al., 2004).

Ski8/Rec103 is a conserved protein containing multiple copies of the ~40 amino-acid WD-repeat, this structure is thought to simultaneously interact with multiple proteins to coordinate their interaction. Ski8 may interact with other components of the Spo11 complex, namely Rec114, Mer2 and Rec104 as suggested by two-hybrid data (Arora et al., 2004). Unlike Ski8, Rec102 and Rec104 appear not to be conserved outside of Saccharomyces and closely related yeasts. Rec104 shows a strong interaction with Rec114 (Arora et al., 2004).

Mei4, Mer2 and Rec114 subcomplex

Rec114, Mer2 and Mei4 form a dynamic subcomplex (Li et al., 2006) and these three proteins are poorly conserved outside of the *saccharomyces* and closely related yeasts. Cyclin-dependent Kinase (Cdk1-Clb5/6) directly phosphorylates Mer2 at two consensus target sites, serine 30 and serine 271 (Henderson et al., 2006). The replication-origin activating Kinase, Cdc7 is also required for Mer2 phosphorylation. Phosphorylation of Mer2, mainly at serine 30 not only promotes Mer2-Mer2 self-interaction, Mer2-Rec114 and Mer2-Xrs2 interactions but is also essential for DSB formation. Notably, mutation of this site causes phenotypes indistinguishable from the *mer2* null mutant (Henderson et al., 2006; Wan et al., 2008a). Phosphorylation of Mer2 at serine 271 appears also to be important for self-interaction and interaction with Xrs2.

Mre11, Rad50, and Xrs2 subcomplex

The MRX complex (Mre11, Rad50 and Xrs2) plays central roles in DNA damage signaling and repair.

Mre11 is a structure selective nuclease comprising a metallo-phosphoesterase nuclease domain and a DNA binding domain (Hopfner et al., 2001). The DNA binding domain of Mre11 is essential for DSB formation but not its nuclease activity (Furuse et al., 1998; Hopfner et al., 2001). The binding of Mre11 to chromatin does not require DSB formation but all other Spo11 complex proteins excepting Rad50 (Borde et al., 2004).

Rad50 is an SMC-family protein with an extended coiled-coil, upon ATP binding, this protein dimerizes to create a DNA binding domain. MRX is able to tether two bound DNA molecules via intermolecular interactions between (Rad50)2-(Mre11)2 heterotetramers (Hopfner et al., 2002; Moreno-Herrero et al.,

2005) and this feature of the MRX complex is required for DSB formation (Wiltzius et al., 2005).

The third component of the MRX subcomplex, Xrs2 contains FHA and tandem BRCT domains which mediate its interaction with phospho-proteins (Becker et al., 2006). Xrs2 is thought to help target MRX to DNA ends and other DNA structures (Trujillo et al., 2003).

The MRX complex has a number of inter-related functions in DNA repair including: sensing and signaling of DNA damage by binding to DSBs and activation of Tel1/Mec1 kinases (ATM and ATR in vertebrates), processing of DSB-ends and ATP-dependent DNA unwinding (Usui et al., 1998; Chen et al., 2005).

Besides the above proteins that are essential for DSB formation, other factors such as chromatin composition (intergenic GC rich sequences), accessibility and modifications (influenced by ATP-dependent chromatin remodelers and post-translational histones modifications) also contribute to DSB formation and repair. And chromosomal axes proteins (Red1, Hop1 and Mek1) are also required for wild type levels of DSBs.

Following DSB formation, 5`- strands of the DSB-ends are resected to provide a 3`- single-stranded tails which are substrates of recombinases Rad51 and Dmc1 to promote pairing and strand exchange with the homologous duplex.

Resection of 5´- DSB ends

The MRX complex cooperates with the Sae2/Com1 protein for the initial removal of Spo11 from the 5-DSB-ends. It was shown that Spo11 is removed from DSB-ends as an oligonucleotide-bound covalent complex (Neale et al., 2005). Separation of function alleles of *MRE11*, RAD50 respectively *mre11S*, *rad50S* and null alleles of *COM1/SAE2* allow DSB formation but block removal of Spo11 (Cao et al., 1990; Keeney et al., 1997b; Nairz and Klein, 1997; Prinz et al.,

1997; Moreau et al., 1999). The 5`-ends of DSBs are further resected by several hundred of nucleotides and Mre11, Exo1 but also Com1 are likely candidate nucleases.

Formation of Rad51 and Dmc1 nucleoprotein filaments

The 3´ssDNA tails produced by the MRX complex and/or the 5`-3` exonuclease are coated by *RPA* to eliminate secondary structures (Sung, 1997), Rad52 protein interacts directly with *RPA* and Rad51 and recruits Rad51 to the *RPA*-ssDNA complex.

The Rad51 nucleoprotein filament formation is further mediated by Rad55/Rad57 and *RPA* is displaced. Once the homologous donor sequence is located, strand invasion (annealing) between donor DNA and the incoming Rad51 nucleoprotein filament is facilitated by the chromatin remodeling, DNA unwinding activities of Rad54 protein, yielding a heteroduplex DNA intermediate often referred to as a joint molecule.A dual side-by-side foci localization of Rad51 and Dmc1 has been observed in a subset of wild type nuclei during meiosis (Shinohara et al., 2000), suggesting that the two recombinases assemble onto opposite DSB-ends.

Dmc1 is a meiosis specific protein required for normal homolog pairing and SC formation. The assembly of Dmc1 nucleoprotein filament requires a lower-order oligomer of Rad51 (Gasior et al., 2001) and is strictly dependent on the meiosis specific Mei5-Sae3 complex (Hayase et al., 2004). The requirement of Mei5-Sae3 complex for the assembly of Dmc1 has also been tested in vitro (Ferrari et al., 2009).

As well as Rad51, Tid1/Rdh4 and Rad54 DNA translocases also promote strand-exchange reactions by biasing the assembly of Dmc1–filaments onto single-stranded DSB tails (Holzen et al., 2006). But homolog pairing and strand-exchange completely fail in the absence of the conserved Hop2 and Mnd1 proteins in budding yeast. It has been proposed that Hop2-Mnd1 binds along

chromosomes and /or at the branch point created during nascent D-loop formation and facilitates recombination (Zierhut et al., 2004; Petukhova et al., 2005; Henry et al., 2006).

Formation and resolution of double Holliday Junctions (dHJs) (pro-crossover factors)

The Rad51 and Dmc1 nucleoprotein filaments serve to find a complementary sequence within a homologous chromosome, at which they instigate single-end strand invasions to generate the D-loop recombination intermediates. If the primary invasion step is stabilized (SEIs) and the second end of the original DSB captured, a double Holliday junction (dHJs) is formed, which can be resolved to generate either a non-crossover or an interhomologue crossover (Schwacha and Kleckner, 1995; Allers and Lichten, 2001a; Bishop and Zickler, 2004) (Figure 3).

In contrast, when the strand invasion is transient and when only a limited amount of DNA synthesis occurs before the invaded strand dissociates and anneals to its partner strand(annealing of the two DSB-ends), as in mitotic synthesis-dependent strand annealing (SDSA), non-crossover is formed. But, using an elegant ectopic recombination system, Allers and Lichten have demonstrated that in budding yeast, SEIs and dHJs are exclusively crossover intermediates and that non-crossover heteroduplex products are formed with the same timing as dHJs, consistent with the idea that crossover and non-crossover are formed through distinct pathways (Allers and Lichten, 2001a).

Analysis of ZMM mutants (discussed in section I.5) further indicates that the decision between crossover and non-crossover is very early at or prior to the establishment of a stable single-end invasion intermediate, that is at the leptotene–zygotene transition (Bishop and Zickler, 2004; (Hunter and Kleckner, 2001; Borner et al., 2004). In addition to ZMM proteins which promote the major crossover pathway in budding yeast, probably by facilitating the stable formation

of recombination intermediates, the structure-specific endonuclease complex between mutagenesis sensitive 81 (Mus81) and Mms4 (Mus81/Mms4 complex) is responsible for generating a subset of crossovers (de los Santos et al., 2003; Argueso et al., 2004).

Recently, a number of resolvases that also possess the biochemical activity to resolve Holliday junctions have been identified in various organisms. The human resolvase XPG-like endonuclease1 (GEN1), and its budding yeast orthologue Yen1 have been shown to have a symmetrical cleavage activity on Holliday junctions (Ip et al., 2008); furthermore Blanco and coworkers have also demonstrated that Yen1 has functional overlap with Mus81 (Blanco et al., 2010).

A role in resolving Holliday junctions has also been reported for the Drosophila protein Mus312. orthologous of the synthetic lethal of unknown function 4 (SLX4) protein. Slx4 interacts with Slx1, and the Slx4-Slx1 complex was shown to possess a robust Holliday junction cleavage activity in vitro (Fekairi et al., 2009; Svendsen et al., 2009), these authors proposed that Slx4 could acts as a platform for different structure-specific endonucleases that are most likely to serve both in meiosis and in DNA repair.

Crossover suppressors (anti-crossover factors)

In contrast to factors described above, that promote crossover recombination, several proteins such as the Sgs1 helicase, suppresses the formation of multi-chromatid joint molecules during meiosis; thereby preventing the formation of aberrant crossing over (Oh et al., 2007), Jessop and coworkers have proposed that Sgs1 is normally antagonized by the ZMM proteins (Jessop et al., 2006). In addition to Sgs1, it has also been reported that Mph1 possess biochemical abilities (Prakash et al., 2009) similar to the *C. elegans* anti-recombinase *RTEL-1* which has the ability to disrupt D-loop recombination intermediates in vitro (Barber et al., 2008; Youds et al., 2010).

Inter-homologue bias

The stable recombination intermediate must have engaged the homologous duplex and not the sister chromatid for proper chromosome segregation. Several proteins participate in the barrier to intersister recombination.

In budding yeast, phosphorylation of the axial element protein Hop1 by Mec1/ Tel1 (Carballo et al., 2008), triggers the dimerization of Mek1 kinase which then phosphorylates its target proteins that prevent the repair of DSBs using the sister chromatid as a template (Niu et al., 2005b). The meiosis-specific cohesin subunit Rec8 promotes sister bias at the very early stage of meiotic prophase I, and Red1/Mek1 promote homolog bias by counteracting this effect (Kim et al., 2010).

Importantly, the axial element Red1 can bind SUMO (small ubiquitin like modifier) polymeric chains.The Red1-SUMO interaction is essential for Hop1 phosphorylation by Mec1/Tel1 (Lin et al., 2010). Mek1 also inhibits Rad51 activity by attenuating the formation of the Rad51-Rad54 complex; and it is thought that with less active Rad51, the activity of Dmc1 is favoured (Niu et al., 2009).

1.5 The synapsis initiation complex

Chromosome synapsis culminates in the formation of the synaptonemal complex (SC) during meiotic prophase I (von Wettstein et al., 1984). Prior to SC formation, each homolog begins to develop a dense, proteinaceous core called an axial element.

In budding yeast, synapsis initiates at one or more sites on each homolog pair before the chromosomes have developed full-length axial cores (Padmore et al., 1991). The Zip1 protein serves as the major building block of the SC central region (Sym et al., 1993). In zip1 mutant, axial cores are formed and are homologously paired (closely connected at multiple sites termed axial

associations) but not intimately synapsed. It has been shown that the formation of axial associations depends on meiotic recombination and that proteins involved in the initiation of chromosome synapsis localize to axial associtions; suggesting that these connections are also the sites where synapsis initiates (Scherthan et al., 1992; Rockmill et al., 1995; Chua and Roeder, 1998; Tsubouchi et al., 2006).

But Tsubouchi and coworkers have recently shown that centromeres are preferred sites for the initiation of synapsis in budding yeast and that initiation of synapsis at centromeres is independent of the Zip3 protein, which plays a major role in synapsis initiation events at noncentromeric locations (Tsubouchi et al., 2008). Polymerization of Zip1 along the lengths of homologs required a protein assembly referred to as the Synapsis Initiation Complex (SIC), SIC components include; Zip2, Zip3, Zip4/Spo22, Spo16, Mer3 and Msh4-Msh5 (Shinohara et al., 2008)

Zip1

Zip1 is the major building block of the transverse filament of the synaptonemal complex (SC) in budding yeast (Sym et al., 1993).. At the sequence level, transverse filaments are poorly conserved but share a broadly similar secondary structure; a long coiled-coil flanked by globular C- and N-termini (Dong and Roeder, 2000). Zip1 protein contains three potential coiled-coil domains and is phosphorylated at serine75 (Zip1-S75) by the ATR-like checkpoint kinase Mec1 (Falk et al., 2010b). Importantly, Zip1-S75 phosphorylation does not affect chromosome synapsis or DSB repair, instead, this phosphorylation event is required to destabilize early homology-independent centromere pairing in response to the initiation of meiotic recombination (Falk et al., 2010a). Zip1 polymerization along the lengths of homologs required its selective interaction with the small ubiquitin-like modifier (SUMO) polymer as a

non-null allele of *UBC9* gene, which encodes the SUMO-conjugating enzyme,impairs chromosome synapsis (Hooker and Roeder, 2006)

Zip2

The meiosis specific Zip2 protein localizes to discrete foci on meiotic chromosomes and these foci correspond to axial associations sites, which closely connected pair of homolog. Zip2 localization to chromosomes required the initiation of meiotic recombination. Zip1 protein fails to localize to chromosomes in zip2 mutant (Chua and Roeder, 1998).

Zip2 is a poorly conserved WD-like repeat protein and could serve as the platform for protein–protein interaction or more specifically could bind multiple substrates simultaneously (Voegtli et al., 2003; Perry et al., 2005a). It was shown by 2-hybrid analysis, that Zip2 interacts with Zip3 and Cdc53, the cullin component of SCF-type (Skp1-Cullin-F box) ubiquitin E3 ligase (Willems et al., 2004); these results have led to the proposal that Zip2, Zip3 and Zip4 comprise a multisubunit ubiquitin E3 ligase (Perry et al., 2005b).

Zip4/Spo22

Zip4/Spo22 is a meiosis specific protein required for synapsis. Unlike in *zip2* mutant, Zip1 localizes to meiotic chromosomes in the absence of Zip4 (in *zip4* mutant) but fails to elongate. Localization of Zip4 to chromosomes is partially dependent on Zip3. Zip2 and Zip4 proteins are mutually dependent for their localization on meiotic chromosomes; suggesting that these two proteins may work as a functional unit (Tsubouchi et al., 2006).

Zip4/Spo22 encodes a conserved large TPR-repeat protein (Tetratrico-peptide repeat). These TPR-repeats are thought to mediate protein-protein

interactions required for the assembly of multiprotein complexes (Perry et al., 2005b).

Zip3

Zip3 protein is a SUMO E3 ligase required for the assembly of the synaptonemal complex (SC). Sumoylation of target proteins is required for timely SC formation.

Synapsis is delayed significantly in ubc9-t which is a non-null allele of the essential SUMO E2 conjugating enzyme *UBC9* in budding yeast. Localization of Zip2 and Zip4/Spo22 to meiotic chromosomes depend on Zip3 and it has been proposed that Zip3 acts upstream of the other SIC proteins to promote synapsis at non-centromeric sites (Agarwal and Roeder, 2000; Hooker and Roeder, 2006; Cheng et al., 2006) but initiation of synapsis at centromeres is independent of Zip3 (Tsubouchi et al., 2008). Recently, MacQueen and Roeder have shown that Zip3 and the proline isomerase Fpr3 ensure that SC formation is dependent upon recombination initiation (Macqueen and Roeder, 2009a; Macqueen and Roeder, 2009b).

Zip3 is a conserved RING-finger protein which interacts with several SC and recombination proteins, including Zip1, Zip2, Msh5, Mre11 and Rad57 Agarwal and Roeder, 2000 ; Jantsch et al., 2004; Perry et al., 2005b)

Spo16

Spo16 is a meiosis-specific protein required for SC formation. In *spo16* mutant, crossover formation and chromosome synapsis are impaired. But unlike other ZMM mutants, the residual crossovers formed in *spo16* and *zip4/spo22* mutants show interference comparable to that in the wild type. In addition, the assembly of the MutS homologs Msh4 and Msh5 occurs in the absence of Spo16 and Spo22 (Shinohara et al., 2008).

Mer3, Msh4 and Msh5

Meiotic recombination 3 (Mer3) and mismatch repair defective 4 and 5 (Msh4 and Msh5, respectively), as other ZMM members also promote crossovers by probably facilitating the stable formation of recombination intermediates (Ross-Macdonald and Roeder, 1994; Hollingsworth et al., 1995). Snowden and coworkers have proposed that Msh4-Msh5 heterodimer acts as a clamp to hold homologous chromosomes together, stabilising thereby the Holliday junction and facilitating crossing over (Snowden et al., 2004).

Mer3 is an ATP dependent 3´-5´ DNA helicase that stimulates Rad51-mediated DNA heteroduplex extension, thereby promoting the formation of SEIs and dHJs (Nakagawa and Ogawa, 1999; Borner et al., 2004; Mazina et al., 2004). Mer3, Msh4 and Mlh1 have recently been shown to play additional roles in homologous chromosome pairing, by avoiding entanglements (interlocks) of homologs during alignment and their resolution respectively (Storlazzi et al., 2010a).

I.6 The synaptonemal complex (SC)

The synaptonemal complex(SC) is a tripartite proteinaceous structure that connects paired of homologous chromosomes in most organisms. The SC consists of two axial elements (derived from axial elements) connected by a central region (element) or transverse filaments.

The axial elements (AE)

The axial element constitutes the rod-like homologue axis along which the chromatin loops of sister chromatids are organized (Figure 4). Evidence supports the hypothesis that the cohesin complex function in LE formation by forming an axial chromosome core on which LE proteins bind and assemble (Klein et al., 1999). The isolation of a meiosis-specific allele of *YCS4* that is defective in recruiting SC proteins, chromosome pairing has also involved the condensin complex in LE assembly (Yu and Koshland, 2003b).

In *S.cerevisiae*, a normal SC does not form in *hop1* and *red1* mutants. The fact that, only fragments of LEs can be form in *hop1* mutant or that LEs are completely absent in *red1* mutant, implicated these proteins in the assembly of LEs (Rockmill and Roeder, 1990; Loidl et al., 1994). A physical interaction of Red1 with Mek1 further involved Mek1 kinase in normal assembly of synapsis (Rockmill and Roeder, 1991).

The transverse filaments

Proteins that form the transverse filaments of the SC have been identified in several species. These proteins include : C(3)G, SCP1, Zip1, SYP-1 and SYP-2 respectively in *Drosophila melanogaster* (Page and Hawley, 2001), in mammalian species (Meuwissen et al., 1992), in *S.cerevisiae* (Sym et al., 1993), and in *C.elegans* (MacQueen et al., 2002a). The common feature of these proteins is that they all share a predicted coiled coils secondary structure eventhough they differ greatly at the primary amino acid sequences level (Page and Hawley, 2004).

Immunolocalization by EM has suggested that Zip1 protein forms parallel dimers through its coiled coil regions and align between homologous chromosomes with the C termini along the LEs and with the N-termini from opposing dimers interacting in an antiparallel manner across the center of the SC to form the transverse filaments (Dong and Roeder, 2000) (Figure 4).

Accordingly, deletion of 34 amino acids (791-824) within the C-terminal globular domain of Zip1 prevents the protein from assembly onto the chromosome, and similarly an in-frame deletion that removes the N-terminal half of the coiled coil domain also prevents synapsis. Importantly, partial deletions that remove the C-terminal half of the coiled coil domain or the N-terminal globular domain of Zip1 do not affect synapsis (Tung and Roeder, 1998).

Mechanism of SC formation

In budding yeast, SC initiation occurs at centromeric as well as at non centromeric locations (Tsubouchi et al., 2008). It has been shown that the protein Red1 can binds Smt3 chains (the yeast small ubiquitin-like modifier (SUMO)) like Zip1 the major SC central element component. The Red1-Smt3 interaction then facilitates firstly the recruitment of Zip1 and Zip3 for SC initiation and secondly promotes the phosphorylation of Hop1 by Mec1/Tel1 upon DSB formation. Hop1 phosphorylation prevents inter-sister recombination to ensure interhomologue recombination (Lin et al., 2010).

SC initiation at centromeric sites is independent of the SUMO E3 ligase Zip3 (Tsubouchi et al., 2008). Other SUMO E3 ligases such as Siz1, Siz2 or Mms21 have been involved in Zip1-Smt3 interaction at centromere (Cheng et al., 2006). After the initiation of SC, other ZMM proteins have been proposed to act as chaperone-like machinery to promote the perpendicular alignment of Zip1 along two axial elements during SC elongation (Cheng et al., 2006). SC elongation might involve an interaction between the Red1-Smt3 chains and Zip1 C-termini globular domains (Cheng et al., 2006; Hooker and Roeder, 2006; Lin et al., 2010).

Roles of the synaptonemal complex (SC)

In most organisms including the budding yeast, mutants that fail to form the mature SC are also defective in crossover formation suggesting that the full length SC plays a role in the maturation of recombination intermediates (SEIs to dHJs, dHJs to crossovers) to crossovers (Blat et al., 2002).

It has also been shown that the full length SC is required to maintain or stabilize the initial pairing of homologs in *C.elegans* as cell progresses through meiosis (MacQueen et al., 2002a). In order to ensure the segregation of achiasmate homologs in some organisms such as the *Bombyx mori* females, a modified form of the SC is maintained until the separation of homolog at anaphase I (Zickler, 1999).

Evolutionary conservation of the SC

The synaptonemal complex (SC) is a highly conserved feature of meiosis. But in several organisms including *S.pombe*, *Drosophila melanogaster* males and *Aspergillus nidulans*, homologous chromosomes pairing occurs normally but a typical tripartite proteinaceous SC structure is not formed.

I.7 Checkpoint control: surveillance mechanisms of the meiotic divisions

DNA breakage is required to connect homologous chromosomes during meiosis. In the absence of interhomolog crossovers, homologous chromosomes segregate randomly during the first meiotic division (MI) and the resulting aneuploidies cause lethality. In rare cases, a disomic germ cell can progress to yield a individual carrying a trisomy. In humans most trisomies are embryonic lethal, but trisomy 21 is the most frequent congenital source of mental retardation in humans. Various surveillance mechanisms function also during meiosis to coordinate the formation and repair of DSBs with the cell cycle progression.

Double-Strand-Breaks are coordinated with premeiotic replication

The intra S-phase checkpoint monitors fork stalling and other irregularities during replication and reacts by downregulating Ddk and Cdc45, in effect slowing down further replication. In the presence of stalled replication forks as a result of hydroxyurea treatment or mutations in ribonucleotide reductase, DSBs are not formed (Borde et al., 2000b; Smith et al., 2001a; Tonami et al., 2005). This is a local phenomenon as a delay in DNA replication on one arm of chromosome III specifically delayed DSB formation on that arm but not on other chromosomes (Borde et al., 2000a).

However, replication is not absolutely required for DSB formation, as inactivation of *CDC6* in meiosis blocks the firing of origins of replication, but allows DSB formation (Hochwagen and Amon, 2006). The activity of S-phase CDKs (Clb5/6-CDK) is required to couple the completion of DNA replication to DSB formation (Smith et al., 2001a). Accordingly, it has also been shown that pre-meiotic DNA replication is coupled to DSB formation by a sequential phosphorylation of Mer2 protein on the adjacent serines S30 and S29 respectively by Cdc28-Clb5 and Cdc7-Dbf4 kinases (Henderson et al., 2006;

Wan et al., 2008b). It was proposed that the coupling between S-phase and DSB formation occurs during passage of the replication fork, which recruits Cdk and Ddk to phosphorylate and activate Mer2 (Murakami and Keeney, 2008). Recently it was shown that Mer2 indeed binds to its chromosomal sites independent of replication, but only is able to recruit the rest of the DSB machinery upon activation by these kinases (Panizza et al., 2011). Activation in the absence of replication is explained by diffusion of kinases, which will eventually also activate the DSB machine.

The pachytene checkpoint

In meiotic prophase a typical consequence of a checkpoint arrest or delay is inhibition of Ndt80 expression. This will delay or suppress pachytene exit and is the reason for the name of this checkpoint. Typical lesions that elicit such a response can be unprocessed DSBs, single stranded DNA termini or lesions left over from S-phase. Unresolved joint molecules do not elicit such a response. Also, even though proposed multiple times, there is no indication that unpaired chromosomes can trigger a checkpoint response.

A number of mutations, which allow the initiation of meiotic recombination but block the processing of recombination intermediates have been characterized. These include a set of non-null alleles of *RAD50 (rad50S)* (Alani et al., 1990), a null mutation of *COM1/SAE2* (Prinz et al., 1997)(McKee and Kleckner, 1997), and *mre11S* (Nairz and Klein, 1997). In these mutants, Spo11 remains covalently bound to the DSBs ends and breaks are not resected.

It has been suggested that the MRX complex (Mre11/Rad50/Xrs2) and Tel1 are the primary sensors of this checkpoint (Usui et al., 2001), and the signal is then relayed through Rad9 and Mek1 to downstream targets.

Mutants that are defective in the initial strand-invasion step of meiotic repair such as *dmc1* (Bishop et al., 1992), *hop2* or *mnd1* (Zierhut et al., 2004), accumulated hyperresected DSBs that leads to large amounts of Rad51-coated

ssDNA. It has been suggested that the Rad51 nucleoprotein filament may constitute a signal recognised by the recombination checkpoint. Tel1 and Rad9 are not essential for this checkpoint (Lydall and Weinert, 1996), however cells lacking *HOP1*, *RED1* or *MEK1* are completely defective in this checkpoint response (Hochwagen and Amon, 2006). And the checkpoint response is also reduced in cells lacking *DOT1* (San-Segundo and Roeder, 2000a). The meiotic recombination checkpoint delay is brought about by the inhibition of CDK and by preventing Ndt80 expression. The activity of the phosphatase PP1/Glc7 would allow cells to bypass the checkpoint delay (Roeder and Bailis, 2000), if not for its inhibitor, the FK506 binding protein Fpr3. Fpr3 associates with and antagonizes the phosphatase PP1/Glc7 function during meiotic recombination (Hochwagen et al., 2005b).

In ZMM mutants (at both 23°C and 33°C), cells undergo a temperature-dependent delay during meiotic recombination (Sym et al., 1993; Chua and Roeder, 1998; Agarwal and Roeder, 2000; Borner et al., 2004). Although, it is not known what may constitute the signal recognised by the zip1 checkpoint, it has been demonstrated that the ATPase Pch2 is required, as the inactivation of Pch2 eliminates the cell-cycle delay of *zip1*Δ, *zip2*Δ mutants (San-Segundo and Roeder, 1999).

1.8 Aims of this study

During meiotic prohase I, homologous chromosomes must align. The molecular mechanism(s) of homologs pairing is not completely understood. Initiation of meiotic recombination is a prerequisite for chromosome alignment and synapsis in budding yeast. Chromosome synapsis initiates at the sites of crossing over as well as at centromeres. A subset of protein assembly referred to as the synapsis initiation complex (SIC) or ZMM proteins is required for polymerization of Zip1 along the lengths of chromosomes, but Zip3 is dispensable for synapsis initiation at centromeres (Chua and Roeder, 1998; Tsubouchi et al., 2006; Tsubouchi et al., 2008).

It has been proposed that Zip1 polymerization along the entire length of homologs requires its interaction with the Red1-Smt3 (Red1-SUMO polychain) complex and that other SIC proteins act as chaperone-like machinery to promote SC elongation (Hooker and Roeder, 2006; Lin et al., 2010). However, the detailed molecular mechanism(s) of SC initiation and elongation remains unknown. The role of SC formation is still debated and enigmatic. Synapsis might provide a means to prevent chromosome interlocking. Several lines of evidences suggest that CO formation and interference between them are not absolutely dependent on SC formation, even though they depend on ZMM factors, which also promote synapsis.

We set out to determine the role of all non-essential genes in SC-formation and elongation. To this end, we have analyzed strains deleted for 3600 non-essential ORFs in budding yeast for their requirement in synapsis. We modified the BY-based deletion library, by introducing the well sporulating SK1 strain background and the Rec8-HA epitope tag to visualize chromosome axes. We used IF-staining of chromosome spreads at a single time point to systematically analyze synapsis and categorized the mutants by the extent of their ability to synapse.

2 Materials and Methods

2.1 Media and Solutions

All media, solutions and equipments detailed in this chapter were sterilized by autoclaving at 121°C at 1.5bar for 15-25 minutes or by baking at 180°C for 3 hours. Heat unstable Media and solutions (e.g. amino acid solutions) were sterilized by filtration using sterile 0.20 μm filter (Iwaki/Asahi Technoglass #2052-025) and a sterile 50 ml syringe (Sarstedt, #62 547 254).

2.1.1 Solid Media

Bacteriological Agar (Agar; Oxoid, # LP0011) was always put directly into glass bottles containing a magnetic stir bar. The premixed medium was then added and the bottles were autoclaved. After autoclaving, the bottle was kept on a magnetic stirrer to cool down below 65°C and it was poured into sterile petri dishes (Sarstedt petridishes 8.4cm #821473) and left for about 2 days at room temperature to dry. The plates were then stored at 4°C.

YPD plates

2% (w/v) Agar (Agar; Oxoid, # LP0011)

Then add mixed with deionized water:

1% (w/v) Yeast extract (Oxoid, # LP0021)

2% (w/v) D(+) - glucose monohydrate (Fluka, # 49159)

2% (w/v) Neutralized bacteriological peptone (Oxoid, # LP0034)

G418 (Geneticin) plates

G418 plates are used to select for the heterozygous dominant marker KanMX (kanamycin) cassette that confers resistance to G418 by coding for an aminoglycoside phosphotransferase which interferes with ribosome function and protein synthesis in eukaryote and procaryote.

Follow the YPD plate recipe.

After autoclaving and cooling the medium to 65°C, add 1 ml per liter medium of the G418 stock solution (200 mg/ml, G418 sulphate, Calbiochem, # 345810) and mixed well.

ClonNAT (nourseothricin) plates

Nourseothricin is an antibiotic that can be used to select for the presence of NatMX marker cassettes, encoding a nourseothricin N-acetyle transferase which confers resistance to the antibiotic.

Follow the YPD plate recipe.

After autoclaving and cooling the medium to 65°C, add 0.5-1 ml per liter medium of the ClonNAT stock solution (200 mg/ml, ClonNAT, dihydrogen sulphate, Werner BioAgents #5.0000) and mixed well.

Cycloheximide plates

Cycloheximide is an antibiotic that can be used to select for mutants who carry a recessive mutation (cyh2 mutant) in the *CYH2* gene encoding for the L29 ribosomal subunit. Cycloheximide binds to wild type ribosomes and blocks further elongation of nascent polypeptide chains, blocking protein synthesis altogether. Because of these properties, the CYH2 gene can be used as a dominant negative marker in the presence of cycloheximide.

Follow the YPD plate recipe.

After autoclaving and cooling the medium to 65°C, add the cycloheximide stock solution (10 mg/ml, Sigma, # C-1988) to a final concentration of 5-10mg per litre medium and mixed well.

5-FOA (5-Fluoro-Orotic acid) plates

5-FOA can be used to select for mutants who fail to utilize orotic acid as the source of the pyrimidine ring. Wild type cells would convert 5-FOA to fluorodeoxyuridine which is quite toxic to the cell. Both ura3 and ura5 null mutants can grow on 5-FOA containing medium, but in practice, only ura3 mutant appears to be uracil auxotroph.

2% (w/v) Agar (Agar; Oxoid, # LP0011)

Mix with one half amounts of water, autoclave and cool to 65°C.

Then mix following ingredients with second half of water, filter sterilize and add to autoclaved agar:

0.17% (w/v) Bacto-yeast nitrogen base w/o amino acids and w/o ammonium sulfate (Difco, # 233520 [0335-15])

0.50% (w/v) Ammonium sulfate (Calbiochem, # 168356)

2% (w/v) D(+)-glucose monohydrate (Fluka, # 491591)

50 mg Uracil (Sigma, # U-0750) per litre

1% URA^- drop out mix (see table 1)

0.10% 5-FOA (5-Fluoro-Orotic acid, BTS Bio Vectra, # 1555)

adjust to pH 4.8 with NaOH

ADE^-,TRP^-,and URA^- drop out plates

Drop out media allows testing of yeast strains for specific auxotrophie (auxotrophic markers). A specific media composition is used in which each of the exhibited auxotrophies is supplemented except the one of interest (the drop out marker).

2% (w/v) Agar (Agar; Oxoid,, # LP0011)

Then add mixed with water:

0.17% (w/v) Bacto-yeast nitrogen base w/o amino acids and w/o ammonium sulfate (Difco, # 233520 [0335-15])

0.5% (w/v) ammonium sulfate (Calbiochem,, # 168356)

2% (w/v) D(+)-glucose monohydrate (Fluka,, # 491591)

1.10% (w/v) Bacto-casamino acids(Difco, # 223120 [0231-17])

Add then:

50 mg L-tyrosine (Sigma, # T-3754) per litre

50 mg Adenine (Sigma,# A-3159) per litre; (**Not** added for ADE^- plates)

50 mg Uracil (Sigma, # U-0750) per litre; (**Not** added for URA^- plates)

Adjust to pH 5.8 with NaOH

After autoclaving and cooling the medium to 65°C,

5 ml of sterile 1% (w/v) L-Leucin (Sigma, # L-8000)

5 ml of sterile 1% (w/v) L-Tryptophan (Sigma, # T-0254); (**Not** added for TRP- plates)

are added per litre and mixed well.

HIS^-,LYS^-, LEU^-, and ARG^- drop-out plates

2% (w/v) Agar (Agar; Oxoid, # LP0011)

Then add mixed with water:

2% (w/v) D(+)-glucose monohydrate (Fluka, # 491591)

0.30% (w/v) Bacto-yeast nitrogen base w/o amino acids and w/o ammonium sulfate (Difco, # 233520 [0335-15])

0.50% (w/v) Ammonium sulfate (Calbiochem, # 168356)

Add then:

60 mg Adenine (Sigma, # A-3159) per litre

60 mg Tyrosine (Sigma, # T-3754) per litre

60 mg Uracil (Sigma, # U-0750) per litre

adjust to pH 5.8 with NaOH

After autoclaving and cooling the medium to 65°C, 10 ml of the sterile 100x HIS^-, LYS^-, LEU^-, or ARG^- drop-out mix (see Table 1) were added per litre of the medium and mixed well.

Table 1: Recipe for 100x drop-out mix.

Amino acid	**Amount in mg/ml**
L-Adenine (Sigma, # A-3159)	2.0
L-Arginine (Sigma, # A-5131)	2.0
L-Histidine (Sigma, # H-8125)	1.0
L-Isoleucine (Sigma, # H-8125)	6.0
L-Leucine (Sigma, # L-8000)	6.0
L-Lysine (Sigma, # L-5751)	4.0
L-Methionine(Sigma, # M-9625)	1.0
L-Threonine (Sigma, # T-8625)	5.0
L-Tryptophan(Sigma, # T-0254)	4.0
L-Uracil (Sigma, # U-0750)	2.0

Each specific drop-out solutions has the appropriate amino acid omitted. after dissolving the ingredients in distilled water, the drop-out solution was filter sterilized (0.2 µm filter) and stored at 4°C in the dark.

SPM plates

2%(w/v) Agar (Agar; Oxoid, #LP0011)

Then add mixed with water:

1% (w/v) Potassium acetate (Merck, #104820)

adjust to pH 7.0 with acetic acid (Not really required) and autoclave.

When setting the meiotic time course experiment, the SPM liquid medium is supplemented with aminoacids (1/5 of the usual amount) and 0.1% (v/v) of a 1% polypropylene glycol stock (1%(v/v) polypropylene glycol P2000, Fluka #81380 in distilled water then autoclave and store at room temperature). Amino acids stock (1.5% Lys, 2% His, 2% Arg, 1% Leu, 0.2% Ura. 1% Trp) filter-sterilized and stored in the dark at +4°C. Use 320µl of amino acids stock per 100ml SPM media.

YPG plates

YPG is a complex medium containing a non-fermentable carbon source (glycerol) which can not support the growth of respiratory deficient mutants such as pet- (petite) mutants.

2% (w/v) Agar (Agar; Oxoid, #LP0011)

Then add mixed with water:

3% (v/v) Glycerol (100%; Sigma, #G7757)

1% (w/v) Yeast extract (Oxoid, #LP0021)

2% (w/v) Neutralized bacteriological peptone (Oxoid, #LP0034)

SM plates

SM is a synthetic minimal medium containing all ingredients ; salts, trace elements, vitamins, a nitrogen and carbon sources; but amino acids. Therefore, only prototrophic cells can grow on SM plates.

2% (w/v) Agar (Agar; Oxoid. #LP0011)

then add mixed with water:

0.17% (w/v) Bacto-yeast nitrogen base w/o amino acids and w/o ammonium sulfate (Difco, #233520 [0335-15])

0.50% (w/v) Ammonium sulfate (Calbiochem, #168356)

2% (w/v) D(+)-glucose monohydrate (Fluka, #491591)

adjust to pH 7.0 with NaOH

2.1.2 Liquid media

For all yeast liquid media, Bacteriological agar (Oxoid, #LP0011) is omitted (see section 2.1.1).

GNA pre-sporulation medium

This medium is for pre-sporulation growth boost in the BY-SK1 K.O. library screen.

1% (w/v) Yeast extract (Oxoid, #LP0021)

5% (w/v) D(+)-glucose monohydrate (Fluka, #491591)

0.17% (w/v) Bacto-yeast nitrogen base w/o amino acids and w/o ammonium sulfate (Difco, #233520 [0335-15])

0.1 - 0.25% (w/v) L-Glutamic acid monosodium salt monohydrate (MSG; Sigma, # G283-4)

adjust to pH 5.8 with NaOH

BY-SK1 hybrid drop-out medium

This medium is used in the BY-SK1 hybrid screen for the selection of the desired genetic marker combinations of sporulated diploid hybrid strains.

Mix following ingredients with water and filter sterilize or autoclave.

0.17% (w/v) Bacto-yeast nitrogen base w/o amino acids and w/o ammonium sulfate (Difco, #233520 [0335-15])

0.25% (w/v) L-Glutamic acid monosodium salt monohydrate (MSG; Sigma, # G283-4)

2% (w/v) D(+)-glucose monohydrate (Fluka, #491591)

50 mg Uracil (Sigma, # U-0750) per litre

Add amino acids according to desired selection

adjust to pH 5.8 with NaOH

Add antibiotic and chemical to desired selection (always after autoclaving the media and cooling down to 65°C):

0.30% Cycloheximide (Sigma, # C-7698)

0.10% 5-FOA (5-Fluoro-Orotic acid, BTS Bio Vectra, # 1555)

0.10% G418 (G418 sulphate, Calbiochem, #345810)

Antibiotics stocks are prepared using deionized water,
filter-sterilized and stored at -20°C.

SPS pre-sporulation medium

This medium is used to prepare yeast cells for sporulation, when a high efficiency of synchrony is needed during sporulation,

0.5%(w/v) Yeast extract (Oxoid, #LP0021)

1% (w/v) Peptone (Oxoid, #LP0034)

0.17% (w/v) Yeast nitrogen base w/o amino acids and w/o ammonium sulphate (Difco, #233520)

1% (wiv) Potassium acetate (Merck, #104820)

0.5% (w/v) Ammonium sulphate (Merck, #101217)

0.05M Potassium biphtalate (10.2g/liter) (Merck, #104874)

adjust to pH 5.5 with KOH

Optionally, a drop of anti-foam is added to prevent excessive foam formation, when setting up the yeast pre-sporulation culture (Antifoam A concentrate, Sigma #A5633-25G).

2.1.3 LB-bacterial culture media

This complex medium is widely for cultivating *Escherichia.Coli b*acteria at 37°C.

1% (w/v) Peptone (Oxoid, #LP0034)

0.5% (w/v) Yeast extract (Oxoid, #LP0021)

1% (w/v) Sodium chloride (Merck, #106404)

Add 2% (w/v) Bacteriological agar (Oxoid, #LP0011) for solid media

To select for resistance to ampicillin (*E.coli* carrying the ampicillin marker), add to the media 100mg/liter ampicillin (Ampicillin sodium salt, Sigma-Aldrich, #A9518). Ampicillin stock concentration of 100mg/ml (in deionized water) is prepared, filter-sterilized and stored at -20°C.

2.2 Manipulating Yeast and E.coli *strains*

2.2.1 Growth and long term storage of Yeast strains

Yeast cells were grown in liquid culture while agitated (at 200 rpm) or on plates at 30°C, or at the indicated temperature for temperature sensitive mutants and were harvested and stored in 1:1 glycerol/YPD mix at -80°C. A stock of 1:1 glycerol/YPD mix is prepared, filter-sterilized and kept at room temperature until needed.

2.2.2 Tetrads dissection and single spores production

After sporulation at 30°C, cells were suspended in 92µl of sterile water and 4µl of 0.5M DTT (Sigma, #D-9779) and 4µl of Zymolyase 20T (stock concenration: 10mg/ml, Seikagaku, #120491) were added. This mixture was incubated at 37°C for 30-60mn; and 1ml of distilled water was added to the suspension to stop the reaction and the digested tetrads were then cooled on ice. Subsequently, 25µl of the mixture were pipetted onto the upper middle area of a YPD plate and the small cell suspension droplet was then forced by gravity to run down the agar surface leaving trail of zymolyase digested tetrads. After drying the plate for 5 minutes at room temperature, the spores of defined, full tetrads were individually separated utilizing a Leitz micromanipulator and the plates were incubated at 30°C for 2-3 days before the analysis of individual segregants was carried out.

When a large number of individual spores is needed or when an homothalic yeast strain has to be crossed to haploid yeast, the production of single spores is required. After sporulation and tetrads digestion, single spores are produced by sonication at lower power. 1.5ml Eppendorf tube containing the digested asci was stacked on top of a plastic tube filled with ice and water, cooling the cell suspension. The sonicator horn was then sterilized by repeated flaming and the spore suspension was sonicated for 5 sec at lower power followed by a 5 sec pause (= cooling step). This cycle was repeated until 95% single spores were produced.

2.2.3 Picking zygotes and meiotic time-course experiments

Meiotic experiments are performed using diploid strains. To produce a diploid yeast strain, two haploid strains of opposite mating type were thoroughly mixed on a YPD plate and incubated at 30°C for 4-6 hours, single zygotes were isolated from the mating mix using a Leitz micromanipulator and this is possible because zygotes exhibit a distinct characteristic morphology (dumb-bell shape, three-lobes shape). The diploid status was confirmed by testing their ability to sporulate and their inability to mate to haploid tester strains (*FKY515* and *FKY516* see appendix).

To analyse the chronological contiguity of meiotic events, meiotic time-course experiments were conducted. An aliquot of on -80°C stored diploid yeast strain was streaked out on YPD plate for single colonies and left growing for 2-3 days. A large colony was then streaked onto a YPG plate to test its proficiency for respiratory growth and was used to inoculate a 4-5 ml YPD culture which is grown for about 24 hours under vigorous agitation (200rpm).

On the next day, cells were spun down at 3000 rpm for 3 minutes and resuspended in 2-5ml of SPS medium and were used to inoculate a desired volume of SPS or GNA media to a starting OD660 of 0.1-0.2 which correspond to 0.2 to 0.4x107 cells per ml culture. The SPS or GNA culture which should not fill more than 1/10th of the flask´s volume; was grown for about 13-16 hours under

vigorous shaking at 200 rpm to reach a cell density of 4x107 cells/ml (OD660 of 1.1).

The cells were then spun down and washed once with 1% potassium acetate and were finally inoculated in 1% potassium acetate supplemented with amino acids mix (320µl/100ml culture) and PPG (polypropylene glycol P2000: 100µl/100ml culture), to a final density of 4x107 cells/ml (OD660 of 1.1), and this corresponds to time point 0-hour of the time course.

As for the SPS or GNA culture, the SPM culture should not fill more than 1/10th of the flask´s volume and the time course is carried out under maximal shaking (200 rpm) at the desired temperature usually 30°C.

2.2.4 Transformation of *S.cerevisiae*

One single colony of the strain which should be transformed was grown overnight in 50 ml of YPD medium. On the next day the cells were diluted to an OD_{660} of 0.1-0.2 and grown until the cell suspension reached an OD_{660} of 0.6-0.8 (= exponential growth range) and were harvested by centrifuging (3mn at 3000 rpm). The cells were then washed twice with 1ml of 1M Lithium acetate and finally transferred in 350µl of 1M Lithium acetate and left incubating for 10-15 minutes at room temperature. Pipetting for the transformation was carried out in the following order:

12µl of the DNA (100-300ng plasmid, 2-5µg PCR generated fragments)

24µl of the competent yeast cells

90µl of 50% (w/v) PEG 3350

8µl of boiled Salmon sperm DNA (10mg/ml, low MW, Fluka

/BioChemika #31149)

Gently finger flicking was employed to mix all components and the suspension was incubated for 35 min at 25°C before adding 6µl of 60%(v/v)

glycerol (Sigma-Aldrich, #G7757). After another 35 mn incubation at 25°C, the cells were heat shocked for 15 minutes at 42°C and plated immediately onto two appropriate selection plates or incubated overnight in 1ml YPD medium if the construct is carrying a resistance marker (KanMX, NatMX). A second transformation procedure was performed in parallel using sterile water in place of the used DNA as a negative control.

Lithium acetate(LiAc)

1M Lithium acetate (Sigma, #L6883) in deionized H2O

adjust to pH 7 with acetic acid and filter sterilize

stored at -20°C

50% PEG 3350 (Polyethyleneglycol)

1.0g PEG 3350 (Sigma, #P3640)

2.0 ml deionized H2O

freshly prepared and filter sterilized

1x TE

10mM Tris buffer grade (Applichen, #A1086)

1mM EDTA (Titriplex; Merck, #108417)

adjust to pH 8 with HCl (Merck, #100319) and filter sterilize

2.2.5 Preparation and transformation of competent *E.coli*

An overnight culture of *E.coli* was diluted to 1:200 in 50 ml fresh LB medium and grown at 37°C until an OD_{600} of 0.3-0.6. The cells were collected by centrifugation at 3500rpm for 10mn at 4°C and cooled on ice for 5 min. The pellet

was resuspended in 25 ml of cold sterile 0.1M CaCl2 and incubated on ice for 30 min. The cells were pelleted at 3500rpm for 10mn at 4°C and resuspended in 2-5ml ice-cold 0.1M CaCl2. The now competent *E.coli* cells were mixed 2:1 with glycerol, aliquoted in 100µl, frozen in liquid nitrogen and stored at -80°C for up to 6 months.

Competent *E.coli* cells were thawed slowly on ice, 3-5µl plasmid DNA was added to 100µl of competent cells and the suspension was mixed by gently finger flicking. After 30mn incubation on ice, a 42°C heatshock was applied for 2 min. 1 ml of LB medium was added and the mixture was incubated for 60min (Ampicillin selection) or 3hours (Kanamycin selection) at 37°C under agitation on a thermomixer. Cells were then collected by centrifugation for 3 min at 6000rpm, the pellet was resuspended in 100µl LB medium and plated onto two appropriate selection plates in a ratio of 10:1.

$CaCl_2$ solution

0.1M calcium chloride (Merck, #102382)

15% (v/v) Glycerol (Sigma-Aldrich, #G7757)

10mM PIPES

adjust to pH 7.0

2.2.6 Flow Cytometric analysis of yeast cells

Approximately 1.10^7 cells (usually 2ml of SPM culture at OD_{660} :1:100 were harvested at indicated meiotic time point and spun down at 3000rpm for 3 minutes. The pellet was resuspended in 1.5ml ddH_2O, 3.5ml of 96% ethanol was added, the cells suspension was gently mixed and incubated overnight at 4°C.

Fixed cells were pelleted at 3000rpm for 3minutes, washed once with 1.5ml ddH_2O and resuspended in 0.5ml of freshly prepared RNase A solution and incubated at 37°C for 6-12 hours. Cells were harvested at 6000rpm for 2minutes

and resuspended in 200µl of protease solution and digested for 15-20 minutes at 37°C. Cells were pelleted at 6000rpm for 2 minutes and resuspended in 0.5ml of 50mM Tris pH 7.5 (after this step cells can be stored at 4°C for a few days (but not more than 5 days) or analysed immediately).

50µl of cells suspension was added to 1ml of Sytox green solution, then sonicated at lower power for 15 seconds and analyzed within 3 hours. Before each measurement, samples were vortexed thoroughly.

RNase A solution

RnaseA (Roche, #10109169001) was prepared at the final concentration of 2mg/ml in (50mM Tris pH 8.0, 15mM NaCl) solution, boiled for 15mn and cooled down slowly at room temperature and stored at -20°C.

Protease solution

5mg/ml pepsin

4.5µl/ml of 32% HCl

ddH_2O to the desired volume

Sytox Green solution

1µM of Sytox green in 50mM Tris pH 7.5

2.3 DNA protocols

2.3.1 Preparation of Yeast genomic DNA

«Quick and dirty» DNA preparation for genotyping

5ml of YPD medium was inoculated with a single yeast colony and grown overnight at 30°C under shaking (200rpm). On the next day, cells were harvested at 3000 rpm for 3mn and resuspended in 200µl of buffer A, 200µl of sterile glass beads (Sartoriusstedim #BBI-8541701, 0.4-0.6mm) and 200µl of PCI were added. After vortexing at maximum speed for 7mn at 4°C, 200µl of TE buffer were added and the cell suspension was again vortexed for 7mn.

The cell suspension was centrifuged down for 5mn at maximum speed and 1ml of 96% ethanol was added to the upper phase, after 5mn incubation on ice, the precipitated nucleic acid was pelleted at maximum speed for 5mn and resuspended in 200µl of TE buffer. RNA was digested by addition of 4µl of 10mg/ml boiled RNaseA (Roche Applied Science, #109169) and incubation at 37°C for 30-60mn. 200µl of CI and 200µl of TE buffer were then added and after spinning down at maximum speed for 5mn, 20µl of 5M potassium acetate (Merck, #106267) and 800µl of 96% ethanol were added to the upper phase, after 5mn incubation on ice, the precipitated DNA was pelleted at maximum speed for 5mn, washed twice with 70% ethanol, dried and resuspended in 50µl of TE buffer.

Buffer A

2% Triton X-100

1% SDS (Merck, #113760)

100mM NaCl

10mM Tris-HCl pH 8.0

1mM EDTA pH 8.0

Store at room temperature

Phenol:Chloroform:Isoamylalcohol (PCI) (25:24:1)

50% (v/v) Phenol, liquefied and Tris saturated pH>7.6 (Biomol, #50734)

48% (v/v) Chloroform (Merck, #102445)

2% (v/v) Isoamylalcohol (Merck, #100979)

Store in the dark at +4°C

Chloroform-Isoamylalcohol (CI) (24:1)

48% (v/v) Chloroform (Merck, #102445)

2% (v/v) Isoamylalcohol (Merck, #100979)

Store in the dark at +4°C

Yeast genomic DNA preparation for southern blotting

8ml of 50% glycerol was added to 35-50ml of meiotic culture and mixed well. The sample was centrifuged down at 4000rpm for 3mimutes at 4°C and the pellet resuspended in 1ml of spheroplasting solution containing 20% glycerol, transferred into 2ml Eppendorf tube and spun down for 3minutes at 4000rpm and 4°C. The cells were frozen in liquid nitrogen or directly stored at -80°C until needed.

The cells were washed with 1ml of ice cold spheroplasting solution, spun down at 6000rpm for 3minutes and resuspended in 400µl of Zymolyase solution. The cells were digested at 37°C for about 10-20minutes until the large majority was spheroplasted, controlled by phase contrast microscopy. The spheroplasts were pelleted at 1500g for 3minutes at room temperature and resuspended by gently vortexing in 350µl of Tris/EDTA solution, to which, 50µl of 10% SDS (Merck, #113760), 12.5µl of 20mg/ml Proteinase K (Roche, #03 115 828 001) and 7-8µl of 10mg/ml boiled RNase A were added. The tube was inverted

several times to mix and finally incubated for 30-60minutes at 55°C. Then after adding 350µl of 5M potassium acetate (Merck, #104820) the tube was again inverted several times and incubated on ice for 30 minutes (or longer). The precipitate was centrifuged down at maximum speed for 10 minutes and the supernatant transferred into a new 2ml eppendorf tube. 1 volume of fresh PCI was added, vortexed for 5 seconds at full speed, left rotating on a wheel for 10 minutes and finally spun down for 5 minutes at full speed. The aqueous phase was transferred into a new 1.5ml eppendorf tube and 120µl of 3M sodium acetate (Merck, #106267) and 1.2ml of 96% ethanol (Merck, #100971) were added to precipitate the DNA, the tube was inverted several times and kept on ice for 30minutes (or longer), then centrifuged down at full speed for 20 seconds. Finally the pellet was washed twice with 1ml of 70% ethanol, dried and resuspended in 50µl 1xTE.

10x Tris/EDTA solution pH 8.0

500mM Tris (AppliChen, #A1086)

200mM EDTA (Merck, #108417)

pH 8.0 using NaOH (Merck, #106498)

1xTE buffer pH 8.0

10mM Tris (AppliChem, #A1086)

1mM EDTA (Merck, #108417)

pH 8.0 with HCl (Merck, #100319)

Proteinase K (20mg/ml)

20mg proteinaseK (Roche Applied Science, #03115879001)

10µl 1M Tris/HCl pH 7.5

20µl 1M CaCl2 (Merck, #102382)

500µl glycerol (Sigma-Aldrich, #G7757)

470µl dH2O

filter sterilized the solution before adding to proteinase K

stored at -20°C

Spheroplasting solution with 20% glycerol

1M sorbitol (Merck, #107758)

50mM KPO_4 buffer pH 7.5

50mM EDTA pH 7.5

20% (v/v) glycerol (Sigma-Aldrich, #G7757)

filter sterilized and stored at 4°C

Spheroplasting solution

1M sorbitol (Merck, #107758)

50mM KPO_4 buffer pH 7.5

50mM EDTA pH 7.5

filter sterilized and stored at 4°C

Zymolyase solution

400µl spheroplasting solution

6µl ß-mercaptoethanol (Sigma-Aldrich, #M3148)

100µg 100T zymolyase (Seikagaku, #120493)

prepared fresh

2.3.2 Plasmid preparation from *E.coli*

Plasmid Midi preparation

An *E.coli* strain carrying a plasmid was grown overnight at 37°C in 50ml LB medium supplemented with antibiotic according to the selection marker on the plasmid. On the next day, the cells were collected by centrifugation at 3500rpm for 20mn and resuspended in 2.5ml of solution 1. 2.5ml of solution 2 was slowly added and after 5mn incubation on ice, 2.5ml of solution 3 was added and the mix was left for another 5mn on ice.

The precipitate was then centrifuged down at 3500 rpm for 10mn and the supernatant transferred through a funnel of Kim-Wipe (Kimtech science tissue wipers, kimberly-clark Professional, #05511) into a new 50ml tube. Nucleic acids were precipitated by addition of 20ml isopropanol (Merck, #109634) and centrifugation at 3500rpm for 15mn at 4°C. The pellet was resuspended in 750µl of 1xTE buffer and the RNA precipitated by addition of 1ml of 5M lithium chloride (Merck, #105679), after 5mn incubation on ice, the precipitate was centrifuged down at 3500 rpm for 10mn and the supernatant containing the plasmid transferred into a new 15ml tube.

The plasmid DNA was collected by addition of 4ml -20°C cold 96% ethanol and centrifugation at 3500 rpm for 10mn. The pellet was resuspended in 300µl 1xTE and 50µg of boiled RNase A (Roche, #109169) added, incubated for 60mn at 37°C. 1 volume of PCI was added and the mix centrifuged down at maximum speed for 5mn, the upper phase was transferred into a new 1.5ml tube to which, 1/10 volume of 3M sodium acetate (Merck, #106267) and 2 volumes of -20°C cold 96% ethanol were added. After 30mn incubation at -20°C, the plasmid DNA was collected by centrifugation at maximum speed for 10mn at 4°C, washed twice with 70% ethanol, dried and resuspended in 100µl 1x TE.

Plasmid Mini preparation

5ml of LB medium supplemented with the appropriate antibiotic, according to the selection marker on the plasmid and containing the *E.coli* strain was grown overnight. On the next day, the cells were spun down at 3500rpm for 10 minutes and the pellet resuspended in 200µl of solution1. 60µg of boiled RNase A (Roche Applied Science. #109169) and 400µl of solution2 were added and the suspension mixed well by inversion without vortexing and incubated at room temperature for 5minutes. Then after adding 300µl of solution3 and incubation for 5 minutes on ice, the precipitate was spun down at maximum speed for 10 minutes at room temperature and the supernatant transferred to a new 1.5ml eppendorf tube.

Precipitation of the DNA was carried out by addition of 700µl isopropanol (Merck, #109634) and centrifugation at maximum speed for 5minutes at 4°C in a microcentrifuge. The pellet was resuspended in 300µl 1xTE and 1 volume of PCI was added, vortexed and finally spun down at maximum speed for 5 minutes at 4°C. The upper phase containing the plasmid DNA transferred to a new 1.5ml Eppendorf tube and 1/10 volume of 3M sodium acetate (Merck, #106267) and 2 volumes of cold 96% ethanol added, left for 30minutes at -20°C and the DNA collected by centrifuging at maximum speed for 10minutes at 4°C. The DNA pellet was washed twice with 70% ethanol, dried and resuspended in 50µl 1x TE.

Solution 1

50mM glucose (Fluka/Biochemika, #49159)

10mM EDTA pH 8.0 (Merck, #108417)

25mM Tris/HCl pH 8.0 (AppliChem, #A1086; Merck, #100319)

filter sterilized and stored at 4°C

Solution 2

1% (w/v) SDS (Merck, #113760)

0.2M sodium hydroxide (Merck, #106498)

prepared fresh every 2 months and stored at room temperature.

Solution 3

2.6M potassium acetate (Merck, #104820)

10% (v/v) acetic acid (Merck, #100063)

stored at 4°C

1x TE buffer pH 8.0

10mM Tris (AppliChem, #A1086)

1mM EDTA (Merck, #108417)

pH 8.0 with HCl (Merck, #100319)

2.3.3 Agarose gel electrophoresis

When DNA molecules are exposed to an electric field in a gel matrix, their mobility is dependent mainly on their size and shape. Taking then the size of the expected DNA fragments into account, 1xTAE gels consisting of 0.5 to 2.5% (w/v) agarose (low electroendosmosis promega, #V3125) were prepared. Pre-weighted agarose was mixed with 1xTAE and melted thoroughly in a microwave oven. After cooling to 65°C, ethidium bromide (final concentration: 100 mg/l) was added to visualize the separated DNA by UV-Light. The agarose was poured into the appropriate gel tray and transferred after polymerization into a electrophoresis chamber. The chamber was filled with 1xTAE optionally supplemented with ethidium bromide (final concentration: of 100 mg/l).

The DNA to be separated was mixed with 6x DNA loading buffer and loaded into the gel slots. A DNA size marker was loaded beside the samples to allow a size estimation of the separated fragments after electrophoresis. Gels were run at 2-10V per cm gel length for approximately 30 – 90 minutes.

50xTAE electrophoresis buffer stock solution

2M Tris (AppliChem, #A1086)

0.1M EDTA (Merck, #108417)

pH 8.5 using 57.1ml acetic acid per litre (Merck, #100063)

6x Orange G loading buffer

40% (w/v) sucrose (Merck, #107654)

75mg Orange G (Sigma-Aldrich, #03756)

60mM EDTA (Merck, #108417)

10mM Tris/HCl pH 8.0

in 50ml, filter sterilized and stored at -20°C

GeneRuler 1kb DNA ladder (Fermentas, #SM0311)

GeneRuler 50bp DNA ladder (Fermentas, #SM0371)

Ethidium bromide

Stock concentration: 0.5 g/l in distilled H2O

Store light protected at +4°C

2.3.4 Gel extraction of DNA fragments

After the separation of a mix of DNA fragments on an agarose gel, specific DNA fragments could be isolated. The band of interest was excised from an ethidium bromide stained agarose gel using illumination of a UV light box. The gel piece was then treated according to the instructions in the kit. Finally, the DNA could be concentrated by addition of 1/10 volume of 3M sodium acetate and 2 volumes of 96% cold ethanol, left for 30minutes (or longer) at -20°C and spun down at maximum speed for 10-15minutes at 4°C, washed twice with 70% ethanol, dried and resuspended in 1xTE.

QIAquick Gel Extraction kit (Qiagen, #28704)

E.Z.N.A Gel Extraction kit (Peqlab, #12-2501-02)

2.3.5 PCR mediated gene targeting in yeast

Gene K.O.s or C-terminal protein tagging were carried out using a PCR-mediated one-step gene targeting method (Wach A., 1996; Goldstein and McCusker, 1999).

K.O.-cassettes and tagging-cassettes were amplified by PCR using specific plasmids (see appendix) or strains already carrying the gene K.O. or gene tag of interest as template.

The primers were designed to contain 38-42bp short flanking homology (SFH) to the gene of interest and a universal sequence designed to amplify various selectable markers from plasmid templates.

If a strain already carrying the gene K.O. or gene tag of interest is used as template, a 18-22 bp primer pairs was engineered in such a way that the amplicon (K.O. cassette) contains approximately 200-500bp long flanking homology (LFH) which offer a higher recombination rate.

After PCR amplification, the specific PCR product was gel purified and approximately 1-3µg were transformed into the appropriate yeast strain.

Stable integration at the targeted region via homologous recombination results in growth of the transformants on appropriate selective media (for example YPD medium plus the antibiotic geneticin to select for resistance to kanamycin).

After restreaking the grown individual clones on selective plates, PCR or southern blot were employed to evaluate the site specific insertion of the construct. Fused C-terminal tags were additionally confirmed by Western blotting.

2.3.6 Southern blotting

After agarose gel electrophoresis, DNA fragments were transferred onto a rigid support, a nylon membrane (Amersham Hybond-N+, GE Healthcare RPN303B) to subsequently probe for specific DNA sequences. The integration of the K.O. cassette at the correct locus and replacement of the targeted gene of interest was verified using this technique. This method was also used to assess the proficiency of some mutant cells on meiotic DSB formation and the formation of crossover and noncrossover recombination products.

An ectopic recombination system engineered and implemented by Thorsten Allers in the laboratory of Michael Lichten was used to monitor the entire process of meiotic recombination (Allers and Lichten, 2001).

2.3.7 DNA restriction digest and electrophoresis

The genomic DNA was carefully quantified by fluorometry or spectrophotometry and digestion conditions were chosen according to the instructions of the enzyme supplier. In a typical reaction setup, 0.3 – 3ug of DNA was digested with 5 –10U of the desired restriction endonuclease in a total volume of 30- 50ul for 1-3hours at the indicated temperature, usually 37°C. For

the recombination assay the genomic DNA was digested in a volume of 30µl with XhoI and XhoI/EcoRI for 2hours at 37°C.

2.3.8 Agarose gel electrophoresis for southern

About 500ng to 1µg of the digested DNA was loaded per lane of a 25 cm long agarose gel. The agarose gel concentration was 0.5% and a thickness of about 5-7mm, no ethidium bromide was present in the gel and the running buffer during the separation. The electrophoresis was performed at low voltage (1.35V/cm) overnight at 4°C (can also be done at RT). During the electrophoresis, the running buffer was recycled using the peristaltic pump, moving running buffer from the buffer reservoir of the anode (+) to the cathode (-).

6x Bromophenol blue, Xylene cyanol FF loading buffer + $MgCl_2$

15% (w/v) Ficoll 400 (Fluka/BioChemika, #46324)

25mM $MgCl_2$ (Merck, #105833)

0.25mM EDTA pH 8

0.25% (w/v) bromophenol blue (Sigma-Aldrich, #B8026)

0.25% (w/v) xylene cyanol F (Sigma-Aldrich, #X4126)

filter sterilized and stored at room temperature

2.3.9 DNA transfer onto a nylon membrane

The agarose gel was stained for 30minutes in 1litre of 0.5µg/ml ethidium bromide solution in water to assess the quality of DNA loading and digest under UV. The $MgCl_2$ was removed by washing the gel twice in 1litre of 10mM EDTA pH 8 for 20minutes each. The agarose gel was washed for 15minutes in dH_2O, followed by acid nicking of the DNA in 1litre of 0.25M HCl for 20minutes, excess of HCl was subsequently removed by two times washes in 1litre of dH_2O for 5 minutes each.

The DNA was transferred onto a nylon membrane using the VacuGene XL blotting system (GE Healthcare, #80 1266 24, #80 1265 15). The porous support of the vaccuum chamber and its gasket were pre-wetted with alkaline transfer buffer, the membrane (Amersham Hybond-N+, GE Healthcare RPN303B) was cut to an appropriate size, pre-wetted in alkaline transfer buffer and placed onto the porous support of the vaccuum chamber. A sealing mask of the transfer system, containing a window according to the area of the gel was carefully placed on top (avoiding air bubbles). The gel was carefully slipped from its casting tray over the window of the sealing mask. The frame of the vaccuum chamber was then put in place over the gasket and fixed while applying slight pressure. The pump was turned on and the DNA was transferred at 50mbar of vaccuum for 1-2 hours.

Once the transfer was completed, the membrane was recovered washed for 5 minutes in 500ml of (0.5M Tris/HCl pH 7.5, 1M NaCl), followed by two rinses in 250ml of 2x SSPE for 2 minutes. The DNA was UV cross-linked to the membrane by two rounds of irradiation with 120mJ/cm^2 (UV Stratalinker 2400, Stratagene). The prehybridization was performed immediately, if not, the membrane was dessicated and stored in a hybridization bag or alternatively between two sheets of whatman filter paper until needed.

Alkaline transfer buffer

1.5M sodium chloride (Merck. #106404)

0.5M sodium hydroxide (Merck, #106498)

freshly prepared

2.3.10 DNA probe labelling, hybridization and detection

Alpha ^{32}P dATP random primed labelling of probe DNA

50ng of template DNA in 7µl dH_2O was denatured by heating to 95°C for 5minutes and subsequent chilling on ice, 3µl of a dCTP/dGTP/dTTP mix (170µM each nucleotide) and 6µl of alpha-^{32}P dATP (10µCi/µl, 6000Ci/mmol, 1.7µM; Amershan Biosciences AA0074) were added. The reaction was initiated by adding 4µl High Prime enzyme and random primer mix (High prime DNA Labelling kit, Roche Applied Science, #11585584001) and incubated at 37°C for 10-15 minutes. The reaction was stopped by addition of 180µl of Tris/EDTA to the reaction mix (approximately 20mM final EDTA concentration).

Radioactive PCR of HisU probe using alpha-^{32}P dATP

Radioactive PCR was performed when small probes below 300 nucleotides were used as for Lichten´s recombination assay.

The HisU probe (163 nucleotides in length) was labelled in the presence of alpha-^{32}P dATP (10µCi/µl, 6000Ci/mmol,1.7µM; Amersham Biosciences AA0074) with VentR (exo-) thermostable DNA polymerase as follows:

Table 2: HisU PCR conditions

PCR reaction composition	Cycling
3µl 10x Buffer	1x 94°C 4min
3µl DCTP, dGTP, dTTP(40µM)	
3.6µl $MgCl_2$ (25mM)	94°C 1min
1µl HisU PCR product(25ng/µl)	10x 58°C 30sec
1.5µl Primer 1965/1966(10pmol/µl)	72°C 1min50sec
0.5µ ddH_2O	
16.5µl alpha-^{32}P dATP (1.7 µM)	1x 72°C 4min
0.9µl VentR	

Sephadex G-50 column purification of labelled probe

After the radioactive labelling of probe DNA, unincorporated nucleotides were removed by filtration through a G-50 sephadex column. Small nucleotides will enter into the pores of the sephadex and will be strongly retarded, while the large molecules (the probe) will elute straight out of the column not penetrating the matrix.

A stock of G-50 sephadex slurry was prepared by equilibrating 5g of G-50 sephadex in 100ml ddH_2O at 37°C for 2hours under gentle shaking. Subsequently, the sephadex slurry was washed twice with 100ml of ddH_2O to remove soluble resin and resuspended in 100ml of TE buffer pH 8.0 and autoclaved at 0.7bar for 15 – 20 minutes.

1ml syringes (B.Braun, Omnifix-F 0.01ml/1ml) mounted into 15ml falcon tubes, were used to prepare the G-50 Sephadex columns. The syringe was blocked at the bottom with autoclaved glass wool and was filled completely with G-50 sephadex slurry and centrifuged down at 1500 rpm for 2 minutes, the procedure was repeated until 2/3 to 3/4 of the syringe was filled.

The probe was added directly on top of the resin in a volume of 200µl and the column centrifuged down at 1500 rpm for 3 minutes in a new 15 ml falcon tube to collect the probe freed of unincorporated nucleotides.

Hybridization of labelled probe to DNA immobilized on the membrane

Unspecific binding sites were first blocked on the membrane prior to the hybridization of the probe to immobilized DNA. 50ml of prehybridization solution was pre-warmed to 50°C, and 1ml of a 10mg/ml salmon sperm DNA (Fluka/BioChemika, #31149) denatured by heating to 95°C for 7minutes and subsequently chilled on ice for 5minutes was added. The prehybridization was performed at 65°C for at least 5 hours. After prehybridization, the labelled probe

was added to 1ml of salmon sperm DNA (10mg/ml) and denatured at 95°C for 7minutes and subsequently chilled on ice for 5minutes. The denatured probe was then added to 40ml of pre-warmed (50°C) hybridization solution. The prehybridization solution was exchanged for the hybridization solution, and hybridization was performed for 20-24hours at 65°C while gentle shaking.

After hybridization, unspecifically bound probes were removed. The hybridization buffer was discarded and the membrane transferred into a large plastic tray and subjected to following washes while shaking: 5 minutes in 500 ml 2x SSPE and 0.5% SDS at RT, 20minutes in 500 ml 2x SSPE and 0.5%SDS at RT, 30minutes in 500 ml 0.2x SSPE and 0.5% SDS at RT, 30 minutes in 500ml 0.2xSSPE and 0.5% SDS at 65°C and 5 minutes in 500 ml 0.2x SSPE at RT. The 65°C wash step was omitted for short probe (HisU probe). The surplus of liquid was removed from the membrane by blotting off on a sheet of Whatman paper and the membrane was tightly wrapped into saran wrap paper for signal detection.

20x SSPE hybridization buffer pH 7.4

3M sodium chloride (Merck, #106404)

20mM EDTA pH 7.4

154.8mM di-sodium hydogen phosphate (Merck, #106586)

45.2mM sodium dihydrogen phosphate dihydrate (Merck #106342)

autoclaved

50x Denhardt´s

1% (w/v) Ficoll 400 (Fluka/BioChemika, #46324)

1% (w/v) PVP360 (Sigma-Aldrich, #PVP360)

1% (w/v) BSA (Fraction V) (Sigma-Aldrich, #A9647)

in dH_2O and stored at -20°C

Prehybridization solution

2 - 6 x SSPE (2x is default, 6x should be for probes <200nt)

1% (w/v) SDS (Merck, #113760)

5x Denhardt´s

freshly prepared and heated to 50°C

Hybridization solution

2 - 6 x SSPE (2x is default, 6x should be for probes <200nt)

1% (w/v) SDS (Merck, #113760)

5% (w/v) dextran sulphate 500 kDa (GE Healthcare/USB, #70796)

freshly prepared and heated to 50°C

Detection of radioactive signals from the membrane

Detection of radioactive signals on membranes from ^{32}P southern hybridizations was performed by exposure on storage phosphor screens (unmounted for general purpose, GE Healthcare/Molecular Dynamics, #63003486).

Before and after the exposure, the screens were erased by exposure to a high intensity light photo screen for 15 minutes (e.g, Storage phosphor screen eraser from BIO-RAD). The image generated on the phosphor screen was digitalized through a phosphor imager (Molecular Imager FX Pro Plus from BIO-RAD) using a scanning laser wavelength of 532 nm and a broad pass emission filter at 390 nm, and corresponding software (QuantityOne 4.6.1, BIO-RAD).

2.4 Protein protocols

2.4.1 TCA protein extracts of *S.cerevisiae*

About 5-10ml of yeast cells (4 x 10^7 cells/ml) were put directly into 15ml tube containing ice-cold 100% TCA (final concentration 20% (v/v) TCA) at the desired time points (optionally, cells from a complex medium for example YPD medium can be washed once with dH2O before adding TCA). The cells were then harvested by centrifugation at 4000rpm and 4°C for 5min. The resulting pellet was then resuspended in 1ml ice-cold 10% (v/v) TCA and transferred to a 1.5 ml eppendorf tube. The harvested cells can then either be frozen in liquid nitrogen and stored at -80°C or processed immediately.

The TCA fixed cells were resuspended in 200µl of cold 10% TCA and 200µl of acid-washed and baked glass beads (diameter 0.40-0.60mm; Sartorius BBI-8541701) was added for subsequent breakage of the cells on a Vibrax (IKA VIBRAX-VXR) at maximum speed at 4°C for 40minutes. The protein extract was transferred to a 1.5 ml eppendorf tube and stored on ice. The beads were subsequently washed 3-5 times with 200µl of 10% TCA and the extract and all washes were pooled in one vial.

The protein sample was spun down for 10minutes at 5000 rpm at 4°C in a microcentrifuge and resuspended in 100-200µl GSD loading buffer, neutralized by addition of 20-35µl of 1M Tris (AppliChem, #A1086). The protein sample was heated for 10min at 95°C and subsequently centrifuged for 10 min at 5000rpm before loading onto a SDS-Polyacrylamide gel. The protein extracts can be stored at -20°C.

Trichloroacetic acid (TCA),100% stock solution

100% (w/v) trichloroacetic acid (Sigma-Aldrich, #T9159)

dissolved in dH_2O and stored at 4°C

1x GSD protein loading buffer

50mM Tris/HCl pH 6.8

8M Urea (Amresco, #0378)

2-3% (w/v) SDS (Merck, #113760)

0.1mM EDTA (Titriplex, Merck, #108417)

2-3% (v/v) ß-mercaptoethanol (Sigma-Aldrich, #M3148)

0.03-0.1% bromophenol blue (Sigma-Aldrich, #B8026)

4-5% (v/v) glycerol (Sigma-Aldrich, #G7757)

stored at -20°C

2.4.2 SDS-Polyacrylamide gel electrophoresis

Proteins bind the detergent SDS to negatively loaded SDS protein complexes with a constant charge-to-mass ratio (1.4g SDS/g protein 1% SDS solutions). SDS denatures the proteins and prevents protein-to-protein interactions thereby allowing their separation by molecular weight in a polyacrylamide gel matrix.

The glass plates of the SDS-PAGE unit (Biorad, Mini Protean II) were cleaned with 70% ethanol and distilled water. The apparatus was assembled and the components of the separation gel were mixed (Table 3) and pipetted between the glass plates, leaving 1.5cm space for the stacking gel. The liquid was then overlaid with 96% ethanol until complete polymerization at room temperature and then removed. The remaining was removed with Whatman 3MM paper. The ingredients of the stacking gel were mixed (Table 4) and poured on top of the solid separating gel to completely fill the gel mould. A clean Teflon comb was then inserted without producing any air bubbles. After the stacking gel had completely solidified, the gel apparatus was transferred into the running tank and filled with 1xSDS running buffer. The comb was removed carefully and the slots

flushed with running buffer to remove any unpolymerized acrylamide. Boiled and centrifuged protein samples, as well as molecular weight protein markers were loaded.

The gels were run at 15V/cm gel for 1-3 hours depending both on the size of the protein to be detected as well as the percentage of the acrylamide gel.

Table 3: Composition of separating gels with different concentrations of polyacrylamide (for 2 Bio-Rad Mini-Protean gels).

Separating gel	**4%**	**6%**	**7%**	**8%**	**9%**	**10%**	**12%**	**15%**
dH_2O (ml)	6.8	6.45	6.10	5.75	5.40	5.05	4.35	3.30
AA/BA (ml) (3.3%C,40%T)	1.75	2.10	2.45	2.8	3.15	3.5	4.2	5.25
1M Tris/HCl (ml) pH 8.8	5.2	5.2	5.2	5.2	5.2	5.2	5.2	5.2
10% SDS (µl)	140	140	140	140	140	140	140	140
10% APS (µl)	100	100	100	100	100	100	100	100
TEMED (µl)	10	10	10	10	10	10	10	10
Approx.linear separation (kDa)	100-250	48-155	40-108	32-85	26-80	20-72	12-58	10-43

Table 4: composition of 10ml stacking gel (for 4 Bio-Rad Mini-Protean gels)

dH_2O (ml)	6.55
AA/BA (ml) (3.3%C,40%T)	1.0
0.5M Tris/HCl (ml) pH 6.8	2.5
10% SDS (µl)	
10% APS (µl)	100
TEMED (µl)	60
	9

Acrylamide/Bisacrylamide solution (29:1, 3.3%C), 40%T (Bio-Rad, #161-0146), stored at 4°C

10X SDS-PAGE running buffer

250mM Tris (AppliChem, #A1086)

1.9M Glycine (AppliChem, #A1067)

1% (w/v) SDS (Merck, #113760)

Store at room temperature

PageRuler Prestained Protein Ladder (Fermentas, #SM0671)

Ammonium persulphate, 10% stock solution

10% (w/v) ammonium persulphate (Sigma-Aldrich, #A3678)

stored at -20°C

TEMED, N,N,N,N-Tetramethylethylenediamine

(Sigma-Aldrich, #T9281), stored at 4°C

2.4.3 Western blot

Protein transfer on a membrane

After separation by SDS polyacrylamide gel electrophoresis, proteins were transferred onto a gel-sized sheet of PVDF membrane (Amersham Hybond-P, GE Healthcare, #RPN303F), for immuno-detection. The gel unit was disassembled and the stacking gel was removed. the transfer sandwich was assembled on the plastic support clamp in following order:

1x fibre pad pre-soaked in transfer buffer

2x sheets of 3MM whatman filter paper pre-soaked in transfer buffer

1x gel

1x methanol activated PVDF membrane

2x sheets of 3MM whatman filter paper pre-soaked in transfer buffer

1x fibre pad pre-soaked in transfer buffer

Air bubbles between gel and membrane were removed using a glass rod. The setup was inserted into the transfer apparatus (Mini Trans-Blot Cell, Bio-Rad), with the gel side oriented to the minus pole. The transfer unit was then filled with ice cold transfer buffer. A pre-cooled cooling unit (-20°C) was inserted and the transfer was performed at 100V for 1-2hours under buffer circulation (by using a stirring bar and a magnetic stirrer). Optionally, the protein transfer was verified by reversible protein staining using the red dye Ponceau S and destaining was performed in 1xTBS for several minutes.

Ponceau S solution

0.5% (w/v) Ponceau S 8 Sigma, #P-3504)

1% (v/v) Acetic acid (Merck, #100063)

prepared fresh every 3 month

5x Transfer buffer

125mM Tris (AppliChem, #A1086)

0.95M Glycine (AppliChem, #1067)

1x Transfer buffer was freshly prepared with 10-20% (v/v) methanol (NEUBER, #441992).

Antibody incubation of the membrane

After the blocking of non-specific epitopes contained on the membrane by incubation with non-fat dry milk for 20-60mn at room temperature while gentle agitated, the blot was incubated in blocking buffer diluted primary antibody for 90minutes at room temperature or overnight at 4°C on a belly dancer. After incubation with the primary antibody, the blot was washed 3 times for 10minutes each with fresh blocking buffer. The secondary antibody was then diluted in blocking buffer and applied for 60-90minutes at room temperature. The blot was then washed 3 times for 10minutes each in 1x TBS-T (or with dH2O). The blot can be detected immediately or stored in 1x TBS-T at 4°C for a few days.

10x TBS (Tris buffered saline) pH 7,5

100mM Tris (AppliChem, #A1086)

1.5M sodium chloride (Merck, #106404)

pH 7.5 with HCl (Merck, #100319)

1x TBS-Tween

1xTBS

0.1% (v/v) Tween 20 (Sigma-Aldrich, #P1379)

freshly prepared

Blocking solution

3-5% (w/v) non-fat dry milk powder (Fixmilch Instant, fat<1.5%, Maresi)

in 1x TBS-Tween

Immunodetection of proteins

proteins bound to the membrane were detected using secondary antibodies coupled with horseradish peroxidase (HRP)-conjugated (see Appendix) and subsequently visualized by application of the „Enhanced Chemi-Luminescence (ECL) Advanced Western Blotting Reagents (GE Healthcare, #RPN2132). The visualization is catalyzed by HRP by the chemiluminescent turnover of a supplied substrate.

The detection procedure was carried out as suggested by the manufacturer. The volume of detection reagent used was 2ml ECL Plus solution for a mini-gel sized membrane (freshly prepared by mixing ECL Plus solution A and Solution B in a ratio of 40:1, kept protected from light, mixed by vortexing and used immediately). The blot was incubated for 5minutes at room temperature and excess detection reagent was removed (optionally by blotting off between two sheets of whatmam paper) and the membrane was wrapped protein side facing upwards into a fresh piece of Saran Wrap. The blot was then transferred into a film cassette and X-ray films (Fuji Medical X-Ray Film 100NIF (13x18cm), FujiFilm Super HR-E30) were exposed for different time interval to the light generated by the ECL process.

Stripping of antibodies from PVDF membranes

To remove primary and secondary antibodies from Western blots that had already been detected, the blot was washed 3 times for 10 minutes each in 1x TBS-T at room temperature while shaking (do not skip this step). The blot was then incubated in stripping solution for 20-45minutes at 70°C under shaking conditions. The blot was then washed 3 times in 1x TBS-T for 10minutes each and any unspecific antibody sites were again blocked with Blocking Buffer for 20-60minutes at room temperature. The blot is now ready for a new antibody detection.

Stripping solution

0.7% (v/v) ß-mercaptoethanol (Sigma-Aldrich, #M3148)

2% (w/v) SDS (Merck, #113760)

62.5 mM Tris/HCl pH 6.8

2. 5 Chromatin Immunoprecipitation (ChIP)

2.5.1 ChIP procedure

This technique is used to identify the binding sites of specific proteins on the chromatin.

Yeast extract preparation

50ml of meiotic time course culture was sampled and incubated with formaldehyde (1% final concentration) for 30 minutes while shaking under a fume hood. The proteins-DNA cross-linking process was then stopped by adding glycine to a final concentration of 131mM and shaking for 5minutes. Cells were collected by centrifugation at 4000rpm for 4minutes and 4°C, then washed twice with ice cold 1xTBS and finally aliquoted in four 1.5ml screw-cap tubes, snap frozen in liquid nitrogen and stored at -80°C.

The cell pellet (10ml = 5x 10^8 cells) was resuspended in 400µl lysis buffer complete and 600µl of glass beads (diameter, 0.40-0.60 mm) was added, cells disruption was performed by placing the tube into the multibeads shocker (YASUI-KIKAI, Osaka, 2500rpm, 30sec ON and 30sec OFF, for 10minutes at 4°C). The breakage efficiency was monitored by phase contrast microscopy.

After breakage, a small hole was poked into the cap of the screw-cap tube, and the tube was placed in an inverted orientation into a 15ml falcon tube, the tube was then spun down at 4000rpm for 4minutes and 4°C, and the cell extract was transferred into a new 1.5ml eppendorf tube. To shear the chromatin, the cell extract was sonicated 5 times at 37% power for 25 seconds each.

After sonication, the yeast extract was centrifuged for 10min at maximum speed and 4°C and the supernatant (cell lysate) transferred to a new 1.5ml eppendorf tube, 20µl was removed to prepare whole cell extract (*WCE*), and kept at 4°C.

Chromatin Immunoprecipitation

200µl blocking buffer (supplied with Adem beads kit) was added into 15µl beads (Adem beads, #04240) and incubated at room temperature for 15minutes while gently agitated. The beads were washed 3 times with 400µl PBS/BSA (beads were fixed at the wall of the tube with the magnet). And finally resupended in 220µl of PBS/BSA, 80µl of primary antibody (e.g., anti-HA antibody for IP against the HA epitope) was added to the beads and incubated for at least 3hours or overnight at 4°C with constant rotation.

The antibody-bound beads were washed 3 times with 400µl (PBS/BSA) and resuspended with cell lysate; and subsequently incubated for 3 hours at 4°C with constant rotation. Beads were then washed; 3 times with 400µl washing buffer, 3 times with 400µl deoxycholate buffer and 1 time with 400µl TE.

Samples were spun down at 1000rpm for 10 seconds and the supernatant was discarded, 200µl of elution buffer was added and incubated at 65°C for 45 minutes under gently shaking. The tube was centrifuged at maximum speed for 1 minute and the supernatant transferred into a new 1.5ml eppendorf tube containing 200µl of TE/1%SDS. 380µl of TE/1%SDS was added to the WCE (20µl), and all samples were incubated overnight at 65°C to reverse the cross-linking.

DNA purification

3µl RNaseA (DNase free, Roche, #) was added to each sample and incubated at 37°C for 30-60 minutes. Then 8µl proteinase K (20mg/ml) was added and incubated for 1 hour at 55°C.

An equal volume of phenol/chloroform/isoamylalcohol (PCI) was added, vortexed briefly and spun down at maximum speed for 5 minutes and the upper phase was recovered carefully to avoid contamination from the interphase. An equal volume of chloroform/isoamylalcohol (24:1) was added to the upper phase, vortexed briefly and centrifuged at maximum speed for 5 minutes and the upper phase transferred to a new 1.5ml eppendorf tube. The recovered phase was supplemented with NaCl (final concentration, 200mM), 2 volumes of 96% ethanol and 2µl of 10mg/ml glycogen, vortexed briefly and incubated at -20°C for at least 30 minutes. The DNA was collected by centrifugation at maximum speed for 30 minutes and 4°C, washed twice with 70% ice-cold ethanol, dried, resuspended in 25µl ddH2O and stored at -20°C until analysed.

2.5.2 Real-Time PCR evaluation of ChIP samples

For real-time analysis of the precipitated DNA, different protocols and reagents are available.Because,it provides a wide dynamic range for monitoring the exponential amplification phase, we used the MESA Green (Eurogentec, #RT-SY2X-03+WOUFL) method. The instrument used was an iQ5 (Biorad).

For DNA quantification of a sample, the instrument needs a minimal series of 3 dilutions of a standard of known concentration and all measurements will be expressed relative to this standard. We used the DNA purified from the WCE as the standard. And in order to obtain meaningful results, ChIP was performed in parallel using the same conditions on cells lacking the tag (as negative control), because only the difference in signals between tagged and untagged is regarded as specific.

Quantitative Real-Time PCR was performed as follows:

A series of four 10-fold dilutions of the WCE sample (e.g., 1/30, 1/300, 1/3000, 1/30000) were prepared for the standard curve.

PCR mix per sample (25µl):

12.5µl MESA Green Mix

2.5µl Primer oligo mix (2µM)

2µl ddH_2O

8µl DNA sample (IP sample or WCE dilution)

IP sample was prepared by adding 0.8µl of IP sample into 7.8µl ddH_2O. One master mix was prepared for all samples per each primer pair and in duplicate. The master mix was first pipetted into the wells of an optical 96-well plate, followed by the DNA samples. A sealing film was placed over the 96-well plate to avoid evaporation and the plate was centrifuged for 1 minute at 500rpm and 4°C, and placed into the real-time thermocycler.

The qPCR was run with the following setting:

Cycle1:(1x)

Step 1: 94.0°C for 3min

Cycle 2:(40x)

Step1: 94.0°C for 15 sec

Step2: 60.0°C for 1min

Data collection and real-time analysis enabled

Step3: 72.0°C for 1min

Cycle 3:(1x)

Step1: 94.0°C for 1min

Cycle 4:(1x)

Step1: 60.0°C for 1min

Cycle 5:(71x)

Step 1: 60.0°C – 95.0°C for 30 sec

Increase set point temperature after cycle 2 by 0.5°C

Melting curve data collection and analysis enabled.

For data interpretation, the amount of chromatin immunoprecipitated relative to the standard curve established for the WCE samples and the fold enrichment obtained for the region of interest and the cold-spot region were evaluated.

2.5.3 ChIP hybridized into High resolution Microarray

DNA-chips (ChIP on chip)

The immunoprecipitated DNA was amplified, fragmented, labeled and hybridized to *S.cerevisiae* Affymetrix Tiling arrays having 25 bp oligo probes with an average probe overlap of 20 nucleotides (currently termed a 5 nucleotides resolution array). This method is used to determine protein-chromatin interactions in a genome wide scale.

Random PCR amplification

A PCR amplification step is required because the amount of immunoprecipitated DNA is very low (below the sensitivity range of the Nanodrop spectrophotometer, which is 2 ng/µl) to be directly detected by hybridization onto a DNA microarray chip.

Round A: Linear amplification

To introduce the consensus sequence into the immunoprecipitated DNA two rounds of linear amplification were performed using a random primer A which contains a consensus sequence at the 5´-end.

Primer A: GTTTCCCAGTCACGATCNNNNNNNNN

Setup:

7µl DNA IP (or 5µl for wce)

2µl Sequenase buffer 5x

1µl Primer A (40µM)

Reaction mix:

Prepare a reaction mix per sample as follows:

1µl Sequenase buffer 5x

1.5µl dNTPs (3mM)

0.75µl DTT (0.1M)

1.5µl BSA (500µg/ml)

0.3µl Sequenase

.....

Total volume = 5.05µl

Furthermore, dilute a sequenase sample as follows (1/4 dilution):

3.6µl sequenase dilution buffer

1.2µl sequenase

. .....

Total volume = 4.8µl

1	95°C	5 min	
2	98°C	20 sec	
3	40°C	30 sec	
4	50°C	30 sec	
5	72°C	3 min	go to step2 31x
6	72°C	7 min	
7	4°C	hold	

The setup mix was incubated at 94°C for 2 minutes, then at 10°C for 5minutes. During this period of time,the reaction mix (5.05µl) was added, followed by incubation at 37°C for 8 minutes, 94°C for 2 minutes, 10°C for 5 minutes. During the 10°C hold, 1.2µl of diluted sequenase was added and the reaction was incubated at 37°C for 8 minutes. Finally, 2µl Exo1 buffer and 1.75µl Exo1 were added and the reaction was incubated at 37°C for 20 minutes and then at 95°C for 5 minutes.

In order to proceed with the exponential amplification, sample was dissolved in ddH_2O for a final volume of 78µl (add 61.75µl).

Round B: Exponential amplification

The exponential amplification was performed in the presence of the consensus primer B which anneals with the consensus sequence introduced during round A.

78µl DNA (from round A)

10µl KOD-XL 10x buffer

1µl Primer B (100pmol/µl)

10µl dNTPs (2mM each)

1µl KOD-XL polymerase

.....

Total volume= 100µl

2.5µl of the amplification product were loaded onto a 1% agarose gel. The amplification product appeared as smear between 300-2000 bp with an average of 500-1000bp (the IP sample presented a broader smear than wce). The remaining sample was purified and concentrated to a volume of 42µl with the microcon columns (MILIPORE YM-100 6000rpm, 15 minutes at room temperature) and the total amount of DNA was estimated with the Nanodrop spectrophotometer. For microarray DNA hybridization, at least 5µg of amplified material is required, eventhough up to 7 to 10µg of DNA per sample can be used.

DNA fragmentation

In order to perform the microarry hybridization, the DNA must be fragmented to an average length of 50-100 bp. This was carried out using a DNAse treatment.

DNase setup:

2µl DNase I (1U/µl)

2µl One-phor-all-buffer plus (10x)

1.2µl CoCl2 (25mM)

8µl ddH_2O

Reaction mix:

40.75µl amplified DNA

2.9µl CoCl2 (25mM)

4.85µl One-phor-all-buffer plus (10x)

1.5µl DNase setup (added when the PCR block has reached 37°C)

37°C 2 minutes, 95°C 15 minutes

2.5µl of digested sample were loaded onto a 2% agarose gel which was run briefly (10-15 minutes). The procedure was repeated (by adding 1µl of DNaseI into the remaining DNase setup and then adding 1.5µl of DNase setup into the reaction mix), until the average fragment size was approximately 100 bp.

Fragmented DNA labelling

Once fragmented, the DNA was labelled at the 5´-ends by using terminal transferase and a biotinylated-N11-ddATP.

47.5µl fragmented DNA (from DNase treatment)

1µl Biotin-N11-ddATP (1nmol/µl, Perkin Elmer NEL 508)

12µl Terminal transferase buffer 5x

1µl Terminal transferase (Roche, #220582)

The reaction was incubated at 37°C during 1 hour

Affymetrix microarray DNA chip hybridization

Once the DNA was 5´-end labelled with Biotinylated ddATP, a hybridization cocktail was prepared as following:The number of microarrays to be hybridized was first equilibrated at room temperature during at least 15 minutes, and 250µl of 1x hybridization buffer were loaded into the microarray and prehybridized at

42°C for at least 15 minutes with constant rotation.During the prehybridization step, the following hybridization cocktail was prepared.

60µl labeled DNA

3.3µl Oligo B2 controls (3nM)

2µl Herring Sperm DNA (10mg/ml)

60µl SSPE 20X

10µl Triton-X 100 (0.1%) or

64.7µl ddH_2O

.....

200µl total volume

The mix was incubated at 99°C for 10minutes,then chilled on ice for 5 minutes and spun down at maximum speed during 5 minutes in order to precipitate insoluble particles. The prehybridization cocktail was removed and 200 µl of hybridization cocktail were loaded into the chip and hybridized at 42°C during 16 hours with constant rotation (80 rpm). On the next day, the hybridization cocktail was removed and kept at -20°C, as it can be rehybridized at least two times). The chip was filled with 250µl of washing bufferA and kept at room temperature until the washing step.

Microarray chips washing and staining procedure

The washing station requires two samples containing thje solution mix (SAPE). And one antibody amplification sample (Ab solution mix).

SAPE (for two microarrays):

1260µl 2 x staining buffer

1134µl dH_2O

108µl BSA

25.2µl SAPE (= Streptavidin/ R-phycoerythrin, 1mg/ml)

.....

2527.2µl total volume(split in 4 eppendorfs,light protected)

Antibody solution (for two microarrays):

630µl 2x staining buffer

560µl dH_2O

50µl BSA (50mg/ml)

12.6µl IgG (10mg/ml)

7.6µl vector (= biotinylated anti-streptavidin, 0.5mg/ml)

.....

1260.2µl total volume (split in two eppendorfs)

Table 5: Fluidic station protocol for washing *S.cerevisiae* 1.0R Tiling arrays

The washing protocol used is called EuKGE-WS2v5 and was performed on the Affymetrix Fluidic station 450.

Automated steps performed into the fluidic station 450	EuKGE-WS2v5 protocol
Post Hyb Wash #1	10 cycles of 2 mixes/cycle with Wash buffer A at 30°C
Post Hyb Wash #1	6 cycles of 15 mixes/cycle with Wash buffer B at 50°C
Stain	Stain the probe array for 10minutes in SAPE at 35°C
Post Stain Wash	10 cycles of 4 mixes/cycle with Wash buffer A at 30°C
2nd Stain	Stain the probe array for 5minutes in antibody solution at 35°C
3rd Stain	Stain the probe array for 5minutes in SAPE at 35°C
Final Wash	15 cycles of 4 mixes/cycle with Wash buffer A at 35°C. The holding temperature is 25°C
Holding buffer	Buffer A loaded in the final was his kept for scanning

Microarray chips scanning

The hybridized microarray DNA chips were scanned using the GeneChip scanner 3000 TG controlled by GeneChip Operating Software (GCOS). The scanning was performed as indicated in the Affymetrix instruction manual (Affymetrix, 2005-2006).

2.6 Cytological Methods

2.6.1 DAPI staining of yeast chromatin

DAPI (4´,6-diamidino-2-phenylindole) is a fluorescent dye, binds specifically to DNA. The excitation maximum of the DAPI-DNA complex is at 364nm and the emission maximum is at 454nm.

To stain the chromatin of whole yeast cells, 100ul of liquid sporulation culture was sampled into 500ul of 96% ethanol. The cells were then centrifuged

at maximum speed for 30 sec, after completely discarding the supernatant, the cells pellet was resuspended in 25ul of DAPI working solution and the resulting suspension was sonicated for 1sec at lower power. The cells were ready for fluoroscence microscope analysis. To monitor the cells progress through the meiotic program during a time course experiment, the fraction of mono-, bi- and tetranucleated cells was counted (n= 100 cells) at indicated time points.

DAPI stock solution

1mg/ml DAPI (Sigma-Aldrich, #D9542)

in dH_2O, stored light protected, frozen at -20°C

DAPI working solution

0.2µg/ml DAPI (Sigma-Aldrich, #D9542)

in dH_2O, stored light protected at +4°C

2.6.2 Spreading and Immunostaining of yeast nuclei

Spreading of yeast nuclei

Yeast nuclei were spread on glass-slides and subsequently stained with the appropriate antibodies to visualize chromatin-associated proteins.

A 1ml aliquot of the sporulating culture was harvested per time point. The cells were pelleted by centrifugation at 6000rpm for 3min and resuspended in 100µl of Digestion Mix. This suspension was incubated at 37°C for 10-25mn. The efficiency of the cell wall digest was checked periodically by phase contrast microscopy by mixing an 5µl aliquot of the sample with 5µl of 1% Sarcosyl solution. Upon addition of Sarcosyl solution, completely digested cells should

burst open and release the nucleus. First check was after 10 min and this check was repeated at 5 minute intervals afterwards until at least 95% of the spheroplasts lysed upon contact with Sarcosyl.

The digest was stopped by placing the sample on ice. For the spreading procedure, 10µl of the digested cells were pipetted on a glass slide placed on an even surface and 100µl of the spreading solution was gently pipetted directly on top of the spheroplasts droplet and the resulting puddle was left to dry for at least 2hours at room temperature. The spreads were frozen at -80°C or used immediately for immunostaining.

Immunostaining of spreads

The glass slides were either first thawed at room temperature (slides from -80°C) or if fresh placed directly in 1x PBS for 5-10minutes to wash away the existing sucrose layer. Unspecific antibody binding epitopes were blocked by incubation of the slide with 50µl of Blocking Buffer under a coverslip for 15-30minutes in a moist chamber. The glass cover slip and excess Blocking buffer were rinsed off and 30µl of the primary antibody diluted in blocking buffer was applied to the slide on a coverslip. The slide was transferred into a moist chamber and incubated for either 2-3hours at 30°C or at 4°C overnight.

The cover slip was rinsed off carefully with 1xPBS and the slide placed into a cuvette containing 1xPBS for 10minutes to wash away excess primary antibody. Then, 30µl of the secondary antibody dilution in blocking buffer was applied to the glass slide on a coverslip and incubated for another 2hours in a moist chamber at 30°C.

The coverslip was rinsed off and the slide washed in 1xPBS for 10minutes. 5µl of Vectashield DAPI solution was applied to the slide on a coverslip to stain the chromatin and protect the fluorescent dyes coupled to the secondary antibodies from fading. The immunostained spreads could now be directly evaluated using a fluorescence microscope or stored frozen at -80°C or –20°C.

Solution 1

1M D(-)-Sorbitol (sorbitol extrapure, Merck, #1.07758) in DMEM

filter sterilized and stored at +4°C

Zymolyase 100T Stock

10 mg/ml Zymolyase (Seikagaku, #120493) in 1M Sorbitol

stored at -20°C (Not filter sterilized)

Digestion Mix

100µl Solution 1

2µl 0.5M DTT (Dithiothreitol, Sigma, #D-9779) in distilled water

2µl Zymolyase 100T Stock

freshly prepared

Sarcosyl solution

1.0% (w/v) N-lauroyl-sarcosine (Sigma, #L-5125) in distilled H_2O

Fixative solution

2.95% (w/v) Sucrose (Merck, #107687)

3.75% (w/v) Paraformaldehyde (Merck, #104005)

Store in the dark at +4°C.

Paraformaldehyde was liquefied at 65-75°C for 4-6hours under shaking. The sucrose was added and the solution filter sterilized (optionally a small drop

of NaOH can be added if after 4-6hrs the paraformaldehyde is not completely dissolved).

Spreading solution

30µl Fixative solution

18µl1% (v/v) Lipsol(LIP., Tel.(0274)593411) in ddH_2O

2-4µl 1% Sarcosyl solution

prepared fresh and kept on ice

Blocking buffer

0.5% (w/v) Bovine Serum Albumin, fraction V (Sigma, #A9647)

0.2% (w/v) Gelatin (Sigma-Aldrich, #G7041-100G)

dissolve in 1x PBS pH 7.25 and store frozen at -20°C; cannot be filter sterilized.

Vectashield DAPI Solution

Vectashield antifade buffer (Vector Laboratories, Sigma-Aldrich, #H1200) 0.3-0.5µg/ml DAPI (stored at +4°C)

10x PBS (Phosphate buffered saline, pH 7.25)

1.3M Sodium chloride (Merck, #106404)

70mM di-sodium hydrogen phosphate (Merck, #106586)

30mM sodiumdihydrogen phosphate dihydrate (Merck, #106342)

Autoclaved

2.6.3 In situ immunostaining of whole yeast cell

This method is used to identify the cellular localization of specific proteins. 300-500µl of 37% formaldehyde (Merck, #104003) was added to a 3-5ml aliquot of cell culture, mixed well, left for 5minutes at room temperature and finally stored at 4°C for up to five days. The cells were harvested by centrifugation for 3minutes at 3000rpm and the pellet washed twice with 1ml buffer I and once with 1ml of buffer II. The digestion of the cell walls was carried out in a digestion mix consisting of 145µl Buffer II + 35µl 0.5M DTT (Sigma-Aldrich, #D9779) + 17µl Zymolyase 20T (Seikagaku, #120491) for 10-25minutes at 37°C. The digest was verified by phase contrast microscopy and was stopped by placing the cells on ice when at least 95% of the cells lost their bright refractive halo. Optionally, spheroplasted cells were washed again twice with buffer II and resuspended in 100µl of buffer II.

10-well containing slides were first coated with 0.1% (w/v) polylysine (poly-L-lysine, Sigma, #P8920) dissolved in dH2O. This is necessary, as the spheroplasts would normally not adhere to the blank glass surface. 5µl of polylysine was added to each well to be used and incubated for 5minutes at room temperature. The remaining liquid polylysine was then carefully aspirated off and the slide was left to dry for at least 5minutes at room temperature.

About 3-5µl of spheroplasts was transferred into the polylysine treated wells and the slides were incubated for 6-10minutes in a moist-chamber, allowing the cells to settle. During the procedure drying out of the cells was avoided. The cells were dehydrated by plunging the slides into a cuvette containing -20°C cold methanol (Neuber, #441992) for 3minutes and subsequently into -20°C cold acetone (Merck, #100014) for 10seconds. To avoid the contamination of wells below, the slides were placed into the cuvette in an angle, with the cell carrying side facing downwards.

The slide was removed and put onto a workbench face up until the acetone was evaporated away. 15µl of blocking buffer was pipetted into each well to block unspecific antibody binding epitopes and the slide was incubated in a moist chamber for 10-20minutes at room temperature. The coverslip was gently rinsed off by placing the slide in 1xPBS, 3-7µl of the primary antibody solution diluted in blocking buffer was added to the wells and the slide was incubated for 2-3 hours at 30°C or alternatively at 4°C overnight in a moist chamber.

Afterwards, the coverslip was rinsed off and the slides were placed in 1xPBS for 10minutes while gently agitated and 3-7µl of the secondary antibody was applied and incubated in a moist chamber for 2-3 hours at 30°C.

The slides were then placed again in 1XPBS for 10minutes while gently agitated. Afterwards, the cells were mounted in a drop of vectashield DAPI solution to stain the chromatin and to protect the fluorescent dyes coupled to the secondary antibodies from fading. The cells were ready for fluorescence microscope analysis. Long-term storage of immunostained slides can be achieved at -80°C (or –20°C).

Buffer I (0.1M potassium phosphate pH 6.4)

27.8mM di-Potassium hydrogen phosphate trihydrate

(Merck, #105099)

72.2mM Potassium dihydrogen phosphate (Merck, #104873)

0.5mM Magnesium chloride (Merck, #105833)

(do not need to filter-sterilize)

Buffer II (0.1M potassium phosphate pH 7.4)

1.2M Sorbitol (Merck, #107758)

80.2mM di-Potassium hydrogen phosphate trihydrate

(Merck, #105099)

19.8mM Potassium dihydrogen phosphate (Merck, #104873)

0.5mM Magnesium chloride (Merck, #105833)

Blocking buffer

0.5% (w/v) Bovine serum albumin, fraction V (Sigma,#A9647)

0.2% (w/v) Gelatin, from cold water fish skin (Sigma, #G7041-100G)

in 1x PBS pH 7.25

do not filter sterilize, stored at -20°C

2.6.4 Microscopy technique

A Zeiss Axioskop epifluorescence microscope equipped with single band pass filters for the excitation of blue (DAPI), red (CY3) and green (both GFP and FITC) and a 100W mercury lamp with an Attoarc regulator was used to carry out cytological analysis of yeast chromatin. The magnified images were obtained while employing a cooled digital black and white CCD camera (Photometrics CH250A).

The acquisition of pictures was controlled by the IPLab 3.0 software (Signal Analytics) and the resulting black and white pictures were then transformed into multi-channel false colour pictures using the IPLab 3.0 software. All images were captured using a 100x objective and a 2.5x eye piece magnification unless otherwise noted.

2.7 Generating a Sk1/BY hybrid library

In order to identify new genes required for chromosome synapsis, we have performed a genome-wide screen in SK1/BY hybrid background. A start-to stop-codon deletion of most non-essential (4800) ORFs in the yeast genome was carried out in BY strain (Winzeler et al., 1999b).

Because BY strains do not sporulate synchronously, a screening strategy that includes bulk mating of the BY haploid deletion collection to a rapidly sporulates SK1 strain background that carries the genetic markers required for further selection and to monitor chromosome morphology (query strain) was developed.

2.7.1 Screening strategy

A diploid SK1/BY hybrid strain, heterozygous of the deletion of interest, was generated by mating of the BY Matalpha haploid that carries the deletion of the gene of interest to a Mata SK1 query strain that carries several markers (HO::HIS3, ste4^{ts}::LYS2, cyh2) needed for the selection of homozygous diploid of the desired genotype. The query strain carries in addition the meiosis-specific cohesin subunit Rec8 tagged at its C-terminal end with 3xHA epitope (REC8-HA3::ura3::LEU2, URA3) to visualize chromosomes axes (Figure 5).

Mating and selection of the heterozygous diploid

The SK1 query strain was incubated on YPD plate at 35°C for 3-4 days. 30mg of query strain cells were dissolved in 50ml of the mating medium (SM + 12% YPD) pre-warmed to 35°C (query strain suspension). 155µl of query strain suspension were pipetted into a new 96-well microtiter plate using a 12 channel pipette and 6.4µl of each candidates (from a BY haploid deletion collection) were added on its corresponding well and mixed thoroughly by pipetting up and down. The mating mix was incubated successively at 20°C and 25°C for two days each.

For selection of the heterozygous hybrid diploid, 4µl of the mating suspension were transferred into 160µl of a freshly prepared SM medium supplemented with G418 at a final concentration of 500µg/ml. The plate was incubated at 30°C for 24hours. The selection procedure was repeated 3 times.

Sporulation of heterozygous hybrid diploids

After the selection, 5µl of heterozygous hybrid diploid were transferred into 160µl of pre-sporulation medium (GNA medium) and incubated at 30°C for 24 hours. 10µl of cells suspension from the pre-sporulation medium were pipetted into 150µl of sporulation medium (SPM medium) supplemented with amino acid

mix (320µl amino acid mix/100 ml SPM medium) and 1%PPG (100µl of 1%PPG/100ml SPM medium). The plate was incubated at 30°C for 5-7 days while shaking (200rpm).

Selection against unsporulated diploids and for correct segregated markers

After sporulation, unsporulated vegetative cells were killed by ether treatment. 100µl of the sporulation culture were pipetted into a 1.2ml 96-well glass plate (Grace Vydac) and 400µl of Diethyl ether were added. The plate was tightly sealed and incubated at room temperature while shaking for 25minutes and under the fume hood. After ether killing, 70µl of cells suspension were carefully transferred into a new microtiter plate containing 200µl of SM medium pre-warmed to 35°C and supplemented with G418 (at a final concentration of 500µg/ml) and cycloheximide (at a final concentration of 3µg/ml): (SM+G418 +Cycloheximide medium).

The plate was incubated at 35°C with open lid for 20minutes and overnight with closed lid. On the next day, 4µl of cells were transferred into 200µl of SM+G418+Cycloheximede medium freshly prepared and pre-warmed to 35°C. The plate was then incubated for 2 days at 35°C.

Generation of homozygous hybrid diploids

Cells were stamped from the selection medium (SM+ G418 + cycloheximide) onto YPD plate supplemented with G418 and were allowed to mate at 20°C for 2 days and at 25°C for another 2 days. Homozygous hybrid diploids cells were finally stamped onto YPG plate and incubated at 30°C for 2-3 days to select against respiratory deficient cells. Cells were ready for cytology, the analysis was carried out immediately or within 10days.

3 RESULTS

3.1 Primary screen: SK1/BY hybrid mutants

Chromosome pairing culminates by the formation of a proteinaceous structure called synaptonemal complex (SC); the SC is morphologically conserved across a wide variety of species (von Wettstein et al., 1984) and it is thought that the SC may control the distribution of crossovers along and between chromosomes and may ensures wild type levels of crossing over (Zickler and Kleckner, 1999). In addition it may serve to avoid entangling of chromosomes during the homology search period (Zickler and Kleckner, 1999; Storlazzi et al., 2010b). The so called ZMM proteins (Zip1, 2, 3, 4, Spo16, Msh4, 5, Mer3) are defined by showing a specific defect in both SC and crossover formation, reviewed in (Page and Hawley, 2004), suggesting, but not proving, that full SC is required for wild type level of crossover formation. The molecular mechanism of SC formation is not fully understood, but at the start of this work it was recognized that some of the ZMM proteins interact to form a SUMO (or Ubiquitin) E3-ligase (Chen et al., 2004; Perry et al., 2005b). Also, the function of the SC is not fully understood. It became clear through the phenotype of synapsis mutants, that synapsis defects often don't produce spore lethality. Therefore spore lethality based genetic screens may have failed to discover parts of the synapsis pathway. In order to contribute to a better understanding of this process of chromosome synapsis, we set out to perform a systematic cytological screen to evaluate the role of all non-essential genes for meiotic SC-formation in *Saccharomyces cerevisiae*, based on the yeast gene deletion library (Winzeler et al., 1999a).

In the yeast gene deletion library almost all non-essential open reading frames (ORFs) of *Saccharomyces cerevisiae* have been deleted and replaced by the kanamycin cassette KanMX4, that confers resistance to the eukaryote specific antibiotic geneticin (G418) in the BY strain background. Unfortunately, the BY strain background is not suitable to study meiosis, because cells sporulate slowly, asynchronously and inefficiently. Only about 50% of asci can be

recovered after 5 days of sporulation under optimal conditions. Therefore the screening strategy involves crossing of all 4.800 mutants of the collection to the well sporulating SK1 background. The screen was then performed in SK1/BY hybrids homozygous for the desired mutation. The technical details of this operation was developed in the lab by a number of previous lab members (Marc Berlinger, Martin Xaver and Alexander Woglar) with the most critical contributions from A. Woglar, who also provided a proof of principle (A. Woglar, master Thesis 2008).

The resulting diploids (each homozygous for a different deletion) were individually synchronized for meiosis and subjected to hypotonic surface spreading (Loidl et al., 1998). The SC-phenotype was then scored under the fluorescence microscope after immunostaining for a synapsis-specific protein (Zip1) and for a protein of the chromosome axis (Rec8-HA3). The technical details of how we obtained diploid hybrid strains homozygous for the desired mutations and for the procedure of synchronization, spreading and staining are described in the Method section. Of the 4800 non-essential ORFs, 3630 have been screened and analyzed within this work. For each candidate, 50 Rec8 positive nuclei were evaluated and classified according to the extent of Zip1 polymerization between homologous axes (and Method section).

Details on the synapsis phentotypes of all 3630 candidates are available as a filemaker database, however here we will concentrate on the categories comprising mutants strongly defective in chromosome synapsis or entry into the meiotic program.

3.1.1 Candidates unable to induce meiosis

We classified candidates as unable to undergo meiosis, if both meiosis specific marker proteins, Rec8 and Zip1, were found nearly absent on nuclear spreads at 6 hours in SPM. Such mutants produced >90% empty nuclei, with a few percent showing unorganized staining or very weak foci. By this criterion, 132/3630 deletions screened did not undergo meiosis (Table 6, Figure 6A).

The largest group of genes required to undergo meiosis was genes involved in aerobic respiration (39 ORFs, 30% of identified ORFs) and/or are located in the mitochondrium (Figure 6A). This is expected, as aerobic respiration is known to be important for meiosis and sporulation (Simchen et al., 1972; Treinin and Simchen, 1993; Jambhekar and Amon, 2008). These studies suggest that respiration acts at multiple levels, but also that a respiration sensing pathway may exist that downregulates meiosis in the absence of respiration. The precise mechanism, how respiration and mitochondrial function impinge on meiotic induction is not understood. So this may be the first comprehensive list of genes, required for both, normal respiration and induction of meiosis. It is important to note here, that also other strongly defective mutant categories, such as Only Zip1 foci contain a large fraction of mitochondrial/respiratory mutations. Thus, different mutations of this class cause phenotypes with gradually differing severity.

Our assignment of ORFs to the group mitochondrial/respiratory was performed manually, on the basis of biological process description and of the protein localization description of the SGD (http://www.yeastgenome.org). GO terms were usually found to be too specific and insufficiently curated, to use them for grouping. For example 61 genes possess the GO term aerobic respiration, 12 genes the term mitochondrial electron transport and 321 the term mitochondrium as manually curated cellular component. Against expectation, only 7 out of the 12 genes listed for mitochondrial electron transport are also part of aerobic respiration. But even more surprisingly, none of the 12 is listed with cellular component mitochondrium. Therefore, we chose to make our own GO term list, based on text description, and on whether mitochondrial localization or

respiratory functions are mentioned in the gene-descriptions. In the absence of a precise number of genes involved in respiration we can't estimate precisely the fraction that is also required for meiosis. However, of the 39 genes we defined as mitochondrial/respiratory mutants only 4 have the GO term aerobic respiration or mitochondrial electron transport (together 66 entries), this is 4/66 (6%). This suggests that 90% of the mutations with these GO terms had initiated meiosis (based on the analysis of 75% of the non-essential genes). On the other extreme, 34 of the 39 (87%) genes identified in our screen have the GO term mitochondrium – as high throughput cellular component (915 entries). This means, only 34/915 (3.7%) of proteins tentatively localized to mitochondria are meiosis deficient. These preliminary results show that only a small set of mitochondrial/respiratory functions are essential for meiotic induction in the BY/SK1 hybrid background. Another set, in the next category, is at least severely compromised with the formation of meiosis specific chromosome structures.

The second largest group (23 genes, 17% of identified candidates) are mutants affecting metabolism (metabolic pathways, ribosome biogenesis, autophagy, Table 6, Figure 6A). Not surprisingly, these processes are involved in meiotic induction. Among the metabolic pathways that affect meiotic induction are nitrogen metabolism and uptake, acetate uptake, gluconeogenesis, nutrient sensing and others. 7 mutants involved either in ribosome biogenesis or in control of protein synthesis with a location at the ribosome, were identified. This small number suggests that also for this category only a small, specific set of genes is essential for meiotic induction. Only 2 genes required for autophagy were identified in this category (**in the first 75% of the screen)**, even though autophagy is an important aspect of meiosis. Meiosis is a response to starvation in yeast and therefore requires autophagy and extensive recycling of cellular components. Some of these functions are linked with the vacuole and the Golgi, which are in the third largest category, detected.

The third largest group (20 genes, 15% of identified candidates) are deleted for proteins associated with the Golgi apparatus, the ER, the vacuole or the plasmamembrane (Table 6, Figure 6A). In general, we believe that these mutants

are defective in either catabolic activities (e.g. vacuole) or anabolic activities (e.g. ER), which are necessary for the major metabolic transitions between mitotic and meiotic states. Transmembrane ATPases or the regulation thereof hint at processes to generate energy by generating gradients across membranes. Certainly, meiosis and spore formation is a very energy consuming process, especially difficult to carry out under starvation conditions.

Dubious and uncharacterized ORFs together make 17 (13%) of the candidates (Table 6, Figure 6A). Completely uncharacterizd ORFs is a class that is shrinking rapidly. We believe that it is not absolutely necessary to produce a protein in order to affect meiotic induction. ncRNA may play important regulatory roles, that could be uncovered by deleting these dubious ORFs. Because diverse biological processes are required for meiotic induction, it is impossible to predict, in which of those processes the newly characterized ORFs are exactly involved. However, the phenotype – no meiotic induction – is certainly a strong, robust phenotype. If confirmed by a second method, this may constitute the first strong phenotype for these mutants.

A small group of mutants hints at the role of the cytoskeleton for meiotic induction, presenting mutants involved in karyogamy (not surprising, as karyogamy should be a prerequisite for meiosis), in spindle positioning and actin bundling (Table 6, Figure 6A). The role of pseudohyphae formation (1 mutant) is less obvious and might be considered preliminary.

We identified the most important positive regulators of meiotic induction, Ime1, Ime2 and Ume6 in our screen (Table 6, Figure 6A). In addition we also found the known meiotic regulator Snf1, thus reidentifying 4 known inducers of the meiotic transcriptional program. Another group of genes known to be involved in DNA metabolism or repair (9, 7%) is somewhat suspicious. Genes like Sgs1, Pph3, Bre1 are known to undergo meiosis in the SK1 background, although being strongly defective. It is therefore likely that the very sensitive BY/SK1 background is responsible for this possible overestimation of their phenotype. Clearly, however, these mutants are strongly defective in meiosis, but if any of

them do indeed not enter the meiotic program can only be determined in a pure SK1 background.

Another 7 genes (5%) are involved in RNA metabolism/transcription. Their roles might be to assist in promoting the transcriptional changes during meiotic differentiation. One gene detected is involved in salt stress. Hsp82, a very abundant chaperone, seems required for meiotic induction.

Two mutations are listed as false positives. Deletion of the mating factor should have caused them to drop out during selection. A failure to sporulate might be due to the presence of largely haploid cells in these cultures. It is unclear, why the *gal4*Δ mutant did not undergo meiosis. The presence of at least some false positives stresses the importance of repeating the results in an independent experiment, before drawing final conclusions. Also, any experimental failure could cause an occasional drop out and prevent sporulation of a culture. The following chapters describe phenotypes that are better internally controlled, because Zip1 figures were taken only from Rec8 positive cells. However, because our primary goal was to identify synapsis mutants, we did not follow up and confirm all the meiosis induction mutants. These results therefore remain preliminary until final confirmation.

3.1.2 Candidates displaying Zip1 foci and/or polycomplexes, but no elongated synaptic stretches

Mutants of this category did initiate the meiotic program and expressed Zip1 and Rec8 in at least a subset of cells. However, at the analyzed time point (6 hours in SPM) no continuous stretches of synapsis were detected in 50 Rec8 positive spreads. Instead a dot-like pattern of Zip1 staining termed foci and/or Zip1 aggregate (s) called polycomplexes (PCs) were observed. Polycomplexes occur by self-assembly of Zip1, which is expressed faster than it can be incorporated into synapsing chromosomes. Most mutants with defective synapsis show increased numbers of PCs. 90 of the 3630 ORFs screened exhibit this phenotype (Table 7 Figure 6B)

We have identified in this category 9 of 12 genes, the deletion of which was previously described to be essential for DSB formation. 2 of these (Mer1 and Nam8) are required for the correct splicing of transcripts of DSB promoting genes, such as for the Mer2 transcript. 2 of the known DSB essential genes were missed (Mei4, Xrs2 and Ski8, the latter appearing in the short Zip1 stretches category). The *mei4*Δ repeatedly gave rise to synapsed chromosomes suggesting that the mutants were either wrongly assigned, contaminated with *MEI4* wild type or inefficiently deleted. Absence of Ski8 may cause a milder phenotype in BY strains than in SK1. 9 more candidates were identified that were previously described with strong synapsis defects. Of the non-essential axial element components, Rec8, Mek1 and Red1 were identified, while Hop1 was not included in the collection. While this observation on Rec8 and Red1 confirms reports of others (Rockmill and Roeder, 1990; Klein et al., 1999), that these factors are essential for synapsis, *mek1*Δ mutants have previously been shown to be able to produce partial synapsis (Rockmill and Roeder, 1991). To reconciliate the two findings, we have analyzed synapsis in *mek1*Δ in pure SK1 and found a maximum of 1% short stretches at 4 hours and 3% at 5 and 6 hours in SPM. This confirms a very strong, though not complete, requirement for Mek1

for synapsis in SK1. We attribute the slightly stronger phenotype to the SK1/BY hybrid background with its generally lower propensity to synapse.

Of the known ZMM pathway components, we identified Zip3 and Mer3 in this class, Zip1 and Zip2 are not included in the analyzed set yet, while Spo16 is in the short Zip1 stretches and Zip4, Msh4 are in the long stretches only category. Msh5 showed reduced SC formation (either >80% foci or >92% short SC).

Other mutants classified in the Zip1 foci category were those involved in meiotic DSB repair. 4 genes were identified: Dmc1 and its loading factor Mei5 (the other loading factor, Sae3, was not analyzed yet), Tid1(Rdh54) and Shu2 (subunit of the Shu complex, together with Shu1, Psy3 and Csm2). Of the other Shu complex subunits, Psy3 was analyzed in this screen and found defective (category long Zip1 stretches), while Shu1 did not show any synapsis phenotype. Csm2, however, was identified in the diploma work of A. Woglar as defective in synapsis. Shu2, Csm2 and Psy3 were still (partially) defective in synapsis when transferred to a pure SK1 genetic background. We presume that the phenotype in mutants defective in DSB repair may be more severe in the BY/SK1 hybrid background, than in pure SK1 or could represent a strong delay. Not detecting SC after 6 hours in SPM in the hybrid of course does not preclude later SC formation. In contrast to DSB formation, DSB repair is not essential for synapsis.

Besides these genes already associated with strong meiotic phenotypes, 11 genes were identified, previously associated with chromatin modification or DNA metabolism. 6 candidates are linked to chromatin modification, 2 to methylation (Rtf1, Cdc73 – both part of the paf1 transcription elongation complex, Paf1 not yet analyzed) 3 to acetylation (Ngg1, Ygl262w interact with SAGA), Ard1 interacts with Nat1 (which was categorized in short Zip1 stretches. 1 candidate is a histone deacetylase, Hst4. (Another deacetylase (Hst1) is in long Zip1 stretches). The other candidates are Rtt107, a mediator protein interacting also with Smc5/6 (not required for synapsis), Ubc13 (a ubiquitin E2 interacting with Mms2 – not analyzed), Apn1 (involved in apurinic repair and ROS (reactive

oxygen species) resistance), Ddr2 (induced in repair), Irc18 (controls mitotic Rad52 foci).

4 genes were identified that are linked to ubiquitin transfer, protein cleavage or protein degradation. Irc25 is a chaperone required for proteasome assembly, *YOL057* is a dipeptyl-peptidase, Ubp15 a ubiquitin isopeptidase and *YLR352* might be a putative novel F-box protein interacting with SCF-ubiquitin ligase.

Similar to the no meiotic induction class, also in Zip1 foci respiratory functions were abundantly identified with 10 candidates and ribosome biogenesis with 7 candidates. The mechanism of these genes might be related to those listed in no meiotic induction, except that they might be less severe. The meiotic program requires a lot of energy and new protein synthesis, and cells compromized in these general, basic functions may either not be able to express the meiotic program at all (no meiotic induction) or not fully (Zip1 foci). This is the most likely explanation, but of course more specific roles for selected candidates is possible. Similarly general roles are possible for the 4 candidates in Metabolism (sugar, nitrogen and lipid metabolism), Golgi/ER (3), Vacuole (3), Autophagy (1) and Membrane (3) classes. However, we expect more specific roles in genes involved in RNA metabolism (Mer1, Nam8 are essential for DSB formation through splicing Mer2 and other important RNAs), Cwc15, Npl3 have also roles in splicing of yet unknown substrates and Dcs1 does decapping of mRNAs.

Proteins involved in transcription may also regulate DSB formation, or may act through regulating important prophase genes. 1 transcription factor (Rtg1) and 2 repressors Maf1 and Rdr1 were found. 2 factors organizing the actin skeleton, Bag7 and Rom1, point at the role of actin for timely synapsis. 4 genes associated with various stress responses were found, such as Sip18, Ypr1, Hal5 and Aha1, the latter activating Hsp82, confirming the role of Hsp82, which is listed under no meiotic induction. Meiosis is carried out under stress conditions, but how exactly these genes contribute to successful meiosis is unclear. One protein, Dbf2, is localized in the nucleolus and is thought to control the activity

and sequestering of Cdc14 phosphatase there. Such mechanism also plays a role in meiosis, for instance in sequestering monopolins until the end of prophase I.

Here again, previously uncharacterized (8) or dubious (3) ORFs were identified. These are of special interest, if confirmed. 4 candidates seem quite unlikely to be real, based on previous characterization. Cts2 chitinase should only affect spore wall formation (however even in pure SK1 this gene was still partially defective in synapsis, see Appendix), His5, Gap1 and Prs5 should make their strains auxotrophic for aminoacids that were selected for. Ideally, they should have dropped out of the screen. Perhaps, in these strains, mating was defective.

3.1.3 Candidates exhibiting both, foci and short stretches of Zip1, but no long stretches of synapsis

In order to differentiate further between nuclei of different degree of synapsis, we defined 3 categories of nuclei containing synapsed chromosomes, short Zip1, long Zip1 and fully synapsed. The category short Zip1 comprises cells, where the total length of synapsis was estimated to be below 25% of a completely synapsed nucleus. The relatively low limit of 25% was chosen to have a strict criterium, which should reduce the number of false positives. Similarly strict, the border between long Zip1 and fully synapsed nuclei was chosen as 50% or at least 8 fully synapsed chromosomes. These definitions are rather conservative to avoid finding too many mutants with weak or borderline phenotypes (Table 8 Figure 6C).

102 candidates were classified as having short Zip1 stretches. These mutants include 7 well known factors previously characterized for their requirement for meiotic recombination and/or SC formation: Ski8/Rec103, Sae2/Com1, Hop2 (Mnd1 NA) and the 9-1-1 complex DNA damage sensors Mec3, Ddc1 (Rad17, Rad24 NA) (Table 8). Of the synapsis formation pathway

(ZMM), only Spo16 was categorized here and Rmr1, which was identified in a previous screen in the lab as being reduced for synapsis and COs (Jordan et al., 2007), while another potential ZMM mutation, *def1*∆ (Jordan et al., 2007) did not produce a phenotype here. The other ZMM mutations were more severe (Zip3, Mer3), not analyzed (Zip1, Zip2) or showed weaker phenotypes (Zip4, Msh4, Msh5).

We found 11 novel candidates annotated before as related to DNA repair (7) or histone modification/chromatin remodelling (4). Interestingly, we found Rad26, which is essential for TCR (transcription coupled repair) and is thought to work in combination with Def1 (previously found to be required for synapsis. The two factors are thought to mediate Pol II ubiquitination and degradation, perhaps to enable access for repair enzymes. Whether the role in synapsis is mediated through the control of ubiquitination or, whether TCR itself is required for synapsis will require further studies.

Another novel candidate is Rev7, an accessory subunit of DNA Pol-zeta, involved in translesion synthesis (TLS). However, Rev7s role in TLS seems not to be important, because the main TLS polymerase (Rev3) has no role in synapsis. However, Rev7 is known to interact with the 9-1-1 complex, whose deletions give the same phenotype as Rev7 mutants. Therefore, this result strengthens the importance of this interaction. Also the identification of AMP-deaminase Amd1 is an important novel finding. This protein is involved in DNA repair by its interaction with crucial kinases like Dbf2 (Zip1 foci) or Hrr25 and Rad53 (both essential, but known to be involved in various meiotic processes).

The other four DNA repair candidates were previously largely uncharacterized. Their role in repair was only inferred from large scale studies, such as being required for reducing Rad52 foci in mitosis (Irc4, Irc11) (Alvaro et al., 2007), for interacting with Rad9 (*YBR259W*, (Giaever et al., 2002)) or for being induced by MMS (*YPL068C*, (Lee et al., 2007)).

Of the 4 chromatin modification factors identified, 2 (Sds3, Sif2) comprize subunits of HDACs (histone deacetylase complexes), one (Sgf29) is a subunit of

a HAT (histone acetyl transferase) and one (Swc2) is a subunit of the Swr1 chromatin remodeling complex.

Sds3 is a component of the Rpd3p/Sin3p deacetylase complex (Rpd3, Sin3 NA), which deacetylates H3 and H4 and antagonizes different forms of transcriptional silencing. Sif2 is part of Set3C histone deacetylase complex (with Hst1, Hos2), which represses early/middle sporulation genes (Pijnappel et al., 2001). It is unlikely that this known role in repression of meiotic genes is responsible for synapsis. Interestingly, Sif2's partner Hst1, was found with almost the exact same phenotype, although falling into long Zip1 category, because of one single nucleus containing long Zip1 stretches. Hos2 did not show a defect, showing that not all subunits are of equal importance. Sgf29 is part of the HAT/Core module of several chromatin remodelling complexes, such as SAGA and SLIK (along with Gcn5 (NA), Ngg1 (Zip1 foci) and Ada2 (no phenotype)). The SAGA complex is implicated by a number of different hits such as (Cti6 (recruits SAGA to silenced chromatin, no meiotic induction), Ngg1 (SAGA-HAT core component, Zip1 foci), *YGL262W* (uncharacterized Sgf29 interacting protein, Zip1 foci), Rpd17 (SAGA-HAT core component, low SC). In summary, it seems likely that histone acetylation/deacetylation, or recognition of acetylated histones may have a direct role in DSB formation or synapsis.

Swc2 is part of a chromatin remodeling complex that exchanges H2AZ for H2A at damaged sites. This protein was analyzed in some detail for its discovered genetic interaction with Pph3 in chapter 3.4.3.

9 novel candidates representing 8 different activities in post translational modification were identified. Among them is a SUMO E3 (Siz2), thought to sumoylate telomeric Ku70/Ku80. Interestingly both its interactors were also identified, although in different categories (Ecm11 long Zip1 and Gis1 high SC). Another novel candidate, Lag2, negatively regulates the SCF (Liu et al., 2009), a ubiquitin E3. It prevents its activation by inhibiting neddylation of the cullin subunit Cdc53. The SCF is required for synapsis, as shown by meiotic specific knock down of Cdc53 (A. Shinohara, personal communication). In addition

Rad52 accumulates in mitotic *lag2*Δ mutants (Alvaro et al., 2007), suggesting accumulation of repair intermediates. Vps7 is a aspartic acid protease so far only implicated in Cell wall morphogenesis and now first implicated in meiotic SC formation. Sam2 is a S-adenosylmethionine and its product AdoMet is involved in the methylation of proteins. A differentially regulated isozyme (SAM1) did not produce a phenotype upon deletion. Last not least 2 Ser/Thr kinases were identified, Yak1 and Ksp1, which until now, also had been implicated in unrelated processes. Yak1 substrates, it regulates mRNA deadenylation, gave no phenotype, when analyzed (Table 8).

8 novel candidates were summarized in a somewhat heterogeneous group as affecting metabolism. Most interestingly, one candidate represents the only non-essential subunit of the proteasome, *PRE9*. It is the alpha 3 subunit of the 20S subcomplex, which apparently is not essential, because it can partially be replaced by the alpha 4 *(PRE6)* subunit. Given that we also identified Poc3 (Zip1 foci) and Poc4 (long Zip1), which are involved in proteasome assembly, and *ECM29* (>92% short SC, tethers 19S and 20S proteasome subunits) this makes a strong case for the importance of the proteasome in synapsis. In addition, we found a hitherto nearly uncharacterized ORF, *YDR179W-A*, which was reported to interact with Pup1, an essential Beta-SU of the proteasome. Taken together our results predict a prominent role of the proteasome in synapsis.

2 genes, *DLD3* and *ZWF1*, are somehow involved in energy metabolism. Importantly, Zwf1, a glucose-6-phosphate dehydrogenase, interacts with Dbf2 kinase (Zip1 foci), which is implicated in DNA repair and Cdc14 activation. 4 genes (including *ZWF1*) are all interfering with the use of nitrogen, but it is questionable, whether this is the reason for the SC defect (*DAL4, TRK1, UGA4*). Oxp1 is a 5-Oxoprolinase, which is required for making glutathione. Similar to the proteasome, also the glutathione metabolism was hit several times by our screen (*YCF1, GLO2* (*TRX1* interacting with *GLO2*), *GRX3*), pointing to the importance of glutathione and protection against oxidative stress for synapsis. Glutathione is important during oxidative stress and for the chemical detoxification of the cells. The last protein of this class is *FSH3*, a putative serine hydrolase.

3 genes known to mediate stress resistance and one novel ORF also implicated in stress resistance were identified in this category. Interestingly, *HYR1* and *YJL206C* mediate resistance to oxidative stress. This emphasizes the above results on the glutathione metabolism and may hint at important functions for ROS management during meiosis. One gene, *ATC1*, is involved in cationic stress response and another one, *HOT1*, in osmotic stress.

11 genes were found which are involved in RNA metabolism and/or transcription. Among the RNA metabolic proteins there is Ski8, a component of the pre-DSB complex that also interacts with Spo11. This mutant was actually expected in the Zip1 foci category. One mutant is defective for respiratory growth, *RSF1*, likely explaining its defect. One mutant highlights the role of the nuclear pore: Nup42. It is not the only nuclear pore component identified – also *NUP170* and *NUP60* as well as *SOY1*. At least Nup170 and Nup60 have been implicated in biological processes like chromosome segregation and DNA repair, in addition to mRNA transport across the pore.

For the genes involved in transcription it is always difficult to separate a role in regulating expression of meiotic genes from a more direct function, as for instance in DSB formation. Several components of RNA polymerase I were identified. *RPA49* (short Zip1), *RPA12* (>80% foci) and *RPA34* (weak SC formation), illustrating a role of this polymerase, which exclusively deals with rDNA transcription. We propose that it exerts its role via ribosome biogenesis, as we also identified 5 other genes in this class (short Zip1), annotated with roles in ribosomal biogenesis. Tup1 is a repressor, thought to be involved in establishing repressive heterochromatin marks via H3 and H4 modification. This could directly effect DSB formation. Swi6 is a TF proposed to regulate genes important for synapsis such as *RNR1*, *CLB5*, *RAD53*. *RDS1* and *ASG1* are Zinc cluster transcripton factors (like Gal4), which can bind DNA in a sequence specific manner.

9 genes are annotated with being required for respiration or mitochondria. The largest group affects the respiratory chain. Among this is, Pet122, a

translational activator for Cox3. Cox1, Cox2 and Cox3 are essential subunits of cytochrome C oxidase and thus not included in the screen. However, genes involved in their activation are discovered in various categories, emphasizing their importance in synapsis. This is further discussed in the next chapter (long Zip1). Pet122 acts together with Pet54 (Zip1 foci) and Pet494 (not analyzed). 4 other genes affect the respiratory chain, from the delivery of electrons (*GUT2*, glycerol-3-phosphate dehydrogenase) via Cox8 (subunit of cytochrome C oxidase) and *QCR7* (cytochrome reductase) to *ATP22* an activator of F1F0 ATP synthase. These results underscore that synapsis is a particularly strongly energy consuming process, which partially derails, or is delayed when ATP runs out. Recently it was shown that after pachytene release inhibition of F1F0 ATP synthase will not interrupt the divisions. This emphasizes that the truly hard and energy consuming part of meiosis in yeast is the identification and connection of homologs, including synapsis formation, while after that it just goes downhill.

SDH3 is Succinate dehydrogenase and required to feed the Krebs cycle. *MDM31* is required for stable mitochondrial inheritance, while *TRX3* is required for redox homeostasis.

5 candidates involved in Golgi/ER processes and 4 candidates affecting vacuolar processes underscore the importance of these organelles and are in line with similar numbers in the Zip1 foci and Long Zip1 categories.

One gene of the category cytoskeleton, *MLP2*, which is myosin-like, was linked to telomere tethering before. This suggests a role in chromosome movement, which is required for synapsis.

Of 3 candidates affecting the cell cycle Cdh1 probably is required for proper B cyclin degradation during the G1 phase preceding meiosis. Vhs2 has a role in G1/S transition and might affect premeiotic S-phase. Sfp1 has also been noted for a role in DNA damage response and might be the most interesting of these 3.

7 candidates are membrane associated, 2 mannoproteins and one mannosylphosphate transferase. These are 3 of a total of 9 genes representing either mannoproteins or mannosyl-metabolizing enzymes. Mannose has so far

been known for its role in the cell wall. The multiple hits in our survey suggest prominent role of mannosylation also in meiotic prophase. This parallels the situation with N-glycosylation, where three genes were identified, *EOS2* and *OST3*, which mediate N-terminal glycosylation and *YND1,* an apyrase, which indirectly helps with glycosylation. The very clear and prominent role of mannosylation and glycosylation for synapsis is a very interesting and unexpected result. This could be the basis of new investigations, into whether this effects recombination via Golgi vesicle transport or whether glycosylated, mannosylated proteins are more directly involved in synapsis.

We also detected 21 largely uncharacterized ORFs, of which 9 are listed as dubious in respect to coding for a protein. Among those 9 dubious ORFs one has been termed Irc11, because its deletion resulted in increased numbers of Rad52 foci in vegetative cells. Another ORF (*YDR134C*) is annotated as interacting with Cdc28, Dbf2 (Zip1 foci) and Mek1; all proteins that play important roles in synapsis.

Of the 12 novel bona fide ORFs, some isolated pieces of information are available. Very interestingly, 1 candidate interacts with the proteasome, one with the DNA damage effector Rad9, one with the DNA ligase Cdc9, one with SUMO and two are induced by exposure to the alkylating DNA damaging agent MMS (methyl methane sulfonate).

These candidates showed a phenotype in SK1/BY hybrids. For selected candidates, SK1 K.O.s were produced. These usually showed a somewhat milder phenotype. Therefore we believe that the hybrid background represents the more sensitive system to test effects on synapsis. For 4 candidates we suspect they may be false positives, as Ura10 and the partially sterile Lrg1 mutants should have dropped out of the selection. Also Gal80 and dytyrosine transporter Dtr1 are not expected to affect synapsis. However, further analysis is required to rule out that one or more of them indeed also have an unexpected role in chromosome biology.

3.1.4 Candidates displaying long stretches of Zip1, but incomplete synapsis

Mutants of this category comprises cells, where the total length of synapsis was estimated to be between 25% and 50% of a completely synapsed nucleus or where less than 8 fully synapsed chromosomes were detected. According to this criterion, 200 mutants displaying long Zip1 stretches on nuclear spreads were identified (Table 9 Figure 6D). Of these, 9% (18/200 of identified ORFs) were factors required for various mitochondrial functions such as 3 mitochondrial genome maintenance genes (*AIM41, IMG1, MDM32*), 3 metal metabolism genes, 3 genes affecting mitochondrial tRNAs and 1 with an unknown function in respiration (Table 9). The largest group of these 18 candidates (8/18) are genes encoding for functions implicated in the electron transport chain at the inner membrane of mitochondria. This electron transport chain is also called respiratory chain and is a multistep process that couples electron transfer from an electron donor molecule (NADH and succinate for mitochondria) to an electron acceptor molecule (molecular oxygen O_2) with the transfer of protons (H^+ ions) across the inner membrane of mitochondria to generate ATP using F0F1 ATP synthase complex. In eukaryotes, the cytochrome oxidase is the terminal enzymatic complex of the respiration chain. In budding yeast cytochrome c oxidase comprises three core subunits (*COX1, COX2, COX3*) encoded by the mitochondrial genome. The three core subunits are not in the yeast deletion library but we have identified three factors that are required for the normal expression of these three core subunits in categories that fail to produce complete SCs: *QRI5* which is required for the accumulation of spliced Cox1 mRNA, *PET111* is a translational activator for the Cox2 mRNA, *PET122* which is the mitochondrial translational activator specific for the Cox3 mRNA appeared in the short Zip1 category. It was shown that the treatment of budding yeast cells with sodium azide an inhibitor of cytochrome c oxidase, prevents Ime1 production and meiotic induction even in the presence of a non-fermentable carbon source (Jambhekar and Amon, 2008). Thus, cytochrome c oxidase

activity is crucial for meiotic induction. Our observations suggest that downregulation of cytochrome c oxidase core components may effect chromosome synapsis without blocking entry into meiosis.

1 gene, *RIM11,* which encodes a protein kinase required for signal transduction during entry into the meiotic program and promotes the interaction between Ime1 and Ume6 was identified. As Ime1/Ume6 complex is a transcriptional activator of meiotic genes, a failure in this process may result in a deficit of DSBs, or their repair, which may translate into reduced synapsis. In this category, there are two poorly characterized ORFs, *YIR016W* and *YLR445W*, whose expression depends on Ume6 (Williams et al., 2002). Ume6 deletion causes a problem with entry into the meiotic program, but its deregulation may cause more subtle defects, which may also be caused by failure to express these two uncharacterized ORFs.

5 other genes known to be required during meiosis were also identified in this class. *MSH4* and *ZIP4/SPO22* are components of the ZMM pathway and 1 gene, *NDJ1* is required for bouquet formation (Conrad et al., 1997) and telomere led chromosome dynamics in zygotene together with Mps3 (essential) and Csm4 (no phenotype) (Kosaka et al., 2008; Wanat et al., 2008). Importantly, these dynamics depend on underlying actin cables, requiring the integrity of actin filaments, which provides a possible link to several mutants affecting actin filaments, described further below in this chapter..

One subunit of the Shu complex (Shu2, Csm2, Psy3, (Shu1)), *PSY3,* was identified in this group, while Shu2 gave a more severe defect (Zip1 foci) while Csm2 was not yet analyzed. *SHU1* deletion did not yield a phenotype. The Shu complex was shown to promote the formation of recombination intermediates (Mankouri et al., 2007) and stimulates Rad51 filament formation in vitro (A. Shinohara, personal Communication). In our lab Shu2, Csm2, Psy3 had been analyzed in a pilot screen, had been identified and reanalyzed in SK1 background (Woglar A, master Thesis). In SK1, all three mutants finally produced synapsis after a delay, but have reduced spore viability and in at least one case

(*csm2*Δ), chromosome missegregation (Rabitsch et al., 2001). We have also identified a DNA- structure specific endonuclease *MMS4* in this class. The Mus81-Mms4 endonuclease generates interference independent crossovers in budding yeast (*MUS81/SLX3,* NA), but was so far not described to affect synapsis.

8.6% (17/200 identified ORFs) were previously assigned to DNA repair and/or chromatin remodeling and modification. Among these are checkpoint factors *DCC1* a subunit of the alternative RFC, interacting with *CTF8* and *CTF18* (no phenotypes) required for 100% sister chromatid cohesion (Mayer et al., 2001). If confirmed this shows a CTF-independent function of Dcc1, probably different from the RFC function. *MRC1,* a component of the fork pausing complex, is also a S-phase checkpoint factor associated with the DNA polymerase epsilon. *MRC1* acts in complex with *TOF1* (no phenotype) and *CSM3* (reduced SC). We also identified *HPR1*, a subunit of the THO/TREX complexes. The THO complex comprises four subunits (*HPR1, THO2(no phenotype)*, *THP1*(no phenotype), *MFT1(NA)*) and is part of the TREX complex that is implicated in coupling transcription to export of mRNAs to the cytoplasm. *HPR1* interacts also with *SAC3* in the TREX-2 complex. The TREX-2 complex has 4 subunits (*SAC3* (Zip1 foci), *THP1* (no phenotype), *SUS1 and CDC31* (both not in library). *HPR1 is also* a component of the PAF1 (NA) complex that associates with RNA polymerase II and is implicated in both transcriptional initiation and elongation. The mixed results for members of the same protein complexes may suggest that Hpr1 exerts its function outside of THO/TREX complexes.

We identified *RAD30,* the DNA polymerase eta which is involved in translesion synthesis. Together with *REV7* (Short Zip1 stretches), an accessory subunit of DNA polymerase zeta also implicated in translesion synthesis, this result hints at a role of this process in synapsis, however *REV3* the catalytic subunit of DNA pol zeta showed only slightly reduced full SC formation (4%), indicating that at least DNA pol zeta is not critical for synapsis. Rev7 may well have Rev3-independent functions, as it is known to interact with the 9-1-1 subunit

Ddc1/Mec3, which shows a similar phenotype. More experiments need to be done to see whether it is the translesion synthesis function of Rad30, that is responsible for the phenotype.

6% (12/200) identified ORFs are genes previously assigned to transcription and 4.5% (9/200) previously implicated in RNA metabolism. One subunit of the elongator complex which comprises 7 SU (*ATS1* (no meiotic induction, *ELP2* (reduced SC), *ELP4* (NA)*, ELP6* (92% short SC), *ELP3* (no phenotype), *IKI1* (not in library)*, IKI3* (NA)*, KTI12* (long Zip1 stretches)) was identified in this category. The elongator complex is involved in the modification of wobble nucleosides in tRNA and also displays histones H3 and H4 acetyltransferase activity. The only subunit of the elongator complex that exhibits histone acetyltransferase activity, *ELP3* seems not to be required for chromosome synapsis, suggesting that the elongator complex may affect synapsis through a different mechanism, although histone acetylation clearly plays a pivotal role in DSB formation and meiotic gene expression.

4.5% (9/200 identified ORFs) are genes involved in various post translational modifications. These candidates include histone deacetylases (*HOS1, HST1, SET3*), but also factors required for the assembly of the proteasome (Poc4, Rpn10). We also identified *FPR4*, a proline isomerase, catalyzing isomerization of proline residues in histones H3 and H4. This affects their lysine methylation. Histone methylation is known to regulate DSB formation (Merker et al., 2008; Borde et al., 2009) and we have identified methyl-transferase in all our categories. *FPR4* interacts with *FPR3*, another proline isomerase, which prevents premature activation of PP1 (Glc7 phosphatase) and whose deletion restores meiotic divisions in *pph3*Δ mutants (section 3.4.5).

As in previous categories, mutants associated with ribosomal biogenesis (8/200 genes), the ER and the Golgi apparatus (7/200), vacuole and peroxisome biogenesis (13/200 genes) and functions involved in transmembrane transport or cell wall organization (14/200 genes) were identified.

16% of identified ORFs, the largest group of genes identified in the long Zip1 category, are factors previously implicated in various metabolic pathways. 2 of these are involved in biotin biosynthesis, *BIO5* and *BIO2* (biotin synthase). This result is complicated by the observation that Bio4, which catalyzes step 2 in biotin synthesis, doesn't show a phenotype (Bio3 NA).

The second largest group of genes identified in this class (29 genes, 15% of identified ORFs) are deleted for proteins of unknown function (19 genes) or dubious ORFs (10 ORFs). 4 genes involved in stress response and 7 genes involved in autophagy were also identified. Meiosis is a response to hunger in budding yeast and requires processes such as autophagy, which is of crucial importance for starving cells as it permits the reallocation of nutrients to processes that are essential for cell survival under stress (for example, ascospore formation in yeast). It is well known that during zygotene, yeast cells undergo nuclear and chromosomal movements, directed by actin filaments, connected with the inside of the nucleus via Sun/Kash domain protein (Mps3 in yeast). These movements are thought to facilitiate partner matching and therefore synapsis, but are not essential for these processes in budding yeast. Therefore it is not unexpected that 4 out of 5 mutations affecting the cytoskeleton actually affect actin fibers.

Surprisingly 3 genes required for ascospore wall assembly were identified, which, if confirmed, would point to additional roles of these genes. Another 5 genes summarized as being involved in cell cycle regulation were identified. Rmd6 was previously found to fail meiotic nuclear divisions in a high throughput analysis (Enyenihi and Saunders, 2003), but went undetected in the Thesis of A. Woglar in our lab. Here it is represented with a somewhat mild phenotype in synapsis. We identified Spo12 and Bns1, a Spo12 related protein that is also partially redundant with Spo12 and was reported to interact with the Srs2 helicase, an important negative regulator of recombination (Grether and Herskowitz, 1999). Spo12 is known to regulate Cdc14 release from the nucleolus, but this process occurs after synapsis. In this group are also two phosphatases, *PPZ1* and *PPH21*. Ppz1 is a serine/threonine phosphatase, which

has a paralog, *PPZ2*, and both together share overlapping functions with PP1 (Glc7) in vegetative cells. The relatively mild phenotype of Ppz1 probably reflects partial redundance with Ppz2. Interestingly, a physical interaction between Ppz1 and Rvs167 was reported. Rvs167 has been identified in the Thesis of A. Woglar, with a strong synapsis defect, however that phenotype could not be reproduced in this work. Similarl to Ppz1, also Pph21 a subunit of Pp2A has a paralog called Pph22. Again, we expect that the full phenotype only will materialize in the double mutants, where both paralogs are eliminated.

In addition, 19 uncharacterized ORFs and 10 dubious ORFs were sorted into this category of long Zip1 stretches. Because of the relatively subtle phenotype in this chapter, confirmation of the candidates by an independent experiment is particularly critical.

3.1.6 Candidates with reduced SC formation

Making us of a database (created with the program Filemaker), we realized, that a number of interesting mutants had very low levels of synapsis, even though one, or a small number of complete SCs were observed. We decided to compile a list of mutants with reduced SC formation by one of two criteria. Mutants displaying at least 80% Zip1 foci only represent the lowest 8% percentile (299) of observed mutants. After subtraction of mutants falling into the previous categories 105 ORFs were collected in this category (Table 10). *SPO13* and *LGE1* fall into this group. This category may contain factors potentially important for synapsis, which clearly can only be supportive, not essential. Spo13 governs the type of chromosome segregation and normally ensures that the first meiotic division is reductional (Sharon and Simchen, 1990). Lge1 interacts physically with Rad6/Bre1 in a high throughput study (Krogan et al., 2006), the latter mediating histone H2B-K123 monoubiquitination and being essential for DSB formation (Yamashita et al., 2004) and synapsis, in SK1 (A. Woglar, Master Thesis).

Mutants exhibiting less than 5 nuclei with long or complete Zip1 stretches represent the lowest 17% percentile of observed mutants. 171 ORFs were not listed in the previous categories and fall exclusively into this group. Some well known genes such as Slx1, Psy2, Dnl4, Msh5 and Rad52 were recovered in this group (Table 8).

We expect mutants, which are not essential, but still important for normal levels of SC formation to be represented in such groups. However, as the system is very sensitive and prone to fluctuations, verification of these ORFs is particularly important.

3.1.7 Candidates displaying increased levels of complete SC

Besides mutants that did not induce meiosis or were defective in SC formation, 67 (1,8% of analyzed ORFS) showed elevated levels of nuclei with long Zip1 stretches or fully synapsed chromosomes (Table 12). Candidates listed in Table 12 were chosen if exhibiting at least 46% of nuclei with long Zip1 stretches or complete SC. The wild type SK1/BY hybrid control strains (ade2Δ, lys2Δ) fluctuated between 5 and 30% in about 50 repeats by this criterion, so that 46% seems well separated from these random fluctuations. Two factors known to accumulate a high levels of fully synapsed nuclei in SK1 background, Pch2 a AAA-ATPase and Ndt80, a transcription factor required for exit from pachytene showed only wild type behavior in this assay in the SK1/BY hybrid background. *ndt80*Δ had 7% long plus complete SC and *pch2*Δ 12%. Possibly the analyzed timepoint is too early as to allow a significant accumulation of SC in these mutants. This would suggest that the mutants obtained are, if confirmed, accumulating SCs very fast, perhaps in part prematurely. This may also explain why this category is relatively small compared to the others that score reduction of SC.

3.2 Secondary screen: SK1 mutants

3.2.1 phenotype of candidates in SK1

As an effort to verify the phenotypes observed we deleted 30 candidate genes in pure SK1 strains, also as a control for the constructs in the collection. These 30 ORFs include mostly uncharacterized ORFs from the four major categories described in the primary screen (No meiotic induction, Zip1 foci, short and long stretches of Zip1). In contrast to the primary screen, the analysis was now more thorough, comprising SC formation (Zip1), DSB turnover (Rad51 foci) and meiotic progression (DAPI) at 4, 5, 6, 7, 8, 10 hours in SPM, instead of a single time point. Of course, this time-resolved analysis is better suited to differentiate between an inability phenotype and a delay. Such time resolved analysis was unfortunately not feasible with the primary screen. Because pre-meiotic DNA replication is intimately linked to DSB formation (Borde et al., 2000), all candidates displaying a significant decrease in chromosome synapsis as compared to wild type, were systematically analyzed by FACs to assess the efficiency of pre-meiotic DNA synThesis. An analysis of meiotic progression by spindle staining (tubulin) was performed only for *rim4*Δ mutants. Detailed phenotypic description of some of the 30 selected candidates in SK1 is depicted below.

In summary the SK1 background produced a meiotic phenotype for most of the mutants identified. Usually, but not always, this phenotype was less severe than in the BY/SK1 hybrid background. Of the 30 mutants which were analyzed in SK1 in parallel, xxx were unable to undergo any synapsis, xxx were unable to accomplish long zip1 regions, and xxx had no or reduced numbers of complete SC. Xxx SK1 mutants did not show any significant meiotic defect. Xxx/xxx had problems in pre-meiotic S-phase. One possibility is, that SK1 cells, which induced the meiotic program very robustly, are less likely to fail in meiosis, because the strong protein expression can balance some of the errors. This opens the possibility to identify partially redundant functions in the sensitized system of the SK1/BY hybrid. In addition, hybrids are sensitized, because their

homology between homologous chromosomes is reduced. Thus small defects will have a stronger impact in this background. We propose, that many of the identified genes with partial defects are in fact absolutely required for meiosis, but have partner proteins with partially overlapping functions.

Wild type SK1

In wild type SK1, Zip1 protein first appears as a dot-like staining termed foci. This corresponds to the leptotene stage of meiotic prophase I (leptotene) (Figure 7A). Chromosome synapsis begins at zygotene when Zip1 starts to be polymerized between homologs axes. At zygotene, linear stretches of Zip1 staining are detected on nuclear spreads (short Zip1 stretches at the early zygotene and long stretches at the end of zygotene) (Figure 7B). As prophase I proceeds, Zip1 is polymerized along the entire length of all chromosomes. This marks the pachytene stage and on nuclear spreads sixteen pairs of homologous chromosomes can be observed (Figure 7C, full SC). Between 8 to 26% of nuclei display fully synapsed chromosomes 4 to 6 hours after meiotic induction in wild type SK1 (n=50 independent timecourses).

In wild type SK1, an average of 17 Rad51 immunostaining foci per nucleus were detected 4 hours after induction of meiosis. This average may vary between 15 and 19 foci in different time courses. The number of Rad51 foci then decreases progressively and almost disappears after 8 hours in SPM (a few residual foci remain, on average 2±1 per nucleus) (Figure 8B). Nuclear division as assayed by DAPI staining is almost completed after 8 hours in liquid SPM (88 - 96% of wild type have passed at least one meiotic division). Wild type yields 90 to 99% viable spores (Figure 8C), depending on possible tagged meiotic proteins. In situ labeling of the spindle with antibody against tubulin showed that more than 60% of meiotic cells have passed the first meiotic division 6 hours after induction of meiosis in wild type SK1 as quantified by the percentage of nuclei displaying an elongated bipolar spindle (anaphase I) and two bipolars spindle (metaphase II, anaphase II) (Figure 10E).

YDR446W/ECM11

Ecm11 has been reported to localize to the nucleus, to show reduced spore viability and a reduction of CO, but not of NCOs (Zavec et al., 2004). In our primary screen *ecm11*Δ mutants showed no complete SCs and a reduced number of nuclei with long fragments of SC (3/50 of nuclei displayed long stretches of Zip1). In pure SK1 *ecm11*Δ cells sporulated with almost wild type timing, however chromosome synapsis was strongly reduced (almost no complete synapsis was observed, (only 1%), Figure 8A). In contrast to *ymr196w*Δ, *ydr333c*Δ, *oxp1*Δ, which accumulate nuclei with Zip1 foci, this mutant showed a lot of short and long SC at 5 and 6 hours in SPM. So while the other mutants fail in the first step of synapsis initiation, *ecm1*Δ cells fail at the elongation step. A significant increase of Rad51 focus formation was detected in *ecm11*Δ mutants (27 Rad51 foci per nucleus compared to 17 foci for the wild type, Figure 8B). These foci disappeared very slowly and were still enhanced several fold over wild type at 8 hours in SPM. This is clear evidence for a problem in Rad51 filament turnover and defines *ecm11*Δ as repair defective mutant. Nuclear division was delayed for 1 hour (Figure 8C), Different from the published results of (Zavec et al., 2004), pre-meiotic DNA replication occured with almost wild type kinetics in our hands (Figure 8D) and spore viability also reached wild type levels (93%, n=20 tetrads dissected). So, while we find a less severe phenotype than (Zavec et al., 2004) for S-phase and spore viability, we have clear evidence for the involvement of this gene in DSB repair.

YMR196W

The function of *YMR196W* gene product is unknown. *ymr196w*Δ mutants showed only Zip1 foci on nuclear spreads at 6 hours in SPM in the primary screen. In pure SK1, *ymr196w*Δ cells displayed a very strong decrease in chromosome synapsis. Both classes, long and complete SCs were almost

eliminated (2% of nuclei with fully synapsed chromosomes at 4 hours in SPM, Figure 8A). The average number of Rad51 foci per nucleus reached nearly wild type levels (15 foci per nucleus) and decreased with a slight delay relatively to wild type (Figure 8B). The spore viability was slightly reduced (77% n=20 tetrads dissected). Pre-meiotic DNA replication was not altered and nuclear divisions occurred on time (Figure 8C,D). The random pattern of spore death (only 3 tetrads with 2 viable and 2 dead spores) that is no increase of 2 or 0 -viable tetrads, argue against chromosome non-disjunction as the primary cause of spore death in this mutant. In summary this mutants suffers from a prominent defect in the progression of synapsis for unknown reasons. This may be accompanied by a slight DSB repair problem.

YDR333C

*ydr333c*Δ represents an uncharacterized ORF, which only showed Zip1 foci on nuclear spreads, but failed to undergo synapses at 6h in SK1/BY. In pure SK1, deletion of *YDR333C* caused a strong decrease in chromosome synapsis (only 3% of nuclei with fully synapsed chromosomes, Figure 8A). Short, long and complete synapsis were all significantly reduced, while the Zip1 foci class was dramatically increased at the 4, 5 and 6 hour timepoints. Pre-meiotic DNA replication and nuclear division occurred with wild type timing, Figure 8C,D). The sporulation efficiency (96%) and spore viability (94% n=20 tetrads dissected) were similar to wild type after 24 hours. A slightly reduced number of 13 Rad51 foci accumulated per nucleus at 4 hours in SPM.. The number of foci started to decrease only at 6 hours (wild type at 5 hours) but disappeared at later time points with wild type kinetics, Figure 8B). This slight reduction in Rad51 focus formation suggests either a slight decrease in DSB formation or a less synchronous formation of DSBs (that is a partial delay) in *ydr333c*Δ, which could contribute to the decrease in chromosome synapsis.

YDR457W/TOM1

Tom1 is an ubiquitin E3 ligase that is involved in the turnover of histones and plays a role in mRNA export from the nucleus (Duncan et al., 2000; Singh et al., 2009). *tom1*Δ mutant showed long fragments of SC (1/50 of nuclei displayed long stretches of Zip1) in the SK1/BY hybrid background. In the absence of *TOM1* in pure SK1, pre-meiotic DNA replication was impaired (Figure 8D), nuclear division was delayed and reduced (65% of *tom1*Δ cells have completed M1 after 10 hours in SPM, Figure 8C). However, chromosome synapsis reached wild type levels (Figure 8A). The average number of Rad51 foci per nucleus (10 foci at 4 hours in SPM) and the spore viability (77% n=20 tetrads dissected) were reduced in *tom1*Δ cells compared to the wild type (Figure 8B). These observations hint at a role of Tom1 in histone turnover for pre-meiotic DNA replication and possibly for wild type levels of DSB formation. Alternatively, the protein may function only during DNA replication, and all the meiotic defects could be a consequence of impaired pre-meiotic DNA replication. It was shown that if DNA replication is delayed in a certain area of a chromosome, DSB formation is also specifically delayed in the same area for about the same time, indicating that the two processes are intimately linked (Borde et al., 2000a).

YKL215C/OXP1

Oxp1 is an ATP-dependent 5-oxoprolinase (Kumar and Bachhawat, 2010) with a known role in glutathione synThesis, which is used in detoxification. In the SK1/BY hybrid background *oxp1*Δ mutant displayed a severe defect in chromosome synapsis with no elongated synapsis at 6 hours in SPM (4/50 nuclei with short Zip1 stretches). In pure SK1, *oxp1*Δ mutants underwent meiotic nuclear division and sporulated with wild type timing (Figure 8C). Chromosome synapsis was reduced for all long SC classes, while Zip1 foci class was strongly elevated (4% complete SCs at 6 hours in SPM, Figure 8A*).* Rad51 foci numbers

were slightly increased (~20 foci per nucleus at 4 hours in SPM compared to 17 foci for the wild type, Figure 8B). Pre-meiotic DNA replication occured with wild type kinetics and efficiency (Figure 8D). These observations suggest a slight defect in the processing of early recombination intermediates in the absence of *OXP1*.

YGL021W/ALK1

Alk1 is a cell cycle regulated kinase and APC substrate (Nespoli et al., 2006), has a paralog (Alk2) and is phosphorylated in response to DNA damage. *alk1*Δ mutants showed a strong reduction of nuclei with fully synapsed chromosomes (1/50 nuclei) in the SK1/BY hybrid background. In pure SK1 background, a much milder decrease in complete chromosome synapsis (5% of nuclei) was observed (Figure 8A). Nuclear division and spore viability (87% n= 20 tetrads dissected) were similar to wild type (Figure 8C). The average number of Rad51 foci was reduced (10 and 12 foci per nucleus at 4 and 5 hours in SPM, respectively, Figure 8B). This result suggests that DSB formation might be reduced or the turnover of Rad51 nucleoprotein filament might be enhanced in *alk1*Δ mutants.

YLR352W

F-box protein of unknown function, *YLR352W* protein interacts with Skp1 and Cdc53 proteins. The *ylr352w*Δ mutant did induce meiosis in SK1/BY hybrid background but only Zip1 foci were detected on nuclear spreads. In pure SK1 background, *ylr352w*Δ mutant showed only a 1 hour delay in chromosome synapsis (Figure 8A). Nuclear division was delayed of about 2 hours and reduced (86% of *ylr352w*Δ cells have executed M1 at 10 hours after transfer to SPM). 11 Rad51 foci (compared to 17 for wild type at 4 hours in SPM) were found per nucleus and were slowly turned over (Figure 8B). Consistently, crossovers and non-crossovers recombination products appeared with 2 hours delay (Figure

16A), These results suggests a role of the SCF in DSB formation and chromosome synapsis.

YNL035C

YNL035C is an uncharacterized ORFs containing three WD-40 repeats (citation) reported to interact with SUMO. In the SK1/BY hybrid background *ynl035c*Δ had no long SC at 6 hours in SPM (9/50 nuclei with short Zip1 stretches). In SK1 *ynl035c*Δ cells sporulated with wild type timing and showed only a weak decrease and delay in chromosome synapsis (7% of nuclei with fully synapsed chromosomes after 6 hours in SPM, Figure 8A). Rad51 foci (~ 12 foci per nucleus) were reduced compared to wild type (Figure 8B). Pre-meiotic DNA replication and spore viability (97%) were not affected by the deletion of *YNL035C* (Figure 8D).

YDR485C/VPS72/SWC2

Swc2 is a subunit of the SWR1 chromatin remodeling complex that binds the histone variant H2A.Z (*HTZ1* in yeast) and is essential for H2A.Z exhanges for chromatin bound histone H2A (Wu et al., 2005). In the SK1/BY hybrid background *swc2*Δ mutant showed no long SC at 6 hours (6/50 nuclei with short Zip1 stretches). In SK1 background, chromosome synapsis and nuclear division were delayed by about 1-2 hours, particularly obvious by the dramatic elevation of the Zip1 foci class at 4 and 5 hours in SPM. SCs eventually reached wild type levels at 6 hours, but remained until 8 hours *(*Figure 9A, C). High levels of Zip1 polycomplexes were observed (see section 3.4.3 for more details on this gene). The average number of Rad51 foci (17 per nucleus) was similar to wild type (Figure 9B). *swc2*Δ mutant displayed wild type level of spore viability (97% n=20 tetrads dissected), but about 25% of spores exhibited a slow growth phenotype.

YOL052C-A/DDR2

Ddr2 is expressed in response to a variety of environmental and physiological stresses, but its molecular function is still unknown. *ddr2*Δ mutants failed to undergo synapsis, but formed Zip1 foci at 6 hours in the primary screen. In SK1, *ddr2*Δ cells sporulated with wild type timing, but displayed a weak decrease in chromosome synapsis (6% of nuclei with fully synapsed chromosmes after 6 hours in SPM, Figure 9A). The average number of Rad51 foci (11 foci per nucleus) was reduced in *ddr2*Δ mutant compared to the wild type (Figure 9B). This result suggests that Ddr2 might be required for wild type levels of DSBs.

YOR296W

YOR296W is an uncharacterized ORF. *yor296w*Δ mutant showed long fragments of SC (4/50 nuclei displayed long stretches of Zip1) in the SK1/BY hybrid background. No pre-meiotic DNA replication was detected in this mutant in two different experiments (Figure 8D). However, in a separate experiment DNA replication must have occurred at some point, as spores were formed and had 90% spore viability. In pure SK1, *yor296w*Δ cells exhibited a strong reduction of synapsis (about 2% of nuclei with fully synapsed chromosomes at 4 hours in SPM). Nuclear division was delayed ~ 4 hours and reduced (only 56% were past M1 after 10 hours in SPM, Figure 9A,C). The spore viability (90% n=20 tetrads dissected) was similar to wild type, of those cells that had formed tetrads (50%). Rad51 foci accumulated to wild type levels (17) and disappeared with similar kinetics as in wild type (Figure 9B). S-phase in this mutant seems to be defective and this might be the primary reason for meiotic defects. How much S-phase is in fact necessary in this strain for initiating synapsis needs to be determined.

YPR068C/HOS1

Hos1 is a class1 histone deacetylase (HDAC) that deacetylates the cohesin subunit Smc3 at the onset of anaphase (Borges et al., 2010; Xiong et al., 2010). Hos1 is the ortholog of human HDAC8, which has recently been shown to be responsible for CdL (Cornelia de Lange Syndrome) a severe condition with malformation of limbs and face. Removal of the acetylation of Smc3 is important to guarantee proper degradation of the kleisin of cohesion after its cleavage by separase. The failure results in prolonged residence of cohesion on chromatin and a delay in anaphase in human cell cultures (derived of CdL patients) (K. Shirahige, personal communication). In the SK1/BY hybrid background *hos1*Δ mutants failed to form complete SC (only 4/50 of nuclei showed long fragments

of SC). In SK1 a clear delay in chromosome synapsis was observed (1-2 hours, 10% complete SC at 7 hours, Figure 9A). Nuclear division was delayed by 2-3 hours (Figure 9C). normal levels of Rad51 foci (15) per nucleus were found (Figure 9B). Whether Hos1 exerts its effects on yeast meiotic prophase via regulation of Smc3-acetylation, or via histone deacetylation is unclear, but based on studies in mouse and humans, the cohesion deacetylation is very important. It will be very interesting to determine, whether this property can explain the synapsis defect.

YHL024W/RIM4

Rim4 is an RNA binding protein required for the expression of early and middle sporulation genes (Soushko and Mitchell, 2000; Deng and Saunders, 2001) and is polyubiquitinated by Rsp5 (Kus et al., 2005). Pre-meiotic DNA synThesis and chromosome segregation were described as defective in *rim4*Δ mutants (Deng and Saunders, 2001).

*rim4*Δ mutant was scored as unable to initiate meiosis in the SK1/BY hybrid bacground. In SK1, rim4Δ mutants displayed a dramatic defect in chromosome synapsis. Initial Zip1 foci formed as in the wild type, but Zip1 elongation was completely abolished (Figure 10A). Nuclear division and sporulation were absent (Figure 10C). The average number of Rad51 foci (12 foci per nucleus at 4 hours in SPM) accumulated to a greater levels (23 foci per nucleus) and remained constantly high after 6 hours in SPM (Figure 10B). In situ immunolabeling of the meiotic spindle revealed the presence of a prophase I spindle (monopolar spindle) until 10 hours in SPM, documenting a solid prophase I arrest, usually caused by DNA damage. A bipolar spindle was never observed (Figure 10E). Rim4-HA3 (obtained from Alain Nicolas, Institute Curie, Paris for collaboration) localized exclusively to the cytoplasm during meiosis (Figure 10D), pointing to a role of Rim4 for the expression of critical prophase genes via mRNA stability, splicing or translational activation.

3.3 Characterization of pilot screen genes

A pioneer screen of 264 candidates carried out in our laboratory by Alexander Woglar (Woglar A, master Thesis) identified 35 genes required for normal levels of synapsis in the SK1/BY background, 28 of which also showed a defect or a delay in pure SK1.

In an attempt to characterize their phenotype in more detail, I repeated FACS analysis of pre-meiotic DNA replication and attempted physical analysis of recombination intermediates using a system developed in Michael Lichten´s laboratory (Figure 12 (Allers and Lichten, 2001b). This system allows to measure the formation of DSBs, crossover and non-crossovers recombination products. I performed it on 12 of the 28 genes.

The Shu complex *(SHU2, CSM2, PSY3)*

The budding yeast RecQ helicase Sgs1 interacts with Top3 and the two proteins act in concert in vivo in regulating homologous recombination during DNA replication. The deletion of *TOP3* gene results in a phenotype of slow growth, DNA damage sensitivity, meiotic defects and hyper-recombination (Wallis et al.,1989; Chakraverty et al., 2001). Mutants of the shu complex (*shu1*Δ*, shu2*Δ*, csm2*Δ*, psy3*Δ*)* were found because they suppress various *sgs1* and *top3* mutant phenotypes (Shor et al., 2005). Previous studies have proposed that the Shu proteins may act to promote the formation of homologous recombination repair intermediates that are processed by the Sgs1-Rmi1-Top3 complex (Mankouri et al., 2007; Ball et al., 2009).

Chromosome synapsis is delayed for 2 to 4 hours in shu mutants (Woglar A Master Thesis). We show here that pre-meiotic DNA replication occurs without delay in all three mutants, and was even slightly faster than wild type in *psy3*Δ and *csm2*Δ (Figure 11A). The average number of Rad51 foci per nucleus was reduced in shu mutants compared to the wild type. 12 foci in *shu2*Δ*,* 10 foci in

csm2Δ and 8 foci in psy3Δ at 4 hours in SPM (Figure 11B). Rad51 foci turnover was similar to wild type in shu2Δ and csm2Δ mutants, but faster in psy3Δ mutant (Figure 11B). The reduction of Rad51 foci in shu mutants suggests either a decrease in DSB formation or the inefficiency of Rad51 loading on broken chromosome ends (ssDNA) or the instability of Rad51 nucleoprotein filament in the absence of these proteins. In the *psy3*Δ mutant, crossovers and noncrossovers appeared with a delay of about 2 hours, and were strongly reduced (Figure 13A,B). These results point at a central role of Psy3 in stabilizing meiotic nucleoprotein filaments formation.

IRC25/POC3

Irc25 is a chaperone component of the 20S proteasome. The 20S proteasome is the catalytic core of the 26S proteasome, the major proteolytic system in the cytosol and nucleus of all eukaryotic cells. Deletion of IRC25 as well as of five other epistatic group of genes (*POC1, POC2, POC4, UMP1* and *PRE9*) suppresses the growth defect of a conditional dominant lethal allele of *RAD53* (RAD53-DL), indicating a role of these proteins in a common pathway of DNA damage response (Le Tallec et al., 2007). Although not essential for normal growth, the deletion of *IRC25* leads to inefficient assembly of the 20S proteasome (Yashiroda et al., 2008).

*irc25*Δ mutants exhibit wild type timing in pre-meiotic DNA replication and a severe reduction in chromosome synapsis (1% of nuclei with fully synapsed chromosomes), nuclear division is reduced (only 59% of *irc25*Δ cells have passed M1 after 10 hours in SPM. The spore viability is unaffected (Woglar A master Thesis). In the physical recombination assay crossovers and non-crossovers products were detected from the initial time point zero on in the *irc25*Δ mutant indicating that cells had started meiosis prematurely. It is possible, but not sure at this point, that this premature initiation is part of the *irc25*Δ phenotype. The *irc25*Δ mutant displayed a specific reduction in crossovers

(~50% of wild type levels) whereas noncrossovers accumulated to almost wild type levels (Figure13A,B). Thus *irc25*Δ showed a specific defect in chromosome synapsis and crossover control, reminiscent of the ZMM phenotype. The SC defect of *irc25*Δ is shared by *pre9*Δ the only non-essential subunit of the proteasome. We propose an important role of the proteasome in the ZMM pathway. This essential role is different from promoting Rec8 cleavage, which is neither necessary for synapsis nor for proper CO levels.

UBC13, RAD33 and YOR029W

Ubc13 is a ubiquitin conjugating enzyme which cooperates with Mms2 and Rad5 proteins in the assembly of polyubiquitin chains on target substrates such as PCNA. Polyubiquitination of PCNA is required for error-free post-replication DNA repair (Brusky et al., 2000; Halas et al., 2011).

Rad33 functions along with the Rad4-Rad23 complex in mediating the initial damage recognition of the Nucleotide Excision Repair (NER) pathway. The role of Rad33 in the Rad4-Rad23 complex seems to be conserved in human (Dulk et al., 2006; 2008).

YOR029W is an uncharaterized dubious ORFs.

*ubc13*Δ*, rad33*Δ and *yor029w*Δ mutants display a slight accumulation of nuclei with fully synapsed chromosomes 6 hours after induction of meiosis (28%, 29% and 31% respectively) compared to a maximum of 26% rarely detected in wild type cells. Nuclear division is slightly delayed in these three mutants, but the spore viability is similar to wild type (Woglar A master Thesis).

Pre-meiotic DNA replication occured with wild type kinetics in the *yor029w*Δ mutant (Figure 14A). DSB formation was reduced and delayed for ~1hour, but the average number of Rad51 foci per nucleus (32 foci) was higher than in the wild type (Figure 14B), suggesting a delay in repair. Only a slight reduction and delay of crossovers was detected while non-crossover levels remained

unaffected (Figure 14C,D). Interestingly, the timing of NCO was advanced relative to CO, as compared to the wild type.

*rad33*Δ mutants showed a delay and reduction in DSB formation and a reduction of both, crossover and non-crossover levels compared to the wild type (Figure 15A, B). This observation together with the accumulation of synapsis detected in the absence of *RAD33* (Woglar A Master Thesis) may suggest the transient activation of the pachytene checkpoint, that is, a delay in Ndt80 activation. Analysis of Ndt80 levels and of Cdc5/polo kinase activation might shed more light on this mechanism. In the SK1/BY hybrid screen, Rad33 interacting partners, Rad23 and Rad4 showed a strong reduction of synapsis for *rad23*Δ mutant (1/50 nucleus with fully synapsed chromosomes) and almost no phenotype for *rad4*Δ (3/50 nuclei with fully synapsed chromosomes).

*Ubc13*Δ displayed a similar delay and reduction of crossover and noncrossover (Figure 16A)

RVS167

Rvs167 is the yeast homolog of the mammalian amphiphysin, which is enriched in a brain, where it is believed to mediate the recruitment of dynamin (is a kinase) to sites of clathrin-mediated endocytosis. In yeast Rvs167 interacts with Rvs161 and both proteins are involved in the regulation of the actin cytoskeleton and endocytosis (Bauer et al., 1993; Lombardi et al., 2001). Rvs161 and Rvs167 function as an obligatory heterodimer in vivo and share similar roles in cell polarity, cell integrity, cell wall synthesis and vesicle trafficking (Friezen et al., 2006). Notably, *rvs161*Δ mutant is more defective in endocytosis and morphogenesis than *rvs167*Δ mutant and both mutations contribute to the virulence of the human fungal pathogen Candida albicans (Douglas et al., 2009).

In the absence of *RVS167* pre-meiotic DNA replication occurs with wild type efficiency, while chromosome synapsis and nuclear divisions were almost completely absent (Woglar A Master Thesis). To our surprise, crossover and

non-crossover recombination products were detected and even accumulated to a substantial amount in *rvs167*Δ mutant (Figure 15A,B).

YGL101W

YGL101W is an uncharaterized ORFs. Chromosome synapsis appears with wild type kinetics in *ygl101w*Δ mutant, nuclear division is slightly delayed and reduced (86% of *ygl101w*Δ cells have undergone M1 10hours upon meiotic induction) (Woglar A Master Thesis). We found that pre-meiotic DNA replication is delayed for ~2hours (Figure 8D) and that crossover and non-crossover recombination products were similarly delayed in *ygl101w*Δ mutant compared to wild type (Figure 16A).

HNT3

Hnt3 is a homolog of the human Aprataxin. Aprataxin was identified as a gene mutated in the neurodegenerative syndrome ataxia oculomotor apraxia type1 (Morara et al., 2001). Aprataxin catalyzes the removal of adenosine monophosphate (AMP) from the 5´-ends of damaged DNA strands, thereby preparing the SSB for ligation. It was also shown that at higher concentrations aprataxin possesses a 3´-processing activity (Takahashi et al., 2007). Deletion of *HNT3*, partially rescued *rad51*Δ and *rad52*Δ mutants while sensitizing *rad50*Δ yeast cells to the DNA damaging agent H2O2.

H2O2 (hydrogen peroxide) creates strand breaks with blocked 3´-termini, such as 3´-phosphate; which could cause abortive ligation if a 5´-phosphate is present. As Rad50 is required for DSBs ends resection, a synthetic sensitivity in *hnt3*Δ, *rad50*Δ double mutant could be explained by the loss of two parallel pathways for 5´AMP removal suggesting that Hnt3 may be required to commit DSB to repair by recombination (Daley et al., 2010).

Chromosome synapsis and nuclear division are delayed in *hnt3*Δ mutant for about 1 hour. A delay of synapsis is further manisfested by an accumulation of SC component (Zip1 polycomplexes) in 52% of nuclei, the spore viability and sporulation efficiency are both delayed and reduced to 65% (Woglar A master Thesis). In this study, we show that the average number of Rad51 foci per nucleus (27 foci at 4 hours in SPM) is higher than in the wild type. Remarkably, numerous Rad51 foci persisted until very late time points (Figure 17B), suggesting a delay in the repair of recombination intermediates. Consistently, crossover and non-crossover recombination products were delayed to ~2 hours and reduced (Figure 17A).

3.4 PP4 phosphatase complex acts in the ZMM pathway to antagonize Pch2 and Fpr3

3.4.1 Phenotypes of mutants in the PP4 complex

The yeast homolog of the protein phosphatase 4 complex (PP4) of higher eukaryotes consists of two components: the catalytic subunit Pph3 and Psy2. A third protein, Psy4, was shown to physically associate with Pph3 and to be required for dephosphorylation of one of PP4's subtrates, histone H2A (Keogh et al., 2006), but not for another important substrate, Rad53 (O´Neill et al., 2007). In response to DNA double-strand breaks (DSBs), ATM/ATR (Tel1/Mec1 in budding yeast) phosphorylate severals substrates including histone H2A at serine 129 in yeast, Rad53 (Chk2 kinase homologue) and single-strand DNA binding protein RPA. Pph3-dependent dephosphorylation of H2A, Rad53 and hRPA2 is required for checkpoint recovery from G2 phase arrest (Keogh et al., 2006; O´Neill et al., 2007; Lee et al., 2010) and to facilitate DSB repair via homologous recombination.

Recently, in parallel to this work, Pph3 was reported to be required in meiosis for full synapsis (Falk et al., 2010) and for resolution of homology-independent centromere-coupling by dephosphorylation of Zip1's critical residue

Serine 75 (Falk et al., 2010). In addition, the *pph3*Δ mutant was found to be delayed in pre-meiotic DNA replication, in DSB repair and a strong delay in spindle pole body (SPB) separation, and to display reduced crossovers (Falk et al., 2010). The meiotic defects of PP4 components were also independently described in our laboratory: We found pre-meiotic DNA replication strongly delayed in the *pph3*Δ mutant, but occurs slightly delayed in *psy2*Δ and with almost wild type kinetics in *psy4*Δ (Figure 18A, see also A. Woglar, master Thesis). Nuclear division is strongly delayed and reduced in all three mutants. ~25% of *pph3*Δ cells completed at least one of the two meiotic divisions 10 hours after transfer into the sporulation medium, compared to ~50% for *psy2*Δ, 67% for *psy4*Δ and 98% for the wild type (Figure 18B). Chromosome synapsis reaches wild type levels in the absence of *PSY4* albeit a slight delay, whereas only 1% of fully synapsed chromosomes is detected on nuclear spreads in *psy2*Δ mutants. This synapsis defect is further exacerbated in *pph3*Δ mutant background where only long fragments of SC are detected (Woglar A master Thesis, shown in Figure 18D). Rad51 foci accumulate to high levels in the absence of any of the PP4 complex subunits and decrease slower than in the wild type (Figure 18C). The *pph3*Δ*,* and *psy2*Δ mutants show a specific reduction in crossover formation, while noncrossovers are unaffected, a hallmark of ZMM mutants. On the other hand the *psy4*Δ mutant displays only a delay affecting crossover and noncrossover formation equally (Figure 18E, F), suggesting that this regulator of Pph3 is not involved in the ZMM functions of the phosphatase. Consistently, the spore viability of *psy4*Δ is similar to wild type, but *pph3*Δ and *psy2*Δ show a decrease in spore viability, 57% for *pph3*Δ (20 tetrads, with *non*-random distribution of dead spores (5 tetrads missing, 6 tetrads with two viable spores, 3 tetrads with three viable spores and 6 tetrads with four viable spores; strain *FKY4571*) and 75% for *psy2*Δ (10 tetrads). To gain further insights into the mechanism by which synapsis is affected by the *PPH3* deletion, we set out to identify suppressors for the synapsis defect of the *pph3*Δ mutant.

3.4.2 Inefficient restoration of synapsis in *pph3*Δ *H2A-S129A*

Phosphorylation of histone H2AX is one of the earliest marks of DSBs in most organisms. Phosphorylation of Serine 129 of yeast histone H2A (H2A-S129-P), serves as a platform for the recruitment of various repair factors at the DSB sites. Following DSB repair, Pph3-dependent dephosphorylation of H2A-S129-P permits the recovery from checkpoint arrest (Keogh et al., 2006).

To determine wether H2A-S129-P is responsible for the synapsis defect of *pph3*Δ mutant, a non-phosphorylatable mutant of histone H2A (kindly provided by Michael Lichten and Rob Shroff, FKY4058, FKY4059), where S129 is replaced by Alanine, was combined with *pph3*Δ.

Indeed, a first strain received from the Lichten lab and transformed to become a *pph3*Δ, *hta1, 2-S129A* triple mutant (FKY4063, FKY4064, FKY4065) displayed wild type levels of nuclei with fully synapsed chromosomes (Figure 19A). However, unexpectedly, the diploid *hta1, 2-S129A* strain (FKY4118, generated from FKY4058 and FKY4059) showed a synapsis defect (only short Zip1 stretches on chromosome spreads) and a very low spore viability (11.5% 20 tetrads). As this result is in stark contrast to the high spore viability (100%) previously observed in Michael Lichten´s lab for this mutant, this called into question, whether the suppression was due to the *hta1, 2-S129A* mutations. It suggests that suppression also involves the presence of an uncharacterized alteration in the genetic background of these strains.

A second set of strains were provided by the Lichten lab (FKY4420, FKY4421). This time the diploid generated from these haploids (FKY4433) had wild type spore viability. However, when combined with the *pph3*Δ mutation, the suppression of the *pph3*Δ phenotype in the triple mutant *pph3*Δ*, hta1, 2-S129A (FKY4450*) was of a much smaller magnitude. Only 0.1% of nuclei displayed fully synapsed chromosomes on nuclear spreads and also the fraction of nuclei displaying partial SC was much reduced compared to the strains analyzed first (Figure 19A,B,C). To make sure the analyzed strains contain the correct mutations, a region of *HTA1* and one of *HTA2* containing position +389 (S129A)

was amplified by PCR (using primers 2356, 2357 for *HTA1* and primers 2415, 2416 for *HTA2*) and subjected to sequencing. Strains FKY4058, FKY4059*,* FKY4063, FKY4064 and FKY4450 were sequenced and confirmed. FKY4450 is a homozygous diploid obtained from FKY4444, and it shows reduced suppression of the phenotype of *pph3*Δ.

Therefore we conclude that the suppression of the SC phenotype in strain *FKY4065* is not due to the *S129A* mutations alone, but to the presence of at least one more suppressor. The fact that also strain FKY4450 shows some level of suppression suggests that the *S129A* mutation may contribute to the restoration of the SC in the *pph3*Δ mutant background. In order to characterize this unknown suppressor, we crossed one haploid containing the suppressor and the *pph3*Δ mutation *(FKY4063*) with one haploid containing only the *S129A* mutations, but no suppressors *(FKY4421*). Of the four segregants of a complete tetrad, two were *pph3*Δ and *PPH3* was knocked out in the other two. Then all four segregants were made diploid by transformation with an HO containing plasmid (p40) and will be tested for their ability to form SC. It is also planned to sequence the four segregants in order to identify sequence variants that correlate with the suppression phenotype.

3.4.3 Deletion of the SWR chromatin remodeling complex subunit *SWC2* restores synapsis in pph3Δ mutants.

Swc2, a subunit of the SWR chromatin remodeling complex that binds to the histone variant H2A.Z (Htz1 in yeast) mediates the replacement of chromatin bound histone H2A with the DNA damage specific histone variant H2A.Z upon DSB formation (van Attikum et al., 2007). In *htz1*Δ mutants, ssDNA formation was found to be significantly delayed and the DNA damage checkpoint is partially defective (Kalocsay et al., 2010).

Because *hta1.2-S129A* mutant showed some suppression of the *pph3*Δ synapsis phenotype and because some H2A is exchanged to H2A.Z in response

to DSB damage in vegetative cells, we asked whether deletion of histone variant H2A.Z might restore synapsis in *pph3*Δ. To address this question, *htz1*Δ and *pph3*Δ, *htz1*Δ double mutants were constructed by PCR mediated gene replacement and analyzed. The *htz1*Δ single mutant showed wild type synapsis and a slight delay in nuclear division. The synapsis phenotype of the *pph3*Δ, *htz1*Δ double mutant was indistinguishable from that of the *pph3*Δ single mutant, indicating that *HTZ1* is not responsible for the synapsis defect of *pph3*Δ mutant (Figure 20B),

In parallel we asked whether the Htz1 binding component of the SWR complex, Swc2, is involved in the defective synapsis of *pph3*Δ mutants. The *swc2*Δ mutant exhibited a defect in chromosome synapsis in the SK1/BY hybrid primary screen, but when deleted in SK1, the *swc2*Δ mutant behaved as the wild type and displayed only a modest delay in chromosome synapsis and nuclear division (see section 3.2.1). To examine the effect of *SWC2* on *pph3*Δ mutant, we constructed a *pph3*Δ*, swc2*Δ double mutant and analyzed it by nuclear spreads. Surprinsingly, chromosome synapsis was fully restored in *pph3*Δ*, swc2*Δ double mutants albeit with a delay, moreover the spore inviability of *pph3*Δ single mutant (60% 20 tetrads) was also rescued (90% spore viability in *pph3*Δ, *swc2*Δ 20 tetrads, Figure 20A B)). As in the *swc2*Δ single mutant, the synapsis delay of *pph3*Δ, *swc2*Δ double mutant is further manifested by an accumulation of SC component (Zip1 polycomplexes) in the majority of cells. These data identify *SWC2* as a mediator of the *pph3*Δ chromosome morphology defect.

This result raised the possibility that a chromatin remodeling complex containing Swc2 interferes with synapsis by binding to chromatin in the absence of Pph3. To determine whether Swc2 is a target of Pph3, a functional version of Swc2 tagged with the hemagglutinin (3HA) epitope was used to compare the localization of the protein on the chromosomes in *pph3*Δ and wild type cells (by chromosome spreading and by ChIP-chip).

First we established the localization of Swc2 in wild type cells. Swc2 localizes periodically all along the chromosomes, with no particular enrichment at

centromeres (Figure 20D). When compared to Rec8, there is a good overlap between peaks at 1kb resolution, establishing a tendency of Swc2 to bind to chromosomal axis sites (Figure 20D). No overlap was found with DSB signals as defined by (Pan et al. 2010; Figure 20E).

Interestingly, in the *pph3*Δ mutant the Swc2 profile was strongly reduced (by a factor of 3 to 4) (Figure 20F). However, signal to background ratio was much less affected, still signal to noise ratio was 20 to 50% higher in the wild type. At this stage this result is to be considered preliminary. The reduction of Swc2 binding on chromosomes in the absence of *PPH3* was confirmed in an independent ChIP-qPCR experiment as shown on Figure 20G. Why would Swc2 then affect synapsis negatively in the *pph3*Δ mutant, if much less of it bound to chromatin? The simplest explanation is that a chromatin unbound form of Swc2 interferes with synapsis, which also helps to explain, why other components of the Swr1 chromatin remodeling complex do not show this phenotype (see below).

In addition to *SWC2* we also analyzed other components of the SWR complex for their ability to suppresss the *pph3*Δ synapsis defect. It is interesting and puzzling that the synapsis phenotype of *pph3*Δ, *ldb7*Δ and *pph3*Δ, swr1Δ is indistinguishable from that of *pph3*Δ single mutants (Figure 20B,C). Ldb7 and Swr1 are subunits of the RSC and SWR chromatin remodeling complexes respectively, implying that the simple disruption of these complexes is not the reason for suppression. Either Swc2 is part of a different complex in meiosis, which needs to be antagonized by Pph3 to allow synapsis, or perhaps, Swc2 acts independently of its role in a remodelling complex to mediate signalling of DSB damage. Pph3 would then be required to localize it efficiently on the chromosome, which may inactivate the signalling.

3.4.4 Restoration of synapsis in pph3Δ, pch2Δ mutant

Pch2 is an AAA+ ATPase family member conserved in evolution between yeast and man, that plays important roles during meiosis. It was found as being required for checkpoint arrest of *zip1*Δ mutant (San-Segundo and Roeder, 1999). In *pch2*Δ single mutants DSBs persist longer and both crossover and noncrossover formation are delayed (Hochwagen et al., 2005; Borner et al., 2008; Zanders et al., 2009). *pch2*Δ is also defective in suppressing intersister repair (Zanders et al., 2011). Pch2 probably monitores the progress of DSB repair and delays pachytene exit upon repair problems. It also negatively regulates axis formation and synapsis (Borner et al., 2008; Joshs et al., 2009; Roig et al., 2010), but how these processes are regulated is unknown.

Because Pch2 is a negative regulator of synapsis, we tested wether Pch2 mediates the synapsis defect of *pph3*Δ. The *pch2*Δ single mutant progresses through meiosis with wild type kinetics and accumulates fully synapsed chromosomes (29% of fully synapsed nuclei compared to typically 10-18% in wild type cells at 5-6 hours in SPM, Figure 21A,B). Disassembly of the SC occurs with normal timing relative to wild type.

Interestingly, synapsis is fully restored in *pph3*Δ*, pch2*Δ double mutant and accumulates above wild type levels similar to the *pch2*Δ single mutant (29% of nuclei with fully synapsed chromosomes at 6 hours in SPM, Figure 21A, B). This indicates that *pch2*Δ is epistatic over *pph3*Δ concerning the ability to synapse. However formation of synapsis is slightly delayed (1-2 hours) in the double mutant compared to both, the *pch2*Δ single mutant and wild type.

The defect of *pph3*Δ mutant in meiotic progression is slightly alleviated by the *pch2*Δ mutation (~61% of *pph3*Δ*, pch2*Δ mutant cells have undergone at least one meiotic division after 10 hours in SPM medium as compared to ~25% in *pph3*Δ single mutant; Figure 21C), indicating that another factor inhibits cell cycle progression in the absence of PP4. Despite restoration of synapsis, spore viability is dramatically reduced in *pph3*Δ*, pch2*Δ double mutant, down to 22.5% (n= 20 tetrads) from 60% (n= 20) in the *pph3*Δ single mutant. Tetrads contained

preferentially 0, 2 or 4 viable spores (10, 5, 1 tetrads, respectively), indicating increased chromosome missegregation caused by a shortage in crossovers and chiasmata. These results identify Pch2 as the key mediator of *pph3*Δ synapsis defect and suggest that the main role of PP4 in synapsis is to downregulate Pch2.

Similar to Pch2, the silencing factors Sir2 and Dot1 also affect the meiotic arrest of the *zip1*Δ mutant (San-Segundo and Roeder, 1999; 2000). However, as shown in Figure 21B,C, the phenotype of the *pph3*Δ, *dot1*Δ double mutant is similar to that of the *pph3*Δ single mutant, indicating that *DOT1* is not required for mediating the synapsis defect of *pph3*Δ mutant.

3.4.5 Deletion of *FPR3* or *MEK1, but not of MEC1* bypasses the meiotic arrest of *pph3*Δ.

The proline isomerase Fpr3 is involved in the meiotic recombination checkpoint, by preventing premature adaptation to chromosomal damage by inhibiting PP1 (Glc7) (Hochwagen et al., 2005). Fpr3 impedes SC assembly in the absence of DSBs and in the absence of SUMO E3 ligase Zip3 (MacQueen et al., 2009). Fpr3 is phosphorylated in response to meiotic DSBs, but the phosphomodification is only seen for molecules interacting with Glc7, after co-immunoprecipitation (Hochwagen et al., 2005). In our hands no phosphoshift was visible after Western blotting, consistent with these earlier results.

The *fpr3*Δ single mutant progresses through meiosis with wild type synapis, wild type kinetics and yields viable spores. However, in contrast to Pch2, deletion of Fpr3 restores synapsis only to a limited extent (4% fully synapsed nuclei at 6 hours, Figure 22B). On the other hand the meiotic arrest of the *pph3*Δ mutant is largely alleviated by the deletion of *FPR3*, although a 1-2 hour delay relative to wild type remains (Figure 22A).

The *pph3*Δ*, fpr3*Δ double mutant sporulates with almost the same efficiency as wild type (97% after 24hours in SPM) and yields mostly inviable spores (22% 20 tetrads) compared to 60% for the *pph3*Δ single mutant (20 tetrads) and the *fpr3*Δ single mutant (93%, 20 tetrads). The number of 0, 2 and 4 viable spore tetrads was (14,3,2), respectively, indicating that, as in the *pch2*Δ*, pph3*Δ double mutant, lack of crossovers may be causing spore lethality here. The kinetics of Rad51 focus formation suggests that DSBs are generated normally in *pph3*Δ*, fpr3*Δ double mutant and are repaired with wild type timing (Figure 22A). This observation suggests that the reason for a lack of sufficient numbers of crossovers may come from a) a defect in designating sufficient crossover numbers or b) a defect in maintaining crossover designation. Because *pph3Δ* behaves like a ZMM mutant (reduced synapsis, normal NCOs, reduced COs), the reduced crossover numbers in the *pph3Δ, fpr3Δ* double mutant may imply that Fpr3 may help buffering the ZMM defect of *pph3Δ* cells. We can't rule out that Fpr3's interaction with PP1, which inhibits PP1 is controlled by Fpr3 phosphorylation, which might in turn be controlled by Pph3.

Mek1 is required for normal levels of DSBs and for continuous synapsis. Mek1 is a meiosis-specific kinase activated via Hop1 phosphorylation and Red1 (Niu H, et al., 2005). After DSB formation Mek1 acts to downregulate inter-sister repair, upon Hop1 and Red1 dimerization following the phosphorylation of Hop1 by Mec1/Tel1 (ATR/ATM). To determine whether *mek1*Δ *or mec1-1 or rad54*Δ suppresses the meiotic defects (chromosome synapsis, nuclear division) of *pph3*Δ cells, the *pph3*Δ*, mek1*Δ ; *pph3*Δ*, mec1-1* and *pph3*Δ*, rad54*Δ double mutants were analyzed. Chromosome synapsis is not rescued in *pph3*Δ*, mek1*Δ, however Rad51 focus formation is dramatically reduced, both in the *mek1*Δ single mutant and in the *pph3*Δ*, mek1*Δ double mutant (Figure 22A,B), consistent with the requirement of Mek1 for wild type levels of DSB formation.

The progression through meiosis is vastly improved compared to the *pph3*Δ single mutant and yields inviable spores (0% 40 tetrads) strongly suggesting that the attenuation of DSB formation in the *mek1*Δ background leads to an

attenuation of the kinase response, which in turn leads to a reduced requirement for the phosphatase PP4 (Figure 22A). Preliminary results of *pph3*Δ*, mec1-1* double mutant showed that neither chromosome synapsis, nor nuclear division defects of *pph3*Δ mutant was improved in the absence of *MEC1* (Figure 22A,B). Nuclear division as well as the synapsis defect of *pph3*Δ were not restored by *RAD54* deletion as suggested by *pph3*Δ*, mek1*Δ double mutant synapsis phenotype (Figure 22A,B).

3.4.6 Restoration of nearly wild type meiosis in *pph3*Δ*, pch2*Δ*, fpr3*Δ triple mutants

We find that *PCH2* and *SWC2* inhibit synapsis in the *pph3*Δ mutant, while *FPR3* prevents meiotic progression. In order to determine whether these factors are the only ones preventing normal meiosis in the *pph3*Δ background, *pph3*Δ, *pch2*Δ, fpr3Δ and *pph3*Δ, swc2Δ, fpr3Δ triple mutants were constructed and analyzed.

Indeed, the *pph3*Δ*, pch2*Δ*, fpr3*Δ triple mutant shows high levels of nuclei with completely synapsed chromosomes (20% at 6 hours in SPM), progresses through meiosis with strongly improved kinetics and generates viable spores (95%, 40 tetrads, Figure 23A, B, C). The average number of Rad51 foci per nucleus decreases similar to wild type but with a slight delay (1-2 hours) indicating that DSB formation and repair are largely restored (Figure 23C).

The *pph3*Δ*, swc2*Δ*, fpr3*Δ triple mutant only shows weak suppression of the synapsis defect (1% of nuclei with fully synapsed chromosomes). However, progression through meiosis is much improved and very similar to the *pph3*Δ*, fpr3*Δ double mutant. Like the double mutant, this triple mutant generates mostly inviable spores (20% spore viability, 40 tetrads, with high numbers of 0, 2 and 4 viable spore tetrads). The kinetics of Rad51 focus formation is similar to the *pph3*Δ*, pch2*Δ*, fpr3*Δ triple mutant (Figure 23A, B, C). That suppression of the

synapsis defect is slightly weaker than for the *pph3*Δ*, swc2*Δ double mutant is surprising, but may be explained by the faster progression in the *fpr3*Δ background. The fact that *swc2*Δ does not improve the suppression in the *fpr3*Δ background, suggests that Swc2 acts in the same pathway as Fpr3, in contrast to Pch2, which clearly acts in a separate pathway. Apparently activation of PP1 via deletion of Fpr3 is sufficient to antagonize the negative effects of Swc2 in a *pph3*Δ mutant background.

3.4.7 Removal of phosphorylated H2A-S129 in *pph3*Δ*, pch2*Δ*, fpr3*Δ triple mutants

To understand better the mechanism of suppression of the *pph3*Δ phenotype by *pch2*Δ and *fpr3*Δ we asked whether the accumulation of H2A-S129-P is also abolished, together with the restoration of SC and meiotic progression. Indeed, the abnormal accumulation of H2A-S129-P, observed in Western blots of *pph3*Δ cells is completely removed in the triple mutant (Figure 23D). This opens the question, whether deletion of *PCH2* or of *FPR3* is sufficient to remove H2A-S129-P, particularly because deletion of *FPR3* is thought to prematurely activate PP1 (Glc7), which could target H2A-S129-P. Surprisingly, deletion of either one was not sufficient to prevent H2A-S129-P accumulation (Figure 23D). Deletion of *PCH2* lead to a somewhat decreased accumulation of H2A-S129-P at 10hours in SPM, while deletion of *FPR3* surprisingly had no effect at all. Therefore it seems that *pch2*Δ and *fpr3*Δ are synthetic concerning the dephosphorylation of H2A-S129-P, suggesting that they may have partially overlapping roles in transducing and maintaining the Mec1/Tel1 checkpoint signal.

Because also *swc2*Δ partially improved the *pph3*Δ synapsis phenotype and spore viability, we also investigated the *pph3*Δ*, swc2*Δ*, fpr3*Δ*.* However, no change of H2A-S129-P levels compared to *pph3*Δ single mutants were observed

(Figure 23D), suggesting that the suppression of the synapsis defect by *swc2*Δ occurs by a fundamentally different mechanism than that by *pch2*Δ.

3.5 Crosstalk between Histones promotes synapsis

3.5.1 H2B-K123 monoubiquitination promotes synapsis

Rad6, Bre1 and Lge1 form a complex that is required for histone H2B monoubiquitination on lysine123 in budding yeast (Robzyk et al., 2000). Rad6 is a ubiquitin conjugating enzyme (E2), Bre1 is a ubiquitin ligase (E3) and Lge1 promotes H2B monoubiquitination by controlling the interaction between Bre1 and Ubp8, a ubiquitin specific protease.

*rad6*Δ, *bre1*Δ and *lge1*Δ mutants were included in a pilot screen (Alexander Woglar, master Thesis) where they were identified with strongly defective chromosome synapsis. This result is in agreement with an earlier report about a decrease in DSB formation in *rad6*Δ and *bre1*Δ mutants (Yamashita et al., 2004). The synapsis defects of *bre1*Δ and *lge1*Δ were also found in a parallel work carried out in our lab (Jordan et al., 2007).

In summary *rad6*Δ and *bre1*Δ cells showed only Zip1 foci and polycomplexes and no partial synapsis (Figure 24A, B). In contrast *lge1*Δ cells had a milder phenotype, producing reduced numbers of nuclei with partial synapsis and even 1% of nuclei with fully synapsed chromosomes after a delay (at 8 hours after induction of meiosis, Figure 24A, B). Nuclear division is almost absent 10 hours after incubation in SPM and FACs analysis reveals a delay in pre-meiotic DNA replication in all three mutants (Woglar A, master thesis). An average of 5 Rad51 foci per nucleus was detected in the *bre1*Δ mutant after 4 and 5 hours in SPM and a maximum of 12 foci at 6 hours, compared to ~18 foci in the wild type where the maximum is at 4 hours (Figure 24C). This confirms a reduction in DSB formation in the *bre1*Δ mutant and agrees with data from the

Shinohara lab (Yamashita et al., 2004). The reduction in DSBs observed by us (Figure 16A) and by the Shinohara lab (Yamashita et al., 2004) doesn't fully explain the complete absence of synapsis observed in *rad6*Δ and *bre1*Δ mutants. This hints at an additional function of these two genes in promoting synapsis, independent of promoting DSB formation. The formation of crossovers and noncrossovers was almost undetectable until 10 hours in SPM in *rad6*Δ mutant (Figure 16A) consistent with the result obtained in the Shinohara lab (Yamashita et al., 2004).

To determine whether Rad6*,* Bre1 and Lge1 dependent monoubiquitination of *H2B-K123* is fully responsible for the synapsis defects in *rad6*Δ and *bre1*Δ mutants, the *H2B-K123R* mutant (*htb1-K123R* and *htb2-K123R*), which prevents H2B monoubiquitination was obtained from A. Shinohara and analyzed.

Indeed*,* the *H2B-K123R* mutant exhibits a strong defect in chromosome synapsis and nuclear division, however not quite as severe as *rad6*Δ and *bre1*Δ. Rather they are more similar to lge1Δ, as small numbers of nuclei with partial SC and even occasional ones with almost complete synapsis were found (Figure 24A, B). Nevertheless, this shows that *H2B-K123R* ubiquitination plays the major role in promoting synapsis. Rad6 and Bre1 seem to have additional targets of minor importance that also promote synapsis. The fact that DSBs are formed, although at reduced numbers suggest that also the ubiquitination of H2B promotes synapsis, also beyond promoting normal DSB formation. Clearly Rad6 and Bre1 have important roles for synapsis, beyond DSB formation.

Meiotic progression was found similarly delayed by *bre1*Δ and by *H2B-K123R* by us, consistent with (Yamashita et al., 2004). Given the prominent defects in synapsis, the mild spore lethality of all of these mutants, except *rad6*Δ*,* which hardly forms any spores, may seem surprising, but more and more evidence accumulates, showing that synapsis is not essential for spore viability. Spore viability of *H2B-K123R* mutants was nearly wild type after producing 52% tetrads in 24 hours in liquid SPM. *bre1*Δ and *lge1*Δ also produce high spore viability (75% and 52%, respectively, Woglar A, master Thesis). In terms of

promoting meiotic progression Rad6 is most important, followed by Bre1 and Lge1 and finally H2B-monoubiquitination in our hands.

3.5.2 H3K4 trimethylation defective cells proceed further in synapsis than H2B-K123R mutants

H2B-K123 monoubiquitination is required for the trimethylation of histone H3K4 by COMPASS (a complex containing Set1 methyltransferase and 7 other subunits) (and H3K79 by Dot1 methyltransferase (Dover et al., 2002: Nakanishi et al., 2009).

The crosstalk between monoubiquitylated histone H2B and trimethylated histone H3K4, H3K79 prompted us to ask, whether H2B-K123 monoubiquitination works through trimethylation of H3K4 and/or H3K79 is required for synapsis. To address this question, *set1*Δ, *dot1*Δ single mutants and *set1*Δ*, dot1*Δ double mutant were generated and analyzed. The deletion of *SET1* causes a slight delay in chromosome synapsis and Zip1 ploycomplexes are more prominent in *set1*Δ mutant cells compared to the wild type. Nuclear division is delayed and reduced in *set1*Δ (85% of cells have passed at least one meiotic division 10 hours after transferred into the sporulation medium compared to 95% in wild type cells after 8 hours in SPM). About 8.5 (4 hours) and 11 (5 hours) Rad51 foci per nucleus are detected in cells lacking *SET1* compared to an average of 18 (4 hours) foci in wild type cells (Figure 24B, C). The spore viability is the same for *set1*Δ and wild type cells, These observations indicate a decrease and a delay in DSB formation in *set1*Δ mutant cells and are consistent with reports by the Nicolas lab (Borde V et al., 2008).

In contrast, cells lacking *DOT1* behave as the wild type during meiosis, indicating that Dot1 is not required during meiosis in an otherwise wild type strain in budding yeast (thus, trimethylation of H3K79 is not essential for normal levels of DSB formation, chromosome synapsis and nuclear division in budding yeast meiosis).

To investigate, whether H3K4 and H3K79 methylation might be partially redundant we examined the *set1*Δ*, dot1*Δ double mutant. The delays observed in the *set1*Δ single mutant were further exacerbated in the *set1*Δ*, dot1*Δ double mutant. The average number of Rad51 foci *was* dramatically reduced to 4 foci at 4 hours in SPM, but went up to 14 foci per nucleus with a 1hour delay. Chromosome synapsis was delayed for about 2hours in the double mutants compared to wild type (Figure 24A, B, C). Nuclear divisions were slightly delayed relative to *set1*Δ (73% of cells have completed the first meiotic division after 10 hours in SPM compared to 85% in *set1*Δ single mutant).

In summary the deletion of *SET1* causes a reduction and a delay in DSB formation and a delay in chromosome synapsis, which nevertheless reaches wild type levels. Thus, H3K4 trimethylation may be required for wild type levels of DSBs and possibly for timely processing of recombination intermediates. 84% of the DSB sites display a significant reduction of DSB frequency in the absence of *SET1 (*Borde V et al., 2008). The meiotic defects of *set1*Δ are further exacerbated in *set1*Δ*, dot1*Δ double mutants, indicating that in the absence of *SET1* the DSB- and synapsis-relevant function of Set1 can to some extent be carried out by Dot1. The double mutant shows extensive, but usually incomplete synapsis and is thus less severely affected than the *htb1,2-K123R* mutant. We conclude that a function of histone H2B-monoubiquitination other than the recruitment of Set1 and Dot1 is responsible for the stronger synapsis defect in *htb1,2-K123R.*

4. DISCUSSION

4.1 A sensitive screen for genes involved in synapsis

By employing a sensitive screen protocol, we have identified mutants affecting meiotic chromosome synapsis from a collection representing precise ORFs deletions of almost all non-essential genes of the yeast *Saccharomyces cerevisiae*. Of the 3630 ORFs screened, 132 candidates were unable to induce the meiotic program and 392 candidates (11%) displayed Zip1 foci or fragments of SC in the SK1/BY hybrid background. These 524 candidates include, genes well described for their roles in the activation of meiosis such as (*IME1, IME2, UME6*); 10/12 genes essential for DSB formation and synapsis (MEI4 and XRS2 missed); genes of known synapsis roles such as (*SPO16, MSH4, MSH5*). We found genes from almost all cellular processes involved in meiotic chromosome synapsis, although to varying degrees (Figure 6, A, B, C, D). Our results document the fact that, rather than being an isolated process within the cell´s nucleus, synapsis rquires the correct execution of a large number of intertwined biological processes within the nucleus, in the cytosol and even the cell´s surrounding. Almost all genes initially contained in the set of 3630 ORFs screened, known to be required for meiotic recombination and/or SC formation were re-identified, arguing for the sensitivity of the screen.

In interpreting the results of this screen, we acknowledge that many biological processes need to function seamlessly, to guarantee normal levels and kinetics of synapsis. These are: Induction of the meiotic program, pre-meiotic S-phase, correct expression of meiotic genes, DSB formation, DNA-repair, chromosome morphogenesis and finally the ZMM pathway (specific pathway that carries out synapsis). As defects in premeiotic S-phase may cause a compromised onset of meiotic recombination, we are aware that a fraction of our mutants actually may not affect meiotic recombination in a strict sense. We have tried to measure the execution of S-phase using FACS analysis in a more detailed analysis, but the best way to differentiate prophase from S-phase defects would be to study meiotic knockdown constructs, such as genes put

under a mitosis specific promoter (e.g. *pCLB2*), or to eliminate proteins using the anchor away technology (Haruki et al., 2008).

When a subset of 30 of the identified ORFs were deleted in the SK1 strain background, the phenotypes could be evaluated in more detail in time courses. All but 4 of the resulting mutants showed clear differences to wild type concerning the extent or the timing of synapsis, or they show an aberrant progression through the different stages of synapsis. Only one candidate was completely devoid of synapsis (rim4Δ) and 3 candidates (*ecm11*Δ*, ymr196*Δ*,* and *yor296*Δ) had very few if any cells showing complete synapsis. We attribute the discrepancy between SK1 and BY/SK1 hybrid phenotypes to the more extensive analysis in the secondary screen (time course!), which uncovers delayed synapsis and to the more robust expression of the meiotic program in SK1 cells. However, we also consider, that some candidates may have been selected because of statistical fluctuations, even though the thresholds were set up to avoid picking up such fluctuations.

4.2 H2B monoubiquitination modulates chromosome synapsis

We have shown that various processes including pre-meiotic DNA replication, DSB formation, chromosome synapsis and nuclear division are strongly impaired or delayed in *rad6*Δ*, bre1*Δ and *lge1*Δ cells. Similar results were reported for *bre1*Δ and *lge1*Δ from an independent screen in our lab (Jordan et al., 2007). Also, *rad6*Δ and *bre1*Δ were reported to be strongly defective for DSB formation, before, but had not been analyzed for SC formation (Yamashita et al., 2004). These three mutants are components of the cellular machinery required for histone *H2B-K123* monoubiquitination (Nakanishi et al., 2009). We find that the meiotic defects of the *H2B-K123R* mutant is very similar, although slightly less severe, to that of *rad6*Δ*, bre1*Δ or *lge1*Δ mutants, which are required for *H2B-K123* monoubiquitylation. Therefore *H2B-K123* monoubiquitination appears to be the major pathway through which Rad6*,* Bre1 and Lge1 modulate

chromosome synapsis, but there seems to be a minor pathway through which they can promote some delayed, residual synapsis without monoubiquitinylating H2B.

4.3 Delayed synapsis in the absence of COMPASS

Our results show that *DOT1 (*H3K79 trimethylation) is dispensable for normal chromosome synapsis. In contrast, synapsis and nuclear divisions are delayed and reduced in *set1*Δ and *set1*Δ*, dot1*Δ double mutants. Rad51 focus formation is also reduced in *set1*Δ and *set1*Δ*, dot1*Δ double mutants. These results are in line with earlier results of others, which showed that COMPASS (H3K4 trimethylation) is required for efficient DSB formation (Borde et al., 2009). This function is likely conserved as the mammalian homologue of COMPASS (*PRMD9*) has also been shown to be an important determinant of meiotic recombination initiation sites, thus in promoting DSB formation (Baudat et al., 2010; Berg et al., 2010). If, as published, global DSB formation is really strongly reduced in *set1*Δ mutants, then finding extensive synapsis in this mutant reveals the presence of a buffering system, were a small fraction of DSBs are sufficient to trigger synapsis, albeit with a delay. Clearly, *set1*Δ*, dot1*Δ double mutants do much better than *H2B-K123R*, arguing for an unidentified role of H2B monoubiquitination beyond the recruitment of a methyltransferase.

4.4 Suppressing the meiotic defects of PP4 mutants.

Previous studies in our and other laboratories (Alexander Woglar, Master Thesis) (Keogh et al., 2006; Falk et al., 2010a) identified the PP4 complex (Pph3, Psy2) as required for several meiotic processes. Here we found independently that Pph3 is required for proper pre-meiotic DNA replication, DSB repair, and crossovers formation. Chromosome synapsis and nuclear divisions are nearly completely abolished. We show that the synapsis defect of *pph3*Δ is very mildly improved in the *hta1, 2-S129A* background. Phospho-H2A-S129 is an important and conserved histone modification in response to DNA damage. It is known that

PP4 dephosphorylates various ATM, ATR substrates including Phospho-H2A-S129 and Rad53, thereby allowing recovery from checkpoint-induced arrest (Keogh et al., 2006; O'Neill et al., 2007). However, mutating H2A-S129 to alanine does not show severe consequences in yeast meiotic recombination.

We could restore synapsis in *pph3*Δ mutant by deleting the SWR complex component *SWC2*. The role of the SWR complex has been reported to be the exchange of H2A with the histone variant H2A.Z (encoded by the *HTZ1* gene in yeast). Surprizingly, deletion of *HTZ1* has no effect on the *pph3*Δ phenotypes. In vegetative DNA repair *swc2*Δ and htz1Δ mutants are both defective in timely resection of DSB ends (van Attikum et al., 2007; Kalocsay et al., 2009) and the recruitment of H2A.Z to the break sites is strictly dependent on *SWC2* (Kalocsay et al., 2009). Other known binding partners of Swc2, such as *swr1*Δ or *ldb7*Δ did not show suppression of the *pph3*Δ synapsis defects. We therefore believe that deletion of *SWC2* suppresses by a mechanism independent of its chromatin remodeling activity. Also, we observed by ChIP that Swc2 protein requires Pph3 for high steady state levels of interaction with chromatin, and that only in PPH3 cells Swc2 protein is modified at about 5 hours in SPM. These observations argue for a mechanism, in which free Swc2 (unbound to chromatin) is responsible for the synapsis defect.

Our main result, illuminating the role of PP4 is a strikingly strong epistatic interaction with Pch2 concerning chromosome synapsis. Intriguingly, *pch2*Δ*,* which accumulates synapsis to higher levels than wild type, is epistatic over *pph3*Δ for the synapsis defect. However, while synapsis reaches very high levels in the double mutant, a 1-2 hour delay relative to the *pch2*Δ single mutant was observed. This delay could stem from problems of the *pph3*Δ mutant causing a delay in premeiotic S-phase. Still, this identifies Pch2 as a key target of PP4 function. We propose that Pch2 anatagonizes synapsis in response to certain phosphorylation events, which signal the presence of unrepaired DNA damage. In this way, Pch2 could coordinate SC formation with repair and make sure that synapsis does not occur prematurely, before the homology check has been successfully concluded. However, Pch2 requires inactivation upon decrease of

checkpoint signaling, which seems to be the key role in synapsis of PP4. Although *pph3*Δ*, pch2*Δ double mutants show higher than wild type levels of synapsis, nuclear divisions remain only partially improved (40% past M1 at t=10 hours, instead of 25%) and spore viability is strongly reduced (22.5% compared to 60% in the *pph3*Δ single mutant). *pph3*Δ*, pch2*Δ double mutant might be reduced for crossovers, judging from the high proportions of tetrads with 2 or zero viable spores. Checkpoint functions of Pch2 during meiosis have been described: *pch2*Δ improves meiotic progression of *zip1*Δ*, zip2*Δ*,* and *dmc1*Δ mutants. In these cases meiosis commences without synapsis and spore viability is further reduced compared to the single mutants (San-Segundo and Roeder, 1999). Our results are strikingly different from these observations, in that *pch2*Δ improves synapsis, but does not affect cell cycle progression very much. In addition a function of Pch2 in promoting timely and efficient recombination have been reported (Borner et al., 2008; Roig et al., 2010; Zanders et al., 2011).

Deletion of DOT1 bypasses the arrest of zip1Δ and dmc1Δ mutants and allows the repair of meiotic DSBs by a Rad54-dependent recombination pathway between sister chromatid (San-Segundo and Roeder, 2000b). These authors proposed that Dot1, Pch2, Sir2 act at the same step in the pachytene checkpoint. In contrast, we found that the deletion of *DOT1* and of *RAD54* have no effect on *pph3*Δ*.*

Interestingly, we found that deletion of the proline isomerase protein *FPR3* almost completely suppresses the meiotic arrest of *pph3*Δ single mutant*, pph3*Δ*, pch2*Δ and *pph3*Δ*, swc2*Δ*.* The double and triple mutants display almost wild type sporulation frequencies. While spore viability in the *pph3*Δ*, fpr3*Δ double mutant was only 20%, unexpectedly, the spore viability of the triple mutant *pph3*Δ*, fpr3*Δ*, pch2*Δ*,* (but not of *pph3*Δ*, fpr3*Δ*, swc2*Δ) was almost wild type. We suggest that in the pph3Δ, pch2Δ double mutant, synapsis is uncoupled from the maturation of important recombination intermediates. This maturation is impaired by the phosphor-status of a (unknown) substrate, which may become dephosphorylated upon premature activation of PP1 (in *fpr3*Δ). But also, *pph3*Δ*, fpr3*Δ mutants have

a problem, because dephosphorylation of that (unknown) substrate in the presence of Pch2 does neither restore synapsis nor spore viability.

Moreover, the accumulation of phospho-H2A-S129 observed in *pph3*Δ mutant completely disappears in the *pph3*Δ*, fpr3*Δ*, pch2*Δ triple mutant, but not in either double mutants (*pph3*Δ*, fpr3*Δ and *pph3*Δ*, pch2*Δ), although a slight decrease in phospho-H2A-S129 levels was observed at 10hours in SPM compared to the *pph3*Δ single mutant. An unknown phosphatase might be activated in the *pph3*Δ*, fpr3*Δ*, pch2*Δ triple mutant that dephosphorylates phospho-H2A-S129. Thus, the meiotic defects of *pph3*Δ mutant are almost completely relieved in *pph3*Δ*, fpr3*Δ*, pch2*Δ triple mutant.

4.5 Repair or checkpoint factor: the meiotic context is paramount

We show that the meiotic prophase I arrest of *pph3*Δ mutant is completely relieved by deletion of *FPR3, MEK1* but not by the point mutant *mec1-1*. This relief of the meiotic block is not due to the suppression of all the meiotic defects of *pph3*Δ mutants as exemplified by the severe reduction in spore viability in *pph3*Δ*, fpr3*Δ and *pph3*Δ*, mek1*Δ compared to *pph3*Δ single mutant. The lower spore viability in the double mutants points to a disruption of checkpoint functions. *FPR3* and *MEK1* were shown to have checkpoint functions (Hochwagen et al., 2005a; Niu et al., 2005a). The *pph3*Δ*, mec1-1* double mutant showed a synthetic phenotype manisfested by almost a complete lack of nuclear division and sporulation. This argues strongly against Pph3's main role being an antagonist to Mec1.

In the course of this work, we found that deletion of *PCH2* fully restores synapsis in the *pph3*Δ mutant, but has little effect on the meiotic arrest, while additional deletion of *FPR3* restores everything. These observations suggest that Pch2 monitors a repair-intermediate to couple its turnover with synapsis (not with cell cycle progression). Fpr3, in contrast, monitors another product to couple its turnover with cell cycle progression. Uncoupling of both surveillance mechanisms

leads to restoration of largely normal meiosis with high spore viability. I believe that further investigations along these lines will continue to greatly improve our understanding of the role of these factors in meiotic recombination. Because these factors are conserved, this should be illuminating, eventually, also for better understanding human meiosis.

Figure legends

Figure 1: Stages of Mitosis and Meiosis.

a) Mitosis: a1 diploid mother cell, a2 DNA replication, a3 Metaphase, a4 2 identical diploid daughter cells.

b) Meiosis: b1 diploid mother cell, b2 DNA replication, b3 crossover formation, b4 segregation of homolog (M1), b5 Metaphase II, b6 segregation of sister chromatids into haploid gametes (modified from Brar and Amon, 2008).

Figure 2: Morphogenesis of chromosomes during meiosis (from Interphase until Telophase II; kindly provided by Prof. Joseph Loidl, University of Vienna, Austria).

Figure 3: Relationships between meiotic recombination and the synaptonemal complex formation from leptotene to diplotene (modified from Hunter, 2006; Martin Xaver (chromosome spreads).

DSBs: DNA double strand breaks

ND: Nascent D-loop

SDSA: Synthesis dependent strand annealing

SEI: Single invasion

DHJs: Double Holliday junctions

Figure 4: Model of the SC assembly;

LE: Lateral elements (refers to axial element) (in blue ovals: cohesin & condensin, in green ovals: Red1, Hop1).

CE: Central region (forms by antiparallel association of Zip1 dimers in the N-terminal region) (Page and Hawley, 2004).

Figure 5: Scheme of the SK1/BY screening procedure to generate homozygous diploids of ORFs deleted in the BY strain background.

Y: Rec8-HA3::ura3::LEU2

Xi: Gene of interest or ORF deleted and replaced by the kanamycin cassette in the BY strain background.

HO: HO endonuclease which is responsible for mating type switching

ste4^{ts}: Temperature sensitive allele of the sterility gene *STE4*

cyh2R: Recessive allele of the *CYH2* gene that confers resistance to cycloheximide.

Figure 6: A, B, C, D: Candidate ORFs were sorted categorized based on GO terms listed in the *Saccharomyces* genome database (SGD). Information contained in this database was used to improve this assignment manually for each ORF.

Figure 7: A, B, C: Zip1 and Rad51 staining during the leptotene, zygotene and pachytene stages of the meiotic prophase 1 in the wild type SK1. A meiotic timecourse experiment was carried out and sampled after 4, 5 and 6 hours in SPM, followed by chromosome spreading and immunostaining with antibodies against Zip1 and Rad51. The spread and labeled chromosomes were analyzed by fluorescence microscopy. Figures represent examples for the different categories used to classify nuclei. See also experimental procedures (2.2.6).

Figure 8: A) Column diagrams showing the frequency of nuclei categorized based on Zip1 appearance on chromosome spreads for each of the indicated mutants. Meiotic timecourse experiments were performed and sampled after 0, 2, 4, 5, 6, 7, 8 and 10 hours in SPM for chromosome spreads, followed by immunolabeling of the SC central component Zip1 and the recombinase Rad51. For each of the candidates, 100 cells were evaluated for Zip1 morphology and classified according to the extent of Zip1 staining of synapsed regions at each timepoint (No Zip1, Zip1 foci, Zip1 short stretches, Zip1 long stretches and almost complete SC). B) Average Rad51 foci per nucleus: 50 nuclei were counted for Rad51 staining (dot-like staining termed foci) and the average number of foci per nucleus plotted as shown on the figure. C) At each timepoint ethanol-fixed, DAPI stained cells containing 1, 2 or 4 nuclei were counted (mononucleates, binucleates, tetranucleates). The graph shows the sum of the percentage of bi- and tetranucleate cells per timepoint, corresponding to the number of cells that have undergone at least the first meiotic division. D) Diagrams displaying the efficiency of pre-meiotic DNA replication. Samples were taken at indicated time points (top right) and subjected to FACs analysis (section 2.2.6). 2C and 4C refer to DNA content (before and after DNA replication).

Figures: 9A,B,C ; 10A,B,C ; The experimental procedures were as described in Figure 8.

Figures 10 D,E: D) Formaldehyde fixed whole cells (taken after 4 hours in SPM) were stained with antibodies against the HA epitope of Rim4-HA3 (see section 2.6.3) and analyzed under Fluorescence microscopy.

E) Formaldehyde fixed whole cells (sampled at different timepoints; 2, 4, 5, 6, 7, 8 and 10 hours in SPM) were immunostained with antibodies to yeast tubulin to visualize the meiotic spindle with the fluorescent microscope. The different morphologies of the spindle were scored (Monopolar or prophase I

spindle = duplicated but unseparated spindle pole body; Bipolar (duplicated and separated spindle pole body); Two bipolars and Post-anaphase II spindle).

Figure 11: A) Diagrams displaying the efficiency of pre-meiotic DNA replication in wild type and shu mutants. Samples were taken at indicated time points and subjected to FACs. 2C and 4C are the percentage of cells with 2C and 4C DNA content at each time point. B): Average number of Rad51 foci per nucleus at indicated timepoints in wild type and (*shu2*Δ*, csm2*Δ and *psy3*Δ*)* mutants.

Figure 12: Ectopic Recombination System (hotspot locus) used to assay DNA double strand breaks (DSBs), crossovers (CO) and noncrossovers (NCO). A 3.5 Kb URA3-ARG4 and URA3-arg4-Ecpal9 constructs insert on the left arm of chromosome III, respectively in the *LEU2* locus (leu2::URA3-ARG4) on one homologue (mom, P1) and in the *HIS4* locus (his4::URA3-arg4-EcPal9) on the other homologous chromosome (dad, P2). The palindrome at +9 of the *ARG4* coding sequence is indicated by a lollipop (see P2). During meiosis, DSBs occur upstream of *URA3* (DSB1) and an upstream of *ARG4* (DSB2) coding sequences and the two inserts frequently recombine. For this study: EcoRI / XhoI digest (bottom panel) was probed with *HIS4* sequence (HISU probe) for the detection of CO, NCO and DSBs (modified from Clyne et al., 2003)

Figure 13: A,B: Southern blots showing DSBs, CO and NCO signals in the wild type SK1, *irc25Δ/poc3* and *psy3Δ* mutants. Meiotic time course experiments were performed and sampled at different timepoints (0, 2, 3, 5, 4, 5, 6, 7, 8, 10 hours in SPM) for genomic DNA preparation, followed by EcoRI / XhoI restriction digest and electrophoresis (see section 2.3). The HisU probe was for the diagnostic of DSBs, CO and NCO, and signals were quantified using the Image Gauge software.

Figure 14: A,B,C,D: Phenotypes of *yor029wΔ* mutants. Experimental procedures were as described in Figures 8 and 13.

Figures 15 A,B; 16 A and **17 A,B**; Experimental procedures were as described in Figures 8 and 13.

Figure 18: A,B,C,D,E,F: Meiotic phenotypes of the PP4 complex, all the experimental procedures were as in Figures 8 and 13.

Figures 19 and **20 A, B,C**: Suppresion of the SC defects of *pph3Δ* mutants by *SWC2* deletion (see Figures 8 for experimental procedures).

Figure 20: D, E, F, G: Chromatin localization of Swc2-HA3. A meiotic time course experiment was conducted and sampled after 4hours in SPM for chromosome spreads and chromatin immunoprecipitation. D) The spreads was stained with antibodies directed to the HA epitope of Swc2-HA3 and analyzed by Fluorescence microscopy. Immunoprecipitated DNA fragments with HA antibody were amplified with specific primers (FK2858, FK2859) for the diagnostic of Swc2-HA3 binding at specific chromosomal locus or hybridzed to a tailing array for a genome-wide mapping of the protein. The example of chromosome III map

of Swc2-HA3 (in green) compared to Rec8 binding sites (in black) and to Swc2-HA3, *pph3*Δ (in red) is shown. E) Swc2-HA3 and Swc2-HA3, pph3Δ chromosomal binding sites were compared to DSBs sites (in blue, Pan et al., 2011). F) Swc2-HA3 (in green) and Swc2-HA3, pph3Δ (in red) chromosomal enrichment were compared. G) qPCR showing the efficiency of DNA binding of Swc2-HA3 in the absence of *PPH3* at position 230.870-230.993 on chromosome III, primer pairs Fk2858 and FK2859 were used to amplify the DNA binding region of interest. And western blot displaying the phosphoshift of Swc2-HA3 in wild type cells: a meiotic time course was carried out and samples taken after 0, 2, 3, 4, 5 and 6 hours in SPM for TCA-proteins extract and subsequent immunoblotting (see section 2.4).

Figure 21: A,B,C; Restoration of synapsis in *pph3*Δ mutants by the deletion of *PCH2*. The experimental procedures were as described in Figure 8.

Figure 22: A,B; Bypasses of the meiotic arrests of *pp4* mutants by *FPR3* and *MEK1* deletion. Experimental procedures as previously described in Figure 8.

Figure 23: A, B, C, D; Wild type like *pp4* mutants. Restoration of synapsis, meiotic progression and spore viability in *pp4* mutants by *PCH2* and *FPR3* double deletion. D) western blotting showing phospho-H2A-S129 dephosphorylation in the absence of *PPH3.* Meiotic time course experiments were performed and sampled at indicated time points for TCA-proteins extract, followed by immunoblotting with antibodies specific to the phosphorylated form of histone H2A at serine 129, and with antibodies to histone H2A as loading controls.

Figure 24: A, B, C; Synapsis phenotypes of *rad6*Δ*, bre1*Δ*, lge1*Δ*, H2B-K123R, set1*Δ*, dot1*Δ*,* and *set1*Δ*, dot1*Δ double mutants*.* All the experiments were conducted as described in Figure 8.

Figure 25 and **Figure 26**: Synapsis phenotypes in a pure SK1 strain background of additional mutants characterized in this work. Experimental procedures were as in Figure 8.

Figure 27: Meiotic progression and Rad51 foci of indicated mutants. The experimental set up were as previously described in Figure 8.

Figure 28: Top2 and Zip1 focus formation during meiotic prophase I. Meiotic time course experiments were performed and sampled after 0, 2, 3, 4, 5, 6, 7, 8 hours in SPM for subsequent chromosomes spreading. The spreads were stained with antibodies against Zip1 and the Myc epitope for Top2-Myc9 and analyzed with Fluorescence microscopy.

Figure 29: Example of nuclei showing Zip1 and Top2-Myc9 staining on chromosomes after 3 and 4 hours in SPM. Experimental procedures were as in Figure 28.

Figure 30: Colocalization of Top2-Myc9 and many DSBs sites. A meiotic time course were carried out and samples taken after 4hours in SPM, for chromatin immunoprecipitation with antibodies against the myc-epitope of Top2-Myc9, Immunoprecipitated DNA fragments were hybridized to a yeast tailing array to determine the DNA binding sites of Top2-Myc9. Chromosomal binding map of Top2-Myc9 (in red) was compared to DSBs map (in blue; Pan et al., 2011) and Rec8 sites (in green). Top2-Myc9 chromosomal binding sites overlap with many DSBs sites as shown for Chromosomes 3, 5, and 9.

Tables

Tables 6 through 12 contain large datasets. They are provided here for completeness, however, because of the small print, it is recommended to access these data in electronic form, in the accompanying CD (e-Appendix). The data there are represented in form of a filemaker database called “SK1BY_SCscreen Part1”. The compilation of data, that correspond to Table 6 through 12 can be accessed in an Excel file called “Table 6 to 12.xls”.

Table 6: **No meiotic induction in BY/SK1 hybrids**

Total number of ORFs: **132**

15	16	21	20	21	20	19
Meiosis 6	DNA metabolism 7	Mitochondria/aerobic respiration 39	Mitochondria/aerobic respiration 39	Metabolism 15	Golgi/ER 8	function unknown 7
BRE1 (H2B mono-ubiquitination) (sporulates weakly in SK1)	**HUR1** (HU sensitive, DNA replication)	**ADE16** (aerobic respiration)	**MRPL37**	**ARO1** (amino acid biosynth?)	**ARF1**	**ICY2**
IME1 (TF, inducer of meiosis, binds Ume6)	**IES2** (associates with Ino80 complex, sporulates normally in SK1)	**AEP2**	**MRPL40**	**YER152C** (transaminase activity, amino acid biosynth?)	**GEF1** (iron/copper homeostasis	**ZSP1 YBR287W** (ER associated)
IME2 (inducer of meiosis, protein kinase, activating Ndt80)	**IRC22** (ER localized, increased Rad52 foci)	**AIM31** (mitochondrial genome maintainence)	**MRPL7**	**FIT2** (nitrogen uptake)	**ICE2**	**YDR114C** (poor growth at elevated pH)
PPH3 PP4 catalytic subunit (sporulates in SK1)	**PHR1** (photoreactivation of thymin dimers after UV exposure)	**CBP1**	**MRPS28**	**TRP4** (nitrogen uptake, tryptophan synthesis	**MNN10 (mannosyl transferase), MNN4** also shows short Zip1	**YDR210W**
SNF1 (kinase, required for starvation response incl sporulation)	**REV1** (interacts with Rev7 (Zip1 foci) abasic site repair, translesion synthesis with DNA polymerase zeta)	**COX10** (4 Cox mutants in no induction, 7 phenotypes out of 12) analzyed	**MRPS35**	**UGA1** (Nitrogen utilization9	**PMT3 (mannosyl transferase)**	**YDR391C**
UME6 (TF for many meiotic genes)	**SAW1** (single-strand annealing together with Rad1/10)	**COX16**	**MRPS5**	**FPS1** (Acetate uptake)	**WSC4** (ER membrane maturation)	**YMR018W**
Cell cycle 2	**SGS1** (Blooms helicase, downregulates recombination and prevents multistrand crossovers, undergoes meiosis in SK1)	**COX6**	**MSS2**	**JLP1** (sulfur catabolism)	**YCT1** (ER component, cysteine transporter)	**YOR352W**
ACM1 (Cdh1 inhibitor to stabilize cyclins)	RNA metabolism 3	**COX9**	**OMS1**	**MDH2** (gluconeogensis)	**ALG5** (asparagine-linked **glycosylation**)	Dubious ORF/ nc RNA? 10
OCA1 (putative phosphatase, cell cycle arrest upon oxidative damage)	**ATS1** (tRNA modifier)	**CYC3**	**OXR1** (oxidative stress resistance)	**SIP4** (gluconeogensis)	vacuole 6	**YDL068W**
Karyogamy 2	**RIM4** (mRNA binding protein, enters meiosis in SK1!!, but no synapsis and no divisions!)	**FMP40** (mitochondrial proteomics)	**PGC1 (Phosphatidyl Glycerol phospholipase C)**	**PFK2** (glycolysis)	**APM3**	**YDR215C**
CIK1 (interacts and regulates Kar3 kinesin, karyogamy)	**TEX1** (mRNA export from nucleus)	**IDH2**	**POS5**	**TCO89** (Tor complex, growth regulation by nutrients)	**FRE6** (iron metabolism)	**YHL041W**
VIK1 (interacts and regulates Kar3 kinesin, karyogamy)	Ribosome biogenesis 7	**IMP2**	**RRG1** (Mitochondrial genome maintenance)	**ARG82** (regulates Nitrogen response genes, Inositol polyphosphate multikinase)	**PEP4** (non specific **protease A)**	**YJL022W**
Spindle/microtubules 1	**ALB1**	**MGR1**	**RRG9** (mitochondrial genome maintenance)	**PHO2** (TF, regulates phosphate metabolism)	**VID30** (proteasome-dependent catabolite degradation)	**YJL150W**
KIP2 (motorprotein, mitotic spidle positioning)	**RPL20A**	**MIP1**	**RSM18**	**RDS2** (TF, gluconeogenesis)	**VPS55** (Vacuolar Protein Sorting)	**YJL211C** (partially overlaps YJL210W)
Cytoskeleton 3	**RPS11A**	**MPA43** (present in purified mitochondria)	**SFC1**	**GAL4** (TF, galactose metabolism)	**VTC4** (Vacuolar Transporter Chaperone)	**YOR135C**
BEM3 (RhoGAP, cell polarity)	**SSB1** (chaperone)	**MRP1** (15 phenotypes of 37 analyzed, **12 no induction,** 1 no synapsis)	**YEA6**	Transcription 4	plasma membrane 6	**YOR379C**
SAC6 (actin bundling)	**RKM2** (Methyltransferase)	**MRP20**	**FMP45** (mitochondrial proteomics)	**CTI6** (activator, recruits SAGA complex to silenced chromatin)	**OPT1**	**YPL136W**
SCP1 (actin bundling)	**SKP2** (SCF component, coIPs with ribosomes)	**MRPL20**	**MAC1** (TF, copper transport, respiratory growth!)	**SET2** (H3-K36 methyltransferase, transcription elongation)	**SSO1** (vesicle fusion, SNARE)	**YOR379C** (partially overlaps YOR378W)
	NBA1 (coIPs with ribosomes)	**MRPL22**	autophagy 2	**SIN4** (Subunit of the RNA polymerase II mediator complex)	**SIA1** (activates Pma1 upon gucose)	pseudohyphae 1
Protein folding 1	salt stress 1	**MRPL23**	**CLG1** (cyclin like gene)	**SNF5** (SWI/SNF chromatin remodeling complex)	**YEH2** (steryl ester hydrolase, like **YEH1** (no phenotype) and **TGL1** (weakish synapsis))	**SFG1**
HSP82 (chaperone, pheromone signalling)	**HAL1**	**MRPL24**	**VPS30** (PI3-kinase also vacuolar protein sorting)	**SPP1** (Subunit of COMPASS (Set1C), methylates H3-K4)	**YOL075C** (transmembrane ATPase)	possible false positives 1
					ASI2 (in nuclear membrane, gene repressor)	**MF(ALPHA)1** (should be non-mater!)

Table 7: **Zip1 foci, no synapsis in BY/SK1 hybrids**

Total number of ORFs: **90**

16	16	17	14	14	13
Meiosis 16	DNA metabolism/chromatin remodelling/chromatin modification 11	Mitochondrial/ aerobic respiration 10	Metabolism 4	Golgi/ ER 3	function unknown 6
SPO11 (DSB essential)	**APN1** (apurinic repair, oxidation resistance)	**FMP31/RDL2** (sulfurtransferase, mitochondrial genome maintenance)	**GPH1** (glycogen catabolism)	**YNL046W** (localizes to ER)	**DOS2** (uncharacterized, interacts with DNM1!)
REC102 (DSB essential)	**RTT107** (Smc5/6 recruitment)	**FMP41** (localizes to mitochondria, uncharacterized)	**TGL3** (lipid metabolism, triglyceride catabolic process, 2 of 3 TGL genes give phenotype, TGL1 has weakish synapsis)	**ERP1** (ER to Golgi transport)	**YGL262W** (uncharacterized, interacts with SGF29 - short Zip1, implicated in SAGA)
REC104 (DSB essential)	**UBC13** (Ubiquitin E2, for Mms2)	**COQ4** (mitochondrial ubiquinone Biosynthesis, 1 no synapsis of 3 analyzed)	**TRM1** (tRNA methyltransferase, nitrogen utilization)	**YDR049W** (involved in ER protein degradation)	**YLR352W** (uncharacterized **F-box** protein, interacts with SKp1 and Cdc53)
MER2 (DSB essential)	**RTF1** (paf1 transcription elongation complex, histone methylation)	**COQ9** interacts but synapses normally	**TNA1** (permease, nicotinic acid uptake, utilization of nitrogen)	Vacuole 3	**YMR196W** (uncharacterized protein, interacts with almost all kinases in yeast!!)
REC114 (DSB essential)	**CDC73** (paf1 transcription elongation complex, histone methylation)	**COX20** (proteolytic processing of COX2, aerobic respiration, 4 no induction, 1 no synapsis, 7 phenotypes out of 12)	RNA metabolism 5	**VPS61** (vacuolar sorting protein)	**YOR111W** (uncharacterized)
Mei4 missed	PAF1 (NA)	**DNM1** (Dynamin GTPase, mitochondrial fission and morphology)	**MER1** (DSB essential, through splicing)	**VTH1** (involved in vacuolar protein sorting)	**CMR3** (uncharacterized, changed mutation rate)
MRE11 (DSB essential)	**NGG1** (transcriptional adaptor, part of SAGA, ADA (Gcn5 (NA) is strong candidate, Ada2 normal), SLIK complexes, **HAT** histone acetylation)	**MRPL17** (component of mitochondrial ribosomal large subunit (MRPs show 15 phenotypes of 37 analyzed, 12 no induction, 1 no synapsis))	**NAM8 / MRE2** (DSB essential through splicing)	**PAI3 (Pep4** inhibitor - perhaps chaperone?)	**YPR078C** (uncharacterized)
Rad50 (DSB essential)	**YGL262W** (uncharacterized, interacts with **SGF29** - short Zip1, implicated in SAGA, **HAT**?)	**ODC2** (mitochondrial inner membrane transporter)	**TGS1** (NA, but expected, through splicing)	Membrane 3	**YDR374C** (uncharacterized)
Xrs2 missed (DSB essential)	**ARD1** (N-terminal acetyltransferase (**HAT** incl histone acetylation) together with Nat1 **(short Zip1!)** and Nat5 (weakish but normal synapsis))	**PET54** (respiratory growth absent, strongest of 15 analyzed PET mutants, 10 are close to wt)	**CWC15** (NTC complex SU, pre-mRNA splicing)	**EXG2** (Exo-1,3-beta-glucanase, cell wall assembly)	Dubious 3
REC8 (axial element)	**HST4 ((HDAC** histone) **deacetylases,** telomere silencing, radiation resistance, 2 of 4 HST genes have a phenotype, HST1 in Long Zip1)	**SNF4** (peroxisome biogenesis, respiratory growth)	**SNT309**(synapses normally)	ERC1 (transmembrane exporter)	**YDR220C**
RED1 (axial element)	**DDR2** (DNA damage responsive, recombination)	**ISN1** (IMP breakdown to inosine, respiratory growth absent)	**NPL3/NOP3** (pre-mRNA splicing)	**HXT12/YIL170W** (pseudogene, hexose transporter)	**YER068C-A**
HOP1 NA missing from library	**IRC18** (enhanced Rad52 foci in del)	Ribosome biogenesis 7	**DCS1** (mRNA decapping)	Autophagy 1	**YPL185W** (partially overlaps YPL186C)
ZIP3 (SUMO E3, synapsis)	Post translational modification 4	**NOP12** (biogenesis of large 60S ribosomal subunit, 2 of 5 tested NOP genes have foci only)	Transcription 3	**ATG11** (autophagy, cytoplasm-to-vacuole targeting)	Sporulation 1
DMC1 (strand invasion)	**YLR352W** (uncharacterized **F-box** protein, interacts with SKp1 and Cdc53)	**SAC3** (Threx SU, **THP1** is normal, biogenesis of the small ribosomal subunit)	**MAF1** (polIII transcription repressor, environmental changes)	Stress response 4	**CTS2** (chitinase, sporulation)
MEI5 (strand invasion)	**IRC25/POC3** (chaperone, proteasome assembly, ubiquitination)	**TMA20** (Translation machinery associated, only 2 of 10 TMA genes have phenotype)	**RDR1 (Repressor (e.g. of Pdr5))**	**SIP18** (Phosphlipid binding hydrophilin, role in dessication resistance, expression induced by osmotic stress)	suspected false positive 3
MER3 (helicase, synapsis)	**YOL057W** (dipeptidyl-peptidase III)	**RPL37B** (component of the 60S ribosomal subunit, 6/42 have pht, 1 no induction, 3 no SC, 1 short, 1 long, 1 reduced)	**RTG1** (transcription factor involved in mitochondria-nucleus signalling	**YPR1** (aldo-keto reductase, expression unduced by osmotic and oxidative stress)	**HIS5** (histidine biosynthesis)
RDH54 (=TID1, strand invasion)	**UBP15** (ubiquitin protease, interacts with Cdh1-APC, only 1 of 7 UBP has strong phenotype)	**RPL40A** (component of the 60S ribosomal subunit)	Cytoskeleton 2	**HAL5** (PH and cation sensitivity, potassium uptake)	**GAP1** (amino acid transmembrane transporter - should not grow as leu-, his- minus strains)
MEK1 (inter sister repair)	Cell cycle 1	**RPS28B** (component of the 40S ribosomal subunit)	**BAG7** (RhoGAP, **actin** cytoskeleton organization)	**AHA1** (binds and activates **HSP82**)	**PRS5** (involved in nucleotid **(URA), histidine,** tryptophan biosynthesis) **should drop out**
SHU2 (strand invasion)	**DBF2 (kinase,** part of MEN, acitvation of Cdc14, but also repair)	**STB3** (rRNA processin, transition from quiescence to growth)	**ROM1** (GDP/GTP exchange protein (GEP) for Rho1p, actin filament organization (ROM2, which is synthetic lethal w ROM1 is normal))		

red: undetected mutations (false neg), grey: (not analyzed, but phenotype expected), orange: phenotype in SK1 less severe, green: (partner proteins without phenotype), violett: tentatively placed under functional heading (duplicate)

Table 8: **Short stretches of Zip1**

Total number of ORFs: **102**

Meiosis 6 (12)	DNA metabolism/**chromatin remodelling/chromatin modification 8** (11)	Mitochondrial/aerobic respiration 8 (17)	Metabolism 9 (15)	Golgi/ER 5 (14)	Function unknown 12 (17)	Dubious 9 (16)
COM1 (5' end resection, Mre11 exonuclease control)	**IRC4** (uncharacterized, increased Rad52p foci in Mitosis)	**GUT2** (**electron transport chain,** Mitochondrial glycerol-3-phosphate dehydrogenase, glycerol utilization)	**PRE9** (Alpha 3 subunit of the **20S proteasome**, only non-essential SU!, sporulation)	**EPS1** (ER protein with chaperone and co-chaperone activity, involved in retention of resident ER proteins)	**YBR259W** (Uncharacterized, interacts with RAD9)	**YGL165C** (partially overlaps with CUP2/YGL166W, NA)
HOP2 (Dmc1 activating factor)	**IRC11** (partially overlaps YOR012C(no phenotype); null mutant displays increased levels of spontaneous Rad52 foci)	**PET122** (Mitochondrial translational activator specific for the COX3 **(electron transport chain)** mRNA, acts together with Pet54p(Zip1 foci) and **Pet494p NA**)	**YDR179W-A** (Uncharaterized, interacts with Pup1, essential SU of proteasome)	**ERP5** (Protein with similarity to Emp24p and Erv25p, member of the p24 family involved in ER to Golgi transport)	**YDL199C** (Uncharacterized, putative sugar transporter)	**YGL214W** (overlaps **SKI8**/YGL213C)
MND1 (Dmc1 activating factor, NA missing from library)	**RAD26** (transcription coupled repair gene, binds to Def1, leads to Ubiquitination & degradation of Pol2)	**COX8** (**electron transport chain,** Subunit VIII of cytochrome c oxidase, terminus of mitochondrial inner membrane electron transport chain)	**DLD3** (**Energy metabolism,** D-lactate dehydrogenase, part of the retrograde regulon (makes pyruvate from lactate))	**ERV2** (Flavin-linked sulfhydryl oxidase, involved in disulfide bond formation within the ER)	**YDR179W-A** (Uncharaterized, interacts with Pup1, essential SU of proteasome)	**YDR134C** (pseudogene, interacts with **CDC28, DBF2, MEK1, ...)**
MEC3 (SU of the PCNA-like 911 complex that recognizes and signals DNA damage, ss/dsDNA junctions)	**Def1 missed** (transcription coupled repair gene, binds to Rad26, promotes Ubiquitination of Pol2 for degradation)	**QCR7** (**electron transport chain,** subunit 7 of the ubiquinol cytochrome-c reductase complex, component of electron transport chain)	**ZWF1 (Energy metabolism,** glucose-6-phosphate dehydrogenase, interacts with **DBF2**, utilization of **nitrogen** absent)	**FMO1** (Flavin-containing monooxygenase, catalyzes oxidation of biological thiols to maintain the ER redox buffer ratio for correct folding of disulfide-bonded proteins)	**YDR333C** (Uncharaterized)	**YDR199W** (overlaps VPS64, NA)
DDC1 (SU of the PCNA-like 911 complex that recognizes and signals DNA damage, ss/dsDNA junctions)	**REV7** (Accessory SU of DNA TLS Pol-zeta (=Rev3/Rev7), Interacts with **Rev1** (no meiotic induction), **Mec3/DDC1**-this category, Hsl1 (kinase NA), involved in TLS & double-strand break repair)	**ATP22 (electron transport chain, oxidative phosphorylation,** Specific translational activator for the mitochondrial ATP6 mRNA, encoding a subunit of F1F0 ATP synthase)	**DAL7** (**Energy metabolism**, Malate synthase, **glyoxylate** cycle)	**TED1** (phosphoesterase that acts together with **Emp24p/Erv25**p in cargo exit from the ER, EMP24 showed no phenotype, ERV25 showed long Zip1 stretches)	**YJL206C** induced by MMS treatment, oxidative stress sensitive	**YDR209C** (partially overlaps uncharacterized gene YDR210W(**no meiotic induction**))
RAD17 NA (SU of the PCNA-like 911 complex that recognizes and signals DNA damage, ss/dsDNA junctions)	Rev3 (Rev3/Rev7 are TLS pol zeta, however, Rev3 not required for SC formation	**SDH2** (**Energy metabolism,** Krebs cycle, SU of succinate dehydrogenase (Sdh1p, Sdh2p, Sdh3p, Sdh4p), SDH4 NA, SDH3 absent, **SDH1** "long Zip1 stretches")	**DAL4** (Allantoin permease, utilization of **nitrogen** absent)	Vacuole 4	**YKL133C** (Uncharacterized, has similarity to Mqr3p)	**YDR467C**
RAD24 NA (Rad24, SU of alt RFC (clamp loader for 911 complex)	**YBR259W** (Uncharacterized, interacts with RAD9)	**MDM31** (required for normal mitochondrial morphology and inheritance)	**TRK1** (Component of the Trk1p-Trk2p potassium transport system, **TRK2** NA, utilization of **nitrogen)**	**RTC1** (associates dynamically with the vacuole, suppresses cdc13-1 temperature sensitivity)	**YNL035C** (Uncharacterized, similar to WD-40 domain containing protein, interacts with **SUMO)**	**YGL165C** (partially overlaps the verified ORF CUP2/YGL166W)
SPO16 (synapsis, ZMM pathway)	**YPL068C** (nuclear protein induced in response to the DNA-damaging agent MMS)	**TRX3** (Mitochondrial thioredoxin, highly conserved oxidoreductase required to maintain the **redox homeostasis** of the cell)	**UGA4** (Permease that serves as a gamma-aminobutyrate (GABA) transport protein involved in the utilization of GABA as a **nitrogen** source)	**SNA3** (Salt sensitive, localized to vacuolar membrane, Sna4 low SC)	**YOR378W** (Uncharaterized, Putative paralog of ATR1, but not required for boron tolerance; member of the DHA2 family of drug:H+ antiporters, interacts with DNA ligase CDC9)	**IRC11** (partially overlaps YOR012C(no phenotype); null mutant displays increased levels of spontaneous Rad52 foci)
RMR1 (Protein required specifically for meiotic CO, but not for DSB formation AND! repair, unclear whether required for GC, ZMM?).	**AMD1** (AMP deaminase,catalyzes the deamination of AMP to form IMP and ammonia, interacts with **DBF2 (zip1 foci),** HRR25, Rad53 (essential, but known to be important in repair and meiosis)	Post translational modifications 6	**OXP1** (5-oxoprolinase, makes glutamate from 5-oxoproline, involved in **glutathione** production)	**VTC2** (Subunit of the vacuolar transporter chaperone (VTC) complex, interacts with CMD1 (calmodulin))	**YPL068C** (nuclear protein induced in response to the DNA-damaging agent MMS, in SK1 irreproducible results, too much or too few SC... **shortlived** SC??)	**SDL1/YIL167W** (L serine ammonia lyase, interacts with **HSP82**)
	SWC2 (Htz1p-binding component of the SWR1 complex, which exchanges histone variant H2AZ (Htz1p) for chromatin-bound histone H2A)	**SIZ2** (SUMO E3 ligase, sumoylates Yku70p/Yku80p, Sir4p for telomere anchoring, interacts with **Ecm11(long** Zip1), **Gis1(high SC**))	**FSH3** (Putative serine hydrolase)	**YCF1** (Vacuolar **glutathione S-conjugate-exporting ATPase** activity)	**YPL150W** (Uncharaterized, phosphatidylinositols and cardiolipin binding)	Suspected false positive 4
	SDS3 (**HDAC** Component of the Rpd3p/Sin3p deacetylase complex required for its structural integrity and catalytic activity, chromatin silencing, sporulation)	**LAG2 (negative regulator** of **SCF** ubiquitin E3 ligase, affects Rad52 distribution)		Membrane 7	**STB2** (interacts with SIN3, in a complex with STB1), STB1 showed no synapsis phenotype, SIN3 NA	**URA10** (biosynthesis of pyrimidines)
RNA metabolism 6		**YAK1 (Serine-threonine kinase** that phosphorylates Pop2p to regulate mRNA deadenylation, and the stress-responsive transcription factors Hsf1p and Msn2p9) POP2, CRF1 and MSN2 synapsed well, HSF1 is essential.	Ribosome biogenesis 5	**YNR066C** (Uncharacterized,localizes to membrane, interacts with a centromere protein **Cse4**)	**YIL166C** (Uncharacterized, similarity with allantoate permease (Dal5p), which has transporter activity)	**GAL80** (represses GAL genes in the absence of galactose, inhibits transcriptional activation by Gal4p)
SKI2 (putative RNA helicase, mediates 3'-5' RNA degradation by the cytoplasmic exosome)		**KSP1 (Ser/thr protein kinase,** haploid filamentous growth)	**YFL034W** (Uncharacterized, interacts with a ribosomal protein Rppop)	**PAU23 (Cell wall mannoprotein,** completely repressed during aerobic growth), similar gene Tir2 low SC, involved in low pH protection	Transcription 5	**DTR1** (dityrosine transporter, required for spore wall synthesis)
SKI8 (mediates 3'-5' RNA degradation by the cytoplasmic exosome; known to be required for meiotic DSB formation - Pht underestimated)	Stress response 3	**YPS7** (aspartic **protease,** involved in cell wall growth and maintenance)	**YJL213W** (Interacts with ribosomes, expressed during yeast metabolic cycle, phosphorylated by MEN)	**PAU24 (Cell wall mannoprotein,** completely repressed during aerobic growth) similar gene Tir2 low SC, involved in low pH protection	**RPA49** (RNA polymerase I subunit A49, the 2 other analyzed SU are either borderline (**RPA34), or >80%foci** (**RPA12**)	**LRG1** (GTPase-activating protein, Mating efficiency decreased)
MSS116 (ATP-dependent RNA helicase required for efficient **splicing** of mitochondrial Group I and II introns, also facilitates strand annealing)	**ATC1** (involved in regulation of cation stress responses and/or in the establishment of bipolar budding pattern, interacts with components of mitotic spindle)	**SAM2** (S-adenosylmethionine synthetase, AdoMet is involved in the **methylation of proteins!**, SAM1 showed no pht, but SAM1, SAM2 are differently regulated)	**RPL23B** (component of the large (60S) ribosomal subunit)	**MNN4** (positive regulator of **mannosylphosphate transferase** Mnn6p, which is normal, **MNN10 no meiotic induction**)	**TUP1 (General repressor** of transcription, establishment of repressive chromatin through I.A. with histones H3 and H4, interactor Rfx1 normal)	Cell cycle 3
NUP42 (Subunit of the nuclear pore complex (NPC),involved in RNA export)	**HYR1** (Thiol peroxidase, cellular response to **oxidative stress)**		**RPP1B** (component of the ribosomal stalk)	**EOS1** (Protein involved in N-**glycosylation,** interacts with WHI3 (NA) which controls Cln3 mRNA)	**SWI6** (Transcription cofactor, Swi4+Swi6+Mbp1=SBF TF at G1/S; involved in meiotic gene expression)	**CDH1** (activator of APC/C, degradation of Cyclins, important for correct expression of meiotic genes)
LIN1 (component of U5 snRNP, interacts with IRR1, may link proteins involved in chromosome segregation, mRNA splicing and DNA replication)	**HOT1** (Transcription factor required for the transient induction of glycerol biosynthetic genes GPD1 and GPP2 in response to **osmo-Stress)**	Cytoskeleton	**ECM32** (modulates translation termination, DNA/RNA helicase)	**OST3** (subunit of the oligosaccharyltransferase complex of the ER lumen, important for N-**glycosylation,** SU **OST1** and **OST2** are essential)	**ASG1** ((Zinc clustertranscriptional regulator, **sequence specific DNA binding,** respiratory deficient)	**SFP1** (transcription factor, regulates G2/M transitions during mitotic cell cycle and DNA-damage response)
RSF1 (ReSpiration Factor mediates the transition to respiratory growth and activate transcription of nuclear and mitochondrial genes)	**YJL206C** (increased by MMS treatment, oxidative stress sensitive	**MLP2** (Myosin-like protein associated with the nuclear envelope,spindle pole body organization,telomere tethering at nuclear periphery)		**YND1** (apyrase, helps promotes **glycosylation,** partially redundant with GDA1), GDA1 NA	**RDS1** (Zinc cluster transcription factor interacts with **HSP82,** MCM16, ACM1)	**VHS2** (suppressor of the synthetic lethality of a sis2 sit4 double mutant), role in G1/S phase progression

Table 9: **Long Zip1**

Total number of ORFs 200

Meiotic recombination 5	DNA metabolism/chromatin remodelling/chromatin modification 17	Mitochondrial/aerobic respiration 18	Metabolism 31	Metabolism 31	Vacuole/peroxisome 13
MSH4 (synapsis), forms a heterodimer with MSH5, **MSH5** showed reduced SC	**CDC40** (Pre-mRNA splicing factor, required for DNA synthesis during mitosis and meiosis)	**ATP11** (**electron transport chain, oxidative phosphorylation**, chaperone required for mitochondrial F1F0 ATP synthase assembly)	**FRM2** (NAD(P)H nitroreductase, negative regulation of fatty acid metabolic process, cell cycle, interacts with **PUB1**)	**MET22** (Bisphosphate-3'-nucleotidase, involved in salt tolerance and methionine biogenesis, interacts with MAK5)	**PRB1** (vacuolar proteinase B, required for protein degradation in vacuole and during sporulation),interacts with CDC53, MMS19, RAD59,SKP1, UBP10..), **MMS19** (long Zip1), **RAD59** (reduced SC)
NDJ1 (bouquet formation, synapsis)	**DCC1** (SU of a complex with CTF8 and CTF18, required for sister chromatid cohesion and chromosome segregation) **CTF8** and **CTF18** showed a reduced synapsis phenotype.	**COA1** (**electron transport chain,** mitochondrial inner membrane protein required for assembly of the cytochrome c oxidase complex (complex IV))	**YHI9** (involved in a membrane regulation metabolic pathway, interacts with ribosomal proteins and **SPP1 (no meiotic induction)**)	**MLS1** (Malate synthase, interacts with **KSS1, FMP48, IKS1**, utilization of carbon source absent)	**YHL008C** (unknown function, transporter, localizes to vacuole)
PSY3 (strand invasion, interacts with SHU1, SHU2, CSM2), **SHU1** (no phenotype), **SHU2** (Zip1 foci) and **CSM2** NA	**ECM11** (chromatin structure, interacts with CDC6, SIZ2, SMT3), **CDC6** essential, **SIZ2 (**short Zip1 stretches)	**CMC1 (electron transport chain,** may be involved in delivering copper from the matrix to the cytochrome c oxidase complex in mitochondria)	**YML082W** (uncharacterized, predicted to have carbon-sulfur lyase activity, interacts with **GIS2** and **MET30**)	**SDH1** (succinate dehydrogenase (Sdh1p, Sdh2p, Sdh3p, Sdh4p), respiratory growth decreased or absent,	**YOR223W** (unknown function, localized to ER and vacuole, interacts with **GIS2** and **LAG1**))
ZIP4 (synapsis)	**MRC1** (SU of the Fork pausing Complex, S-phase checkpoint kinase (TOF1-MRC1-CSM3) tethered to Pol Epsilon), **CSM3** (reduced synapsis) and **TOF1** (no phenotype)	**PET100** (**electron transport chain,** Chaperone that specifically facilitates the assembly of cytochrome c oxidase)	**YNL108C** (uncharacterized, possibly involved in glucose metabolism, shows similarity to **TFC7**, interacts with **RPN11** (SU of 19S regulatory particle of the 26S **proteasome**)	**PHM8** (Lysophosphatidic acid (LPA) phosphatase, cellular response to phosphate starvation)	**HHY1** (Dubious ORF, hypersensitive to hygromycin B indicative of defects in vacuolar trafficking)
YBR098W/SLX2/MMS4 (structure specific endonuclease)	**APN2** (endonuclease, removes 3'phosphates in DNA repair, interacts with **HTL1** (RSC complex), **POL30** (PCNA complex), **RIM1** (ssDNA binding)	**PET111** (**electron transport chain,** Mitochondrial translational activator specific for the COX2 mRNA)	**DAP1** (heme binding protein, damage responsive, telomeres, mitochondria, sterol biosynthesis)	**PRO2** (Gamma-glutamyl phosphate reductase, catalyzes the second step in proline biosynthesis, interacts with **MSH2**)	**IST1** (late endosome to vacuole transport via multivesicular body sorting pathway, function with **DID2**, interacts with **BUB1, MEC1, TEL1**)
RNA metabolism 7	**DUN1** (Chk2 paralog, like Rad53 and Mek1, needs Rad53 phosphorylation and binding for its own activation.)	**PET191** (**electron transport chain,** Protein required for assembly of cytochrome c oxidase)	**ADO1** (Adenosine kinase, required for the utilization of S-adenosylmethionine (AdoMet)), interacts with HRR25,**SPO12** (long Zip1), **SSB1**(no meiotic induction) AdoMet is involved in the methylation of proteins!,	**SER33** (3-phosphoglycerate dehydrogenase, catalyzes the first step in serine and glycine biosynthesis, isozyme with **SER3**)	**PCD1** (Peroxisomal nudix pyrophosphatase, may function to remove potentially toxic oxidized CoA disulfide from peroxisomes , **resistance to MMS decreased)**
STP3 (**Zinc-finger**, sequence specific DNA binding, pre-tRNA splicing)	**HHO1** (linker histone H1, suppresses DNA repair involving homologous recombination)	**QCR10** (**electron transport chain,** SU of the ubiquinol-cytochrome c oxidoreductase complex, part of the mitochondrial respiratory chain)	**ARO10** (Phenylpyruvate decarboxylase, catalyzes the first specific step in the Ehrlich pathway(production of fusel acids & fusel alcolols from branched-chain amino acids, aromatic amino acids & methionine)	**TKL2** (Transketolase, similar to **TKL1**, involved in pentose phosphate pathway,needed for synthesis of aromatic amino acids)	**PCS60** (Peroxisomal protein that binds AMP and mRNA, interacts with **IPL1, PTC1**, ASH1)
KTI12 (plays a role with elongator complex in modification of wobble nucleosides in tRNA, interacts with ELP2, ELP3 (normal SC)	**HPR1** (SU of THO/TREX complexes that couple transcription elongation with mitotic recombination and with mRNA metabolism and export, interacts with **AHA1**(Zip1 foci), CSE4, PAF1, **SAC3** (Zip1 foci),SSB1...)	**QRI5** (**electron transport chain,** required for accumulation of spliced COX1 mRNA)	**ATG26** (sterol 3-beta-glucosyltransferase, not involved in autophagy, plays a role in cell cycle progression)	**TRP3** (Bifunctional enzyme exhibiting both indole-3-**glycerol-phosphate synthase** and anthranilate synthase activities, tryptophan biosynthesis, interacts with **AHA1, DBF2, DMC1, GCN5**, SPO12, TUB3)	**PEP7** (Golgi to vacuole transport, phosphatidylinositol-3-phosphate binding, Golgi to endosome transport, UV resistance decreased, sporulation absent and respiratory growth decreased, interacts with **MEK1, HSP82(**no meiotic induction**), PHO85, PEP12(**long Zip1**)**)
LSM6 (mRNA decay, RNA processing, **LSM1**(reduced SC) and LSM2-8, NA)	**IRC3** (ATP-dependent RNA helicase, increased levels of spontaneous RAD52 foci)	**SOV1** (mitochondrial protein of unknown function, r**espiratory growth** decreased or absent)	**BDH1** (NAD-dependent (R,R)-butanediol dehydrogenase, interacts with **BDH2, PHO85**	**YBR139W** (serine hydrolase, serine-type carboxypeptidase, phytochelatin biosynthesis, interacts with **GCN5**)	**PEX12** (C3HC4-type RING-finger peroxin and E3 ubiquitin ligase, required for peroxisome biogenesis)
TOM1 (E3 ubiquitin ligase,involved in mRNA export from the nucleus and degradation of excess histones.interacts with **HSP82**(no induction**), NGG1(**Zip1 foci**), RAD53, (E), SPT5 (E), STP1** (no phenotype)	**IRC5** (putative ATPase, increased levels of spontaneous RAD52 foci, interacts with KSS1 (MAPK kinase, normal SC), SWE1(kinase that inhibits CDC28, normal SC), **TPK1** (long Zip1), **ATG1** (no pht)	**MDM32** (required for normal mitochondrial morphology and inheritance)	**BIO5** (BIO5 is in a cluster of 3 genes (BIO3, BIO4, and BIO5) that mediate biotin synthesis,	**YPL113C (Glyoxylate** reductase; acts on **glyoxylate** and hydroxypyruvate substrates, interacts with WHI3)	**PEX21** (Peroxin required for targeting of peroxisomal matrix proteins containing PTS2,redundant with PEX18, interacts with **SES1**)
TUM1 (Rhodanese domain sulfur transferase, accepts persulfite from Nfs1p and transfers it to Uba4p in the pathway for 2-thiolation of the wobble uridine base of tRNAs), interacts with **PHO85** (>91% short)	**KIN3/YAR018C** (kinase, possible role in DNA damage, interacts with LGE1(reduced SC), which interacts with Rad6/Bre1	**AIM41** (uncharaterized, **mitochondrial genome maintenance**, interacts with **DMA1**(spindle positioning and orientation) and **HRR25** (regulation of chromosome segregation))	**BIO2** (Biotin synthase, conversion of dethiobiotin to biotin,	**PGS1 (Phosphatidylglycerolphosphate synthase,** cardiolipin biosynthesis, respiratory growth absent, inviable)	**PEX27** (control peroxisome size and number, interacts with PEX25,interacts with **SPC1**)
MOD5 (tRNA isopentenyl transferase, tRNA dimethylallyltransferase)	**MMS19/MET18** (DNA repair and TFIIH regulator, required for both **nucleotide excision repair** (NER) and Pol II transcription)	**IMG1** (required for respiration and **maintenance of mitochondrial genome**)	**BNA3** (Kynurenine aminotransferase, biosynthesis of nicotinic acid, chromosome maintenance decreased, interacts with **CDC28, MAD2,**	**GRX3** (Hydroperoxide and superoxide-radical responsive **glutathione**-dependent oxidoreductase, along with **GRX4** and **GRX5;** protects cells from oxidative damage)	**SPS19** (Peroxisomal 2,4-dienoyl-CoA reductase, ascospore formation, interacts with **CHS1**(chitin synthase 1))
HUB1 (Ubiquitin-like protein modifier; promotes **alternative splicing** of SRC1 pre-mRNA, interacts with **HBT1** (>91% short))	**RAD7** (SU of **nucleotide excision repair** factor 4 (NEF4) and the Elongin-Cullin-Socs (ECS) ligase complex.Binds the DNA with **Rad16** (no phenotype)	**ISA2** (required for maturation of mitochondrial and cytosolic Fe/S proteins, localizes to the mitochondrial intermembrane space)	**ERG5** (C-22 sterol desaturase, ergosterol biosynthesis,respiratory growth absent)	**HMG1** (One of two isozymes of HMG-CoA reductase that catalyzes the conversion of HMG-CoA to mevalonate, which is a rate-limiting step in sterol biosynthesis,interacts with **CSE4, RAD51, SPO75**)	**YCK3** (vacuolar membrane-localized casein kinase I isoform, hares essential functions with **HRR25**, vesicle-mediated transport, interacts with GAL7, YCK1)
Cytoskeleton 5	**RIF1** (binds **RAP1** c-terminus, acts synergistically with **RIF2 (NA)** in telomere capping and silencing (maintenance))	**PRD1** (Zinc metalloendopeptidase, with **CYM1**, involved in degradation of mitochondrial proteins)	**GCY1** (Putative NADP(+) coupled **glycerol dehydrogenase,** glycerol catabolism, mRNA binding, oxidative stress response, interacts with **ASH1**, PRP6)		
ARK1 (ser/thr kinase,involved in regulation of the cortical **actin** cytoskeleton, interacts with **BMH2**,	**RTT101** (Cullin SU of a **ROC1** dependent ubiquitin E3 ligase, plays a role in anaphase progression, **MMS22** dependent DNA repair, and with **MMS1** in nonfunctional rRNA decay, modified by RUB1)	**MRS4** (iron transporter across the inner mitochondrial membrane)	**GLO2 (**Cytoplasmic **glyoxalase** II, catalyzes the hydrolysis of S-D-lactoylglutathione into **glutathione** and D-lactate, interacts with **TRX1)**		
GIM4 (SU of the cochaperone prefoldin complex(GIM3, GIM5, PAC10, PFD1, YKE2), binds specifically to cytosolic chaperonin and transfers target proteins to it , **tubulin** assembly,	**IRC13** (dubious ORF, null mutant displays increased levels of spontaneous Rad52 foci)	**SLM3** (mitochondrial tRNA thio-modification)	**GLT1** (NAD(+)-dependent **glutamate** synthase (GOGAT), interacts with **CSE4, MCM2, SPC24)**		
HSP42 (heat shock protein with chaperone activity,involved in cytoskeleton reorganization after heat shock, interacts with **CDC14, CSE4, DBF2, ORC1, SRS2, TUB2**)	**RAD30** (DNA **polymerase Eta,** involved in translesion synthesis during post-replication repair, interacts with **SNF4** (Zip1 foci), **SNF1**(no induction), **POL30**)	**MST1** (Mitochondrial threonyl-tRNA synthetase)	**GLY1** (Threonine aldolase, glycine biosynthesis from threonine, interacts with **DBF2**(Zip1 foci), HHF1(histoneH4), **SMC3)**		
RGA1 (GTPase-activating protein for the polarity-establishment protein Cdc42p, **actin filament** organization, interacts with CIN2, **LGE1**)		**PTH1** (peptidyl-tRNA hydrolases, required for **respiratory growth** on minimal medium)	**GPD1** (NAD-dependent **glycerol-3-phosphate dehydrogenase,** key enzyme of glycerol synthesis, interacts with **RAD1**)		
ABP140 (AdoMet-dependent tRNA methyltransferase and actin binding protein, **actin filament** bundle assembly, interacts with **IME2**, YCK2, YCK1..)					

Post translational modifications 10	Transcription 12	Ribosome biogenesis 10	Membrane 14	Function unknown 19	Dubious 10
FPR4 (proline isomerase, catalyzes isomerization of proline residues in histones H3 and H4, which affects **lysine methylation** of those histones, interacts with FPR3, GCN5, GLC7, HTA2, HTZ1…)	**WTM1** (Transcriptional modulator involved in regulation of meiosis,expression of RNR genes)	**YET2** (unknown function, colocalizes with ribosomes)	**PNS1** (enriched in plasma membrane fraction)	**SPR6** interacts with CDC28	**YMR031W-A** (partially overlaps YMR031C, may be involved in telomere maintenance)
JHD2 (H3K4 specific demethylase)	**CAT8** (Zinc cluster transcriptional activator, sequence specific DNA binding)	**ARX1** (Shuttling pre-60S factor, ribosomal large subunit biogenesis)	**AST1** (protein targeting to the plasma membrane,interacts with CBK1, KSP1	**GFD2** (high-copy suppressor of a dbp5 mutation, interacts with **GIS2** and **RVS167** (Zip1 foci in SK1))	**YBR116C** (partially overlaps TKL2)
HOS1 (HDAC, deacetylates SMC3 on lysine 112 & 113 residues at the onset of anaphase) Cornelia de Lange syndrome in human.	**GTS1** (involved in Arf3 regulation and in transcription regulation, interacts with **BMH1** (14-3-3 protein), SLA1, SSA1, SSA2…)	**RPL17B** (ribosomal protein,interacts with HMO1)	**DNF2** (Aminophospholipid translocase (flippase),involved in intracellular protein transport, cell polarity, interacts with **CDC28, TOR1, TOR2)**	**YDL121C** (localizes to ER interacts with **GIS2**)	**YCL023C** (partially overlaps KCC4)
HST1 (HDAC, SU of the (SUM1/RFM1/HST1) complex, which represses middle sporulation specific genes, **SUM1** (reduced SC), RFM1 NA, and of the SET3 complex (CPR1,HOS2, HOS4, HST1, SNT1, SIF2, SET3), **SET3** (long Zip1), **SIF2** (short Zip1), CPR1, HOS2 (normal SC)	**HAP5** (SU of the heme-activated, glucose-repressed Hap2/3/4/5 CCAAT-binding complex, a transcriptional activator and global regulator of respiratory gene expression, DNA binding,interacts with DOC1, GAL4, SPC24 (SU of NDC80 complex)…)	**RPL31B** (ribosomal protein, interacts with ORC1, BRE5)	**ECM33** (GPI-anchored protein of unknown function, fungal-type cell wall organization)	**YDL206W**	**YER067C-A** (partially overlaps YER067W)
SET3 (HDAC, meiosis specific repressor of sporulating genes, acts in complex with CPR1, HOS2, HOS4, SIF2, SNT1,**HST1,see above)**	**MTH1** (Negative regulator of the glucose-sensing signal transduction pathway, required for repression of transcription by Rgt1p, interacts with RGT1, SNF3 and RGT2 glucose sensors)	**RPP2B** (Ribosomal protein P2 beta, involved in the interaction between translational elongation factors and the ribosome)	**MMP1** (High-affinity S-methylmethionine permease, required for utilization of S-methylmethionine as a sulfur source)	**YDL241W**	**YER119C-A** (deletion mutation blocks replication of Brome mosaic virus in S. cerevisiae, but this is likely due to effects on the overlapping gene SCS2)
YNG1 (SU of NuA3 HAT,acetylates histone H3)	**PDR8** (transcription factor, targets include genes involved in the pleiotropic drug resistance, interacts with **CTF19**, SFH5, RPC19)	**RPS10B** (ribosomal protein of small subunit)	**MOG1** (Ran GTPase binding, protein import into nucleus)	**RTR2**	**YJL135W** (partially overlaps YJL134W/LCB3)
POC4 (heterodimeric Poc4p-Irc25p chaperone involved in assembly of **alpha subunits into the 20S proteasome, POC3** shows a reduced SC in SK1	**PHD1** (transcription activator, regulates expression of FLO11, pseudohyphal growth, interacts with **CDC28**, CYC8, SMT3, TUP1)	**RPS14B** (Ribosomal protein S9 of the small subunit, required for ribosome assembly and 20S pre-rRNA processing)	**PKH3** (kinase, MAPKKK cascade involved in cell wall biogenesis, reconstituted complex (**SHP1, RTR1, RNR4, RIM4**, PRS1, PAC10, OCA1, MFT1, JJJ3, FRS1, DRS1, CSM3,CCT6, BUD27, ATG19, ARP8)	**PAL1** (interacts with BMH2, CDC28, RSP5, SGF29)	**YKL118W** (partially overlaps VPH2)
RPN10 (Non-ATPase base SU of the **19S regulatory** particle (RP) of the 26S **proteasome,** binds selectively to polyubiquitin chains)	**SPT8** (SU of SAGA transcriptional regulatory complex, required for SAGA mediated repression of some promoters)	**TMA108** (involved in ribosome biogenesis)	**PMP2** (Proteolipid associated with plasma membrane H(+)-ATPase (Pma1p), cation transpor)	**YER130C/COM2** (sequence specific DNA binding)	**YML035C-A**
RIM11 (Kinase, phosphorylates Ime1 to repress meiosis under glucose conditions by regulating IME1-UME6 complex formation)	**SWI4** (SU of the SBF complex (SWI4-**SWI6(short Zip1)**), a transcriptional activator that regulates late G1 specific transcription of targets including cyclins and genes required for DNA synthesis and repair in concert with MBF complex (**MBP1-SWI6**)	**MRT4** (Protein involved in mRNA turnover and ribosome assembly, interacts with several factors including **HTA2, UBP3**…)	**PRM3** (Pheromone-regulated protein required for nuclear envelope fusion during karyogamy, interacts with **CDC5**(E))	**YHL008C** (localizes to vacuole, chloride transport, interacts with LSM5, **RVS167** (Zip1 foci in SK1) WHI3 NA)	**YNL198C**
PTC4 (Cytoplasmic type 2C **protein phosphatase** (PP2C), interacts with GIN4, HAT1, **HRR25, SSB1**)	**WHI5** (repressor of G1 transcription that binds to SCB binding factor (SBF), interacts with **HOS1**(long Zip1**), HSP82(**no induction**),** …)	**NSR1** (required for pre-rRNA processing and ribosome biogenesis, interacts with **ORC1**(E)**, SGF2, UBP3**..)	**SAT4/HAL4** (Ser/Thr Kinase, involved in salt tolerance, funtions in regulation of Trk1p-Trk2p potassium transporter; partially redundant with **HAL5(**Zip1 foci**)**; has similarity to NPR1(no phenotype)), interacts with RVS161,**RVS167**(Zip1 foci in SK1)	**YHR140W**	**YOR248W**
	YOX1 (repressor of transcription, binds to Mcm1p and to early cell cycle boxes (ECBs) in the promoters of cell cycle-regulated genes expressed in M/G1 phase,interacts with **CDC28**..		**SNF3** (Plasma membrane low glucose sensor that regulates glucose transport, negative regulation of meiosis, interacts with **GCN5(**NA**), TAF5**(E))	**YHR162W**	Stress response 4
Autophagy 7	**RTR1** (dephosphorylation of RNA polymerase II C-terminal domain, shuttles between the nucleus and cytoplasm, interacts with **BIK1**)	Golgi/ER 7	**STE23** (Metalloprotease,involved with homolog **AXL1** in peptide pheromone maturation)	**YIL055C**	**ALD3** (aldehyde dehydrogenase, involved in beta-alanine synthesis, induced by stress and repressed by glucose), interacts with ALD2
YIL165C (putative nitrilase, autophagy and mitophagy decrease. interacts with **KIN1**, likely constitute a single ORF with YIL164C)	Cell cycle 6	**COG5** (SU of the Golgi complex, involved in protein trafficking to mediate fusion of transport vesicles to Golgi compartments) intaracts with **HSP82**	**PRM7** (Pheromone-regulated protein, predicted to have one transmembrane segment, interacts with **HAL5, YCK2**)	**YJL132W** (interacts with **PRE1**)	**DOT5** (Nuclear thiol peroxidase, cellular response to oxidative stress, interacts with CMK1, **IPL1**, PHO85)
YML018C (uncharacterized, interacts with **ATG27**, suggesting a role in autophagy)	**SPO12** (involved in regulating release of Cdc14p from the nucleolus in early anaphase)	**ERV25** (in complex with **ERP1**(Zip1 foci), ERP2, and EMP24), ER to golgi transport, member of the p24 family)	**RTT10** (Cytoplasmic protein involved in endosomal recycling and in the regulation of Ty1 transposition, interacts with **RAD1**, SSB1)	**YLR445W** (transcription is regulated by Ume6p and induced in response to alpha factor)	**PST2** (induced by oxidative stress, interacts with CDC7, DUN1, SNF4, **XRS2, YKU80**)
ATG10 (Conserved E2-like conjugating enzyme that mediates formation of the Atg12p-Atg5p conjugate, which is a critical step in autophagy)	**BNS1/YGR230W** (Protein with some similarity to Spo12p; overexpression bypasses need for Spo12p, but not required for meiosis , interacts with **SRS2**	**EUG1** (disulfide isomerase, function overlaps with that of **PDI1**)		**YNL193W** (interacts with **DOC1** (substrate recognition factor of APC/C)	**TPK1** (cAMP-dependent protein kinase catalytic subunit, partially redundant with TPK2 and TPK3, predicted stress response and cell cycle,interacts with **CDC20**)
ATG21 (phosphatidylinositol binding, autophagy decreased, interacts with **MEK1, PHO85, ATG1** (no pht) **, TPK1 (**long Zip1))	**YIR016W** (uncharacterized, expression regulated by **UME6,** interacts with **CBK1 kinase** and its activator **MOB2**)	**FLC3** (Putative FAD transporter, similar to FLC1 and FLC2)	Sporulation 3	**YOL131W** (interacts with **SWI6** (short Zip1 foci)	
CCZ1 (involved in vacuolar assembly, essential for autophagy and the cytoplasm to-vacuole pathway, interacts with **SGF29**	**PPH21** (SU of protein phosphatase 2A (pp2A), involved in signal transduction and regulation of mitosis, **redundant with PPH22**)	**MPD1** (protein disulfide isomerase,inhibits thechaperone activity of CNE1(involved in folding and quality control of ER glycoproteins) interacts with **IPL1, GIN4, MPS3**, ORC1, **TPK1**(long Zip1))	**DIT2** (N-formyltyrosine oxidase, required for spore wall formation)	**YOL159C** (deletion mutants show elevated levels of Ty1 retrotransposition and Ty1 cDNA)	Suspected false positive 2
ATG32 (mitochondrial transmembrane receptor, essential for mitophagy (the selective vacuolar degradation of mitochondria in response to starvation)	**PPZ1** (Serine/threonine protein phosphatase Z, **isoform of Ppz2p**, involved in regulation of potassium transport, which affects osmotic stability, cell cycle progression, and halotolerance), interacts with **RVS167**, SDS22, SMT3..)	**VPS27** (required for recycling Golgi proteins, forms a complex with HSE1)	**FKS3** (ascospore wall assembly, **FKS1** no phenotype and **GSC2** NA	**YOR296W** (sporulation, interacts with **SUS1, PFK26, HEK29**)	**ADE1** (required for 'de novo' purine nucleotide biosynthesis)
PEP12 (Golgi to vacuole transport, autophagy and mitophagy absent), interacts with **SPO20, HSP82, PEP7(**long Zip1**))**	**RMD6** (meiotic nuclear division, interacts with **RDS1** (short Zip1)	**YOS9** (ER quality-control lectin, ER-associated protein catabolism)	**SSP2** (ascospore wall assembly)	**YIR016W**	**AFR1** (required for pheromone-induced projection (shmoo) formation, has an RVXF motif that mediates targeting of **GLC7** to mating projections), interacts with CDC12…

Table 10: **At least 80% non-SC**

Total number of ORFs:	133				4
RNA metabolism 4	DNA metabolism/chromatin remodelling/chromatin modification 13	Mitochondrial/aerobic respiration 10	Metabolism 18	Golgi/ER 2	Function unknown 10
BRR1 (snRNP protein component of spliceosomal snRNPs, required for pre-mRNA splicing and snRNP biogenesis)	**WSP1** (uncharacterized, induced in response to MMS)	**ISF1** (respiration)	**BNA6** (de novo biosynthesis of NAD fr	**BST1/PER17** (GPI inositol deacylase)	**YBR090C**
ELP2 (SU of Elongator complex, tRNA wobble uridine modification)	**LGE1** (H2B monoubiquitination)	**PKP2** (kinase kinase that negatively regulates activity of the pyruvate dehydrogenase complex)	**SCT1 (glycerol-3-phosphate O-acyltransferase)**	**DSS4** (guanyl-nucleotide exchange factor, post-Golgi vesicle-mediated transport)	**YGL015C**
SYF2/NTC31 (nuclear mRNA splicing, via spliceosome)	**MCM21/CTF5** (component of the COMA complex (Ctf19p, Okp1p, Mcm21p, Ame1p) that bridges kinetochore subunits that are in contact with centromeric DNA and the subunits bound to microtubules)	**ATP20** (SU g of the mitochondrial F1F0 ATP synthase9	**SNO4** (chaperone and cysteine protease,pyridoxine metabolism)	Vacuole 3	**YGR273C**
LSM1 (forms heteroheptameric complex (with Lsm2p, Lsm3p, Lsm4p, Lsm5p, Lsm6p, and Lsm7p) involved in degradation of cytoplasmic mRNAs)	**HTA1** (histone H2A, chromatin assembly, DNA repair)	**MRPL39** (Mitochondrial ribosomal protein)	**AAD3** (Putative aryl-alcohol dehydrogenase)	**VAM10** (vacuole morphogenesis)	**YLR283W**
Ribosome biogenesis 3	**ACK1** (induced in response to the DNA-damaging agent MMS, cell cycle progression abnormal)	**COX18** (membrane insertase, protein insertion into mitochondrial membrane from inner side)	**ARG4** (Argininosuccinate lyase, arginine biosynthesis)	**PMC1** (vacuolar calcium-transporting ATPase, calcium ion homeostasis)	**YDR444W**
SSD1 (translational repressor)	**LOH1** (unknown function, genome maintenance, sporulation)	**RMD9** (role in delivering mitochondrial mRNAs to ribosomes, respiratory growth absent, sporulation absent)	**PUS4** (Pseudouridine synthase, formation of pseudouridine-55 (Psi55))	**VPS62** (Vacuolar protein sorting (VPS) protein required for cytoplasm to vacuole targeting of proteins)	**YJL070C** (similar to AMP deaminases)
RPL41A (protein L47 of the large (60S) ribosomal subunit)	**HHT2** (histone H3, chromatin assembly or disassembly, nucleotide excision repair)	**MRPL16** (Mitochondrial ribosomal protein, respiratory growth absent)	**GLG2** (glucosyltransferase, glycogen biosynthesis9	Membrane 8	**YDR370C**
YAR1 (link ribosome biogenesis and adaptation to osmotic and oxidative stress)	**TOF2** (involved in rDNA silencing and mitotic rDNA condensation, stimulates Cdc14p phosphatase activity, required for condensin recruitment to the replication fork barrier site)	**COX5B** (Subunit Vb of cytochrome c oxidase, mitochondrial electron transport, cytochrome c to oxygen)	**STE24** (Highly conserved zinc metalloprotease, involved in a-factor maturation, mating decreased)	**YHR048W** (uncharaterized, drug transpor)	**YPL216W**
Transcription/Translation 7	**SUM1** (Transcriptional repressor required for mitotic repression of middle sporulation-specific genes, involved in telomere maintenance, chromatin silencing; regulated by pachytene checkpoint)	**GEP3/FMP38/AIM40** (Unknown function, defective in respiration)	**MET13** (Major isozyme of methylenetetrahydrofolate reductase, methionine biosynthesis)	**AGP3** (Low-affinity amino acid permease, supply the cell with amino acids as nitrogen source in nitrogen-poor conditions)	**YML002W** (uncharacterized, expresiom induced by heat and calcium shortages)
CCR4 (Component of the CCR4-NOT transcriptional complex, regulation of gene expression)	**NUP170** (SU of the nuclear pore complex involved in RNA export from nucleus, chromosome segregation)	**IMP1** (mitochondrial inner membrane peptidase complex, required for maturation of mitochondrial proteins of the intermembrane space; complex contains Imp1p and IMP2 (both catalytic subunits), and SOM1)	**ADI1** (Acireductone dioxygenease, L-methionine salvage from methylthioadenosine)	**PEX32** (negative regulation of peroxisome size; partially functionally redundant with PEX31, acts downstream of PEX28, PEX29)	**YML033W/YML034W** (merged ORFs)
STB5 (transcription factor, regulates multidrug resistance and oxidative stress response)	**SIM1** (Protein of the SUN family (Sim1p, Uth1p, Nca3p, Sun4p) that may participate in DNA replication)	Post translational modifications 9	**YMR1** (Phosphatidylinositol 3-phosphate (PI3P) phosphatase; involved in various protein sorting pathways)	**YGL114W** (uncharateized, oligopeptide transporter activity)	Dubious 10
RPA12/RRN4 (RNA polymerase I subunit A12.2, termination of RNA polymerase I transcription)	**SPO13** (involved in maintaining sister chromatid cohesion during meiosis I as well as promoting proper attachment of kinetochores to the spindle during meiosis I and meiosis II)	**PAA1** (Polyamine acetyltransferase)	**BNA5** (de novo NAD biosynthetic process from tryptophan)	**LRE1** (control of cell wall structure and stress response)	**YPL102C**
TIF4632 (Translation initiation factor eIF4G, SU of the mRNA cap-binding protein complex (eIF4F))	**NUP60** (SU of the nuclear pore complex, nvolved in nuclear export and cytoplasmic localization of specific mRNAs such as ASH1 and in DSBs repair)	**UBP5** (ubiquitin protease, protein deubiquitination)	**TGL1** (Steryl ester hydrolase(triglyceride lipase), acts in complex with (YEH1, YEH2)	**PEX25** (regulation of peroxisome size and maintenance)	**YIL059C** (overlaps YIL060W)
NCL1 (S-adenosyl-L-methionine-dependent tRNA, tRNA methylation)	Cell cycle 2	**HPM1** (Histidine Protein Methyltransferase, methylation of ribosomal protein Rpl3, decreased sprorulation efficiency)	**MUQ1** (Ethanolamine-phosphate cytidylyltransferase, phosphatidylethanolamine biosynthesis)	**DAL5** (Allantoate permease; ureidosuccinate permease,dipeptide transport)	**YGR226C** (overlaps AMA1/YGR225W)
UME1 (required for repression of a subset of meiotic genes during vegetative growth, binding of histone deacetylase Rpd3p required for activity)	**RNQ1** ([PIN(+)] prion, involved in cell cycle)	**SIP1** (alternate beta SU of the Snf1p kinase complex, protein phosphorylation, protein complex assembly, signal transduction)	**SCS3** (involved in triglyceride droplet biosynthesis)	**RTN2** (Reticulon homolog, possibly endomembrane establishment)	**YGR069W**
ABP140/TRM140 ((S-adenosyl-L-methionine)AdoMet-dependent tRNA methyltransferase, tRNA methylation)	**RRD2** (Activator of the phosphotyrosyl phosphatase activity of PP2A,peptidyl-prolyl cis/trans-isomerase, mitotic spindle organization)	**RKM3** (Ribosomal lysine methyltransferase specific for monomethylation of Rpl42ap and Rpl42bp (lysine 40))	**OSH3** (oxysterol-binding protein, sterol metabolism)	Budding 3	**YDL050C**
Apoptosis 2	Stress response 4	**PIB1** (RING-type ubiquitin ligase of the endosomal and vacuolar membranes, binds phosphatidylinositol(3)-phosphate, replicative lifespan increase)	**YHL012W** (uncharacterized, glycogen biosynthesis)	**BUD28** (budding pattern abnormal,98% of ORF overlaps the verified gene RPL22A)	**YOR121C** (overlaps GCY1/YOR120W)
YMR074C (overexpression promotes H2O2-induced apoptosis)	**ATX1** (copper transporter, cellular response to oxidative stress)	**PMT5** (Protein O-**mannosyltransferase,** transfers mannose residues from dolichyl phosphate-D-mannose to protein serine/threonine residues, acts in complex with **PMT3** or PMT2)	**TCB1** (unknown function, lipid binding protein)	**BUD25** (budding pattern)	**YER188W**
NMA111 (Serine protease and general molecular chaperone; involved in response to heat stress and promotion of apoptosis, sporulation normal)	**PSR2** (plasma membrane phosphatase involved in the general stress response, redundant with PSR1)	**RXT2/RAF60** (SU of the histone deacetylase Rpd3L complex)		**BUD30** (diploid displays a weak budding pattern phenotype, positive regulation of PolII transcription, 96% of ORF overlaps the verified gene RPC53)	**YDR433W**
Cytoskeleton 1	**PAU7** (seripauperin, active during alcoholic fermentation, stress response)	**MAK10/NAA35** (Non-catalytic subunit of N-terminal acetyltransferase of the NatC type, N-terminal protein amino acid acetylation)		Suspected false positive 1	**YBL095W** (uncharaterized, invasive growth absent)
ACF2/ENG2/ PCA1 (Intracellular beta-1,3-endoglucanase, cortical actin cytoskeleton assembly)	**PAU11** (uncharacterized, seripauperin)			**STE11** (Signal transducing MEK kinase involved in pheromone response, **sterile**)	**YNL057W**

Table 12: More than 46% long or full SC

Post translational modifications 5	DNA metabolism/chromatin remodelling/chromatin modification 4	Dubious 10	Metabolism 10	Golgi/ER 8	Function unknown 10
PFA5 (protein-cysteine S-palmitoleyltransferase, Palmitoyltransferase)	**RLF2/CAC1** (Largest subunit (p90) of the Chromatin Assembly Complex (CAF-1) with Cac2p and Msi1p that assembles newly synthesized histones onto recently replicated DNA)	**YGR051C**	**FAA4** (Long chain fatty acyl-CoA synthetase, long chain fatty acid import,localized to lipid particles)	**TPO5** (involved in excretion of putrescine and spermidine, polyamine transmembrane transporter)	**YFR039C** (uncharacterized, may be involved in response to high salt and changes in carbon source)
GIS1 (histone demethylase and transcription factor; involved in expression of genes during nutrient limitation)	**TRS85** (SU of TRAPPIII (transport protein particle), ER to Golgi vesicle-mediated transport, late post-replication meiotic role, protein localization to pre-autophagosomal structure)	**YMR304C-A** (partially overlaps the verified gene SCW10)	**ADH4** (alcohol dehydrogenase, involved in glucose fermentation, leucine, isoleucine, tryptophan,phenylalanine and valine degradation)	**YIP5** (localized to late Golgi vesicles, possible role in vesicle-mediated transport)	**YMR253C**
SCM4 (Potential regulatory effector of CDC4 function, suppresses a temperature-sensitive allele of CDC4, cell cycle progression abnormal)	**MMS1/RTT108** (SU of an E3 ubiquitin ligase complex involved in resolving replication intermediates, nonfunctional rRNA decay, recombinational repair)	**YKL177W** (partially overlaps SET3)	**NQM1** (Transaldolase of unknown function)	**YPT32** (Rab family GTPase, mediates intra-Golgi traffic or the budding of post-Golgi vesicles from the trans-Golgi)	**YMR265C**
CKA2 (alpha catalytic SU of casein kinase2 (CK2),a ser/thr kinase comprising (CKA1, CKA2, CKB1 CKB2) inovlved in protein phosphorylation includind transcription factors and all RNA polymerase)	**SCP160** (Essential RNA-binding G protein effector of mating response pathway, chromatin silencing, chromosome segregation, telomere clustering, introcellular mRNA localization)	**YJR128W** (overlaps RSF2)	**CHO2** (phosphatidylethanolamine N-methyltransferase,phosphatidic acid and phospholipid biosynthesis)	**ERV15** (ER to Golgi vesicle-mediated transport)	**YML079W**
CLA4 (Cdc42p-activated signal transducing kinase of the PAK (p21-activated kinase) family, along with Ste20p and Skm1p; involved in septin ring assembly, vacuole inheritance, cytokinesis, sterol uptake regulation; phosphorylates Cdc3p and Cdc10p)	Transcription/Translation 3	**YAR047C**	**AIM22/LIP3/RRG3** (Putative lipoate-protein ligase, null mutant displays reduced frequency of mitochondrial genome loss)	**BCH1** (Golgi to plasma membrane transport, Member of the ChAPs family (Chs5p-Arf1p-binding proteins: Bch1p, Bch2p, Bud7p, Chs6p))	**YGL242C**
Vacuole 3	**FUN12** (GTPase, required for general translation initiation by promoting Met-tRNAiMet binding to ribosomes, sporulation absent)	**YMR057C** (partially overlaps AAC1)	**SGA1** (glucan 1,4-alpha-glucosidase, glycogen catabolism)	**RER1** (ER to Golgi transport vesicle, protein retention in ER lumen)	**YGR042W** (uncharacterized, maintenance of telomere)
ROY1 (GTPase inhibitor with similarity to F-box proteins, physically interacts with Skp1p, protein targeting to vacuole)	**HMS1** (Basic helix-loop-helix protein, sequence-specific DNA binding transcription factor)	**YOL150C**	**BUD17** (pyridoxal kinase, a key enzyme in vitamin B6 metabolism, budding pattern abnormal)	**GYP1** (Cis-golgi GTPase-activating protein (GAP) for the Rab family members Ypt1p (in vivo) and for Ypt1p, Sec4p, Ypt7p, and Ypt51p (in vitro); involved in vesicle docking and fusion)	**COS12** (member of the DUP380 subfamily of conserved, often subtelomerically-encoded proteins)
ZRT3 (transports zinc from storage in the vacuole to the cytoplasm when needed)	**FRA2/AIM15** (negative regulation of transcription from RNA polymerase II promoter in response to iron)	**YGR039W** (partially overlaps ARS722)	**ACB1** (Acyl-CoA-binding protein, transports newly synthesized acyl-CoA esters from fatty acid synthetase (Fas1p-Fas2p) to acyl-CoA-consuming processes)	**FLC2** (Putative FAD transporter; required for uptake of FAD into endoplasmic reticulum; involved in cell wall maintenance)	**YLR049C**
VID27 (possibly involved in vacuolar protein degradation)	Ribosome biogenesis 4	**YKL102C** (confers sensitivity to citric acid)	**PHO8** (Repressible vacuolar alkaline phosphatase, dephosphorylates phosphotyrosyl peptides; contributes to NAD+ metabolism)	Membrane 4	**YMR262W**
Mitochondrial/aerobic respiration 3	**YMR295C** (uncharacterized, colocalizes with ribosomes)	**YEL028W**	**SCS7** (Sphingolipid alpha-hydroxylase)	**MUP1** (High affinity methionine permease, also involved in cysteine uptake)	**GFD1** (Coiled-coiled protein of unknown function, identified as a high-copy suppressor of a dbp5 mutation)
YBR238C (Mitochondrial membrane protein with similarity to Rmd9p; not required for respiratory growth but causes a synthetic respiratory defect in combination with rmd9 mutations)	**RPS30B** (component of the small (40S) ribosomal subunit)	Stress response 1	Meiosis 1	**PDR18** (ATPase activity, coupled to transmembrane movement of substances)	Cytoskeleton 2
ATP12 (required for the assembly of mitochondrial F1F0 ATP synthase, respiratory growth absent)	**RPS0B** (component of the small (40S) ribosomal subunit)	**TRX1/LMA1** (Cytoplasmic thioredoxin isoenzyme of the **thioredoxin system** which protects cells against **oxidative and reductive** stress)	**IML3/MCM19** (role in kinetochore function, localizes to the outer kinetochore in a Ctf19p-dependent manner, interacts with Chl4p and Ctf19p, establishment of mitotic and meiotic sister chromatid cohesion)	**IZH3** (Membrane protein involved in zinc ion homeostasis, apoptosis absent)	**MDM1** (Intermediate filament protein, required for nuclear and mitochondrial transmission to daughter buds, specifically binds phosphatidylinositol 3-phosphate)
FZO1 (mitochondrial genome maintenance)	**RPL26B** (component of the large (60S) ribosomal subunit)			**RSN1** (overexpression suppresses NaCl sensitivity of sro7 mutant cells by restoring sodium pump (Ena1p) localization to the plasma membrane)	**JNM1** (Component of the yeast dynactin complex, consisting of Nip100p, Jnm1p, and Arp1p; required for proper nuclear migration and spindle partitioning during mitotic anaphase B)

Table 13: list of antibodies used in this study

AB-ID	antigen	dilution	source	supplier	product number	conjugated to
FKα14	Mouse	cytology 1:500	Goat	Jackson ImmunoResearch	115-165-146	CY3
FKα17	Rabbit	cytology 1:300	Goat	Sigma-Aldrich	F9887	FITC
FKα18	Rat	cytology 1:100	Rabbit	Sigma-Aldrich	F-1763	
FKα26	yeast Tubulin	cytology 1:200	Rat	Serotec	MCA78S	
FKα65 (9E10)	MYC	cytology 1:50 Western 1:300	Mouse		Cell line 9E10	
FKα75	Mouse	Western 1:100000	Goat	Pierce	31444	HRP
FKα79	Rabbit	Western 1:60000	Swine	Daco		HRP
FKα97	HA (16B12)	cytology 1:8000 Western 1:10000	Mouse	Ralf Hess	MMS-101R	
FKα133	Swi6	Western 1:10000	Rabbit			
FKα160	Rad51	cytology 1:75	Mouse	Neomarkers Fremont		
FKα214	Zip1	cytology 1:400	Rabbit		20.7.2000 final bleed	
FKα231	yeast phospho-H2A-S129	Western 1:40000	Rabbit	Upstate	07-745	
FKα234	Histone H2A	cytology 1:40000	Rabbit	Upstate	39235	
FKα244	Fpr3 C-terminus(281-413)	Western 1:10000	Rabbit	Thorner lab	1138	

Table 14: list of oligonucleotides used in this study

number	sequence (5`-------3`)	purpose
FK749	ccaactcctcaggacgtgac	amplication of threonine hotspot (DSB1)
FK750	caaccacctgcgtgagtgtg	amplication of threonine hotspot (DSB1)
FK794	GGTGATGATTGCTCTCTGCC	amplification of ADP1 (coldspot)
FK795	CGTCACAATTGATCCCTCCC	amplification of ADP1 (coldspot)
FK1965	TGGTCTCCAAGTGGCAAAATCC	amplification of HISU probe
FK1966	GGTCGTGGCGTTTATTATTCTCG	amplification of HISU probe
FK2011	GAATTTCCCGCACATCTTTG	amplification of DSB3 (chrIII)
FK2012	CTAATTTGCCGTGCTTCGTC	amplification of DSB3 (chrIII)
FK2015	TGGATGGCAACTGAAGGAGC	amplification of Core1(chrIII)
FK2016	CAGCCAGGAAAATTCACCAC	amplification of Core1(chrIII)
FK2165	aaatgcgaggcggttaaaagagagtgacaacaatttcatacgtacgctgcaggtc gac	for PCH2 K.O.
FK2166	gaaagtatgctacatgagtatgagacaaaagaaagaagcgaaatcgatgaattc gagctc	for PCH2 K.O.
FK2167	TAGATTTGCCGTTGACAATAAG	checking PCH2 K.O.
FK2168	taagcatgaaagcgagcaac	checking PCH2 K.O.
FK2356	TGCCAAACATCCATCAAA	checking HTA1-S129A
FK2357	GCAACAGTGCCCAATGAA	checking HTA1-S129A
FK2415	GCCCAAGGTGGTGTTTTG	checking HTA2-S129A
FK2416	TGCGAGATCGAGGGAAAA	checking HTA2-S129A
FK2498	TTTCAACTGGCTTGCTTCCT	for FPR3 K.O.
FK2499	CGACCATCCAGTAGCACTCA	for FPR3 K.O.
FK2549	CCCGGAGAAAAGAGCTTAGG	for HTZ1 K.O.
FK2550	TTTCCGGGTATGCAAAGTTC	for HTZ1 K.O.
FK2551	TGCAAGAAGTCTTGGCAATG	for SWC2 K.O.
FK2552	TACGAAAGTTGCGAATGACG	for SWC2 K.O.
FK2614	CTAGATAAGACCCAAAGCATTCGATTACTGCATTTGAGA G cgtacgctgcaggtcgac	for SWR1 K.O.
FK2615	GAGTACATTACCATAAAAACCAAGAGGCGATAGTGTTGT C atcgatgaattcgagctc	for SWR1 K.O.
FK2616	GATTTAAGTCAAAGACCTGCAAAAGGTGTTCCTGAAGGA TTTTCCGGTTCTGCTGCTAG	C-terminal SWC2 tagging with 3XHA

FK2617	CGTATAAAGTATATTTTTATGTAAAATGATCTTTATGATT CCTCGAGGCCAGAAGAC	C-terminal SWC2 tagging with 3XHA
FK2618	CTTGAAGAAAGAGTGCAAAGG	checking SWR1 K.O.
FK2619	TGTTCAATGGAATCTTGCTC	checking SWR1 K.O.
FK2621	AGTTGAAGCTTTCACCAGAA	checking SWC2 tagging (reverse primer)
FK2659	GATCGAAGACCGTCAAATCC	checking SWR1 K.O. (used with FK2619)
FK2671	GTCTAATGAATACAAATAGAAGTGAAACCGAAGCAAATT C cgtacgctgcaggtcgac	for SWC2 K.O. (NatMX cassette)
FK2672	GTCTAATGAATACAAATAGAAGTGAAACCGAAGCAAATT C cgtacgctgcaggtcgac	for SWC2 K.O. (NatMX cassette)
FK2673	CTTTGCTGGTAAGCCAAAAT	checking SWC2 K.O. (forward primer)
FK2681	ACAATGATTAAGGCGGAACA	for IES2 K.O.
FK2682	GTCTGCCTTACGTGGTTCTG	for IES2 K.O.
FK2742	TTGGTTCCCTTCCCGTTATT	for ALK1 K.O.
FK2743	TTGACTCCCAAAATGGAAGC	for ALK1 K.O.
FK2744	AGGGTTTGACAAGTTGAACGA	for CMR3 K.O.
FK2745	CGTCTTTGTGCGTCCAAGTA	for CMR3 K.O.
FK2746	TTCTTTTCCCCTGTTTCCAT	for DDR2 K.O.
FK2747	AGAGACGAACTGGAAGAAGAGA	for DDR2 K.O.
FK2748	CGTCATCGACACTGCTCACT	for ECM11 K.O.
FK2749	AACGTTTCCGCTCAAAGAGA	for ECM11 K.O.
FK2750	TTTGCCATTCCTTTTTCGTC	for FMP41 K.O.
FK2751	TCCCTTGACCTCGAGATTTG	for FMP41 K.O.
FK2752	AATTGGTGGCTCCAAACAAG	for HAL5 K.O
FK2753	TCCATGCCTCTACATTACATCG	for HAL5 K.O
FK2754	GTTCTGAAGTTTTCCCAGTTGC	for HOS1 K.O.
FK2755	TGTCACGGTTTCCAGTACAATC	for HOS1 K.O.
FK2782	TGTGGTTCATGCTGAGAGGA	for IRC3 K.O.
FK2783	TCAGAAAGGGTGTGATCCAA	for IRC3 K.O.
FK2784	GCCTAATTGAAGCAGGCAAA	for IRC4 K.O
FK2785	TGAGGCTATGGTAAGCGTAAGA	for IRC4 K.O
FK2786	TCCTCCCAAATGAAGATCAA	for IRC18 K.O.
FK2787	CAAAAGGGTGGGTATGTTTG	for IRC18 K.O.
FK2788	TGAGACTCAACGTAACATGC	for PAI3 K.O.
FK2789	TGAGACTCAACGTAACATGC	for PAI3 K.O.
FK2790	GGAGAAGATGGAAGCTGTCTTG	for YJL049W K.O.
FK2791	TTCTCAATTGCGACAAAACG	for YJL049W K.O.
FK2792	TCCCGTATCGTGCGATAAAT	for RDR1 K.O.
FK2793	GCAATTTGCATTTGGTTCAG	for RDR1 K.O.
FK2794	TCATCTACCTTTGGTGGAAC	for RTC1 K.O.
FK2795	ACCACGACTCAGATTTATCG	for RTC1 K.O.
FK2796	TAAAACCTAATGTTGGAAAGAAAGAGCTACGTCAGCAAG AGcgtacgctgcaggtcgac	for RTT102 K.O.
FK2797	AATATATAAATATATATATATATATATATATATATATATGat cgatgaattcgagctc	for RTT102 K.O.
FK2798	GGCGATAAAACCTAATGTTGGA	checking RTT102

		K.O.
FK2799	GGGTGGTGTAGCATCCTTTACT	checking RTT102 K.O.
FK2800	CGAGACCTCAACTTCACCTCA	for TMA20 K.O.
FK2801	AGAAGGTTAACAGCCCATCG	for TMA20 K.O.
FK2802	TGCCGCTTTGTGATAATGAG	for TOM1 K.O.
FK2803	CTTCCTTGGGCAAGTGTTGT	for TOM1 K.O.
FK2804	GGTATATGAACTCAGTTTTAAGGTGTAGTTTATTTTATAG TCCGTACGCTGCAGGTCGAC	for YBR259W K.O.
FK2805	TACAAAACTTGCTAAGGTCCAACTCCCTGTCTTCACGGT TGATCGATGAATTCGAGCTCG	for YBR259W K.O.
FK2806	CTGTGTTTCAGCTTCGCTAAAT	checking YBR259W K.O.
FK2807	TCCAAGCAACCTTCCATGA	checking YBR259W K.O.
FK2808	CTTCGTGGTTCAAACAGTGC	for YDR220C K.O.
FK2809	CCAGCGGCATCTGTACACTA	for YDR220C K.O.
FK2810	AACGCCACCGAAAAATCTTA	for YDR333C K.O.
FK2811	GTAAACGTCGGACCACTCGT	for YDR333C K.O.
FK2812	GGTGCTTTAGATGGAGTTGC	for YGL262W K.O.
FK2813	TCCAAGGACGGTATCTACAC	for YGL262W K.O.
FK2814	GCTGGTACGTAGCGTAGCTT	for YJL213W K.O.
FK2815	CCTCCTTGAGGTGTTCTATT	for YJL213W K.O.
FK2816	CGTGGTGTTGAAGAAAGAATG	for OXP1 K.O.
FK2817	CGAAACATTGTTAAGTGCCTGT	for OXP1 K.O.
FK2818	GTGTACCCTCCCCTCCTCAT	for YLR352 K.O.
FK2819	TTCGTTTCCGAAAAGTCTGG	for YLR352 K.O.
FK2824	ATCAAGCCTTCGTCAGCATT	for YLR445W K.O.
FK2825	CCGAGTAATAAGGCCAGTTG	for YLR445W K.O.
FK2826	GGCAAGCCAAGAAAACCTGC	for YMR196W K.O.
FK2827	ATGCCATTATCGCAGTCCTT	for YMR196W K.O.
FK2828	AAGGCACCGTGCTAATAACG	for YNL035C K.O.
FK2829	GTTCTGCCGAAATCTCTTGC	for YNL035C K.O.
FK2830	GCATTGGTGGACGTAAGAGC	for YNL046W K.O.
FK2831	GAAGCGTGGGCAGGTAAATA	for YNL046W K.O.
FK2832	CACAGGTGCATCTGCTTGTT	for YOR111W K.O.
FK2833	AAGGCCTTTTTGAAGGTGAA	for YOR111W K.O.
FK2834	CTCCATTACCCGGAGTTGAA	for YOR223W K.O.
FK2835	TTGATTCGTCGTTAGCAGCA	for YOR223W K.O.
FK2836	TTAACATTCCCGGGTGAAAA	for YOR296W K.O.
FK2837	GACGCTCAAATATAGGGTGGA	for YOR296W K.O.
FK2838	TCAGCATGCCAAAATGCTAC	for YPL068C K.O.
FK2839	AGGCGAAGCAAAGAAAAATG	for YPL068C K.O.
FK2840	TGGAAGCAAGTTCTCCTTATCC	for YPL150W K.O.
FK2841	TCGCGAGTTCATACAGATGC	for YPL150W K.O.
FK2842	TGAAAGCATTCCTGGGATTT	for YPR078C K.O.

FK2843	CAGGACAATGGGGCATTATT	for YPR078C K.O.
FK2844	GATATCGAGAGTCTATCATGCCCTTTGCACAACAAAACT ACGTACGCTGCAGGTCGAC	for RMD6 K.O
FK2845	CCTACAGTTTATTCAAATAGAGTGTGTACGGGACTATAC CAATCGATGAATTCGAGCTCG	for RMD6 K.O
FK2846	CTTGGTCGTGATTGAAAACG	checking RMD6 K.O
FK2847	TTGCAGCAAAACAAGGAACC	checking RMD6 K.O
FK2848	CTTGAGGAGGCGAGAAAATG	checking TOM1 K.O. (used with FK2802)
FK2858	GGCGTGGATGTTTATTCTGT	for SWC2 qPCR (enrichment on ChrIII)
FK2859	ATTACCGCTATCGTTGGAAG	for SWC2 qPCR (enrichment on ChrIII)
FK2886	CCAGTAATTGTGCGCTTTGGTTACATTTTGTTGTACAGT Acgtacgctgcaggtcgac	for DOT1 K.O.
FK2887	TAGTTATTCATACTCATCGTTAAAAGCCGTTCAAAGTGC Catcgatgaattcgagctc	for DOT1 K.O.

Table 15: yeast strains used in this study

Strain	Relevant genotype
FKY1	Mat a/alpha, HO
FKY515	MATalpha, his7, hom3, spo13
FKY516	MATa, his7, hom3, spo13
FKY1084	Mat a/alpha, REC8-HA3::URA3, ura3
	REC8-HA3::URA3, ura3
FKY3091	Mat a/alpha, arg4Δ(eco47III-hpa1), leu2-RV::URA3-(Sma1-Eco47III)-[ARG4cloned], REC8-HA3::URA3
	arg4Δ(eco47III-hpa1),his4Δ(Sal1-Cla1)::URA3-Δ(Sma1-Eco47III)-arg4-EcPal(1691),REC8-HA3::URA3
FKY3108	Mat a/alpha, arg4Δ(eco47III-hpa1), leu2-RV::URA3-(Sma1-Eco47III)-[ARG4cloned],
	arg4Δ(eco47III-hpa1),his4Δ(Sal1-Cla1)::URA3-Δ(Sma1-Eco47III)-arg4-EcPal(1691)
FKY3391	Mat a/alpha, TOP2ΔC-9Myc-TRP1, Rec8-3HA::URA3, trp1::hisG
	TOP2ΔC-9Myc-TRP1, Rec8-3HA::URA3, trp1::hisG
FKY3484	Mat a/alpha, TOP2::3HA-TRP1, trp1::hisG
	TOP2::3HA-TRP1, trp1::hisG
FKY3593	Mat a/alpha, arg4Δ(eco47III-hpa1), leu2-RV::URA3-(Sma1-Eco47III)-[ARG4cloned], irc25::KanMX
	arg4Δ(eco47III-hpa1),his4Δ(Sal1-Cla1)::URA3-Δ(Sma1-Eco47III)-arg4-EcPal(1691), irc25::KanMX
FKY3596	Mat a/alpha, arg4Δ(eco47III-hpa1), leu2-RV::URA3-(Sma1-Eco47III)-[ARG4cloned], rad33::KanMX
	arg4Δ(eco47III-hpa1),his4Δ(Sal1-Cla1)::URA3-Δ(Sma1-Eco47III)-arg4-EcPal(1691), rad33::KanMX
FKY3598	Mat a/alpha, arg4Δ(eco47III-hpa1), leu2-RV::URA3-(Sma1-Eco47III)-[ARG4cloned], psy2::KanMX
	arg4Δ(eco47III-hpa1),his4Δ(Sal1-Cla1)::URA3-Δ(Sma1-Eco47III)-arg4-EcPal(1691), psy2::KanMX
FKY3601	Mat a/alpha, arg4Δ(eco47III-hpa1), leu2-RV::URA3-(Sma1-Eco47III)-[ARG4cloned], ynl196c::KanMX
	arg4Δ(eco47III-hpa1),his4Δ(Sal1-Cla1)::URA3-Δ(Sma1-Eco47III)-arg4-EcPal(1691), ynl196c::KanMX
FKY3604	Mat a/alpha, arg4Δ(eco47III-hpa1), leu2-RV::URA3-(Sma1-Eco47III)-[ARG4cloned], yor029w::KanMX
	arg4Δ(eco47III-hpa1),his4Δ(Sal1-Cla1)::URA3-Δ(Sma1-Eco47III)-arg4-EcPal(1691), yor029w::KanMX
FKY3607	Mat a/alpha, arg4Δ(eco47III-hpa1), leu2-RV::URA3-(Sma1-Eco47III)-[ARG4cloned], arp8::KanMX
	arg4Δ(eco47III-hpa1),his4Δ(Sal1-Cla1)::URA3-Δ(Sma1-Eco47III)-arg4-EcPal(1691), arp8::KanMX
FKY3610	Mat a/alpha, arg4Δ(eco47III-hpa1), leu2-RV::URA3-(Sma1-Eco47III)-[ARG4cloned], hnt3::KanMX
	arg4Δ(eco47III-hpa1),his4Δ(Sal1-Cla1)::URA3-Δ(Sma1-Eco47III)-arg4-EcPal(1691), hnt3::KanMX
FKY3628	Mat a/alpha, arg4Δ(eco47III-hpa1), leu2-RV::URA3-(Sma1-Eco47III)-[ARG4cloned], csm2::KanMX
	arg4Δ(eco47III-hpa1),his4Δ(Sal1-Cla1)::URA3-Δ(Sma1-Eco47III)-arg4-EcPal(1691), csm2::KanMXX
FKY3634	Mat a/alpha, arg4Δ(eco47III-hpa1), leu2-RV::URA3-(Sma1-Eco47III)-

	[ARG4cloned], ldb7::KanMX
	arg4Δ(eco47III-hpa1),his4Δ(Sal1-Cla1)::URA3-Δ(Sma1-Eco47III)-arg4-EcPal(1691), ldb7::KanMXX
FKY3336	Mat a/alpha, arg4Δ(eco47III-hpa1), leu2-RV::URA3-(Sma1-Eco47III)-[ARG4cloned], psy4::KanMX
	arg4Δ(eco47III-hpa1),his4Δ(Sal1-Cla1)::URA3-Δ(Sma1-Eco47III)-arg4-EcPal(1691), psy4::KanMXX
FKY3639	Mat a/alpha, arg4Δ(eco47III-hpa1), leu2-RV::URA3-(Sma1-Eco47III)-[ARG4cloned], bre1::KanMX
	arg4Δ(eco47III-hpa1),his4Δ(Sal1-Cla1)::URA3-Δ(Sma1-Eco47III)-arg4-EcPal(1691), bre1::KanMXX
FKY3645	Mat a/alpha, arg4Δ(eco47III-hpa1), leu2-RV::URA3-(Sma1-Eco47III)-[ARG4cloned], shu2::KanMX
	arg4Δ(eco47III-hpa1),his4Δ(Sal1-Cla1)::URA3-Δ(Sma1-Eco47III)-arg4-EcPal(1691), shu2::KanMXX
FKY3648	Mat a/alpha, arg4Δ(eco47III-hpa1), leu2-RV::URA3-(Sma1-Eco47III)-[ARG4cloned], ubc13::KanMX
	arg4Δ(eco47III-hpa1),his4Δ(Sal1-Cla1)::URA3-Δ(Sma1-Eco47III)-arg4-EcPal(1691), ubc13::KanMXX
FKY3651	Mat a/alpha, arg4Δ(eco47III-hpa1), leu2-RV::URA3-(Sma1-Eco47III)-[ARG4cloned], rvs167::KanMX
	arg4Δ(eco47III-hpa1),his4Δ(Sal1-Cla1)::URA3-Δ(Sma1-Eco47III)-arg4-EcPal(1691), rvs167::KanMXX
FKY3654	Mat a/alpha, arg4Δ(eco47III-hpa1), leu2-RV::URA3-(Sma1-Eco47III)-[ARG4cloned], rad6::KanMX
	arg4Δ(eco47III-hpa1),his4Δ(Sal1-Cla1)::URA3-Δ(Sma1-Eco47III)-arg4-EcPal(1691), rad6::KanMXX
FKY3657	Mat a/alpha, arg4Δ(eco47III-hpa1), leu2-RV::URA3-(Sma1-Eco47III)-[ARG4cloned], ygl101w::KanMX
	arg4Δ(eco47III-hpa1),his4Δ(Sal1-Cla1)::URA3-Δ(Sma1-Eco47III)-arg4-EcPal(1691), ygl101w::KanMXX
FKY3660	Mat a/alpha, arg4Δ(eco47III-hpa1), leu2-RV::URA3-(Sma1-Eco47III)-[ARG4cloned], ybr090c::KanMX
	arg4Δ(eco47III-hpa1),his4Δ(Sal1-Cla1)::URA3-Δ(Sma1-Eco47III)-arg4-EcPal(1691), ybr090c::KanMXX
FKY3663	Mat a/alpha, arg4Δ(eco47III-hpa1), leu2-RV::URA3-(Sma1-Eco47III)-[ARG4cloned], ynr068c::KanMX
	arg4Δ(eco47III-hpa1),his4Δ(Sal1-Cla1)::URA3-Δ(Sma1-Eco47III)-arg4-EcPal(1691), ynr068c::KanMX
FKY3666	Mat a/alpha, arg4Δ(eco47III-hpa1), leu2-RV::URA3-(Sma1-Eco47III)-[ARG4cloned], ctf8::KanMX
	arg4Δ(eco47III-hpa1),his4Δ(Sal1-Cla1)::URA3-Δ(Sma1-Eco47III)-arg4-EcPal(1691), ctf8::KanMX
FKY3672	Mat a/alpha, arg4Δ(eco47III-hpa1), leu2-RV::URA3-(Sma1-Eco47III)-[ARG4cloned], psy3::KanMX
	arg4Δ(eco47III-hpa1),his4Δ(Sal1-Cla1)::URA3-Δ(Sma1-Eco47III)-arg4-EcPal(1691), psy3::KanMX
FKY3677	Mat a/alpha, arg4Δ(eco47III-hpa1), leu2-RV::URA3-(Sma1-Eco47III)-[ARG4cloned], taf14::KanMX
	arg4Δ(eco47III-hpa1),his4Δ(Sal1-Cla1)::URA3-Δ(Sma1-Eco47III)-arg4-EcPal(1691), taf14::KanMX
FKY3766	Mat a/alpha, rim4Δ::KanMX
	rim4Δ::KanMX
FKY3800	Mat a/alpha, REC8-HA3::URA3, ura3
	REC8-HA3::URA3, ura3

FKY3819	Mat a/alpha, pch2Δ1::KanMX4
	pch2Δ1::KanMX4
FKY4065	Mat a/alpha, hta1-S129A hta2-S129A, pph3:KanMX4
	hta1-S129A hta2-S129A, pph3:KanMX4
FKY4073	Mat a/alpha, htb1-K123R::KlURA3, htb2-K123R::kanMX6
	htb1-K123R::KlURA3, htb2-K123R::kanMX6
FKY4102	Mat a/alpha, arg4Δ(eco47III-hpa1), leu2-RV::URA3-(Sma1-Eco47III)-[ARG4cloned], hos1::KanMX
	arg4Δ(eco47III-hpa1),his4Δ(Sal1-Cla1)::URA3-Δ(Sma1-Eco47III)-arg4-EcPal(1691), hos1::KanMX
FKY4105	Mat a/alpha, arg4Δ(eco47III-hpa1), leu2-RV::URA3-(Sma1-Eco47III)-[ARG4cloned], ylr352w::KanMX
	arg4Δ(eco47III-hpa1),his4Δ(Sal1-Cla1)::URA3-Δ(Sma1-Eco47III)-arg4-EcPal(1691), ylr352w::KanMX
FKY4118	Mat a/alpha, hta1-S129A, hta2-S129A (related to FKY406, old sending from lichten´s lab)
	hta1-S129A, hta2-S129A
FKY4134	Mat a/alpha, arg4Δ(eco47III-hpa1), leu2-RV::URA3-(Sma1-Eco47III)-[ARG4cloned], ydr333c::KanMX
	arg4Δ(eco47III-hpa1),his4Δ(Sal1-Cla1)::URA3-Δ(Sma1-Eco47III)-arg4-EcPal(1691), ydr333c::KanMX
FKY4137	Mat a/alpha, arg4Δ(eco47III-hpa1), leu2-RV::URA3-(Sma1-Eco47III)-[ARG4cloned], ykl215c::KanMX
	arg4Δ(eco47III-hpa1),his4Δ(Sal1-Cla1)::URA3-Δ(Sma1-Eco47III)-arg4-EcPal(1691), ykl215c::KanMX
FKY4140	Mat a/alpha, arg4Δ(eco47III-hpa1), leu2-RV::URA3-(Sma1-Eco47III)-[ARG4cloned], ymr196w::KanMX
	arg4Δ(eco47III-hpa1),his4Δ(Sal1-Cla1)::URA3-Δ(Sma1-Eco47III)-arg4-EcPal(1691), ymr196w::KanMX
FKY	Mat a/alpha,
FKY4150	Mat a/alpha, set1Δ::KanMX4, dot1Δ::NatMX4
	set1Δ::KanMX4, dot1Δ::NatMX4
FKY4240	Mat a/alpha, dot1Δ::NatMX4
	dot1Δ::NatMX4
FKY4257	Mat a/alpha, fpr3Δ::KanMX4
	fpr3Δ::KanMX4
FKY4275	Mat a/alpha, set1Δ::KanMX4
	set1Δ::KanMX4
FKY4287	Mat a/alpha, pph3Δ::KanMX4, fpr3Δ::KanMX4
	pph3Δ::KanMX4, fpr3Δ::KanMX4
FKY4295	Mat a/alpha, htz1Δ::KanMX
	htz1Δ::KanMX
FKY4358	Mat a/alpha, pph3Δ::kanMX4, pch2Δ1::KanMX4
	pph3Δ::kanMX4, pch2Δ1::KanMX4
FKY4433	Mat a/alpha, hta1-S129A hta2-S129A (new sending from lichten´s lab)
	hta1-S129A hta2-S129A
FKY4450	Mat a/alpha, hta1-S129A hta2-S129A, pph3::KanMX
	hta1-S129A hta2-S129A, pph3::KanMX
FKY4456	Mat a/alpha, pph3Δ::KanMX, htz1Δ::KanMX,
	pph3Δ::KanMX, htz1Δ::KanMX,
FKY4570	Mat a/alpha, arg4Δ(eco47III-hpa1), leu2-RV::URA3-(Sma1-Eco47III)-[ARG4cloned], pph3::KanMX
	arg4Δ(eco47III-hpa1),his4Δ(Sal1-Cla1)::URA3-Δ(Sma1-Eco47III)-arg4-EcPal(1691) pph3::KanMX

FKY4471	Mat a/alpha, arg4Δ(eco47III-hpa1), leu2-RV::URA3-(Sma1-Eco47III)-[ARG4cloned], pph3::KanMX
	arg4Δ(eco47III-hpa1),his4Δ(Sal1-Cla1)::URA3-Δ(Sma1-Eco47III)-arg4-EcPal(1691) pph3::KanMX
FKY4479	Mat a/alpha, mek1::LYS2, lys2
	mek1::LYS2, lys2
FKY4572	Mat a/alpha, shp1::KanMX6::pCLB2-HA3-SHP1
	shp1::KanMX6::pCLB2-HA3-SHP1
FKY4580	Mat a/alpha, pph3Δ::KanMX, swr1Δ::NatMX4
	pph3Δ::KanMX, swr1Δ::NatMX4
FKY4590	Mat a/alpha, pph3Δ::KanMX4, ldb7::KanMX4
	pph3Δ::KanMX4, ldb7::KanMX4
FKY4622	Mat a/alpha, swc2Δ::NatMx4
	swc2Δ::NatMx4
FKY4623	Mat a/alpha, pph3Δ::KanMX, swc2Δ::NatMX4
	pph3Δ::KanMX, swc2Δ::NatMX4
FKY4634	Mat a/alpha, Swc2-3HA::TRP1, trp1::hisG
	Swc2-3HA::TRP1, trp1::hisG
FKY4657	Mat a/alpha, pph3Δ::KanMX4, Swc2-3HA::KTRP1, trp1::hisG
	pph3Δ::KanMX4, Swc2-3HA::KTRP1, trp1::hisG
FKY4702	Mat a/alpha, RIM4-HA3::KanMX6
	RIM4-HA3::KanMX6
FKY4758	Mat a/alpha, ies2Δ::KanMX4
	ies2Δ::KanMX4
FKY4799	Mat a/alpha, dot1Δ::NatMX4, pph3Δ::KanMX4
	dot1Δ::NatMX4, pph3Δ::KanMX4
FKY4809	Mat a/alpha, pph3Δ::KanMX4, rad54Δ::KanMX4,
	pph3Δ::KanMX4, rad54Δ::KanMX4,
FKY4812	Mat a/alpha, pph3Δ::KanMX4, fpr3Δ::KanMX4, swc2Δ::NatMX4
	pph3Δ::KanMX4, fpr3Δ::KanMX4, swc2Δ::NatMX4
FKY4824	Mat a/alpha, pph3Δ::KanMX4, fpr3Δ::KanMX4, pch2Δ::NatMX4
	pph3Δ::KanMX4, fpr3Δ::KanMX4, pch2Δ::NatMX4
FKY4838	Mat a/alpha, mek1Δ::LYS2. pph3Δ::KanMX4, lys2
	mek1Δ::LYS2. pph3Δ::KanMX4, lys2
FKY4850	Mat a/alpha, hal5Δ::KanMX4
	hal5Δ::KanMX4
FKY4853	Mat a/alpha, ynl035cΔ::KanMX4
	ynl035cΔ::KanMX4
FKY4856	Mat a/alpha, ynl046wΔ::KanMX4
	ynl046wΔ::KanMX4
FKY4859	Mat a/alpha, cmr3Δ::KanMX4
	cmr3Δ::KanMX4
FKY4862	Mat a/alpha, alk1Δ::KanMX4
	alk1Δ::KanMX4
FKY4865	Mat a/alpha, fmp41Δ::KanMX4
	fmp41Δ::KanMX4
FKY4868	Mat a/alpha, tma20Δ::KanMX4,
	tma20Δ::KanMX4,
FKY4871	Mat a/alpha, ypl150wΔ::KanMX4
	ypl150wΔ::KanMX4
FKY4874	Mat a/alpha, cts2Δ::KanMX4
	cts2Δ::KanMX4
FKY4877	Mat a/alpha, irc3Δ::KanMX4

	irc3Δ::KanMX4
FKY4880	Mat a/alpha, ddr2Δ::KanMX4
	ddr2Δ::KanMX4
FKY4883	Mat a/alpha, yor111wΔ::KanMX4,
	yor111wΔ::KanMX4,
FKY4886	Mat a/alpha, irc4Δ::KanMX4
	irc4Δ::KanMX4
FKY4889	Mat a/alpha, ydr220cΔ::KanMX4
	ydr220cΔ::KanMX4
FKY4892	Mat a/alpha, rdr1Δ::KanMX4
	rdr1Δ::KanMX4
FKY4895	Mat a/alpha, ypl068cΔ::KanMX4
	ypl068cΔ::KanMX4
FKY4901	Mat a/alpha, yor296wΔ::KanMX4
	yor296wΔ::KanMX4
FKY4907	Mat a/alpha, irc18Δ::KanMX4
	irc18Δ::KanMX4
FKY4910	Mat a/alpha, ecm11Δ::KanMX4
	ecm11Δ::KanMX4
FKY4913	Mat a/alpha, yjl049wΔ::KanMX4,
	yjl049wΔ::KanMX4,
FKY4916	Mat a/alpha, tom1Δ::KanMX4
	tom1Δ::KanMX4
FKY4919	Mat a/alpha, rtc1Δ::KanMX4,
	rtc1Δ::KanMX4,
FKY4922	Mat a/alpha, ybr259wΔ::KanMX4
	ybr259wΔ::KanMX4
FKY4925	Mat a/alpha, ypr078cΔ::KanMX4
	ypr078cΔ::KanMX4
FKY4958	Mat a/alpha, mec1-1, slmX, pph3Δ::KanMX4
	mec1-1, slmX, pph3Δ::KanMX4

Additional phenotypes of candidates in pure SK1

YDR540C/IRC4: (see also Figures 25, 26 and 27)

Nuclear division Rad51 foci (50 nuclei counted)

hoursinSPM	mono-	bi-	tetra-	Rad51 positive	totalfoci	total average	average of Rad51 positive
4	100	0	0	39	850	17,0	21,8
5	87	13	0	29	839	16,8	28,9
6	46	14	40	18	389	7,8	21,6
7	25	11	64	20	360	7,2	18,0
8	23	4	73	12	158	3,2	13,2
10	12	1	88	8	85	1,7	10,6

Synapsis: Zip1 staining

hours in SPM	No Zip1	Zip1 foci	Short stretches	long stretches	Almost full SC
4	10	27	30	22	12
5	29	21	17	21	12
6	46	11	12	15	16
7	54	19	16	9	2
8	77	8	10	5	0
10	91	5	3	1	0

Spore viability: 57/60

YJL037W/IRC18

Nuclear division Rad51 foci (50 nuclei counted)

hoursinSPM	mono-	bi-	tetra-	fill	totalfoci	total average	average of Rad51 positive
4	100	0	0	45	898	18,0	20,0
5	98	2	0	30	454	9,1	15,1
6	60	27	13	17	222	4,4	13,1
7	28	5	67	23	349	7,0	15,2
8	10	2	88	22	288	5,8	13,1
10	9	0	91	27	233	4,7	8,6

Synapsis: Zip1 staining

hours in SPM	No Zip1	Zip1 foci	short stretches	long stretches	almost complete
4	10	43	28	13	6
5	24	17	23	29	7
6	42	10	17	20	11
7	49	34	11	6	0
8	47	28	19	6	0
10	37	51	10	2	0

Spore viability: 50/60

YBL058W/SHP1

Nuclear division (DAPI staining) Rad51 foci (50 nuclei counted)

hours in SPM	mono-	bi-	tetra-	fill	totalfoci	total average	average of Rad51 positive
4	100	0	0	44	889	17,8	20,2
5	99	1	0	34	547	10,9	16,1
6	68	31	1	27	456	9,1	16,9
7	40	15	45	15	217	4,3	14,5
8	18	11	72				
10	7	2	91				

Synapsis: Zip1 staining

hours in SPM	No Zip1	Zip1 foci	short stretches	long stretches	almost complete

hours in SPM	mono-	bi-	tetra-	fill	totalfoci	total average	average of Rad51 positive
4	100	0	0	31	745	14,9	24,0
5	82	18	0	23	502	10,0	21,8
6	26	27	47	28	522	10,4	18,6
7	17	2	81	21	332	6,6	15,8
8	7	3	90	9	56	1,1	6,2
10							

4	10	67	18	5	0
5	16	47	21	15	1
6	47	30	10	10	3
7	51	22	10	12	5
8	82	7	8	2	1
10					

YDR220C/Dubious

Nuclear division: DAPI staining Rad51 foci (50 nuclei counted)

hours in SPM	mono-	bi-	tetra-	fill	totalfoci	total average	average of Rad51 positive
4	100	0	0	31	745	14.9	24.0
5	82	18	0	23	502	10.0	21.8
6	26	27	47	28	522	10.4	18.6
7	17	2	81	21	332	6.6	15.8
8	7	3	90	9	56	1.1	6.2
10							

Synapsis : Zip1 staining

hours in SPM	No Zip1	Zip1 foci	short stretches	long stretches	almost complete
4	17	22	30	26	6
5	35	22	18	13	12

6	32	15	9	22	22
7	46	38	13	3	0
8	53	33	12	2	0
10	66	30	3	1	0

Spore viability: 56/60

YPR078C

Nuclear division: DAPI staining Rad51 foci (50 nuclei counted)

hours in SPM	mono-	bi-	tetra-	fill	totalfoci	total average	average of Rad51 positive
4	100	0	0	32	669	13,4	20,9
5	80	20	0	24	495	9,9	20,6
6	52	21	27	22	391	7,8	17,8
7	11	2	88	13	134	2,7	10,3
8	8	2	90	10	93	1,9	9,3
10							

Synapsis: Zip1 staining

hours in SPM	No Zip1	Zip1 foci	short stretches	long stretches	almost complete
4	8	17	24	27	24
5	38	14	18	16	14
6	34	25	15	16	10
7	48	40	12	0	0
8	40	47	13	0	0
10					

Spore viability: 55/56

YOR380W/RDR1

Nuclear division : DAPI staining Rad51 foci (50 nuclei counted)

hours in SPM	mono-	bi-	tetra-	fill	totalfoci	total average	average of Rad51 positive
4	100	0	0	41	736	14,7	18,0
5	95	5	0	25	410	8,2	16,4
6	54	26	20	27	294	5,9	10,9
7	23	7	70	20	199	4,0	10,0
8	10	0	90	19	166	3,3	8,7
10							

Synapsis : Zip1 staining

hours in SPM	No Zip1	Zip1 foci	short stretches	long stretches	almost complete
4	4	28	21	35	12
5	25	35	20	14	6
6	39	38	10	11	2
7	40	50	6	3	1
8	48	38	11	3	0
10					

Spore viability: 50/56

YNL046W

Nuclear division: DAPI staining Rad51 foci (50 nuclei staining)

hours in SPM	mono-	bi-	tetra-	fill	totalfoci	total average	average of Rad51 positive
4	100	0	0	29	590	11,8	20,3
5	69	29	2	10	356	7,1	35,6
6	28	13	59	26	431	8,6	16,6
7	9	3	88	27	252	5,0	9,3
8	5	0	95	20	185	3,7	9,3
10							

Synapsis: Zip1 staining

hours in SPM	No Zip1	Zip1 foci	short stretches	long stretches	almost complete
4	14	59	13	11	3
5	50	40	3	4	3
6	47	19	7	16	11
7	53	18	14	12	4
8	65	22	4	7	2
10					

Spore viability: 56/60

YPL165C/HAL5

Nuclear division: DAPI staining Rad51 foci (50 nuclei counted)

hours in SPM	mono-	bi-	tetra-	fill	totalfoci	total average	average of Rad51 positive
4	100	0	0	40	657	13,1	16,4
5	77	23	0	23	318	6,4	13,8
6	50	13	37	25	383	7,7	15,3
7	18	7	75	12	115	2,3	9,6
8	13	2	85	8	130	2,6	16,3
10							

Synapsis: Zip1 staining

hours in SPM	No Zip1	Zip1 foci	short stretches	long stretches	almost complete
4	9	45	21	15	10
5	30	31	18	12	9
6	30	24	20	19	7
7	57	17	13	9	4
8	74	17	5	4	1
10					

Spore viability: 59/60

YOL138C/RTC1/SEA2

Nuclear division: DAPI staining Rad51 foci (50 nuclei counted)

hours in SPM	mono-	bi-	tetra-	fill	totalfoci	total average	average of Rad51 positive
4	100	0	0	39	644	12,9	16,5
5	67	33	0	25	426	8,5	17,0
6	22	14	64	22	302	6,0	13,7
7	9	0	91	9	100	2,0	11,1
8	4	0	96	15	189	3,8	12,6
10							

Synapsis: Zip1 staining

hours in SPM	No Zip1	Zip1 foci	short stretches	long stretches	almost complete
4	14	29	19	21	19
5	25	26	11	24	14
6	36	24	12	14	14
7	46	26	15	11	2
8	73	14	4	7	2
10					

Spore viability: 58/60

YBR259W

Nuclear division: DAPI staining Rad51 foci (50 nuclei counted)

hours in SPM	mono-	bi-	tetra-	fill	totalfoci	total average
4	100	0	0		251	5,0
5	93	7	0		234	4,7
6	45	29	26		106	2,1
7	24	12	64		62	1,2
8	17	3	80			0,0
10	10	0	90			

Synapsis: Zip1 staining

hours in SPM	No Zip1	Zip1 foci	short stretches	long stretches	almost complete
4	28	47	20	5	0
5	48	27	13	6	4
6	69	11	3	10	6
7	69	30	0	1	0
8	98	2	0	0	0
10					

YDR371W/CTS2

Nuclear division: DAPI staining

hours in SPM	mono-	bi-	tetra-
4	100	0	0
5	63	37	0
6	32	35	33
7	18	10	72
8	10	10	80
10	3	1	96

Synapsis: Zip1 staining

hours in SPM	No Zip1	Zip1 foci	short stretches	long stretches	almost complete
4		53	24	19	4
5		63	22	13	2
6		52	26	18	4
7		95	5	0	0
8					

YER007C-A/TMA20

Nuclear division: DAPI staining

hours in SPM	mono-	bi-	tetra-
4	100	0	0
5	91	9	0
6	75	23	2
7	33	57	10
8	11	16	73
10	6	3	91

Synapsis: Zip1 staining

hours in SPM	Zip1 foci	short stretches	long stretches	almost complete
4	78	22	0	0
5	46	20	4	0
6	57	29	13	2
7	77	15	7	2
8	58	30	11	0
10	87	6	6	1

Spore viability: 52/60

The chromatin localization map of Top2

In yeast, a temperature sensitive allele of the DNA topoisomeraseII (*top2*^{ts}) was shown to display a dramatic spore lethality at a restrictive temperature. The spore inviability was suppressed or prevented by nocodazole treatment (Holm et al., 1985). Kinetics of pre-meiotic DNA synthesis of *top2*^{ts} mutants was shown to be similar to wild type, but recombined chromosomes were unable to segregate during the first meitic division (Rose and Holm, 1990). It was also shown that the SUMO (Smt3) isopeptidase *smt4*Δ mutant exhibits an increased frequency of precocious centromere separation and notably fails to maintain cohesion at centromere proximal regions that normally do not disjoin prior to anaphase (Bachant et al., 2002); and *top2-SNM* mutant that is resistant to Smt3 modification was found to suppress the *smt4*Δ cohesion defects (Bachant et al., 2002).

We set out to investigate the chromatin localization pattern of DNA topoisomerase II, a tagged version of Top2 (Top2-Myc9) was analyzed by ChIP on chip. Interstingly, we found a striking overlap between many DSB hotspots and the Top2 signals, as illustrated in Figure 30. This is an unusual case, as very few proteins so far are labelling the DSB sites in our hands. Further analysis is required to see whether this localization is dependent on DSB formation and recombination.

Summary

During the meiotic cell cycle, one round of DNA replication is followed by two rounds of chromosome segregation in which the two pairs of homologous sister centromeres segregate from each other during the first division while sister centromeres are partitioned in the second division. Hereby, the chromosome set of a diploid cell is reduced to half and four haploid cells are generated as precursors of gametes. A highly conserved meiosis-specific chromosomal structure called synaptonemal complex (SC) is formed during meiotic prophase I, connecting the axes of paired homologous chromosomes. The SC has a tripartite proteinaceous structure consisting of two axial elements connected by a central region called transverse filament. In most organisms including the budding yeast *Saccharomyces cerevisiae*, mutants that fail to form mature SC are also defective in crossover formation between the homologous chromosomes, which is required for accurate segregation of the homologs during the first meiotic division (Börner et al, 2004). The molecular mechanism of SC formation is not understood very well.

In order to identify a comprehensive set of genes required for chromosome synapsis, I have performed a systematic, genome-wide visual screen for mutations affecting chromosome morphology. Of the 4800 non-essential ORFs represented in the deletion library, I have analyzed 3630 in a primary round. Nearly 14.5% (524) of the deletions affected synapsis or were unable to induce the meiotic program. Nearly all mutants previously known to be essential for meiotic recombination and SC formation were re-identified, if analyzed. Of the 524 identified mutants with strong phenotypes, 132 were unable to initiate the meiotic program, 90 failed to undergo synapsis, 102 only underwent exclusively very short synapsis and 200 failed to form complete or nearly complete SC. The identified ORFs had been annotated with a wide variety of biological processes, such as respiration, RNA and DNA metabolism, membrane biology or meiosis.

For closer characterization, a set of 30 identified ORFs from various classes were deleted in the SK1 strain background. The respective mutants were

characterized for chromosome synapsis during a meiotic time course and selected mutants were subjected to FACS analysis and to physical recombination assays. Only one of these (*rim4*Δ) is unable to synapse at all, whereas 3 (*ecm11*Δ*, ymr196*Δ*,* and *yor296*Δ) show nearly no complete synapsis. All other ORFs, show complete synapsis in SK1, but either in too few nuclei, or they show an aberrant progression through the different stages of synapsis. Only 4 deletions behaved very similar to wild type (*irc4*Δ*, hal5*Δ*, rtc1*Δ*, ynl046*Δ*),* although not perfectly identical.

I also contributed to the characterization of 22 mutants, which were previously identified in a pilot screen carried out in our lab by A. Woglar (master thesis 2008). Rad6 and Bre1 are required for the monoubiquitination of histone H2B at lysine 123. (Robzyk et al., 2000). I showed that the synapsis defect in *htb1-K123R, htb2-K123R* double mutants is similar to, but not as rigorous as, in *bre1*Δ and *rad6*Δ, or lge1 mutants. This indicates a major role of histone H2B-K123 ubiquitination in synapsis, but also hints at additional roles of Rad6/Bre1. H2B-K123 monoubiquitination is required for histone H3K4 and H3K79 trimethylation by COMPASS (Set1) and Dot1 (Nakanishi et al., 2009) respectively. Interestingly, elimination of both, *SET1* and *DOT1,* which should eliminate H3K4 and H3K79 trimethylation, does not eliminate extensive synapsis, although it causes ca. a 2 hours delay. These observations suggest that H2B-K123 monoubiquitination may promote synapsis through an additional pathway, other than H3K4,K79 trimethylation.

The PP4 phosphatase complex anatagonizes the phosphorylation of various targets by he checkpoint kinases ATM/ATR (Tel1/Mec1) including histone H2A-S129, enabling checkpoint recovery after DNA damage (Keogh et al, 2006). We found *pph3*Δ to be defective in pre-meiotic DNA replication, chromosome synapsis, crossover formation and nuclear division (Woglar A, master thesis; this work), observations also made by others (Falk et al., 2010a). Interestingly, pch2Δ is epistatic to *pph3*Δ concerning synapsis, overcompensating the synapsis defect. Also deletion of *SWC2* can restore extensive synapsis in *pph3*Δ mutants. In contrast deletion of *MEK1* or of *FPR3* suppressed the nuclear

division defects of *pph3*Δ mutants. Interestingly, the triple mutant *pph3*Δ*, pch2*Δ*, fpr3*Δ progressed through meiosis almost normally, underwent synapsis and produced viable spores. We conclude, that Pch2 prevents synapsis in response to the ATM, ATR mediated checkpoint response, and that the role of PP4 is to downregulate that signal upon repair, to inactivate Pch2 and to allow synapsis. We propose that this constitutes a module to coordinate synapsis with completion of DSB repair. Fpr3 rather is an inhibitor of an alternative way to antagonize ATM/ATR, that is PP1 (Glc7-phosphatase), normally only activated shortly before the division.

Zusammenfassung

Im meiotischen Zellzyklus folgen einer Runde DNA-Replikation zwei Runden Chromosomensegregation in denen zunächst in der ersten Zellteilung die zwei Paare homologer Schwesterzentromere von einander segregieren, währen die Schwesterzentromere in der zweiten Teilung separiert werden. Als Folge wird der Chromosomensatz halbiert und aus einer diploiden Zelle gehen vier Zellen mit einem nun haploiden Genom hervor, als Vorläufer der Gameten. Im Laufe der meiotischen Prophase 1 bildet sich eine meiosespezifische, hoch konservierten Struktur aus, der sogenannte Synaptonemale Komplex (SC), welcher die Axen gepaarter homologer Chromosomen verbindet. Der SC hat eine dreigliedrige proteinöse Struktur, bestehend aus zwei seitlichen axialen Elementen, verbunden durch eine zentrale Region, dem Transversalfilament. In den meisten Organismen, einschließlich der Hefe Saccharomyces cerevisiae weisen Mutanten, die an der Bildung eines normalen SC scheitern ebenfalls Defekte in der Bildung von Crossovern zwischen den homologen Chromosomen auf, welche notwendig für die korrekte Aufteilung der Homologen während der ersten meiotischen Teilung sind (Börner et al, 2004). Über die molekularen Mechanismen der SC-Bildung besteht bisher nur sehr geringe Kenntnis.

Mit dem Ziel jene Gene, welche für die Synapsis der Chromosomen in Saccharomyces cerevisiae erforderlich sind umfassend zu identifizieren, habe ich in einem systematischen Screen genomweit, unter Zuhilfenahme visuell-mikroskopischer Methoden, nach Mutationen gesucht, welche die Chromosomenmorphologie beeinträchtigen.

Von den 4800 nicht essentiellen Genen, repräsentiert durch eine Gendeletionsbibliothek, habe ich 3630 in einem ersten Lauf analysiert. Nahezu 14.5% (524) der Gendeletionen beeinträchtigten Synapsis, oder führten zum Unvermögen das meiotische Programm in Gang zu setzen. Beinahe alle Mutanten von Genen – so denn analysiert –, die bereits zuvor als essentiell für meiotische Rekombination und SC-Bildung bekannt waren, konnten erneut

identifiziert werden. Von den 524 gefundenen Mutanten mit ausgeprägtem Phenotyp waren 132 nicht in der Lage das meiotische Programm zu initiieren, 90 konnten keinen SC bilden, 102 waren ausschliesslich zu sehr kurzer Synapsis befähigt, und 200 konnten keinen vollständigen oder ausgedehnten SC bilden. Die identifizierten Gene sind breitgefächert vielen verschiedenen biologischer Prozessen zugeordnet, wie zum Beispiel der Zellatmung, dem RNA und DNA Metabolismus, dem Membranaufbau, oder der Meiose.

Für eine genauere Charakterisierung wurden 30 der identifizierten Gene, einer breiten Auswahl unterschiedlicher Klassen, in einem reinen SK1 Stammhintergrund deletiert. Die resultierenden Mutanten wurden charakterisiert anhand ihrer Chromosomensynapsis in einer Zeitserie durch die Meiose, und ausgewählte Mutanten wurden zudem einer FACS-Analyse und einer physischen Rekombinationsmessung unterzogen. Nur eine dieser Mutanten (rim4Δ) ist dabei überhaupt nicht in der Lage SCs zu bilden, wohingegen drei (ecm11Δ, ymr196Δ, und yor296Δ) im wesentlichen keine vollständige Synapsis zustande bringen. Alle anderen Mutanten zeigen in SK1 vollständige Synapsis, jedoch entweder in zu wenigen Kernen, oder unter aberrantem Verlauf durch die verschiedenen Stadien der Synapsis. Nur vier Deletionen (irc4Δ, hal5Δ, rtc1Δ, and ynl046Δ) verhielten sich sehr ähnlich zum Wildtyp, wenn auch nicht völlig identisch.

Ebenso habe ich zu der Charakterisierung 22 weiterer Mutanten beigetragen, welche zuvor in einem Pilot-Screen identifiziert wurden, durchgeführt in unserem Labor durch A. Woglar (Diplomarbeit, 2008). Rad6 und Bre1 werden für die Monoubiquitinierung von Histon H2B an Lysin 123 (K123) benötigt (Robzyk et al., 2000). Ich konnte zeigen, dass der Synapsisdefekt einer htb1-K123R htb2-K123R Doppelmutante, bre1Δ und rad6Δ, oder lge1Δ ähnlich, jedoch nicht so ausgeprägt ist. Dies weist auf eine wesentliche Rolle von Histon H2B-K123 Ubiquitinierung für Synapsis hin, deutet aber auch zusätzliche Funktionen von Rad6/Bre1 an. Monoubiquitinierung von H2B-K123 ist wiederum notwendig für Trimenthylierung von Histon H3K4 durch COMPASS (Set1), beziehungsweise H3K79 durch Dot1 (Nakanishi et al., 2009). Interessanterweise führt die gemeinsame Eliminierung von SET1 und DOT1, welche auch H3K4 und

H3K79 Trimethylierung eliminieren sollte, nicht zum Verlust von ausgedehnter Synapsis, obgleich es zu einer Verzögerung von ungefähr zwei Stunden kommt. Diese Beobachtungen legen nahe, dass H2B-K123 Monoubiquitinierung über einen anderen Weg als H3K4/K79 Trimethylierung an Synapsis beteiligt ist.

Der PP4 Phosphatasekomplex (Pph3, Psy2 und Psy4) wirkt der Phosphorylierung zahlreicher Substrate der Checkpointkinasen ATM/ATR (Tel1/Mec1) entgegen, inklusive Histon H2A Serin 129 (S129), und erlaubt somit den Austritt aus dem Checkpointarrest nach erfolgter Reparatur von DNA-Schäden (Keogh et al, 2006). Wir haben für pph3Δ Defekte in der pre-meiotischen DNA Replikation, Synapsis, der Bildung von Crossovern, und den meiotischen Kernteilungen gefunden (Woglar A., Diplomarbeit; diese Arbeit), welche auch durch andere nachgewiesen wurden (Falk et al., 2010). Interessanterweise beobachteten wir, dass pch2Δ bezüglich Synapsis epistatisch über pph3Δ ist, und in pph3Δ Synapsis unter Überkompensierung wieder herstellt. Auch die Deletion von SWC2 erlaubt wieder ausgedehnte Synapsis in pph3Δ Mutanten. Dagegen bewirkt eine Deletion von MEK1 oder FPR3 die Suppression des Kernteilungsdefektes der pph3Δ Mutanten. Bemerkenswerterweise liessen sich in der Tripelmutante pph3Δ pch2Δ fpr3Δ die meiotischen Defekte der pph3Δ Mutante praktisch vollständig aufheben. pph3Δ pch2Δ fpr3Δ durchläuft nahezu normal das meiotische Programm, hat Synapsis, und produziert lebensfähige Sporen. Wir schliessen daraus, dass Pch2 Chromosomensynapsis als Antwort auf ATM/ATR Checkpointkinasenaktivität verhindert, und dass PP4 die Funktion einnimmt dieses Checkpointsignal nach erfolgter DNA-Reparatur zu eliminieren um Pch2 zu inaktivieren und Synapsis zu erlauben. Wir legen damit nahe, dass es sich hierbei um ein funktionelles Modul handelt, welches Synapsis mit der Vervollständigung der DNA-Reparatur koordiniert. Fpr3 hingegen wirkt als Inhibitor auf einen anderen Antagonisten von ATM/ATR, PP1 (Glc7-Phosphatase), welche normalerweise erst kurz vor der Kernteilung aktiviert wird.

References

Alani, E., Padmore, R., and Kleckner, N. (1990). Analysis of wild-type and rad50 mutants of yeast suggests an intimate relationship between meiotic chromosome synapsis and recombination. Cell *61*, 419-436.

Allers, T., and Lichten, M. (2001a). Differential timing and control of noncrossover and crossover recombination during meiosis. Cell *106*, 47-57.

Allers, T., and Lichten, M. (2001b). Intermediates of yeast meiotic recombination contain heteroduplex DNA. Mol Cell *8*, 225-231.

Alvaro, D., Lisby, M., and Rothstein, R. (2007). Genome-wide analysis of Rad52 foci reveals diverse mechanisms impacting recombination. PLoS Genet *3*, e228.

Argueso, J.L., Wanat, J., Gemici, Z., and Alani, E. (2004). Competing crossover pathways act during meiosis in Saccharomyces cerevisiae. Genetics *168*, 1805-1816.

Arora, C., Kee, K., Maleki, S., and Keeney, S. (2004). Antiviral protein Ski8 is a direct partner of Spo11 in meiotic DNA break formation, independent of its cytoplasmic role in RNA metabolism. Mol Cell *13*, 549-559.

Baarends, W.M., and Grootegoed, J.A. (2003). Chromatin dynamics in the male meiotic prophase. Cytogenetic and genome research *103*, 225-234.

Barber, L.J., Youds, J.L., Ward, J.D., McIlwraith, M.J., O'Neil, N.J., Petalcorin, M.I., Martin, J.S., Collis, S.J., Cantor, S.B., Auclair, M.*, et al.* (2008). RTEL1 maintains genomic stability by suppressing homologous recombination. Cell *135*, 261-271.

Bardhan, A., Chuong, H., and Dawson, D. (2010). Meiotic cohesin promotes pairing of nonhomologous centromeres in early meiotic prophase. Mol Biol Cell *21*, 1799-1809.

Baudat, F., Buard, J., Grey, C., Fledel-Alon, A., Ober, C., Przeworski, M., Coop, G., and de Massy, B. (2010). PRDM9 is a major determinant of meiotic recombination hotspots in humans and mice. Science *327*, 836-840.

Baudat, F., and Nicolas, A. (1997). Clustering of meiotic double-strand breaks on yeast chromosome III. Proc Natl Acad Sci U S A *94*, 5213-5218.

Becker, E., Meyer, V., Madaoui, H., and Guerois, R. (2006). Detection of a tandem BRCT in Nbs1 and Xrs2 with functional implications in the DNA damage response. Bioinformatics *22*, 1289-1292.

Berg, I.L., Neumann, R., Lam, K.W., Sarbajna, S., Odenthal-Hesse, L., May, C.A., and Jeffreys, A.J. (2010). PRDM9 variation strongly influences recombination hot-spot activity and meiotic instability in humans. Nature genetics *42*, 859-863.

Bishop, D.K., Park, D., Xu, L., and Kleckner, N. (1992). DMC1: a meiosis-specific yeast homolog of E. coli recA required for recombination, synaptonemal complex formation, and cell cycle progression. Cell *69*, 439-456.

Bishop, D.K., and Zickler, D. (2004). Early decision; meiotic crossover interference prior to stable strand exchange and synapsis. Cell *117*, 9-15.

Blanco, M.G., Matos, J., Rass, U., Ip, S.C., and West, S.C. (2010). Functional overlap between the structure-specific nucleases Yen1 and Mus81-Mms4 for DNA-damage repair in S. cerevisiae. DNA repair *9*, 394-402.

Blat, Y., Protacio, R.U., Hunter, N., and Kleckner, N. (2002). Physical and functional interactions among basic chromosome organizational features govern early steps of meiotic chiasma formation. Cell *111*, 791-802.

Bolte, M., Steigemann, P., Braus, G.H., and Irniger, S. (2002). Inhibition of APC-mediated proteolysis by the meiosis-specific protein kinase Ime2. Proceedings of the National Academy of Sciences of the United States of America *99*, 4385-4390.

Borde, V., Goldman, A.S., and Lichten, M. (2000a). Direct coupling between meiotic DNA replication and recombination initiation. Science *290*, 806-809.

Borde, V., Goldman, A.S., and Lichten, M. (2000b). Direct coupling between meiotic DNA replication and recombination initiation. Science *290*, 806-809.

Borde, V., Lin, W., Novikov, E., Petrini, J.H., Lichten, M., and Nicolas, A. (2004). Association of Mre11p with double-strand break sites during yeast meiosis. Mol Cell *13*, 389-401.

Borde, V., Robine, N., Lin, W., Bonfils, S., Geli, V., and Nicolas, A. (2009). Histone H3 lysine 4 trimethylation marks meiotic recombination initiation sites. EMBO J *28*, 99-111.

Borges, V., Lehane, C., Lopez-Serra, L., Flynn, H., Skehel, M., Rolef Ben-Shahar, T., and Uhlmann, F. (2010). Hos1 deacetylates Smc3 to close the cohesin acetylation cycle. Mol Cell *39*, 677-688.

Borner, G., Barot, A., and Kleckner, N. (2008). Yeast Pch2 promotes domainal axis organization, timely recombination progression, and arrest of defective recombinosomes during meiosis. Proc Natl Acad Sci U S A *105*, 3327-3332.

Borner, G.V., Kleckner, N., and Hunter, N. (2004). Crossover/noncrossover differentiation, synaptonemal complex formation, and regulatory surveillance at the leptotene/zygotene transition of meiosis. Cell *117*, 29-45.

Cao, L., Alani, E., and Kleckner, N. (1990). A pathway for generation and processing of double-strand breaks during meiotic recombination in S. cerevisiae. Cell *61*, 1089-1101.

Carballo, J.A., Johnson, A.L., Sedgwick, S.G., and Cha, R.S. (2008). Phosphorylation of the axial element protein Hop1 by Mec1/Tel1 ensures meiotic interhomolog recombination. Cell *132*, 758-770.

Cha, R.S., Weiner, B.M., Keeney, S., Dekker, J., and Kleckner, N. (2000). Progression of meiotic DNA replication is modulated by interchromosomal interaction proteins, negatively by Spo11p and positively by Rec8p. Genes Dev *14*, 493-503.

Chen, L., Morio, T., Minegishi, Y., Nakada, S., Nagasawa, M., Komatsu, K., Chessa, L., Villa, A., Lecis, D., Delia, D.*, et al.* (2005). Ataxia-telangiectasia-mutated dependent phosphorylation of Artemis in response to DNA damage. Cancer Sci *96*, 134-141.

Chen, Y., Leng, C., Olivares, H., Lee, M., Chang, Y., Kung, W., Ti, S., Lo, Y., Wang, A., Chang, C.*, et al.* (2004). Heterodimeric complexes of Hop2 and

Mnd1 function with Dmc1 to promote meiotic homolog juxtaposition and strand assimilation. Proc Natl Acad Sci U S A *101*, 10572-10577.

Chua, P.R., and Roeder, G.S. (1998). Zip2, a meiosis-specific protein required for the initiation of chromosome synapsis. Cell *93*, 349-359.

Collins, I., and Newlon, C.S. (1994). Chromosomal DNA replication initiates at the same origins in meiosis and mitosis. Mol-Cell-Biol *14*, 3524-3534.

Conrad, M.N., Dominguez, A.M., and Dresser, M.E. (1997). Ndj1p, a meiotic telomere protein required for normal chromosome synapsis and segregation in yeast [see comments]. Science *276*, 1252-1255.

Corbett, K.D., and Berger, J.M. (2003). Emerging roles for plant topoisomerase VI. Chemistry & biology *10*, 107-111.

Davis, L., Barbera, M., McDonnell, A., McIntyre, K., Sternglanz, R., Jin, Q., Loidl, J., and Engebrecht, J. (2001). The Saccharomyces cerevisiae MUM2 gene interacts with the DNA replication machinery and is required for meiotic levels of double strand breaks. Genetics *157*, 1179-1189.

de los Santos, T., Hunter, N., Lee, C., Larkin, B., Loidl, J., and Hollingsworth, N.M. (2003). The Mus81/Mms4 endonuclease acts independently of double-Holliday junction resolution to promote a distinct subset of crossovers during meiosis in budding yeast. Genetics *164*, 81-94.

Dehe, P.M., and Geli, V. (2006). The multiple faces of Set1. Biochemistry and cell biology = Biochimie et biologie cellulaire *84*, 536-548.

Deng, C., and Saunders, W.S. (2001). RIM4 encodes a meiotic activator required for early events of meiosis in Saccharomyces cerevisiae. Molecular genetics and genomics : MGG *266*, 497-504.

Dernburg, A.F., McDonald, K., Moulder, G., Barstead, R., Dresser, M., and Villeneuve, A.M. (1998). Meiotic recombination in C. elegans initiates by a conserved mechanism and is dispensable for homologous chromosome synapsis. Cell *94*, 387-398.

Diaz, R.L., Alcid, A.D., Berger, J.M., and Keeney, S. (2002). Identification of residues in yeast Spo11p critical for meiotic DNA double-strand break formation. Mol Cell Biol *22*, 1106-1115.

Dirick, L., Goetsch, L., Ammerer, G., and Byers, B. (1998). Regulation of meiotic S phase by Ime2 and a Clb5,6-associated kinase in Saccharomyces cerevisiae. Science *281*, 1854-1857.

Dong, H., and Roeder, G.S. (2000). Organization of the yeast Zip1 protein within the central region of the synaptonemal complex. The Journal of cell biology *148*, 417-426.

Enyenihi, A.H., and Saunders, W.S. (2003). Large-scale functional genomic analysis of sporulation and meiosis in Saccharomyces cerevisiae. Genetics *163*, 47-54.

Falk, J.E., Chan, A.C., Hoffmann, E., and Hochwagen, A. (2010a). A Mec1- and PP4-dependent checkpoint couples centromere pairing to meiotic recombination. Dev Cell *19*, 599-611.

Falk, J.E., Chan, A.C., Hoffmann, E., and Hochwagen, A. (2010b). A Mec1- and PP4-dependent checkpoint couples centromere pairing to meiotic recombination. Developmental cell *19*, 599-611.

Fekairi, S., Scaglione, S., Chahwan, C., Taylor, E.R., Tissier, A., Coulon, S., Dong, M.Q., Ruse, C., Yates, J.R., 3rd, Russell, P.*, et al.* (2009). Human SLX4 is a Holliday junction resolvase subunit that binds multiple DNA repair/recombination endonucleases. Cell *138*, 78-89.

Ferrari, S.R., Grubb, J., and Bishop, D.K. (2009). The Mei5-Sae3 protein complex mediates Dmc1 activity in Saccharomyces cerevisiae. The Journal of biological chemistry *284*, 11766-11770.

Fink, M., Imholz, D., and Thoma, F. (2007). Contribution of the serine 129 of histone H2A to chromatin structure. Mol Cell Biol *27*, 3589-3600.

Furuse, M., Nagase, Y., Tsubouchi, H., Murakami-Murofushi, K., Shibata, T., and Ohta, K. (1998). Distinct roles of two separable in vitro activities of yeast Mre11 in mitotic and meiotic recombination. EMBO J *17*, 6412-6425.

Gambus, A., Jones, R.C., Sanchez-Diaz, A., Kanemaki, M., van Deursen, F., Edmondson, R.D., and Labib, K. (2006). GINS maintains association of Cdc45 with MCM in replisome progression complexes at eukaryotic DNA replication forks. Nature cell biology *8*, 358-366.

Gasior, S.L., Olivares, H., Ear, U., Hari, D.M., Weichselbaum, R., and Bishop, D.K. (2001). Assembly of RecA-like recombinases: distinct roles for mediator proteins in mitosis and meiosis. Proc Natl Acad Sci U S A *98*, 8411-8418.

Giaever, G., Chu, A.M., Ni, L., Connelly, C., Riles, L., Veronneau, S., Dow, S., Lucau-Danila, A., Anderson, K., Andre, B.*, et al.* (2002). Functional profiling of the Saccharomyces cerevisiae genome. Nature *418*, 387-391.

Grether, M.E., and Herskowitz, I. (1999). Genetic and biochemical characterization of the yeast spo12 protein. Mol Biol Cell *10*, 3689-3703.

Guacci, V., Koshland, D., and Strunnikov, A. (1997). A direct link between sister chromatid cohesion and chromosome condensation revealed through the analysis of MCD1 in S. cerevisiae [see comments]. Cell *91*, 47-57.

Guttmann-Raviv, N., Boger-Nadjar, E., Edri, I., and Kassir, Y. (2001). Cdc28 and Ime2 possess redundant functions in promoting entry into premeiotic DNA replication in Saccharomyces cerevisiae. Genetics *159*, 1547-1558.

Hagstrom, K.A., Holmes, V.F., Cozzarelli, N.R., and Meyer, B.J. (2002). C. elegans condensin promotes mitotic chromosome architecture, centromere organization, and sister chromatid segregation during mitosis and meiosis. Genes & development *16*, 729-742.

Haruki, H., Nishikawa, J., and Laemmli, U. (2008). The anchor-away technique: rapid, conditional establishment of yeast mutant phenotypes. Mol Cell *31*, 925-932.

Hayase, A., Takagi, M., Miyazaki, T., Oshiumi, H., Shinohara, M., and Shinohara, A. (2004). A protein complex containing Mei5 and Sae3 promotes the assembly of the meiosis-specific RecA homolog Dmc1. Cell *119*, 927-940.

Henderson, K.A., Kee, K., Maleki, S., Santini, P.A., and Keeney, S. (2006). Cyclin-dependent kinase directly regulates initiation of meiotic recombination. Cell *125*, 1321-1332.

Henry, J.M., Camahort, R., Rice, D.A., Florens, L., Swanson, S.K., Washburn, M.P., and Gerton, J.L. (2006). Mnd1/Hop2 facilitates Dmc1-dependent

interhomolog crossover formation in meiosis of budding yeast. Molecular and cellular biology *26*, 2913-2923.

Hochwagen, A., and Amon, A. (2006). Checking your breaks: surveillance mechanisms of meiotic recombination. Current biology : CB *16*, R217-228.

Hochwagen, A., Tham, W., Brar, G., and Amon, A. (2005a). The FK506 binding protein Fpr3 counteracts protein phosphatase 1 to maintain meiotic recombination checkpoint activity. Cell *122*, 861-873.

Hochwagen, A., Tham, W.H., Brar, G.A., and Amon, A. (2005b). The FK506 binding protein Fpr3 counteracts protein phosphatase 1 to maintain meiotic recombination checkpoint activity. Cell *122*, 861-873.

Hollingsworth, N.M., Ponte, L., and Halsey, C. (1995). MSH5, a novel MutS homolog, facilitates meiotic reciprocal recombination between homologs in Saccharomyces cerevisiae but not mismatch repair. Genes & development *9*, 1728-1739.

Holzen, T.M., Shah, P.P., Olivares, H.A., and Bishop, D.K. (2006). Tid1/Rdh54 promotes dissociation of Dmc1 from nonrecombinogenic sites on meiotic chromatin. Genes & development *20*, 2593-2604.

Honigberg, S.M., and Purnapatre, K. (2003). Signal pathway integration in the switch from the mitotic cell cycle to meiosis in yeast. Journal of cell science *116*, 2137-2147.

Hooker, G.W., and Roeder, G.S. (2006). A Role for SUMO in meiotic chromosome synapsis. Current biology : CB *16*, 1238-1243.

Hopfner, K.P., Craig, L., Moncalian, G., Zinkel, R.A., Usui, T., Owen, B.A., Karcher, A., Henderson, B., Bodmer, J.L., McMurray, C.T.*, et al.* (2002). The Rad50 zinc-hook is a structure joining Mre11 complexes in DNA recombination and repair. Nature *418*, 562-566.

Hopfner, K.P., Karcher, A., Craig, L., Woo, T.T., Carney, J.P., and Tainer, J.A. (2001). Structural biochemistry and interaction architecture of the DNA double-strand break repair Mre11 nuclease and Rad50-ATPase. Cell *105*, 473-485.

Hunter, N., and Kleckner, N. (2001). The single-end invasion: an asymmetric intermediate at the double-strand break to double-holliday junction transition of meiotic recombination. Cell *106*, 59-70.

Ip, S.C., Rass, U., Blanco, M.G., Flynn, H.R., Skehel, J.M., and West, S.C. (2008). Identification of Holliday junction resolvases from humans and yeast. Nature *456*, 357-361.

Jambhekar, A., and Amon, A. (2008). Control of meiosis by respiration. Curr Biol *18*, 969-975.

Jessop, L., Rockmill, B., Roeder, G.S., and Lichten, M. (2006). Meiotic chromosome synapsis-promoting proteins antagonize the anti-crossover activity of sgs1. PLoS genetics *2*, e155.

Jiao, K., Bullard, S.A., Salem, L., and Malone, R.E. (1999). Coordination of the initiation of recombination and the reductional division in meiosis in Saccharomyces cerevisiae. Genetics *152*, 117-128.

Jordan, P., Klein, F., and Leach, D. (2007). Novel roles for selected genes in meiotic DNA processing. PLoS Genet *3*, 2368-2380.

Kalocsay, M., Hiller, N., and Jentsch, S. (2009). Chromosome-wide Rad51 spreading and SUMO-H2A.Z-dependent chromosome fixation in response to a persistent DNA double-strand break. Mol Cell *33*, 335-343.

Keeney, S., Giroux, C., and Kleckner, N. (1997a). Meiosis-specific DNA double-strand breaks are catalyzed by Spo11, a member of a widely conserved protein family. Cell *88*, 375-384.

Keeney, S., Giroux, C.N., and Kleckner, N. (1997b). Meiosis-specific DNA double-strand breaks are catalyzed by Spo11, a member of a widely conserved protein family. Cell *88*, 375-384.

Keeney, S., and Neale, M.J. (2006). Initiation of meiotic recombination by formation of DNA double-strand breaks: mechanism and regulation. Biochem Soc Trans *34*, 523-525.

Keogh, M., Kim, J., Downey, M., Fillingham, J., Chowdhury, D., Harrison, J., Onishi, M., Datta, N., Galicia, S., Emili, A*., et al.* (2006). A phosphatase complex that dephosphorylates gammaH2AX regulates DNA damage checkpoint recovery. Nature *439*, 497-501.

Kim, K.P., Weiner, B.M., Zhang, L., Jordan, A., Dekker, J., and Kleckner, N. (2010). Sister cohesion and structural axis components mediate homolog bias of meiotic recombination. Cell *143*, 924-937.

Kleckner, N. (2006). Chiasma formation: chromatin/axis interplay and the role(s) of the synaptonemal complex. Chromosoma *115*, 175-194.

Kleckner, N., Zickler, D., Jones, G.H., Dekker, J., Padmore, R., Henle, J., and Hutchinson, J. (2004). A mechanical basis for chromosome function. Proc Natl Acad Sci U S A *101*, 12592-12597.

Klein, F., Mahr, P., Galova, M., Buonomo, S.B., Michaelis, C., Nairz, K., and Nasmyth, K. (1999). A central role for cohesins in sister chromatid cohesion, formation of axial elements, and recombination during yeast meiosis. Cell *98*, 91-103.

Kosaka, H., Shinohara, M., and Shinohara, A. (2008). Csm4-dependent telomere movement on nuclear envelope promotes meiotic recombination. PLoS Genet *4*, e1000196.

Koszul, R., Kim, K., Prentiss, M., Kleckner, N., and Kameoka, S. (2008). Meiotic chromosomes move by linkage to dynamic actin cables with transduction of force through the nuclear envelope. Cell *133*, 1188-1201.

Koszul, R., and Kleckner, N. (2009). Dynamic chromosome movements during meiosis: a way to eliminate unwanted connections? Trends Cell Biol *19*, 716-724.

Krogan, N.J., Cagney, G., Yu, H., Zhong, G., Guo, X., Ignatchenko, A., Li, J., Pu, S., Datta, N., Tikuisis, A.P*., et al.* (2006). Global landscape of protein complexes in the yeast Saccharomyces cerevisiae. Nature *440*, 637-643.

Kumar, A., and Bachhawat, A.K. (2010). OXP1/YKL215c encodes an ATP-dependent 5-oxoprolinase in Saccharomyces cerevisiae: functional characterization, domain structure and identification of actin-like ATP-binding motifs in eukaryotic 5-oxoprolinases. FEMS yeast research *10*, 394-401.

Kus, B., Gajadhar, A., Stanger, K., Cho, R., Sun, W., Rouleau, N., Lee, T., Chan, D., Wolting, C., Edwards, A.*, et al.* (2005). A high throughput screen to identify substrates for the ubiquitin ligase Rsp5. The Journal of biological chemistry *280*, 29470-29478.

Lee, B., and Amon, A. (2001). Meiosis: how to create a specialized cell cycle. Curr Opin Cell Biol *13*, 770-777.

Lee, M.W., Kim, B.J., Choi, H.K., Ryu, M.J., Kim, S.B., Kang, K.M., Cho, E.J., Youn, H.D., Huh, W.K., and Kim, S.T. (2007). Global protein expression profiling of budding yeast in response to DNA damage. Yeast *24*, 145-154.

Li, J., Hooker, G.W., and Roeder, G.S. (2006). Saccharomyces cerevisiae Mer2, Mei4 and Rec114 Form a Complex Required for Meiotic Double-Strand Break Formation. Genetics *173*, 1969-1981.

Lin, F.M., Lai, Y.J., Shen, H.J., Cheng, Y.H., and Wang, T.F. (2010). Yeast axial-element protein, Red1, binds SUMO chains to promote meiotic interhomologue recombination and chromosome synapsis. The EMBO journal *29*, 586-596.

Liu, Y., Mimura, S., Kishi, T., and Kamura, T. (2009). A longevity protein, Lag2, interacts with SCF complex and regulates SCF function. The EMBO journal *28*, 3366-3377.

Loidl, J., Klein, F., and Engebrecht, J. (1998). Genetic and morphological approaches for the analysis of meiotic chromosomes in yeast. In Nuclear structure and function, M. Berrios, ed. (San Diego, Academic Press.), pp. 257-285.

Loidl, J., Klein, F., and Scherthan, H. (1994). Homologous pairing is reduced but not abolished in asynaptic mutants of yeast. The Journal of cell biology *125*, 1191-1200.

Lydall, D., and Weinert, T. (1996). From DNA damage to cell cycle arrest and suicide: a budding yeast perspective. Current opinion in genetics & development *6*, 4-11.

Macqueen, A., and Roeder, G. (2009a). Fpr3 and Zip3 ensure that initiation of meiotic recombination precedes chromosome synapsis in budding yeast. Curr Biol *19*, 1519-1526.

MacQueen, A.J., Colaiacovo, M.P., McDonald, K., and Villeneuve, A.M. (2002a). Synapsis-dependent and -independent mechanisms stabilize homolog pairing during meiotic prophase in C. elegans. Genes & development *16*, 2428-2442.

MacQueen, A.J., Colaiacovo, M.P., McDonald, K., and Villeneuve, A.M. (2002b). Synapsis-dependent and -independent mechanisms stabilize homolog pairing during meiotic prophase in C. elegans. Genes Dev *16*, 2428-2442.

Macqueen, A.J., and Roeder, G.S. (2009b). Fpr3 and Zip3 ensure that initiation of meiotic recombination precedes chromosome synapsis in budding yeast. Current biology : CB *19*, 1519-1526.

Mankouri, H.W., Ngo, H.P., and Hickson, I.D. (2007). Shu proteins promote the formation of homologous recombination intermediates that are processed by Sgs1-Rmi1-Top3. Mol Biol Cell *18*, 4062-4073.

Matos, J., Lipp, J., Bogdanova, A., Guillot, S., Okaz, E., Junqueira, M., Shevchenko, A., and Zachariae, W. (2008). Dbf4-dependent CDC7 kinase links DNA replication to the segregation of homologous chromosomes in meiosis I. Cell *135*, 662-678.

Mayer, M.L., Gygi, S.P., Aebersold, R., and Hieter, P. (2001). Identification of RFC(Ctf18p, Ctf8p, Dcc1p): an alternative RFC complex required for sister chromatid cohesion in S. cerevisiae. Mol Cell *7*, 959-970.

Mazina, O.M., Mazin, A.V., Nakagawa, T., Kolodner, R.D., and Kowalczykowski, S.C. (2004). Saccharomyces cerevisiae Mer3 helicase stimulates 3'-5' heteroduplex extension by Rad51; implications for crossover control in meiotic recombination. Cell *117*, 47-56.

McKee, A.H., and Kleckner, N. (1997). A general method for identifying recessive diploid-specific mutations in Saccharomyces cerevisiae, its application to the isolation of mutants blocked at intermediate stages of meiotic prophase and characterization of a new gene SAE2. Genetics *146*, 797-816.

McKim, K.S., Green-Marroquin, B.L., Sekelsky, J.J., Chin, G., Steinberg, C., Khodosh, R., and Hawley, R.S. (1998). Meiotic synapsis in the absence of recombination [see comments]. Science *279*, 876-878.

Merker, J., Dominska, M., Greenwell, P., Rinella, E., Bouck, D., Shibata, Y., Strahl, B., Mieczkowski, P., and Petes, T. (2008). The histone methylase Set2p and the histone deacetylase Rpd3p repress meiotic recombination at the HIS4 meiotic recombination hotspot in Saccharomyces cerevisiae. DNA Repair (Amst) *7*, 1298-1308.

Meuwissen, R.L., Offenberg, H.H., Dietrich, A.J., Riesewijk, A., van Iersel, M., and Heyting, C. (1992). A coiled-coil related protein specific for synapsed regions of meiotic prophase chromosomes. The EMBO journal *11*, 5091-5100.

Moreau, S., Ferguson, J.R., and Symington, L.S. (1999). The nuclease activity of Mre11 is required for meiosis but not for mating type switching, end joining, or telomere maintenance. Molecular and cellular biology *19*, 556-566.

Moreno-Herrero, F., de Jager, M., Dekker, N.H., Kanaar, R., Wyman, C., and Dekker, C. (2005). Mesoscale conformational changes in the DNA-repair complex Rad50/Mre11/Nbs1 upon binding DNA. Nature *437*, 440-443.

Murakami, H., and Keeney, S. (2008). Regulating the formation of DNA double-strand breaks in meiosis. Genes Dev *22*, 286-292.

Murakami, H., and Nurse, P. (2001). Regulation of premeiotic S phase and recombination-related double- strand DNA breaks during meiosis in fission yeast. Nat Genet *28*, 290-293.

Nairz, K., and Klein, F. (1997). mre11S--a yeast mutation that blocks double-strand-break processing and permits nonhomologous synapsis in meiosis. Genes & development *11*, 2272-2290.

Nakagawa, T., and Ogawa, H. (1999). The Saccharomyces cerevisiae MER3 gene, encoding a novel helicase-like protein, is required for crossover control in meiosis. The EMBO journal *18*, 5714-5723.

Nakanishi, S., Lee, J.S., Gardner, K.E., Gardner, J.M., Takahashi, Y.H., Chandrasekharan, M.B., Sun, Z.W., Osley, M.A., Strahl, B.D., Jaspersen,

S.L.*, et al.* (2009). Histone H2BK123 monoubiquitination is the critical determinant for H3K4 and H3K79 trimethylation by COMPASS and Dot1. The Journal of cell biology *186*, 371-377.
Nasmyth, K., and Haering, C. (2009). Cohesin: its roles and mechanisms. Annu Rev Genet *43*, 525-558.
Neale, M.J., Pan, J., and Keeney, S. (2005). Endonucleolytic processing of covalent protein-linked DNA double-strand breaks. Nature *436*, 1053-1057.
Nespoli, A., Vercillo, R., di Nola, L., Diani, L., Giannattasio, M., Plevani, P., and Muzi-Falconi, M. (2006). Alk1 and Alk2 are two new cell cycle-regulated haspin-like proteins in budding yeast. Cell cycle *5*, 1464-1471.
Niu, H., Wan, L., Baumgartner, B., Schaefer, D., Loidl, J., and Hollingsworth, N.M. (2005a). Partner choice during meiosis is regulated by Hop1-promoted dimerization of Mek1. Mol Biol Cell *16*, 5804-5818.
Niu, H., Wan, L., Baumgartner, B., Schaefer, D., Loidl, J., and Hollingsworth, N.M. (2005b). Partner choice during meiosis is regulated by Hop1-promoted dimerization of Mek1. Molecular biology of the cell *16*, 5804-5818.
Niu, H., Wan, L., Busygina, V., Kwon, Y., Allen, J.A., Li, X., Kunz, R.C., Kubota, K., Wang, B., Sung, P.*, et al.* (2009). Regulation of meiotic recombination via Mek1-mediated Rad54 phosphorylation. Molecular cell *36*, 393-404.
Novak, I., Wang, H., Revenkova, E., Jessberger, R., Scherthan, H., and Hoog, C. (2008). Cohesin Smc1beta determines meiotic chromatin axis loop organization. J Cell Biol *180*, 83-90.
O'Neill, B.M., Szyjka, S.J., Lis, E.T., Bailey, A.O., Yates, J.R., 3rd, Aparicio, O.M., and Romesberg, F.E. (2007). Pph3-Psy2 is a phosphatase complex required for Rad53 dephosphorylation and replication fork restart during recovery from DNA damage. Proc Natl Acad Sci U S A *104*, 9290-9295.
Obeso, D., and Dawson, D. (2010). Temporal characterization of homology-independent centromere coupling in meiotic prophase. PLoS One *5*, e10336.
Ofir, Y., Sagee, S., Guttmann-Raviv, N., Pnueli, L., and Kassir, Y. (2004). The role and regulation of the preRC component Cdc6 in the initiation of premeiotic DNA replication. Molecular biology of the cell *15*, 2230-2242.
Oh, S.D., Lao, J.P., Hwang, P.Y., Taylor, A.F., Smith, G.R., and Hunter, N. (2007). BLM ortholog, Sgs1, prevents aberrant crossing-over by suppressing formation of multichromatid joint molecules. Cell *130*, 259-272.
Padmore, R., Cao, L., and Kleckner, N. (1991). Temporal comparison of recombination and synaptonemal complex formation during meiosis in S. cerevisiae. Cell *66*, 1239-1256.
Page, S.L., and Hawley, R.S. (2001). c(3)G encodes a Drosophila synaptonemal complex protein. Genes & development *15*, 3130-3143.
Page, S.L., and Hawley, R.S. (2004). The genetics and molecular biology of the synaptonemal complex. Annual review of cell and developmental biology *20*, 525-558.
Pan, J., Sasaki, M., Kniewel, R., Murakami, H., Blitzblau, H.G., Tischfield, S.E., Zhu, X., Neale, M.J., Jasin, M., Socci, N.D.*, et al.* (2011). A Hierarchical

Combination of Factors Shapes the Genome-wide Topography of Yeast Meiotic Recombination Initiation. Cell *144*, 719-731.

Panizza, S., Mendoza, M.A., Berlinger, M., Huang, L., Nicolas, A., Shirahige, K., and Klein, F. (2011). Spo11-accessory proteins link double-strand break sites to the chromosome axis in early meiotic recombination. Cell *146*, 372-383.

Panizza, S., Tanaka, T., Hochwagen, A., Eisenhaber, F., and Nasmyth, K. (2000). Pds5 cooperates with cohesin in maintaining sister chromatid cohesion. Curr Biol *10*, 1557-1564.

Perry, J., Kleckner, N., and Borner, G.V. (2005a). Bioinformatic analyses implicate the collaborating meiotic crossover/chiasma proteins Zip2, Zip3, and Spo22/Zip4 in ubiquitin labeling. Proceedings of the National Academy of Sciences of the United States of America *102*, 17594-17599.

Perry, J., Kleckner, N., and Borner, G.V. (2005b). Bioinformatic analyses implicate the collaborating meiotic crossover/chiasma proteins Zip2, Zip3, and Spo22/Zip4 in ubiquitin labeling. Proc Natl Acad Sci U S A.

Peters, A.H., O'Carroll, D., Scherthan, H., Mechtler, K., Sauer, S., Schofer, C., Weipoltshammer, K., Pagani, M., Lachner, M., Kohlmaier, A.*, et al.* (2001). Loss of the Suv39h histone methyltransferases impairs mammalian heterochromatin and genome stability. Cell *107*, 323-337.

Petronczki, M., Siomos, M., and Nasmyth, K. (2003). Un menage a quatre: the molecular biology of chromosome segregation in meiosis. Cell *112*, 423-440.

Petukhova, G.V., Pezza, R.J., Vanevski, F., Ploquin, M., Masson, J.Y., and Camerini-Otero, R.D. (2005). The Hop2 and Mnd1 proteins act in concert with Rad51 and Dmc1 in meiotic recombination. Nature structural & molecular biology *12*, 449-453.

Pijnappel, W.W., Schaft, D., Roguev, A., Shevchenko, A., Tekotte, H., Wilm, M., Rigaut, G., Seraphin, B., Aasland, R., and Stewart, A.F. (2001). The S. cerevisiae SET3 complex includes two histone deacetylases, Hos2 and Hst1, and is a meiotic-specific repressor of the sporulation gene program. Genes Dev *15*, 2991-3004.

Prakash, R., Satory, D., Dray, E., Papusha, A., Scheller, J., Kramer, W., Krejci, L., Klein, H., Haber, J.E., Sung, P.*, et al.* (2009). Yeast Mph1 helicase dissociates Rad51-made D-loops: implications for crossover control in mitotic recombination. Genes & development *23*, 67-79.

Prieler, S., Penkner, A., Borde, V., and Klein, F. (2005). The control of Spo11's interaction with meiotic recombination hotspots. Genes & development *19*, 255-269.

Prinz, S., Amon, A., and Klein, F. (1997). Isolation of COM1, a new gene required to complete meiotic double-strand break-induced recombination in Saccharomyces cerevisiae. Genetics *146*, 781-795.

Rabitsch, K.P., Toth, A., Galova, M., Schleiffer, A., Schaffner, G., Aigner, E., Rupp, C., Penkner, A.M., Moreno-Borchart, A.C., Primig, M.*, et al.* (2001). A screen for genes required for meiosis and spore formation based on whole-genome expression. Curr Biol *11*, 1001-1009.

Robzyk, K., Recht, J., and Osley, M.A. (2000). Rad6-dependent ubiquitination of histone H2B in yeast. Science *287*, 501-504.

Rockmill, B., and Roeder, G.S. (1990). Meiosis in asynaptic yeast. Genetics *126*, 563-574.

Rockmill, B., and Roeder, G.S. (1991). A meiosis-specific protein kinase homolog required for chromosome synapsis and recombination. Genes & development *5*, 2392-2404.

Rockmill, B., Sym, M., Scherthan, H., and Roeder, G.S. (1995). Roles for two RecA homologs in promoting meiotic chromosome synapsis. Genes & development *9*, 2684-2695.

Roeder, G.S., and Bailis, J.M. (2000). The pachytene checkpoint. Trends in genetics : TIG *16*, 395-403.

Roig, I., Dowdle, J., Toth, A., de Rooij, D., Jasin, M., and Keeney, S. (2010). Mouse TRIP13/PCH2 Is Required for Recombination and Normal Higher-Order Chromosome Structure during Meiosis. PLoS Genet *6*.

Ross-Macdonald, P., and Roeder, G.S. (1994). Mutation of a meiosis-specific MutS homolog decreases crossing over but not mismatch correction. Cell *79*, 1069-1080.

Rousseaux, S., Caron, C., Govin, J., Lestrat, C., Faure, A.K., and Khochbin, S. (2005). Establishment of male-specific epigenetic information. Gene *345*, 139-153.

San-Segundo, P.A., and Roeder, G.S. (1999). Pch2 links chromatin silencing to meiotic checkpoint control. Cell *97*, 313-324.

San-Segundo, P.A., and Roeder, G.S. (2000a). Role for the silencing protein Dot1 in meiotic checkpoint control. Molecular biology of the cell *11*, 3601-3615.

San-Segundo, P.A., and Roeder, G.S. (2000b). Role for the silencing protein Dot1 in meiotic checkpoint control. Mol Biol Cell *11*, 3601-3615.

Scherthan, H., Loidl, J., Schuster, T., and Schweizer, D. (1992). Meiotic chromosome condensation and pairing in Saccharomyces cerevisiae studied by chromosome painting. Chromosoma *101*, 590-595.

Scherthan, H., and Schonborn, I. (2001). Asynchronous chromosome pairing in male meiosis of the rat (Rattus norvegicus). Chromosome research : an international journal on the molecular, supramolecular and evolutionary aspects of chromosome biology *9*, 273-282.

Schwacha, A., and Kleckner, N. (1995). Identification of double Holliday junctions as intermediates in meiotic recombination. Cell *83*, 783-791.

Sharon, G., and Simchen, G. (1990). Mixed segregation of chromosomes during single-division meiosis of Saccharomyces cerevisiae [published erratum appears in Genetics 1991 Mar;127(3):630]. Genetics *125*, 475-485.

Shinohara, M., Gasior, S.L., Bishop, D.K., and Shinohara, A. (2000). Tid1/Rdh54 promotes colocalization of Rad51 and Dmc1 during meiotic recombination. Proc Natl Acad Sci U S A *97*, 10814-10819.

Shinohara, M., Oh, S.D., Hunter, N., and Shinohara, A. (2008). Crossover assurance and crossover interference are distinctly regulated by the ZMM proteins during yeast meiosis. Nature genetics *40*, 299-309.

Simchen, G. (2009). Commitment to meiosis: what determines the mode of division in budding yeast? Bioessays *31*, 169-177.

Simchen, G., Pinon, R., and Salts, Y. (1972). Sporulation in Saccharomyces cerevisiae: premeiotic DNA synthesis, readiness and commitment. Experimental cell research *75*, 207-218.

Smith, K.N., and Nicolas, A. (1998). Recombination at work for meiosis. Curr Opin Genet Dev *8*, 200-211.

Smith, K.N., Penkner, A., Ohta, K., Klein, F., and Nicolas, A. (2001a). B-type cyclins CLB5 and CLB6 control the initiation of recombination and synaptonemal complex formation in yeast meiosis. Current biology : CB *11*, 88-97.

Smith, K.N., Penkner, A., Ohta, K., Klein, F., and Nicolas, A. (2001b). B-type cyclins CLB5 and CLB6 control the initiation of recombination and synaptonemal complex formation in yeast meiosis. Curr Biol *11*, 88-97.

Snowden, T., Acharya, S., Butz, C., Berardini, M., and Fishel, R. (2004). hMSH4-hMSH5 recognizes Holliday Junctions and forms a meiosis-specific sliding clamp that embraces homologous chromosomes. Molecular cell *15*, 437-451.

Soushko, M., and Mitchell, A.P. (2000). An RNA-binding protein homologue that promotes sporulation-specific gene expression in Saccharomyces cerevisiae. Yeast *16*, 631-639.

Storlazzi, A., Gargano, S., Ruprich-Robert, G., Falque, M., David, M., Kleckner, N., and Zickler, D. (2010a). Recombination proteins mediate meiotic spatial chromosome organization and pairing. Cell *141*, 94-106.

Storlazzi, A., Gargano, S., Ruprich-Robert, G., Falque, M., David, M., Kleckner, N., and Zickler, D. (2010b). Recombination proteins mediate meiotic spatial chromosome organization and pairing. Cell *141*, 94-106.

Storlazzi, A., Tesse, S., Gargano, S., James, F., Kleckner, N., and Zickler, D. (2003). Meiotic double-strand breaks at the interface of chromosome movement, chromosome remodeling, and reductional division. Genes & development *17*, 2675-2687.

Stuart, D., and Wittenberg, C. (1998). CLB5 and CLB6 are required for premeiotic DNA replication and activation of the meiotic S/M checkpoint. Genes Dev *12*, 2698-2710.

Sung, P. (1997). Function of yeast Rad52 protein as a mediator between replication protein A and the Rad51 recombinase. J Biol Chem *272*, 28194-28197.

Svendsen, J.M., Smogorzewska, A., Sowa, M.E., O'Connell, B.C., Gygi, S.P., Elledge, S.J., and Harper, J.W. (2009). Mammalian BTBD12/SLX4 assembles a Holliday junction resolvase and is required for DNA repair. Cell *138*, 63-77.

Sym, M., Engebrecht, J.A., and Roeder, G.S. (1993). ZIP1 is a synaptonemal complex protein required for meiotic chromosome synapsis. Cell *72*, 365-378.

Szekvolgyi, L., and Nicolas, A. (2010). From meiosis to postmeiotic events: homologous recombination is obligatory but flexible. FEBS J *277*, 571-589.

Tonami, Y., Murakami, H., Shirahige, K., and Nakanishi, M. (2005). A checkpoint control linking meiotic S phase and recombination initiation in fission yeast. Proceedings of the National Academy of Sciences of the United States of America *102*, 5797-5801.

Treinin, M., and Simchen, G. (1993). Mitochondrial activity is required for the expression of IME1, a regulator of meiosis in yeast. Curr-Genet *23*, 223-227.

Trujillo, K.M., Roh, D.H., Chen, L., Van Komen, S., Tomkinson, A., and Sung, P. (2003). Yeast xrs2 binds DNA and helps target rad50 and mre11 to DNA ends. J Biol Chem *278*, 48957-48964.

Tsubouchi, T., Macqueen, A.J., and Roeder, G.S. (2008). Initiation of meiotic chromosome synapsis at centromeres in budding yeast. Genes & development *22*, 3217-3226.

Tsubouchi, T., Zhao, H., and Roeder, G.S. (2006). The meiosis-specific zip4 protein regulates crossover distribution by promoting synaptonemal complex formation together with zip2. Developmental cell *10*, 809-819.

Tung, K.S., and Roeder, G.S. (1998). Meiotic chromosome morphology and behavior in zip1 mutants of Saccharomyces cerevisiae. Genetics *149*, 817-832.

Usui, T., Ogawa, H., and Petrini, J.H. (2001). A DNA damage response pathway controlled by Tel1 and the Mre11 complex. Molecular cell *7*, 1255-1266.

Usui, T., Ohta, T., Oshiumi, H., Tomizawa, J., Ogawa, H., and Ogawa, T. (1998). Complex formation and functional versatility of Mre11 of budding yeast in recombination. Cell *95*, 705-716.

van Attikum, H., Fritsch, O., and Gasser, S.M. (2007). Distinct roles for SWR1 and INO80 chromatin remodeling complexes at chromosomal double-strand breaks. The EMBO journal *26*, 4113-4125.

Vazquez-Nin, G.H., Echeverria, O.M., Ortiz, R., Scassellati, C., Martin, T.E., Ubaldo, E., and Fakan, S. (2003). Fine structural cytochemical analysis of homologous chromosome recognition, alignment, and pairing in Guinea pig spermatogonia and spermatocytes. Biology of reproduction *69*, 1362-1370.

Voegtli, W.C., Madrona, A.Y., and Wilson, D.K. (2003). The structure of Aip1p, a WD repeat protein that regulates Cofilin-mediated actin depolymerization. The Journal of biological chemistry *278*, 34373-34379.

von Wettstein, D., Rasmussen, S.W., and Holm, P.B. (1984). The synaptonemal complex in genetic segregation. Annual review of genetics *18*, 331-413.

Wahls, W.P. (1998). Meiotic recombination hotspots: shaping the genome and insights into hypervariable minisatellite DNA change. Curr Top Dev Biol *37*, 37-75.

Wan, L., Niu, H., Futcher, B., Zhang, C., Shokat, K.M., Boulton, S.J., and Hollingsworth, N.M. (2008a). Cdc28-Clb5 (CDK-S) and Cdc7-Dbf4 (DDK) collaborate to initiate meiotic recombination in yeast. Genes Dev *22*, 386-397.

Wan, L., Niu, H., Futcher, B., Zhang, C., Shokat, K.M., Boulton, S.J., and Hollingsworth, N.M. (2008b). Cdc28-Clb5 (CDK-S) and Cdc7-Dbf4 (DDK)

collaborate to initiate meiotic recombination in yeast. Genes & development *22*, 386-397.

Wanat, J., Kim, K., Koszul, R., Zanders, S., Weiner, B., Kleckner, N., and Alani, E. (2008). Csm4, in collaboration with Ndj1, mediates telomere-led chromosome dynamics and recombination during yeast meiosis. PLoS Genet *4*, e1000188.

Webster, K.E., O'Bryan, M.K., Fletcher, S., Crewther, P.E., Aapola, U., Craig, J., Harrison, D.K., Aung, H., Phutikanit, N., Lyle, R.*, et al.* (2005). Meiotic and epigenetic defects in Dnmt3L-knockout mouse spermatogenesis. Proceedings of the National Academy of Sciences of the United States of America *102*, 4068-4073.

Willems, A.R., Schwab, M., and Tyers, M. (2004). A hitchhiker's guide to the cullin ubiquitin ligases: SCF and its kin. Biochimica et biophysica acta *1695*, 133-170.

Williams, R., Primig, M., Washburn, B., Winzeler, E., Bellis, M., Sarrauste de Menthiere, C., Davis, R., and Esposito, R. (2002). The Ume6 regulon coordinates metabolic and meiotic gene expression in yeast. Proc Natl Acad Sci U S A *99*, 13431-13436.

Winzeler, E., Shoemaker, D., Astromoff, A., Liang, H., Anderson, K., Andre, B., Bangham, R., Benito, R., Boeke, J., Bussey, H.*, et al.* (1999a). Functional characterization of the S. cerevisiae genome by gene deletion and parallel analysis. Science *285*, 901-906.

Winzeler, E.A., Lee, B., McCusker, J.H., and Davis, R.W. (1999b). Whole genome genetic-typing in yeast using high-density oligonucleotide arrays. Parasitology *118 Suppl*, S73-80.

Wu, W.H., Alami, S., Luk, E., Wu, C.H., Sen, S., Mizuguchi, G., Wei, D., and Wu, C. (2005). Swc2 is a widely conserved H2AZ-binding module essential for ATP-dependent histone exchange. Nature structural & molecular biology *12*, 1064-1071.

Wysocka, M., Rytka, J., and Kurlandzka, A. (2004). Saccharomyces cerevisiae CSM1 gene encoding a protein influencing chromosome segregation in meiosis I interacts with elements of the DNA replication complex. Experimental cell research *294*, 592-602.

Xiong, B., Lu, S., and Gerton, J.L. (2010). Hos1 is a lysine deacetylase for the Smc3 subunit of cohesin. Current biology : CB *20*, 1660-1665.

Yamashita, K., Shinohara, M., and Shinohara, A. (2004). Rad6-Bre1-mediated histone H2B ubiquitylation modulates the formation of double-strand breaks during meiosis. Proc Natl Acad Sci U S A *101*, 11380-11385.

Youds, J.L., Mets, D.G., McIlwraith, M.J., Martin, J.S., Ward, J.D., NJ, O.N., Rose, A.M., West, S.C., Meyer, B.J., and Boulton, S.J. (2010). RTEL-1 enforces meiotic crossover interference and homeostasis. Science *327*, 1254-1258.

Yu, H.G., and Koshland, D.E. (2003a). Meiotic condensin is required for proper chromosome compaction, SC assembly, and resolution of recombination-dependent chromosome linkages. J Cell Biol *163*, 937-947.

Yu, H.G., and Koshland, D.E. (2003b). Meiotic condensin is required for proper chromosome compaction, SC assembly, and resolution of recombination-dependent chromosome linkages. The Journal of cell biology *163*, 937-947.

Zanders, S., Brown, M.S., Chen, C., and Alani, E. (2011). Pch2 Modulates Chromatid Partner Choice During Meiotic Double-Strand Break Repair in Saccharomyces cerevisiae. Genetics *188*, 511-521.

Zavec, A., Lesnik, U., Komel, R., and Comino, A. (2004). The Saccharomyces cerevisiae gene ECM11 is a positive effector of meiosis. FEMS Microbiol Lett *241*, 193-199.

Zickler, D. (1999). [The synaptonemal complex: a structure necessary for pairing, recombination or organization of the meiotic chromosome?]. J Soc Biol *193*, 17-22.

Zickler, D., and Kleckner, N. (1998). The leptotene-zygotene transition of meiosis. Annu Rev Genet *32*, 619-697.

Zickler, D., and Kleckner, N. (1999). Meiotic chromosomes: integrating structure and function. Annu Rev Genet *33*, 603-754.

Zierhut, C., Berlinger, M., Rupp, C., Shinohara, A., and Klein, F. (2004). Mnd1 is required for meiotic interhomolog repair. Current biology : CB *14*, 752-762.

Curriculum vitae

Personal Data

Full name: Jean Mbogning
Date of birth: 00/00/1970
Place of Birth: Baleveng
Nationality: Cameroonian

Education

1977-1983: Primary school in Baleveng (Cameroon)
1983-1991: Secondary school in Dschang (Cameroon)
1992-1996: Undergraduate studies of Biochemistry at the University of Yaoundé I
1997-2001: Master thesis (Biochemistry) at the University of Yaoundé I
2001-2006: PhD student at the University of Yaoundé I
2006- 2011: PhD student at the University of Vienna

List of publications

Master´s thesis:
Jean Mbogning : Identification and characterization of proteases of adult worms of *onchocerca volvulus* (2002) University of Yaoundé I, Cameroon.

Contributions at conferences

09/2003**:** Attending the 6th **European Meiosis Meeting,EMBO workshop on meiosis in Obertraun, Austria**

.

09/2009: Attending the **European Meiosis Meeting,EMBO workshop on meiosis in**
in France:
Poster presentation: A Systematic Visual Screen for Chromosome morphology in *S.cerevisiae*

11/2009**:** Attending the **SAB** (Scientific Advisory Board) meeting,Vienna,Austria

Poster presentation: A Visual Survey for the Involvement of genes in Meiotic chromosome synapsis.

09/2011: attending the EMBO meeting, Vienna, Austria

Poster presentation: **A screen for mutations affecting synaptonemal complex formation in budding yeast.**

Acknowledgements

First I would like to thank my supervisor Prof.Franz Klein for giving me the opportunity to carry out this work in his laboratory. Furthermore for his counsel and criticism during the five years that I have spent in his laboratory. I highly appreciate his financial an intellectual support when I was a PhD student in my home country university in Cameroon. I hope that his efforts to teach us what good science is all about will be fruitful in the future.

I would like to thank the AAI-Wien (Afro Asiatisches Institut in Wien) for the scholorships awarded, without which this work would never have been performed.

Special thanks to members of my PhD committee (Prof.Friedrich Propst and Dr.Juraj Gregan) for their intellectual input and advice during this work.

I would like to thank Prof.Giora Simchen and Dr.Verena Jantsch for accepting to evaluate this work and for the fast review of the manuscript.

Thanks to Prof.Michael Jantsch for providing me with severals molecular biology books and my first laptop.

I would like to thank the other past and present colleagues from the Department of chromosome biology, especially to Martin Xaver, who also helped with the german translation of the Summary, Alexander Woglar, Marco Antonio Mendoza, Silvia Panizza, Benjamin Brenhoffer, Philip Jordan, Dagmar Schöninklee, Ahmad Shazia, Lingzhi Huang, Susanne Zich, Feng Peng, Edlinger Bernd, Marc Berlinger for their friendship, technical support, stimulating discussions and advises.

I am indebted to my family especially to my parents, my wife and children for their constant support and understanding.

Fig 1

Comparison of mitosis and meiosis

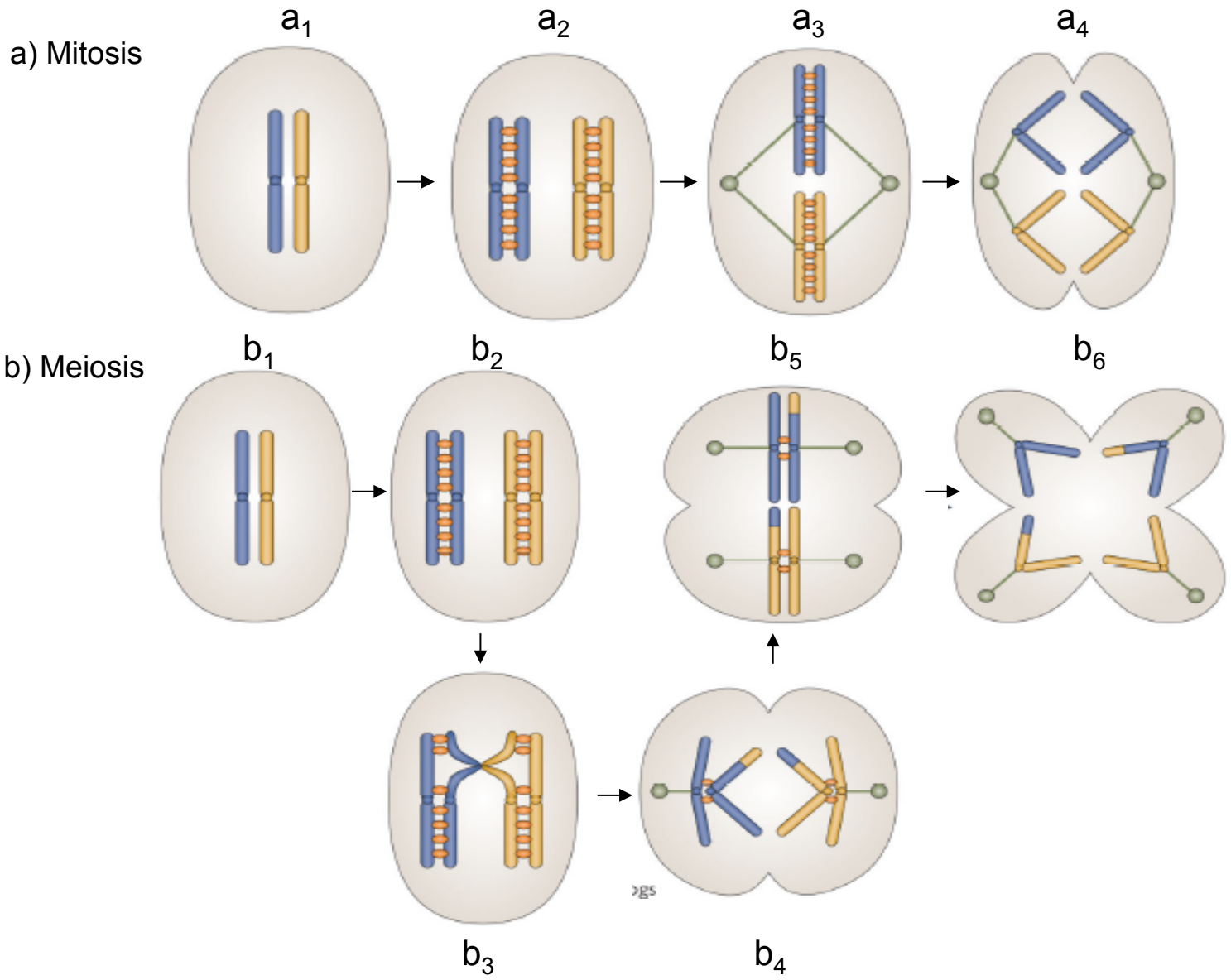

Fig 2

Chromosomal morphogenesis during meiosis

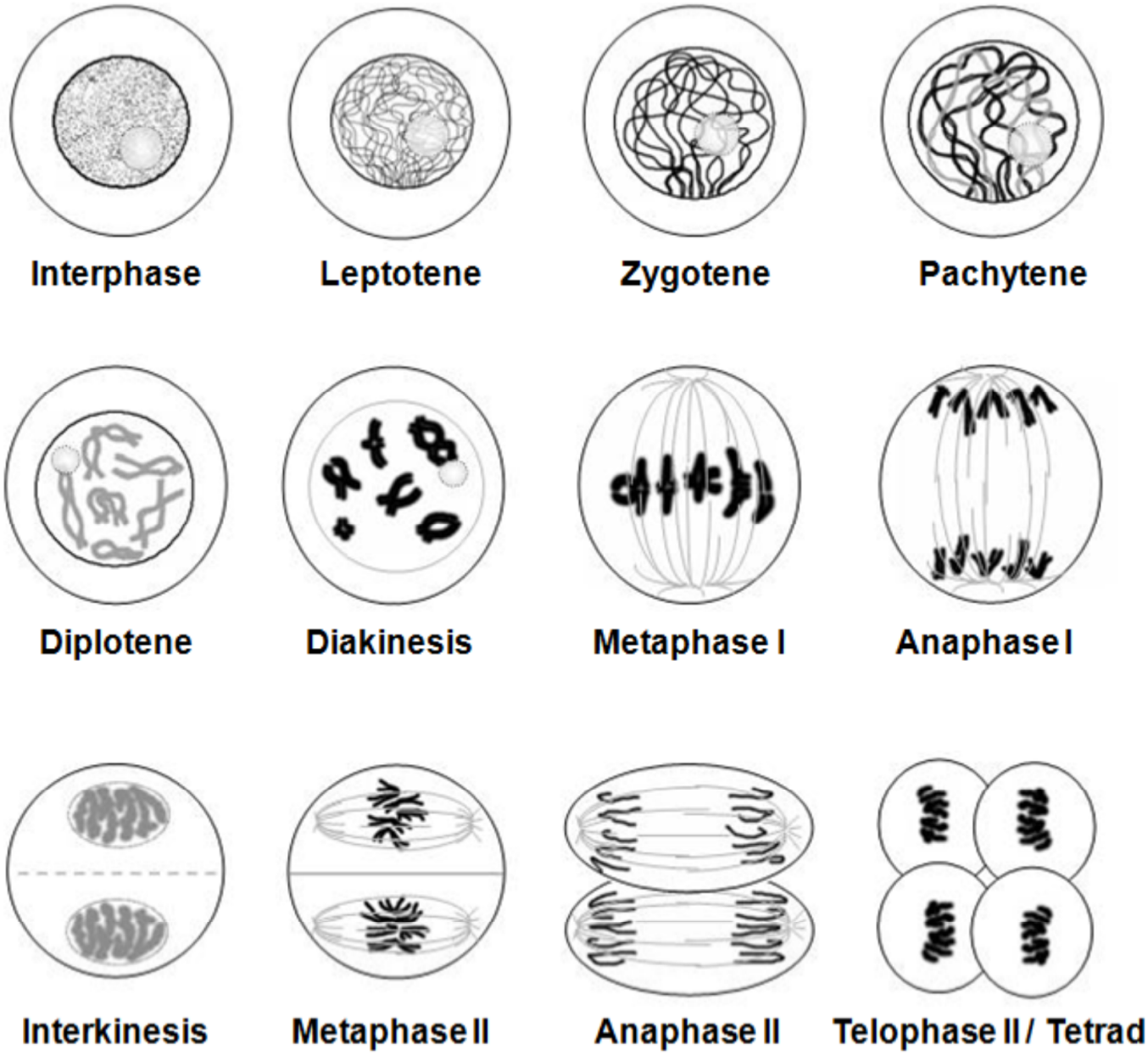

Fig 3

Correlation between DSB formation and repair and the synaptonemal complex formation

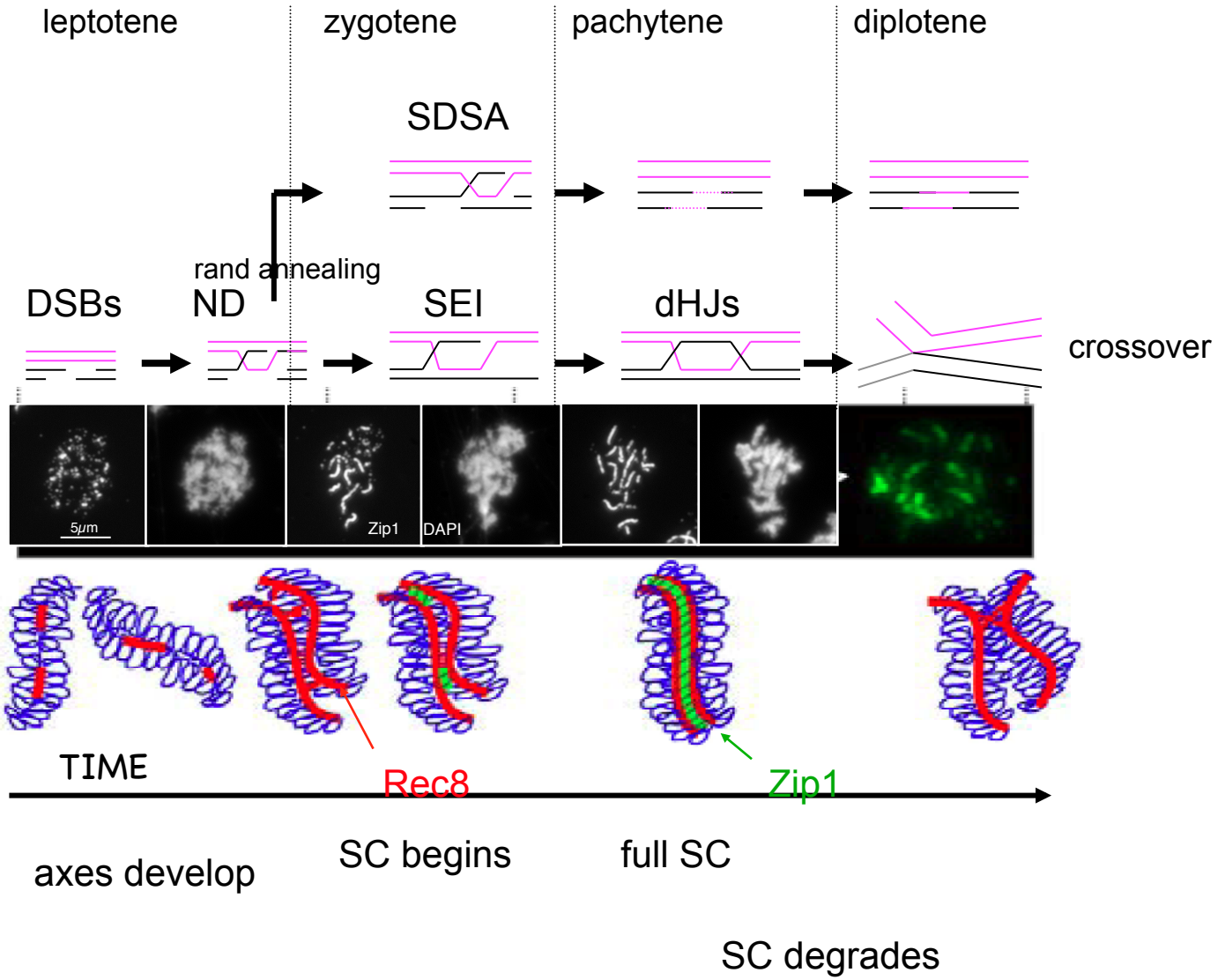

Fig 4

Model of SC structure

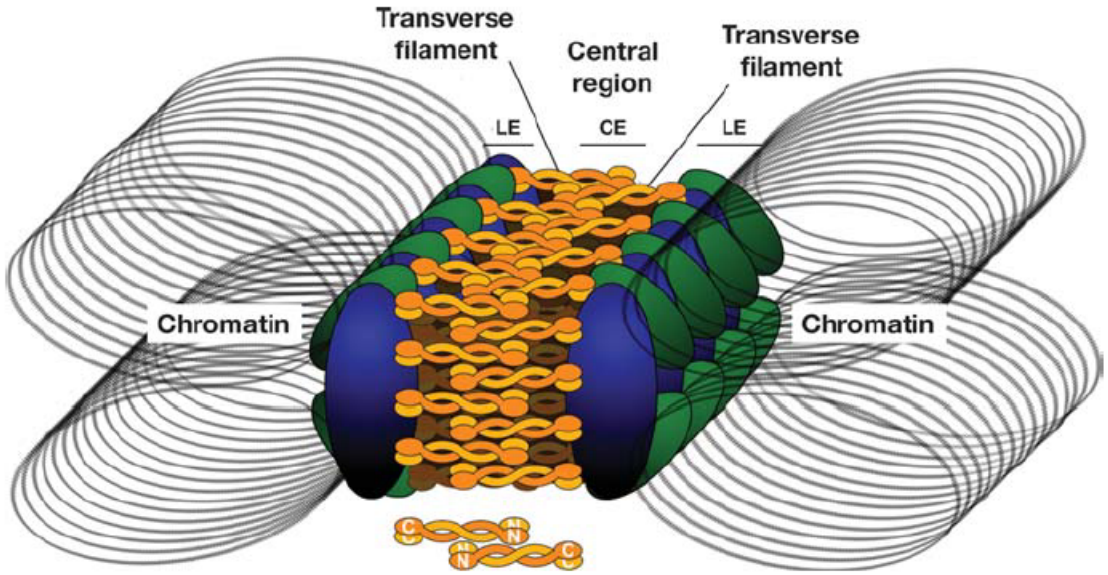

Fig 5

Generating homozygous SK1/BY hybrid diploids from the Euroscarf BY-deletion collection

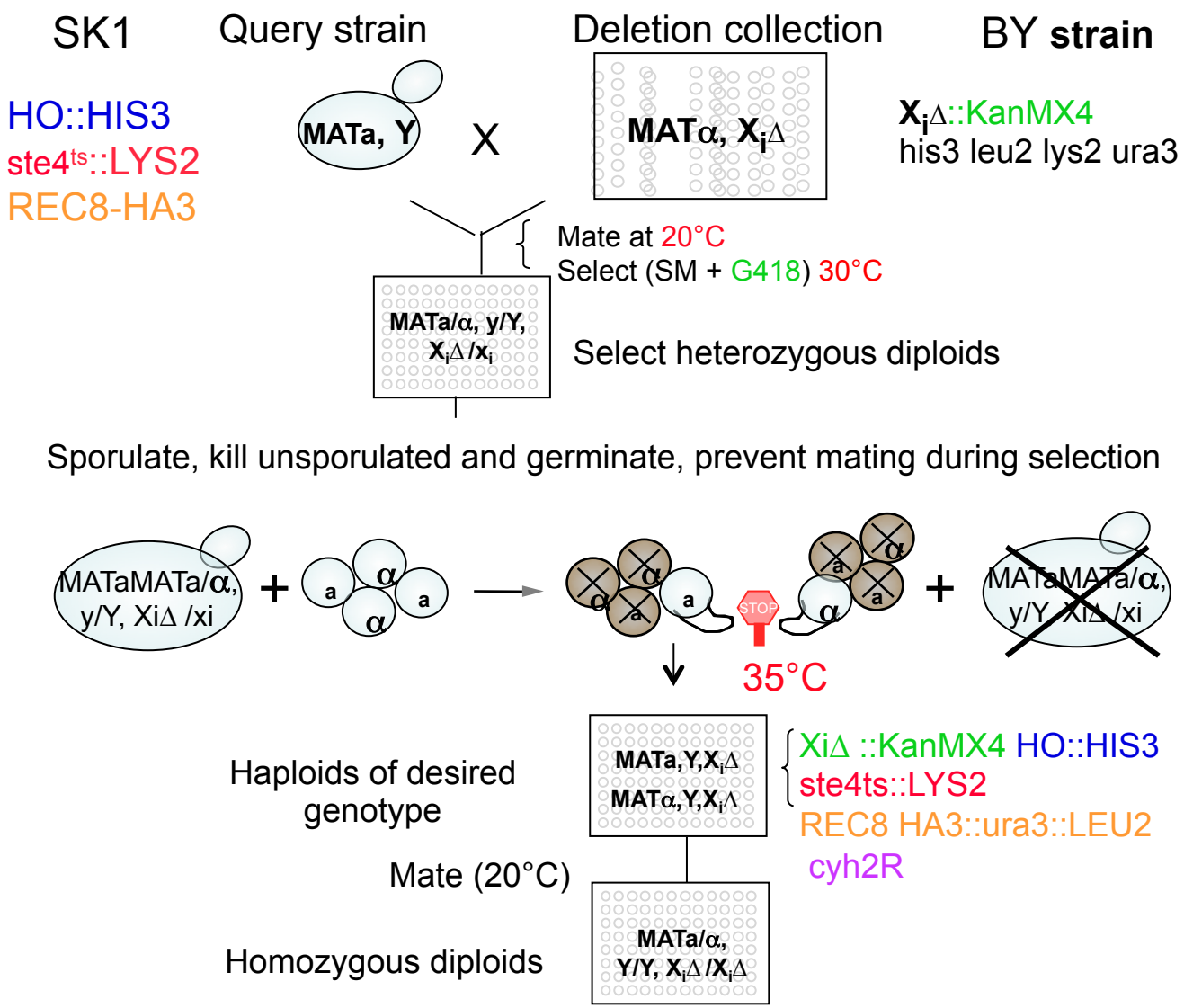

Fig 6A

No meiotic induction – previous annotation of candidate ORFs

Total **ORFs** identified: **132**

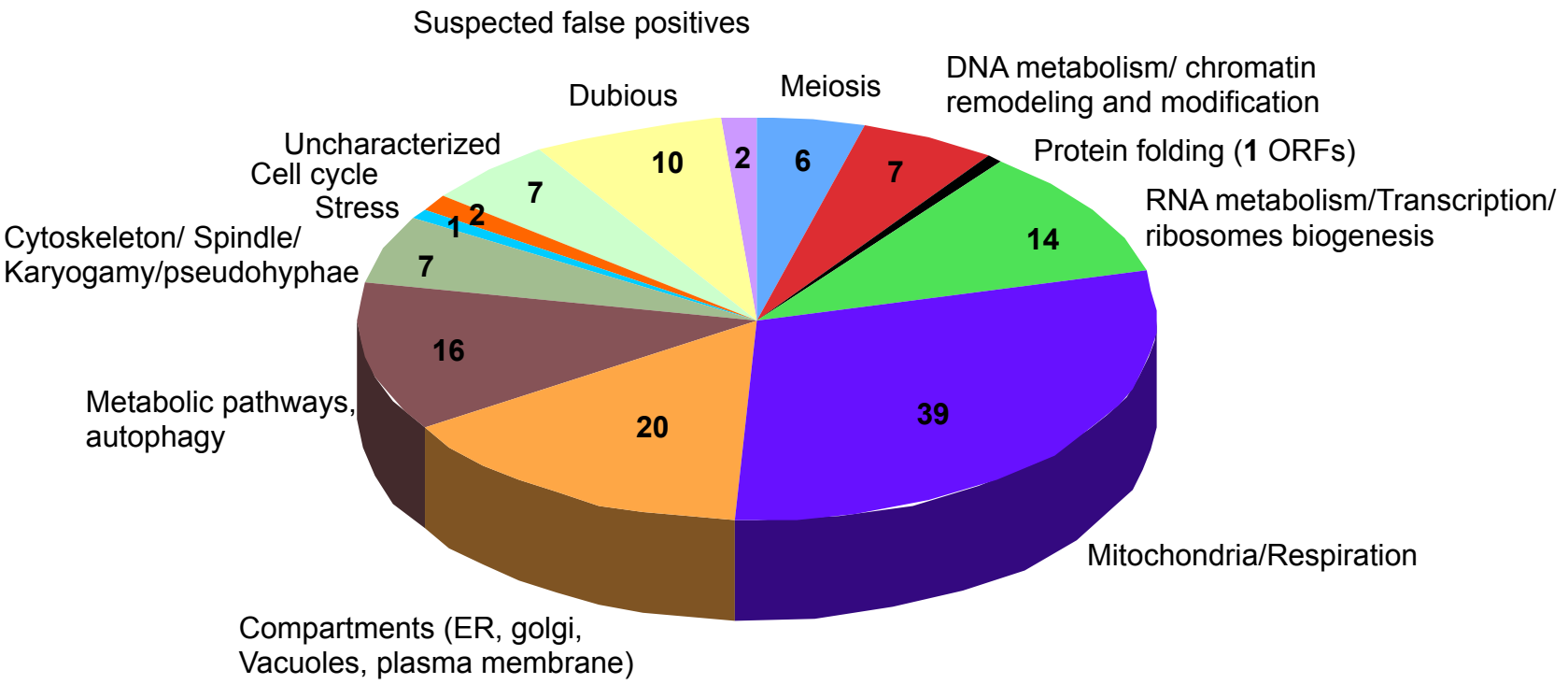

Fig 6B

Zip1 foci – previous annotation of candidate ORFs

Total **ORFs** identified in this class: **90**

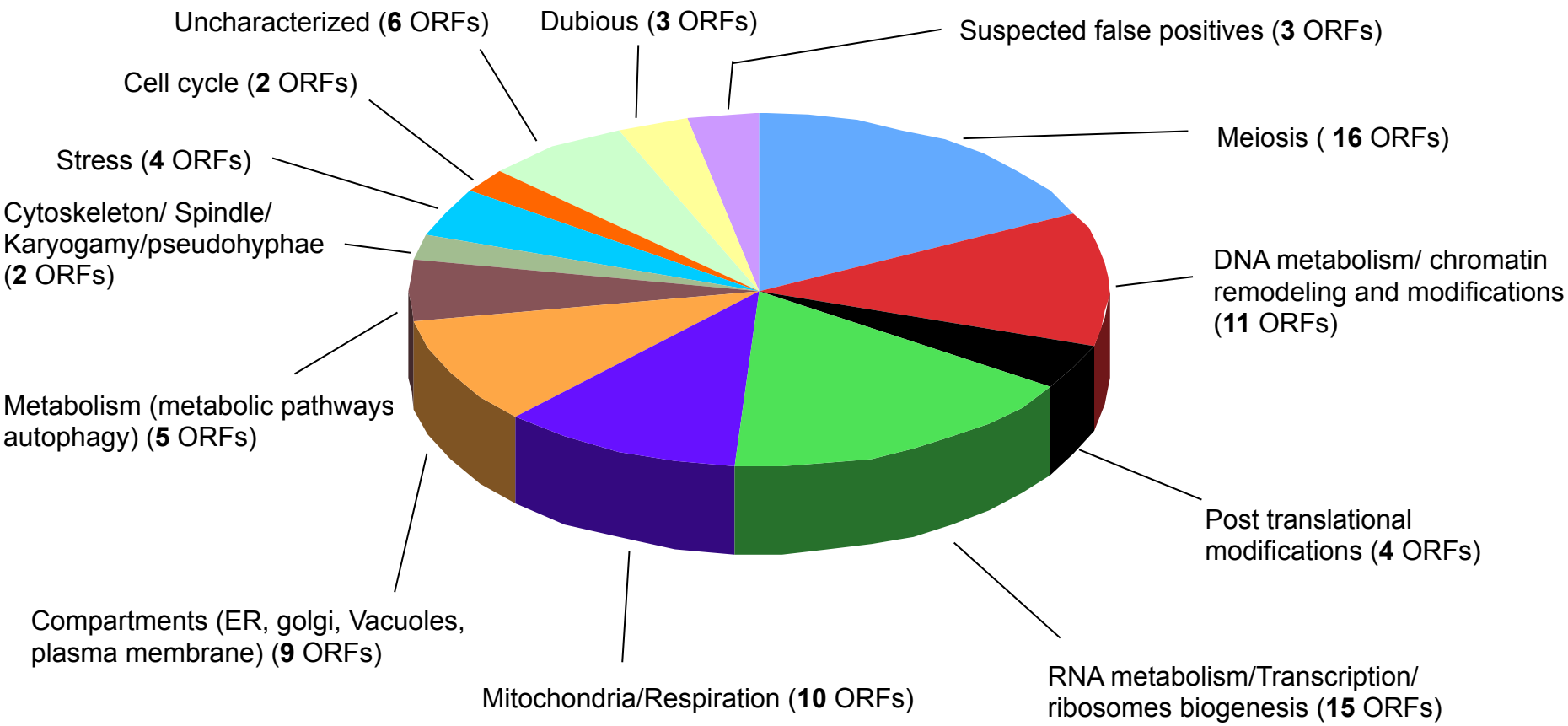

Fig 6C

Short Zip1 stretches - previous annotation of candidate ORFs

Total **ORFs** identified in this class: **102**

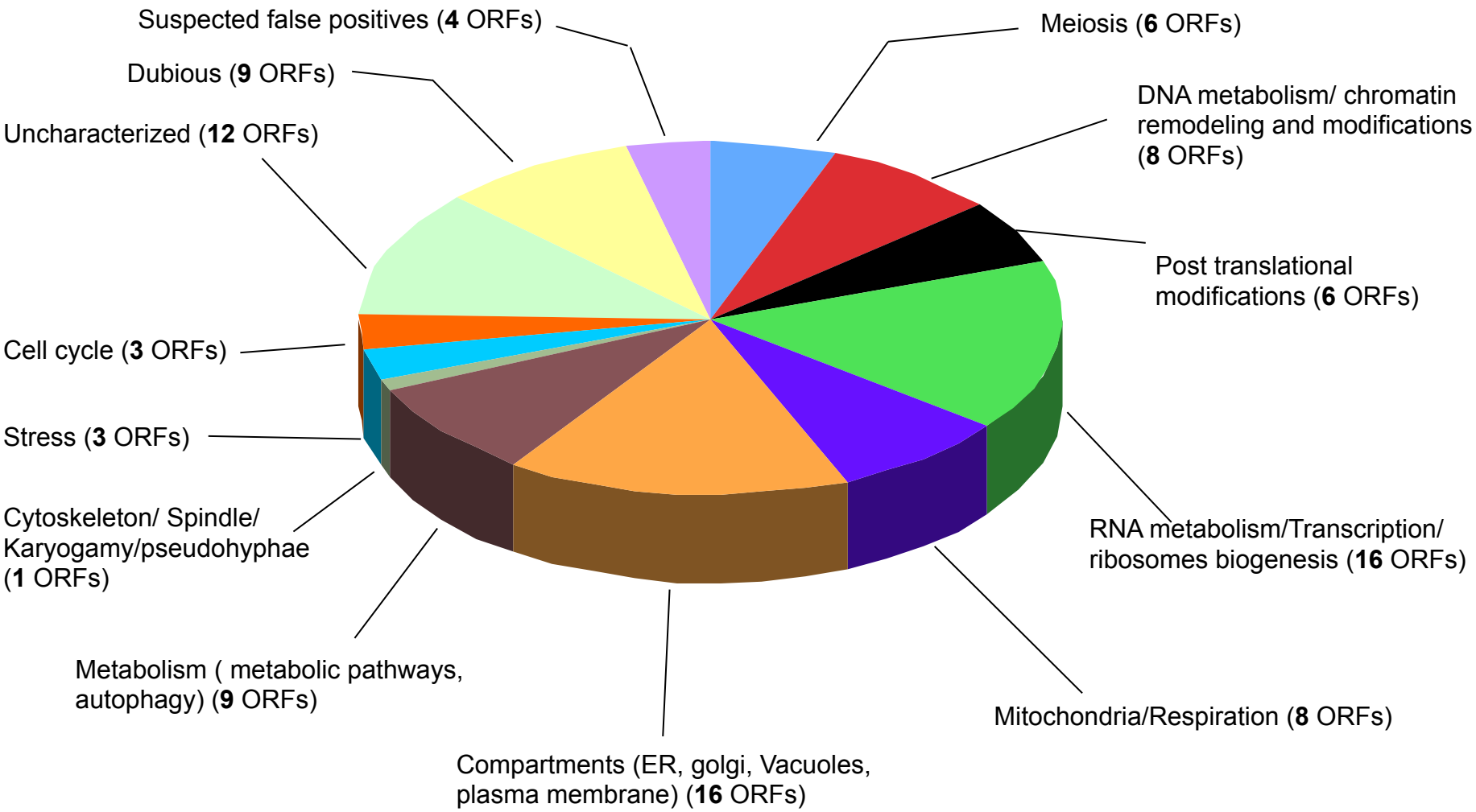

Fig 6D

Long Zip1 stretches - previous annotation of candidate ORFs

Total **ORFs** identified in this group: **200**

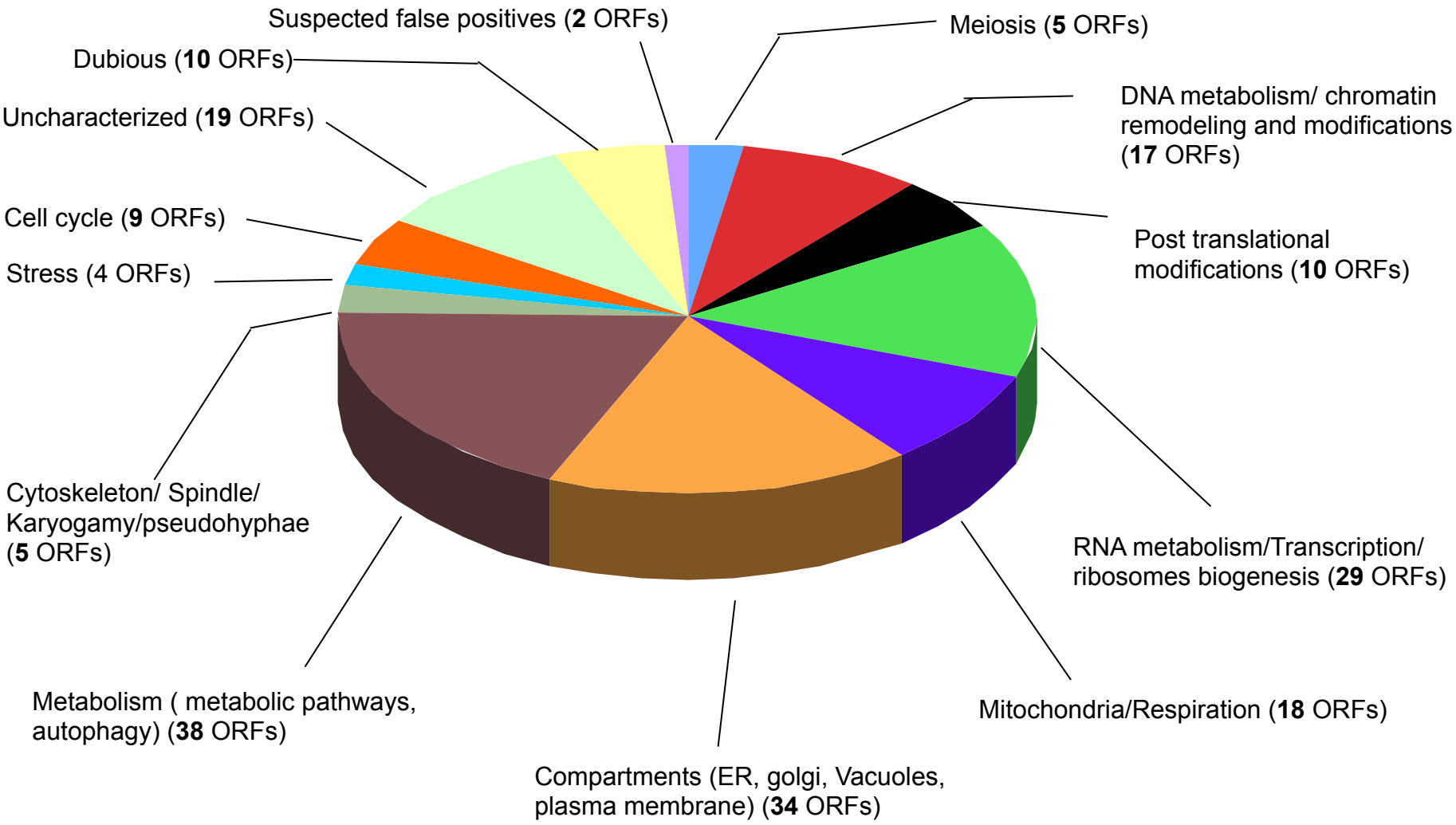

Fig 7A,B In WT Zip1 appears as foci during leptotene, forms linear stretches during zygotene on chromosome spreads

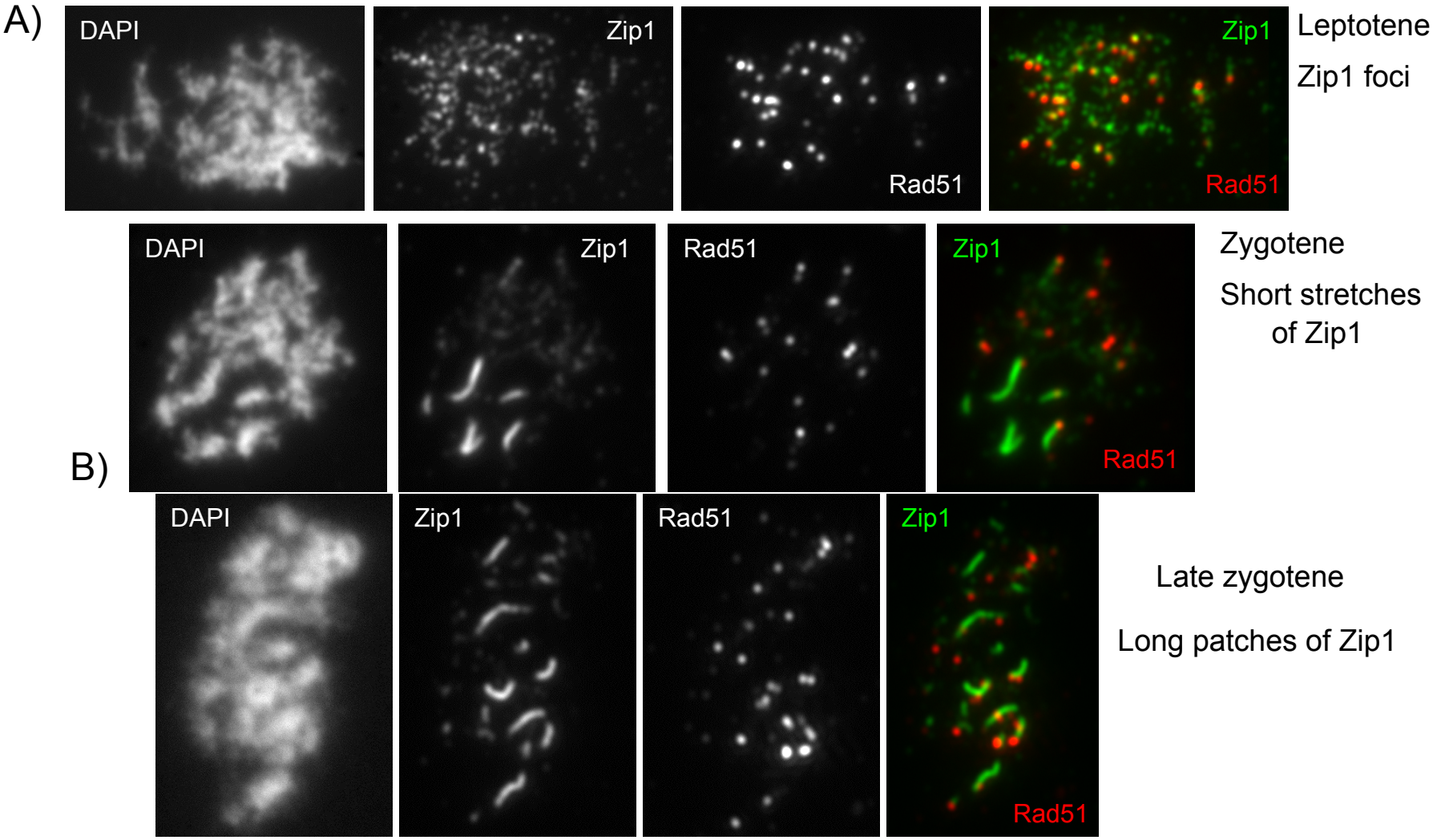

Fig 7C

In pachytene of wild type SK1 nuclei show a maximum of synapsis

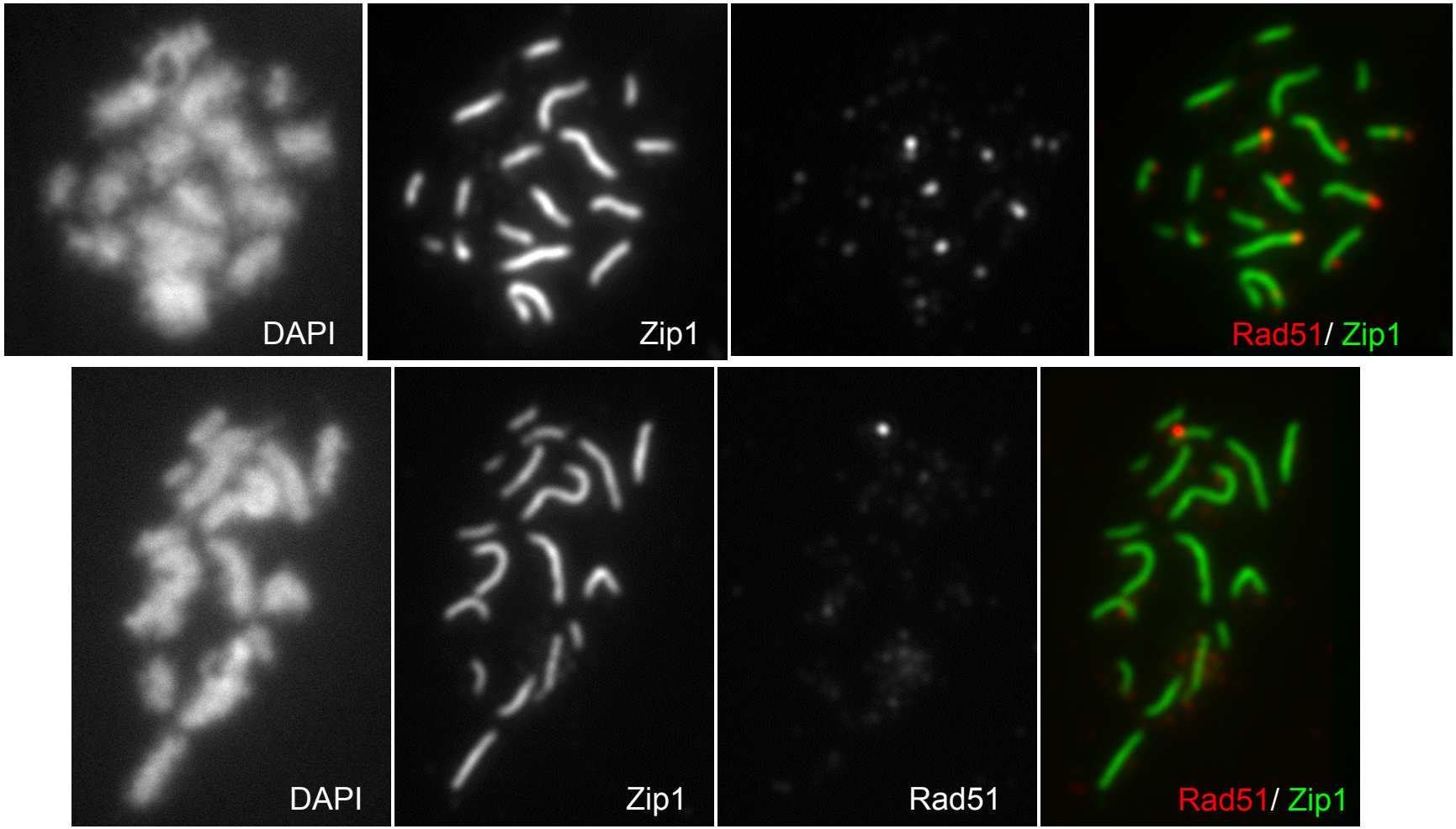

Fig 8A

ecm11Δ, *ymr196wΔ*, *oxp1Δ* and *ydr333cΔ* display a significant decrease in chromosome synapsis.

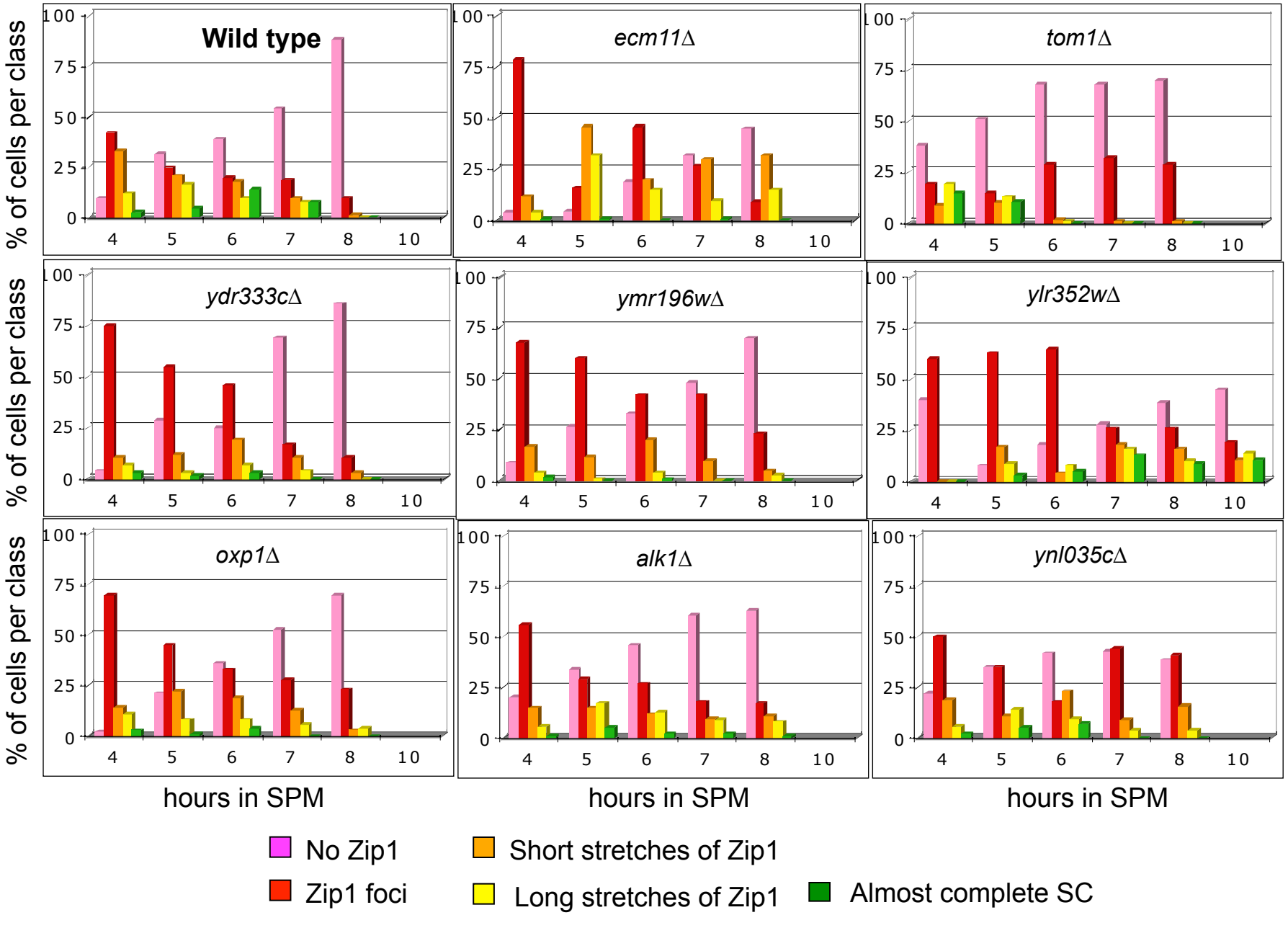

Fig 8B,C

Meiotic progression is delayed in *tom1*Δ and *ylr352w*Δ, and *ecm11*Δ shows increased numbers of Rad51 foci

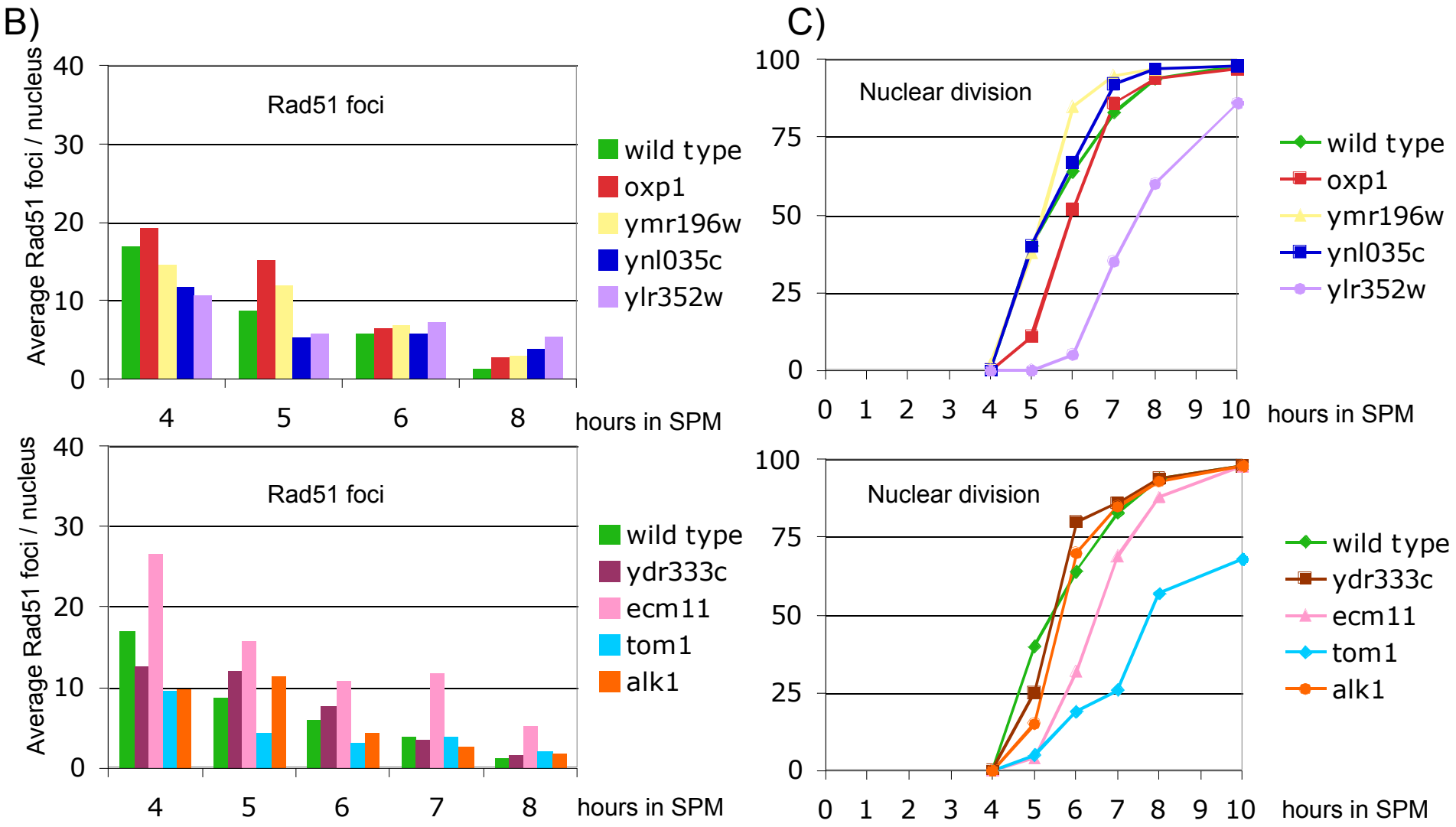

Fig 8D

*tom1*Δ and *yor296w*Δ are defective in pre-meiotic DNA replication

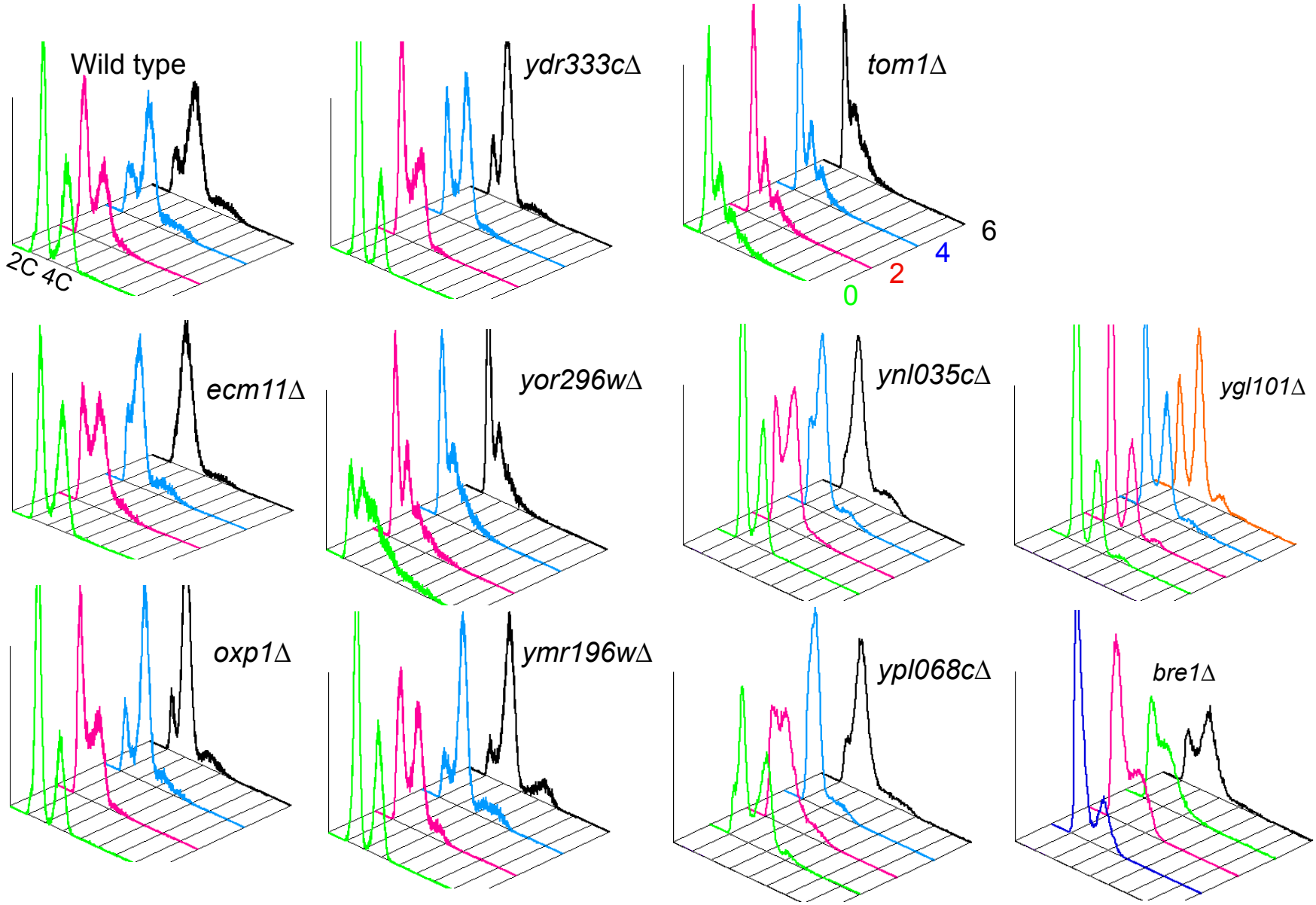

Fig:9A

Synapsis is reduced in *yor296wΔ*, *ddr2Δ* and delayed in *hos1Δ*, *swc2Δ*

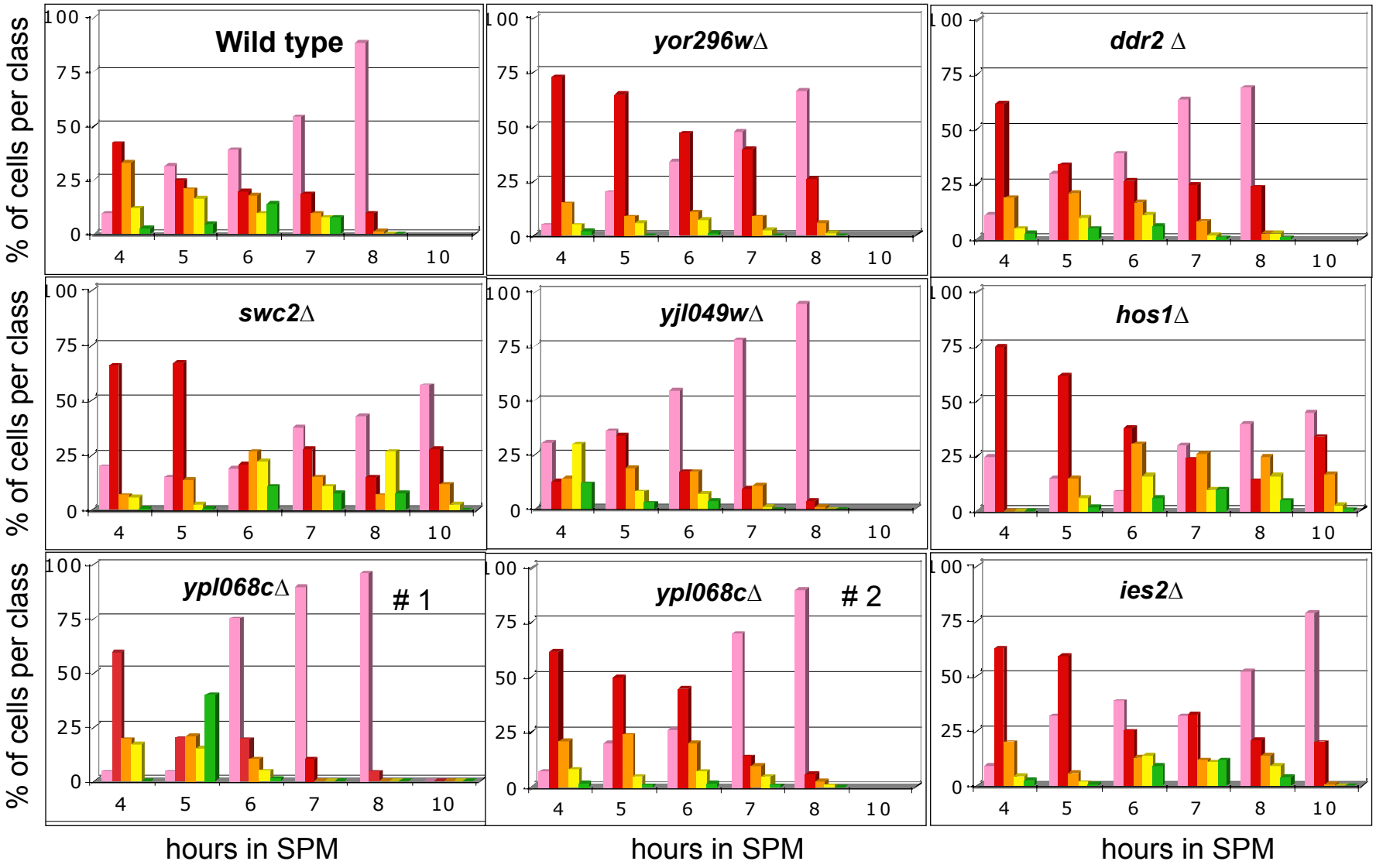

Fig 9B,C Meiotic progression is delayed in *hos1Δ, yor296wΔ* and *swc2Δ*.

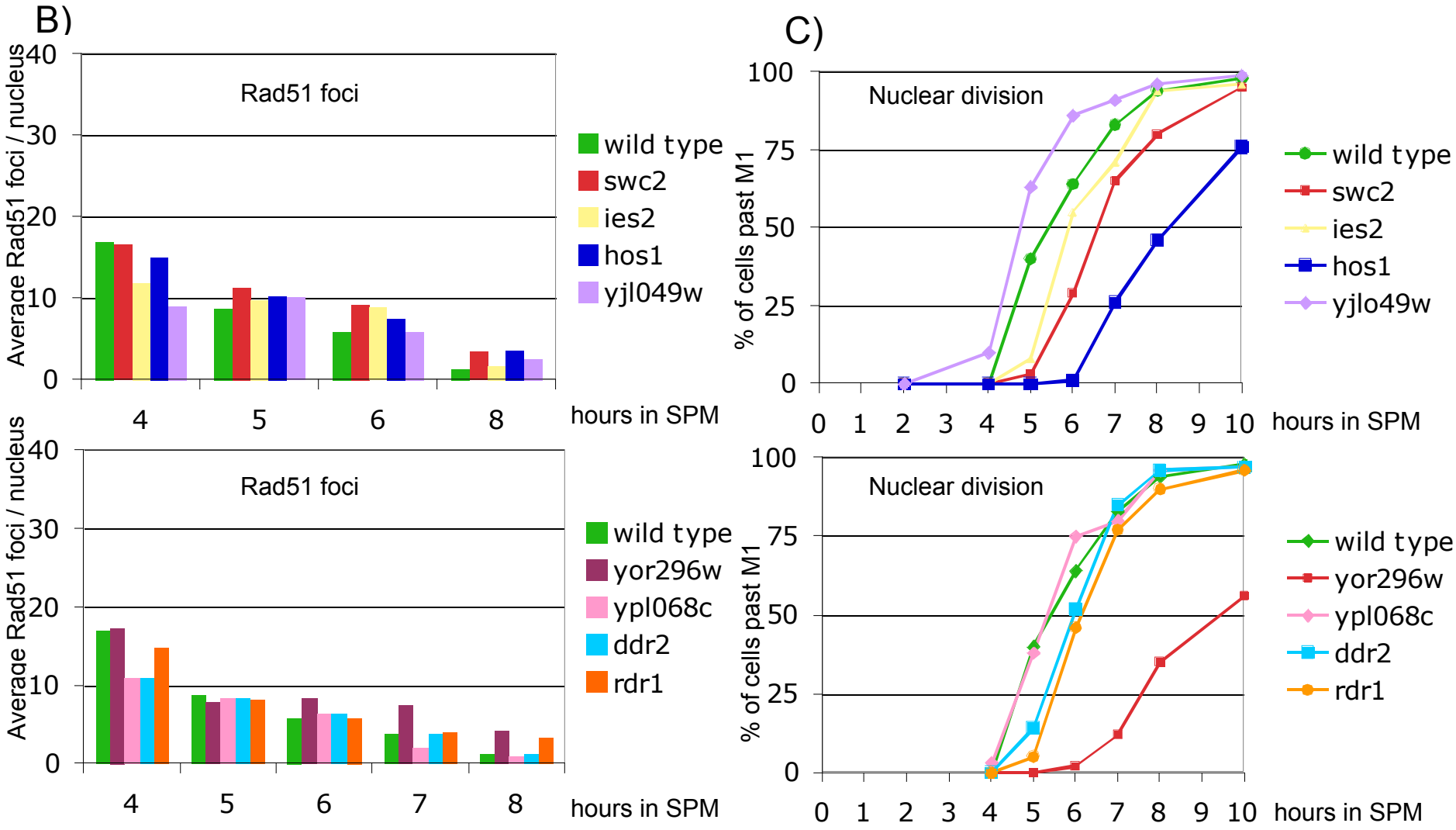

Fig 10A,B,C

*rim4*Δ is nearly devoid of synapsis, shows no meiotic progression and impaired Rad51 turnover

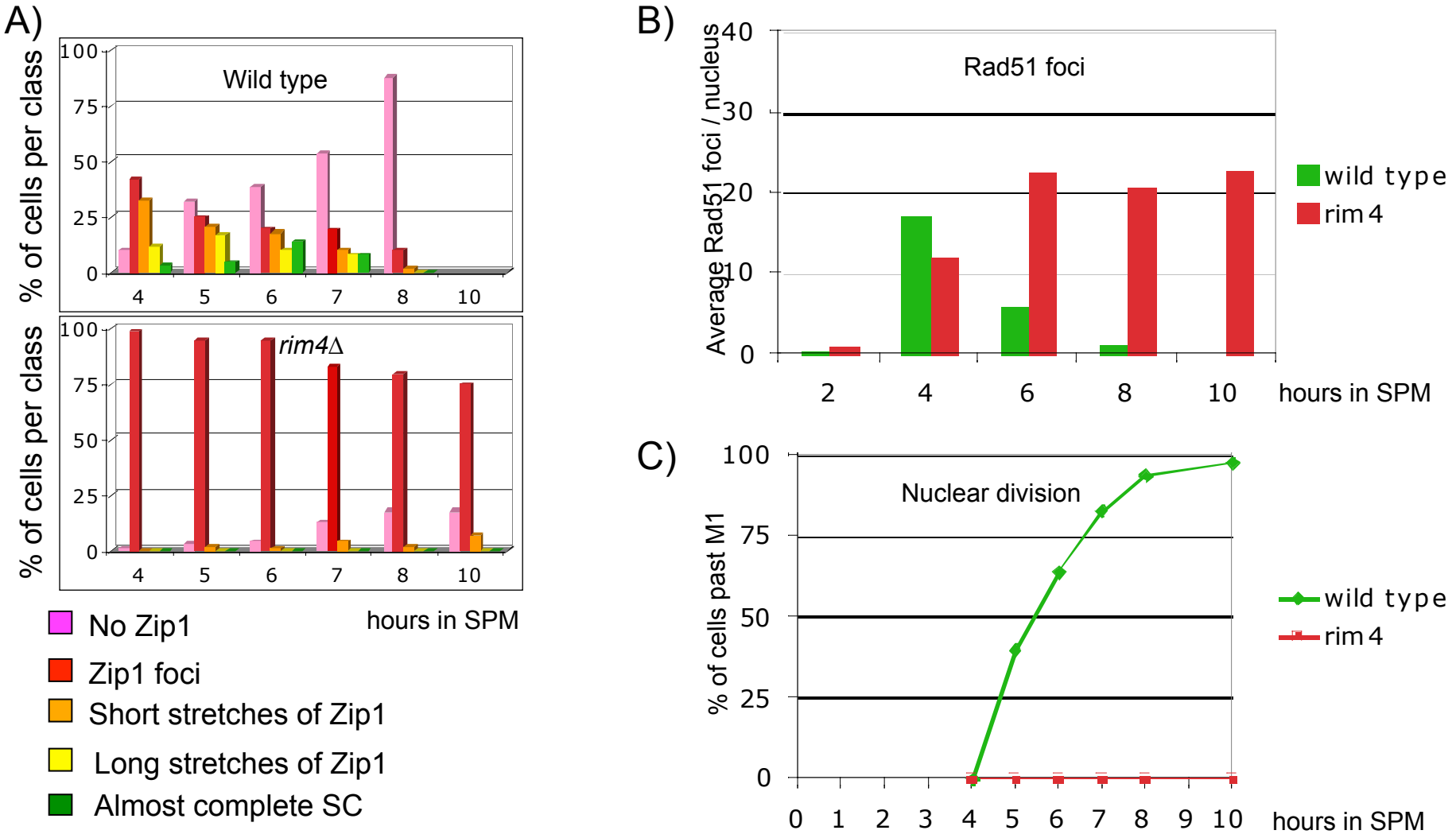

Fig 10D,E

Rim4-HA3 localizes in the cytoplasm, while *rim4*Δ mutants arrest with a prophase I spindle.

D)

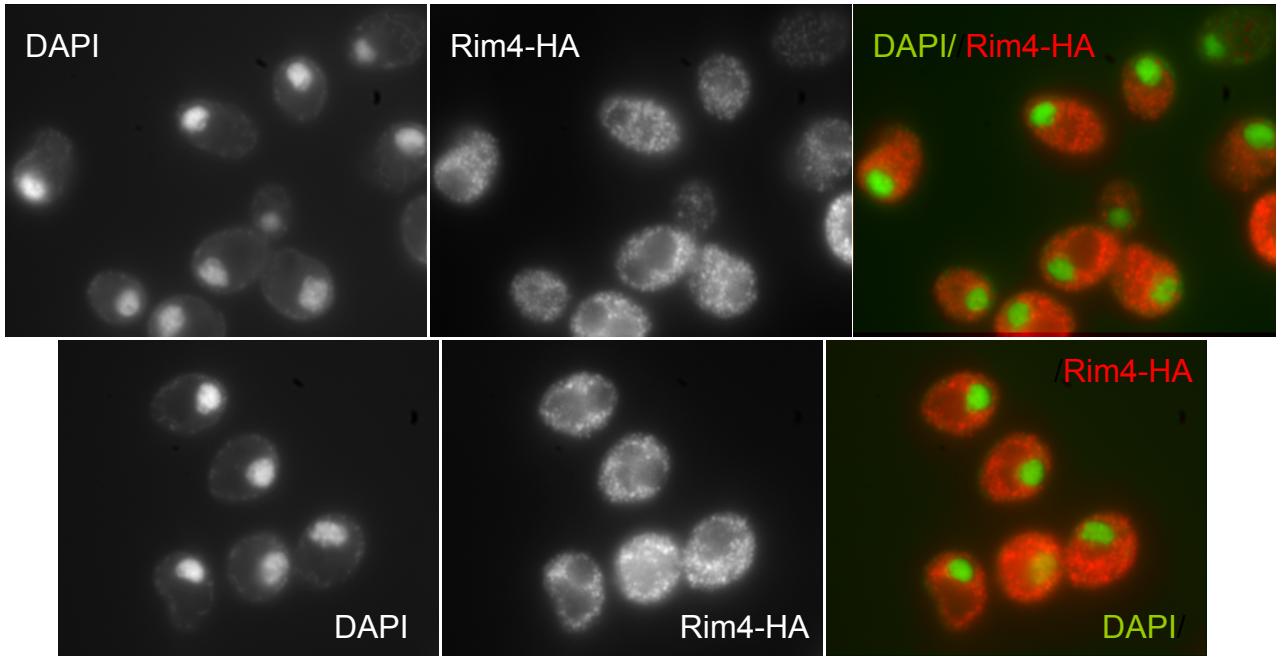

E)

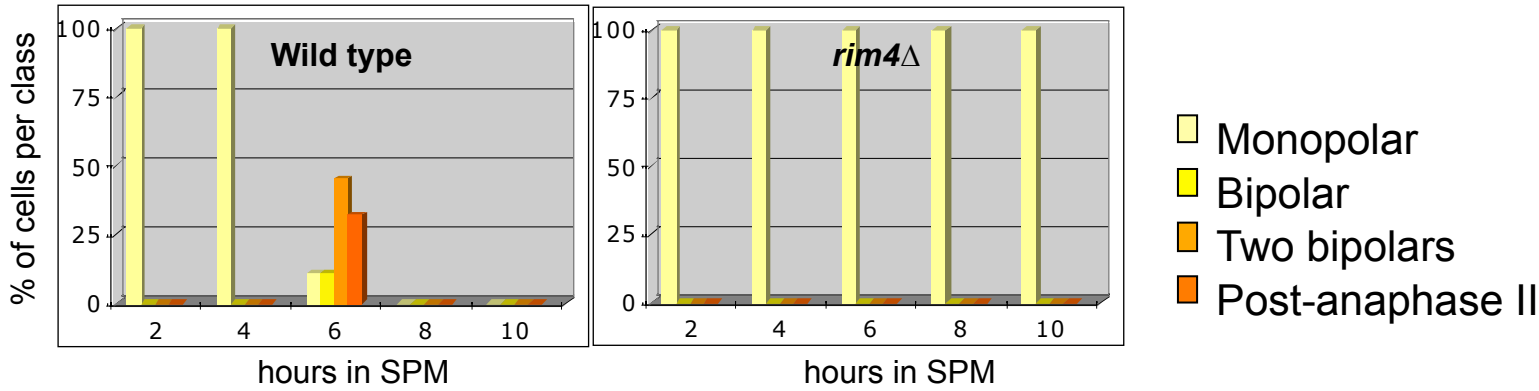

Fig 11A,B Mutants of the Shu complex undergo premeiotic S-phase, but display reduced numbers of Rad51 foci

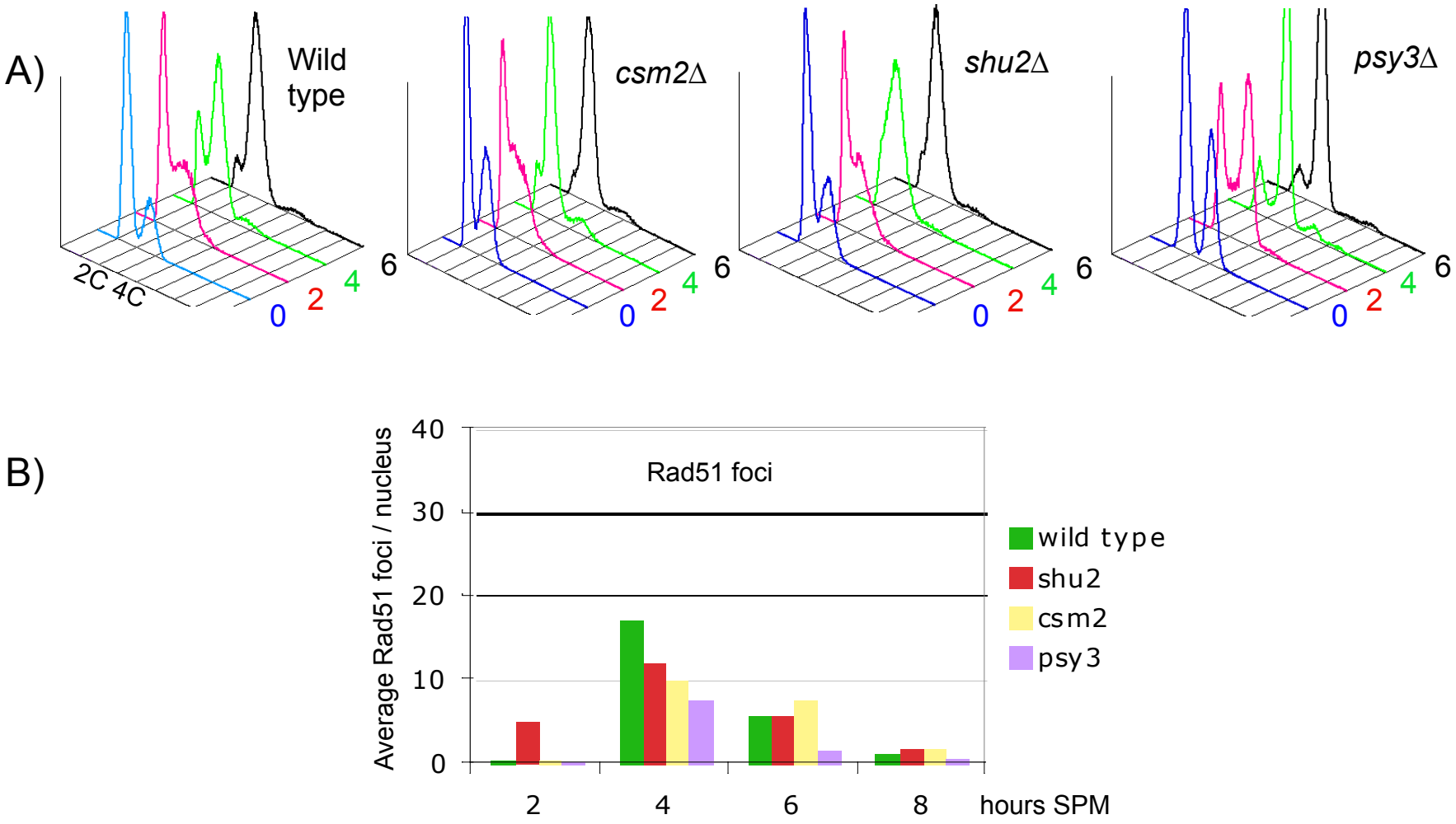

Fig 12

Scheme of CO, NCO detection system.

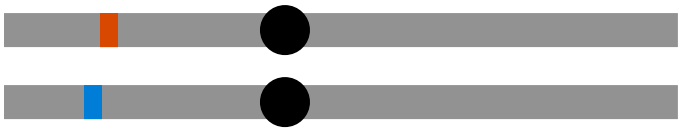

‘mom’

‘dad’

Chr3

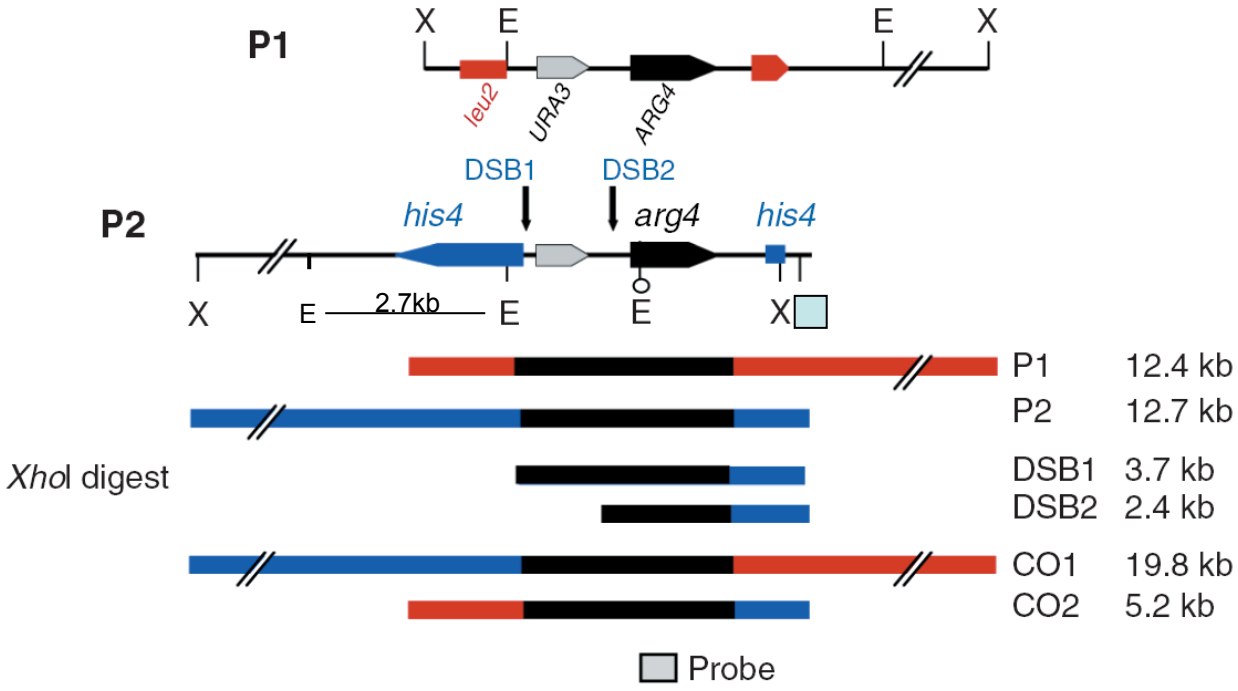

EcoRI/XhoI - Assay

DSBs, CO, NCOs

Fig 13A,B

CO and NCO are delayed and reduced in *psy3Δ*, while *irc25Δ/poc3Δ* is specifically reduced for CO

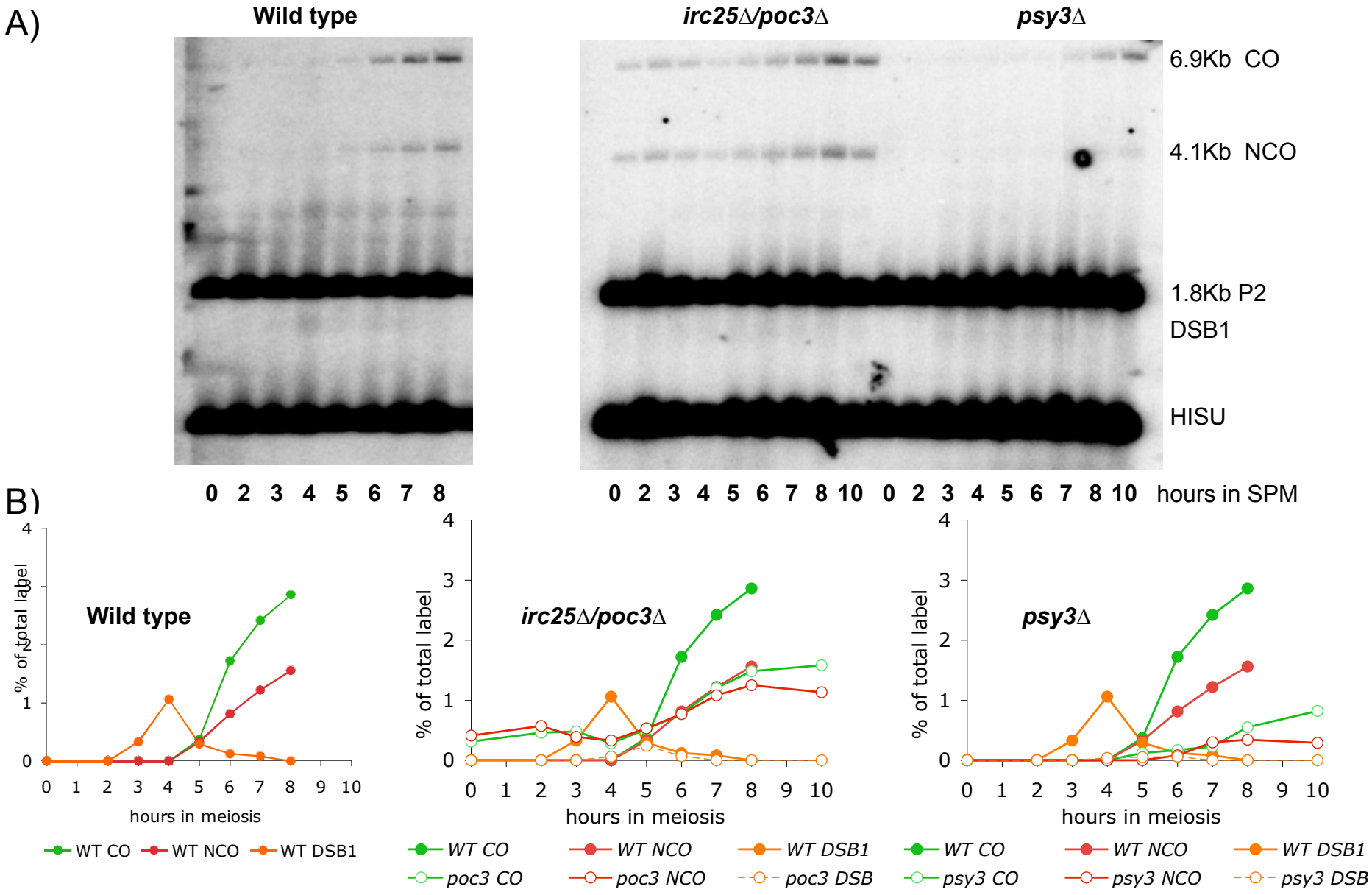

Fig 14ABCD

*yor029w*Δ shows a delay in DSB formation, increased Rad51 foci levels and a mild reduction in COs

A)

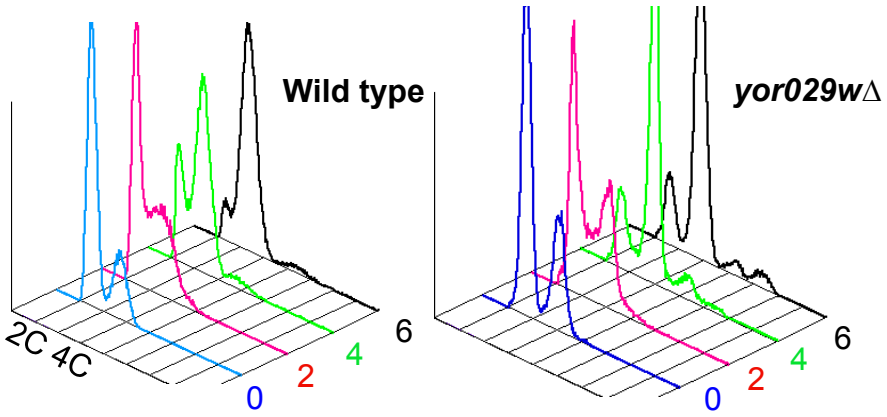

B)

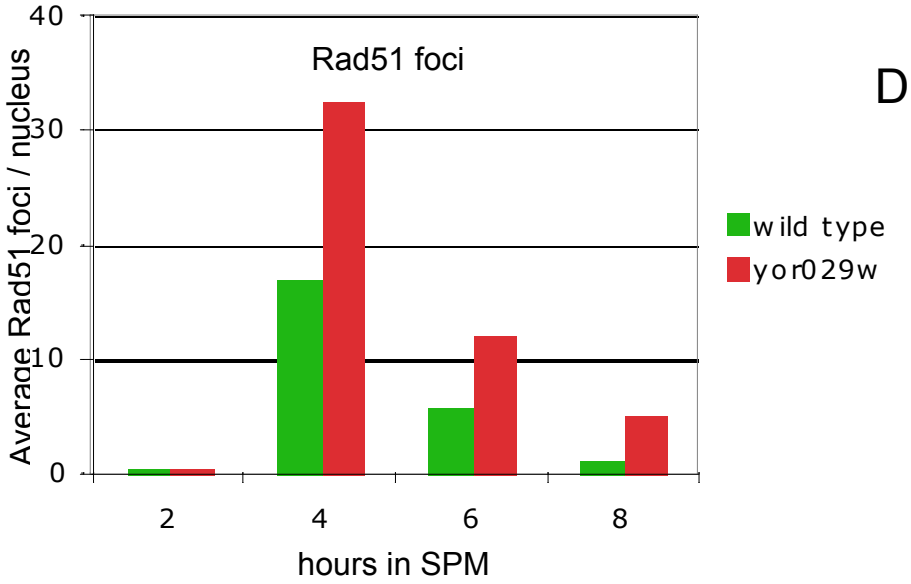

C)

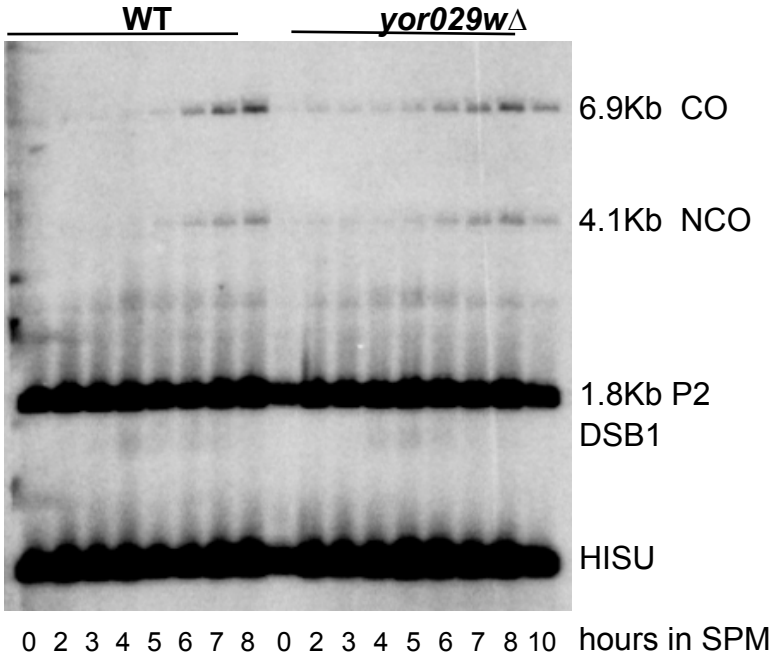

D)

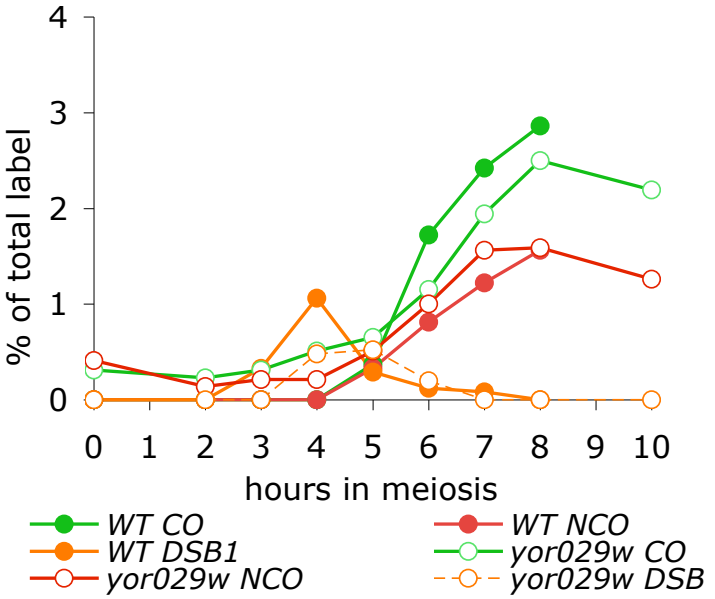

Fig 15A,B

*rad33*Δ shows a slight reduction in CO and NCO, *rvs167*Δ shows a reduction in NCO

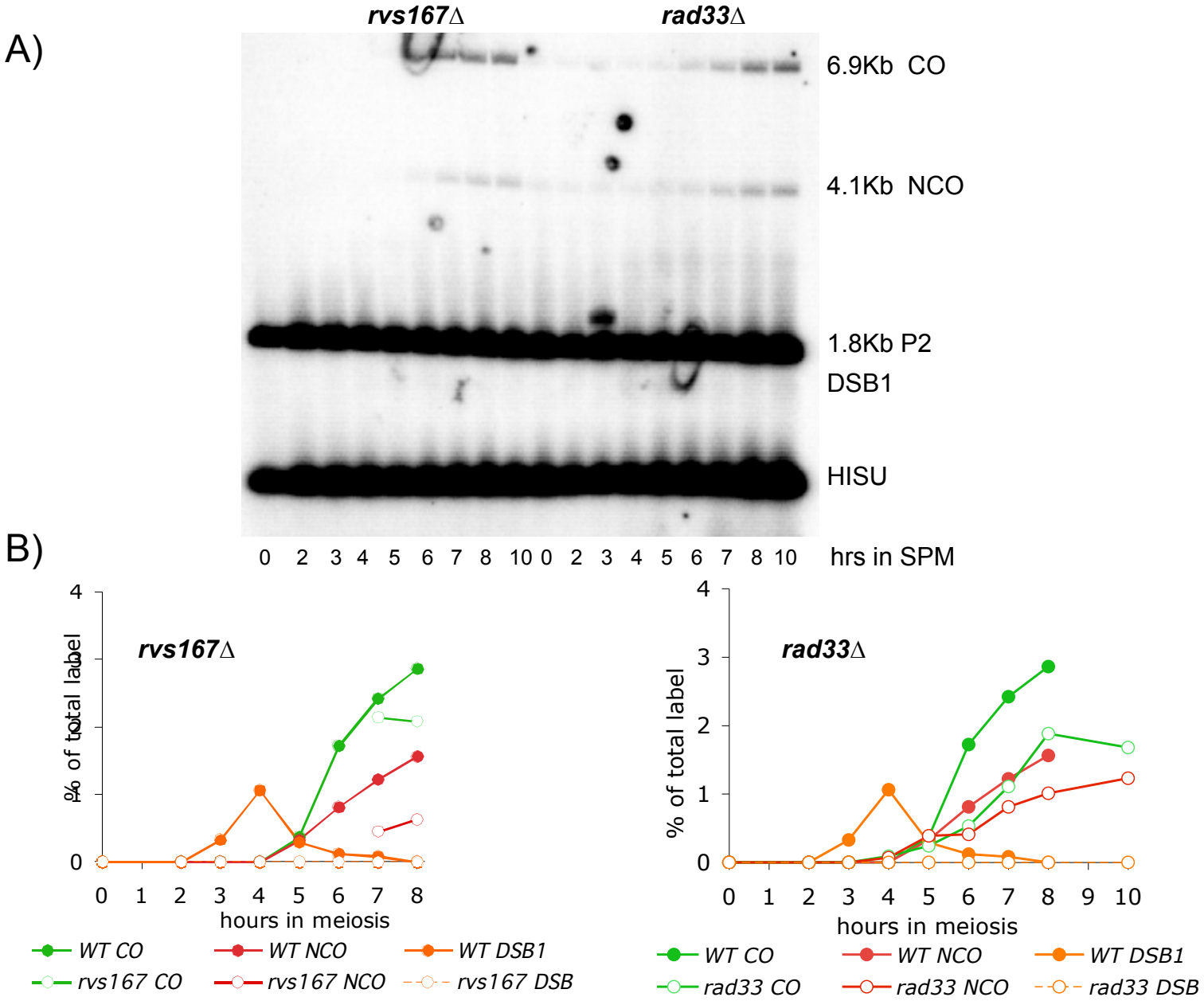

Fig 16A

*rad6*Δ is defective in CO and NCO, *ylr352w*Δ shows a delay in CO and NCO

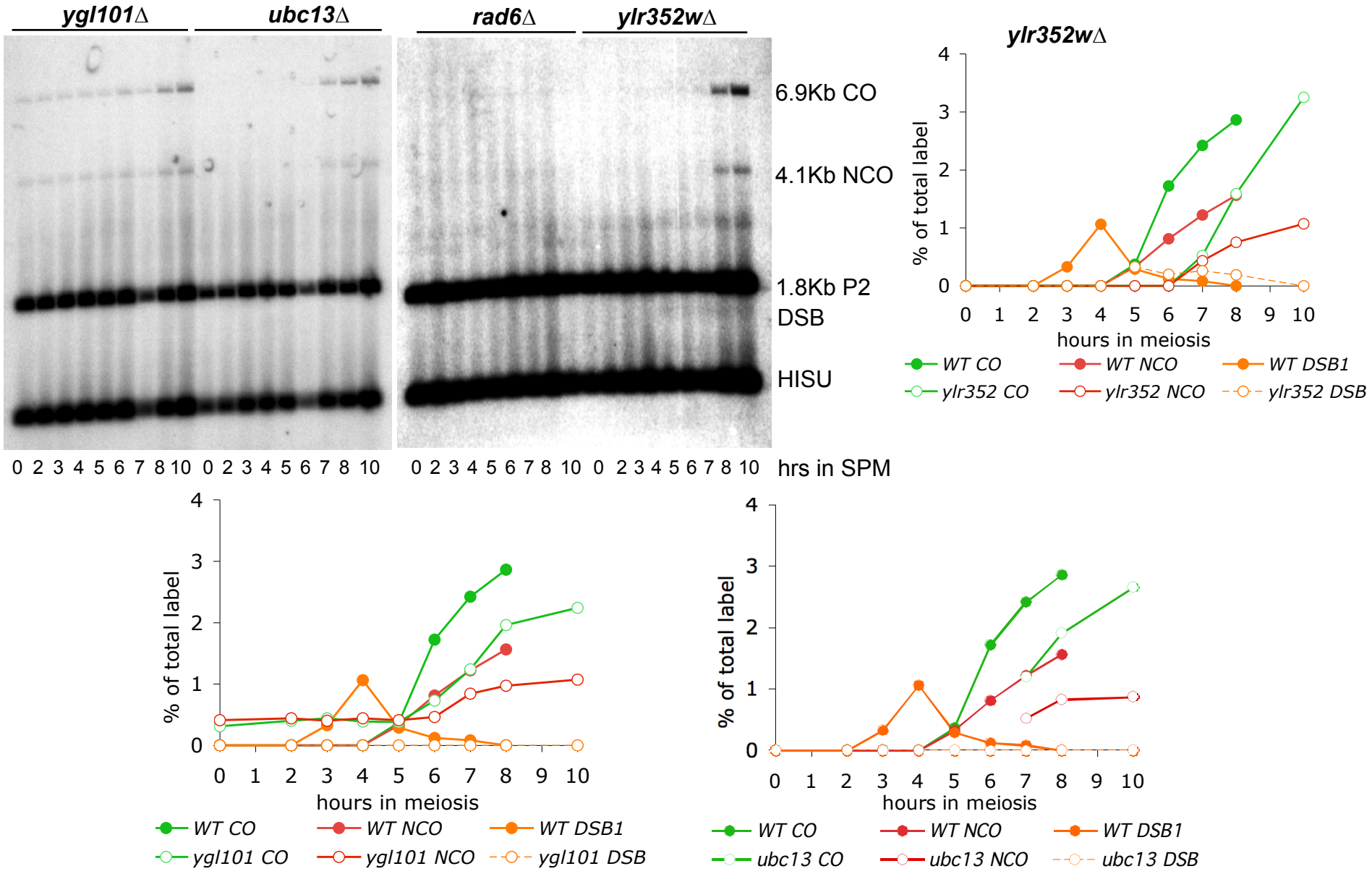

Fig 17A,B

hnt3Δ displays a reduction in CO and NCO, and a delay in Rad51 foci turnover

A)

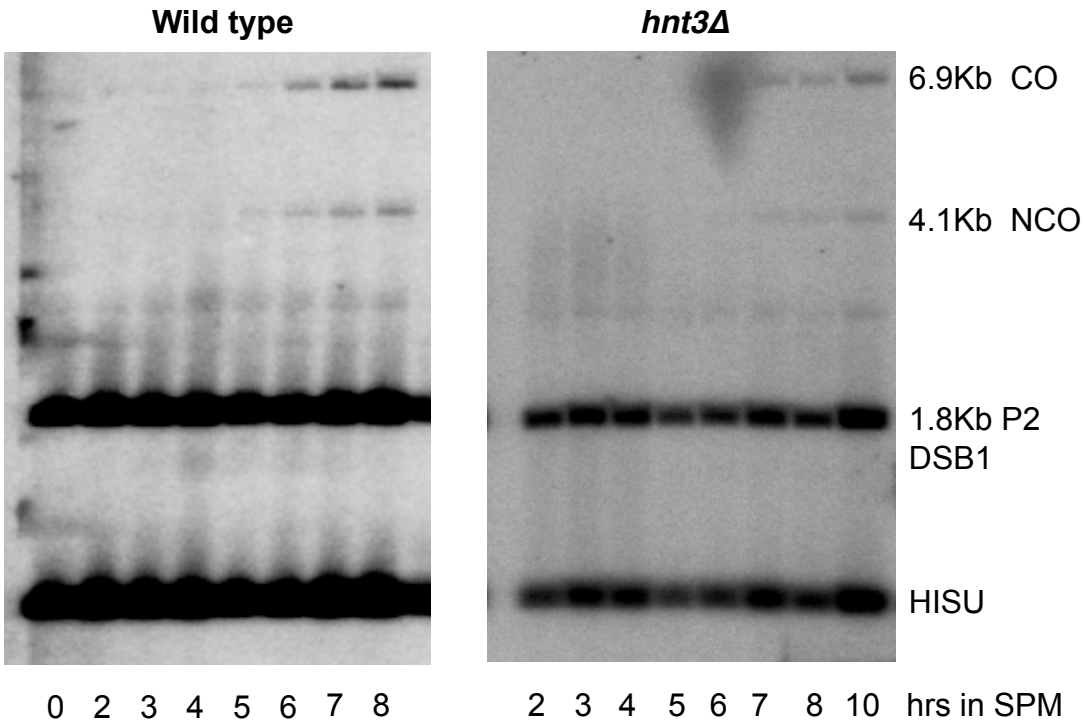

B)

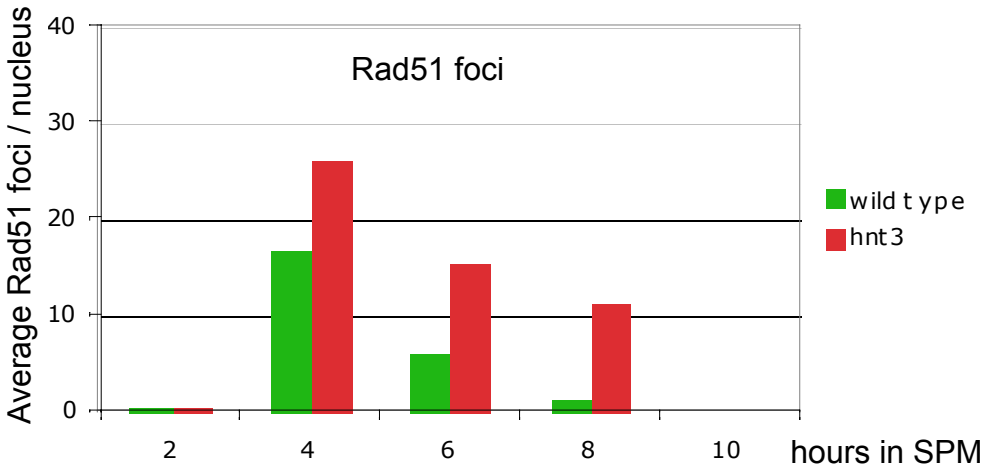

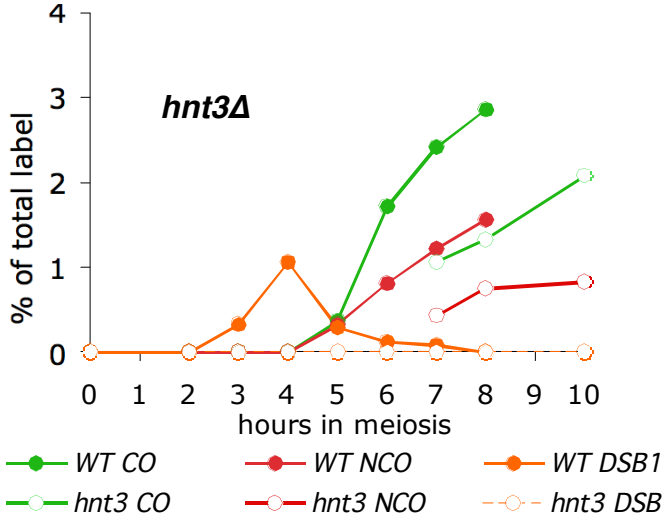

Rad51 foci turnover and nuclear division are delayed in *pph3*Δ, *psy2*Δ and *psy4*Δ mutants, while pre-meiotic DNA replication is impaired only in *pph3*Δ.

Fig 18A,B,C

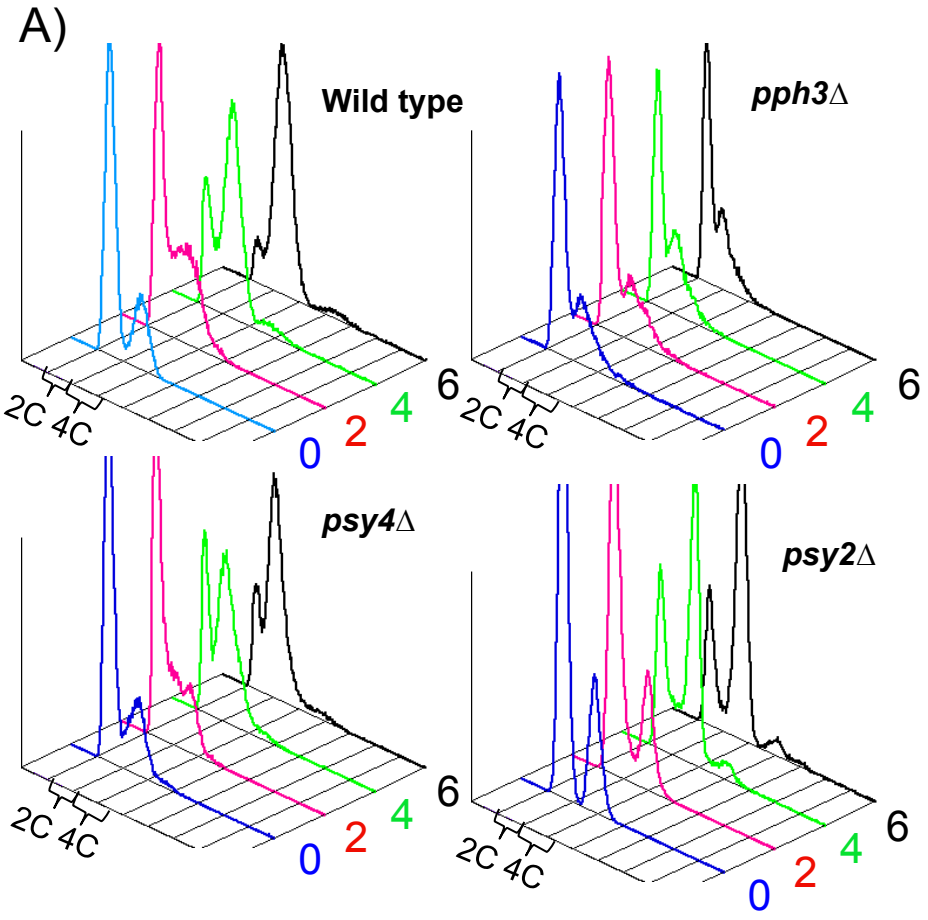

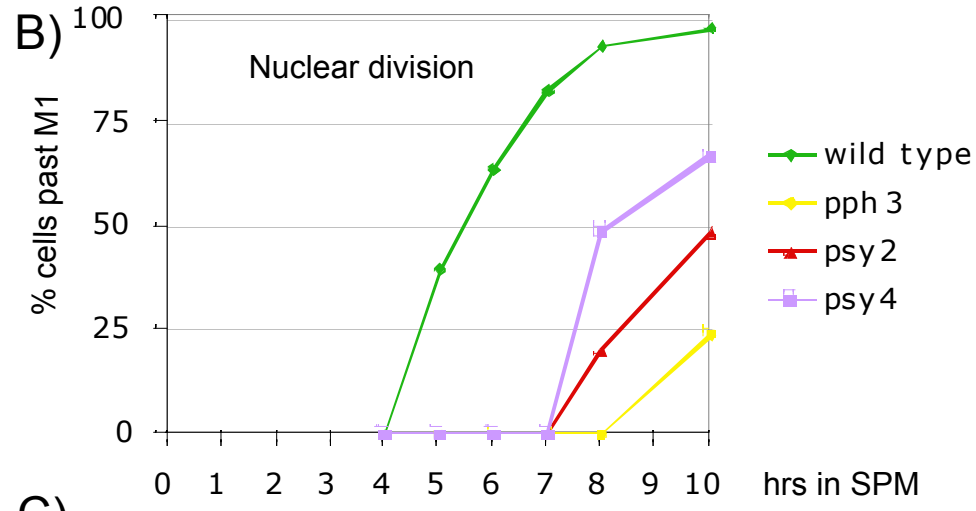

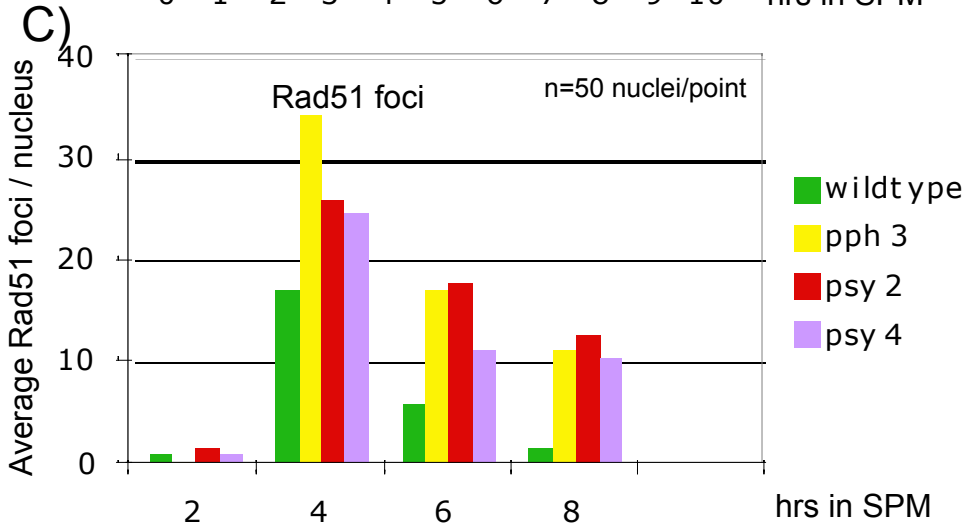

Fig 18D

Synapsis is strongly impaired in *pph3*Δ and *psy2*Δ and delayed in *psy4*Δ mutants.

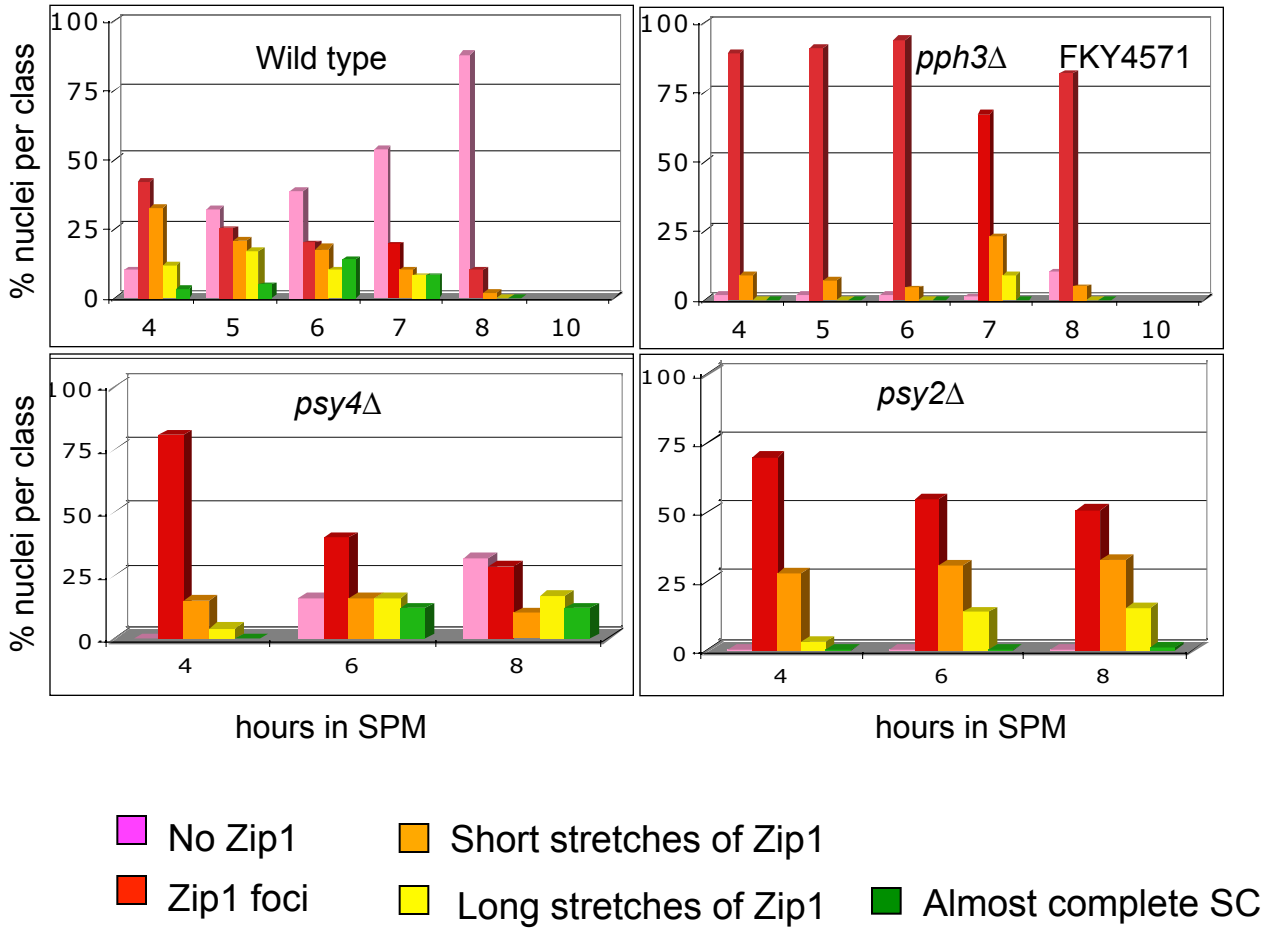

Fig 18E,F

*psy2*Δ shows a specific reduction in COs,
while COs and NCOs appear with a delay and a reduction in *psy4*Δ.

E)

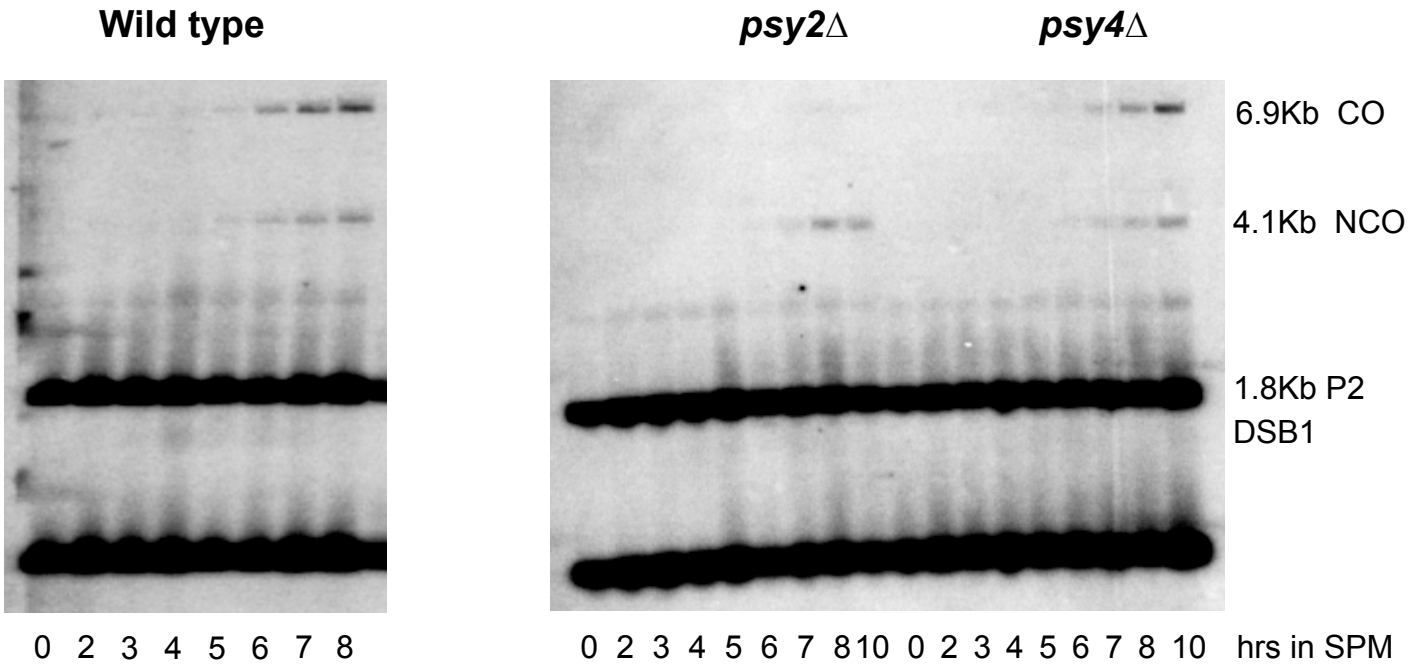

F)

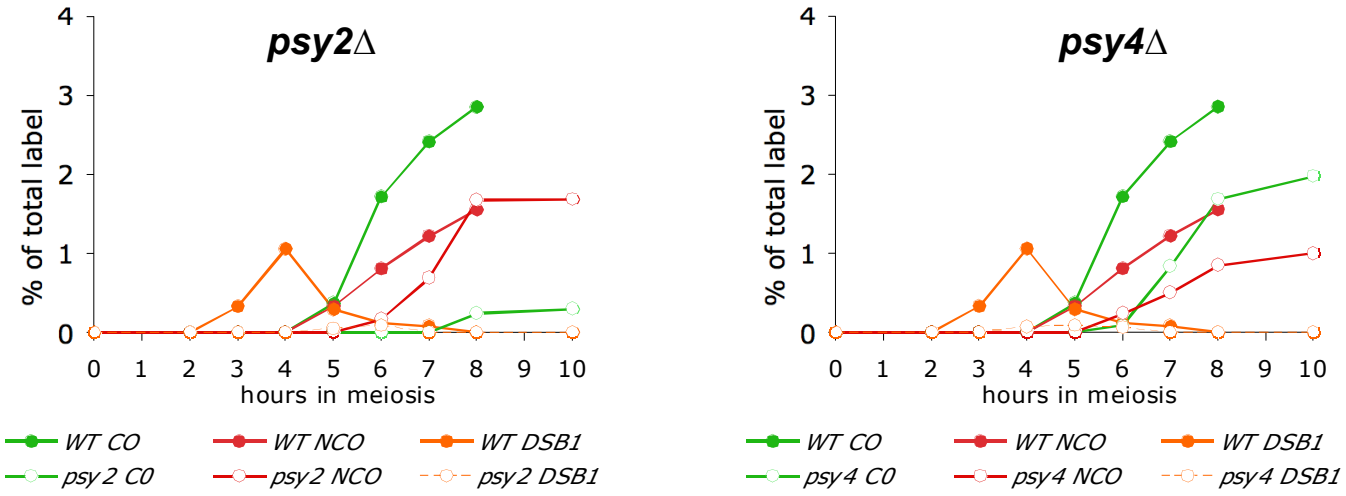

Fig 19A

hta1.2-S129A mutations mildly alleviate the synapsis defect of pph3Δ

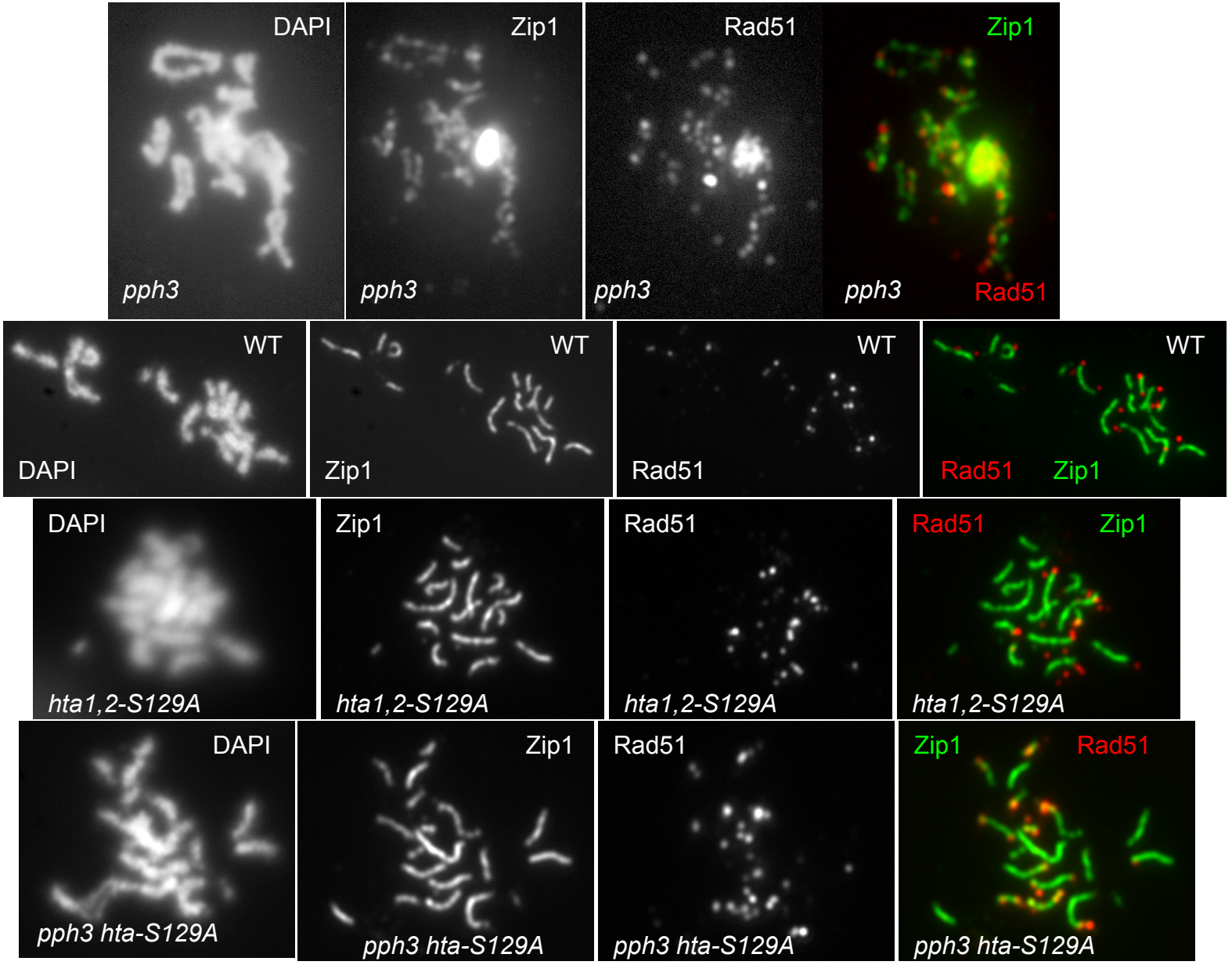

Fig 19B

hta1.2-S129A mutations mildly alleviate the synapsis defect of *pph3Δ*

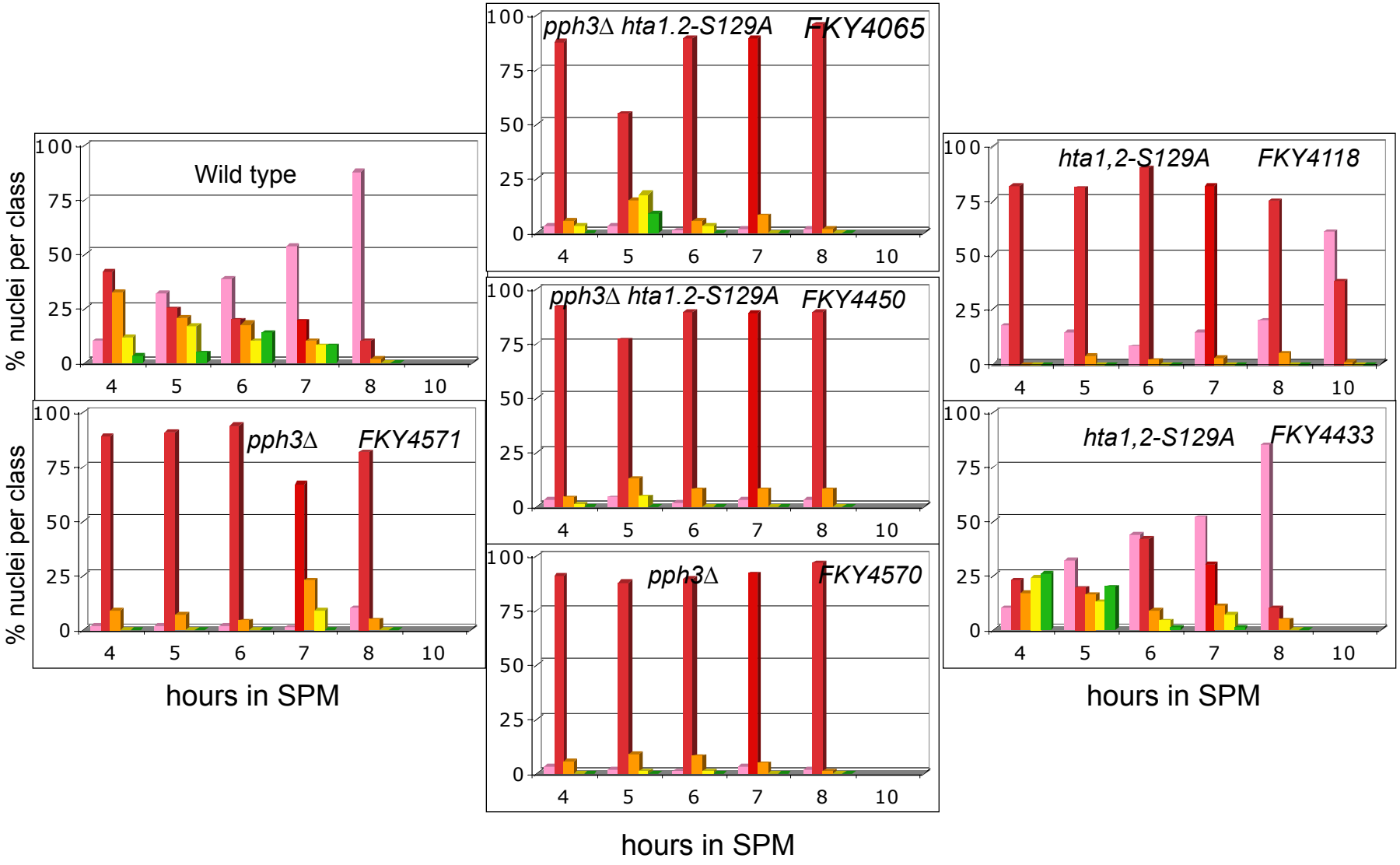

Fig 19C

pph3Δ and hta1,2-S129A mutations are additive concerning nuclear division delay

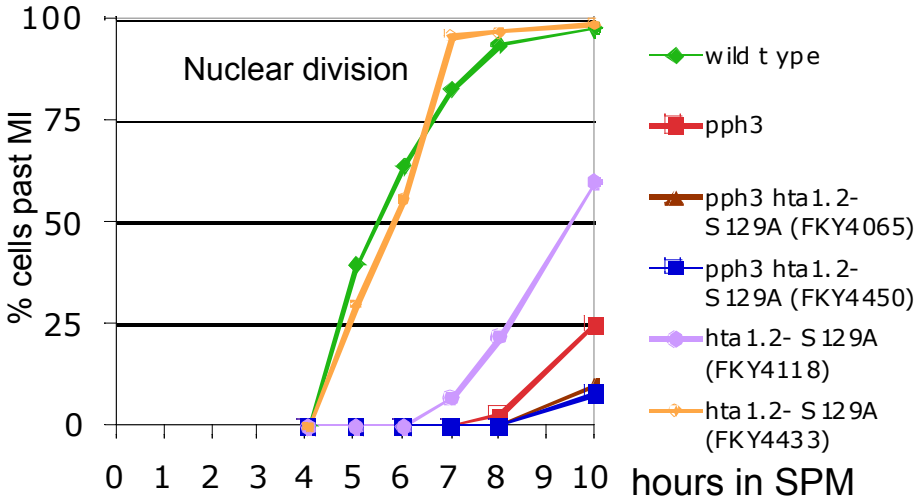

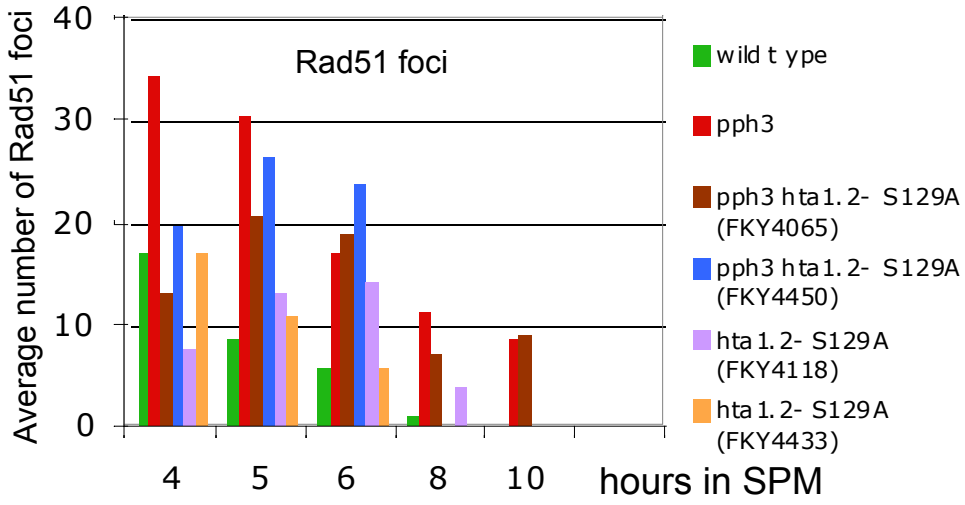

Fig 20A

Deletion of *SWC2* restores full synapsis in *pph3*Δ mutants, although with delay

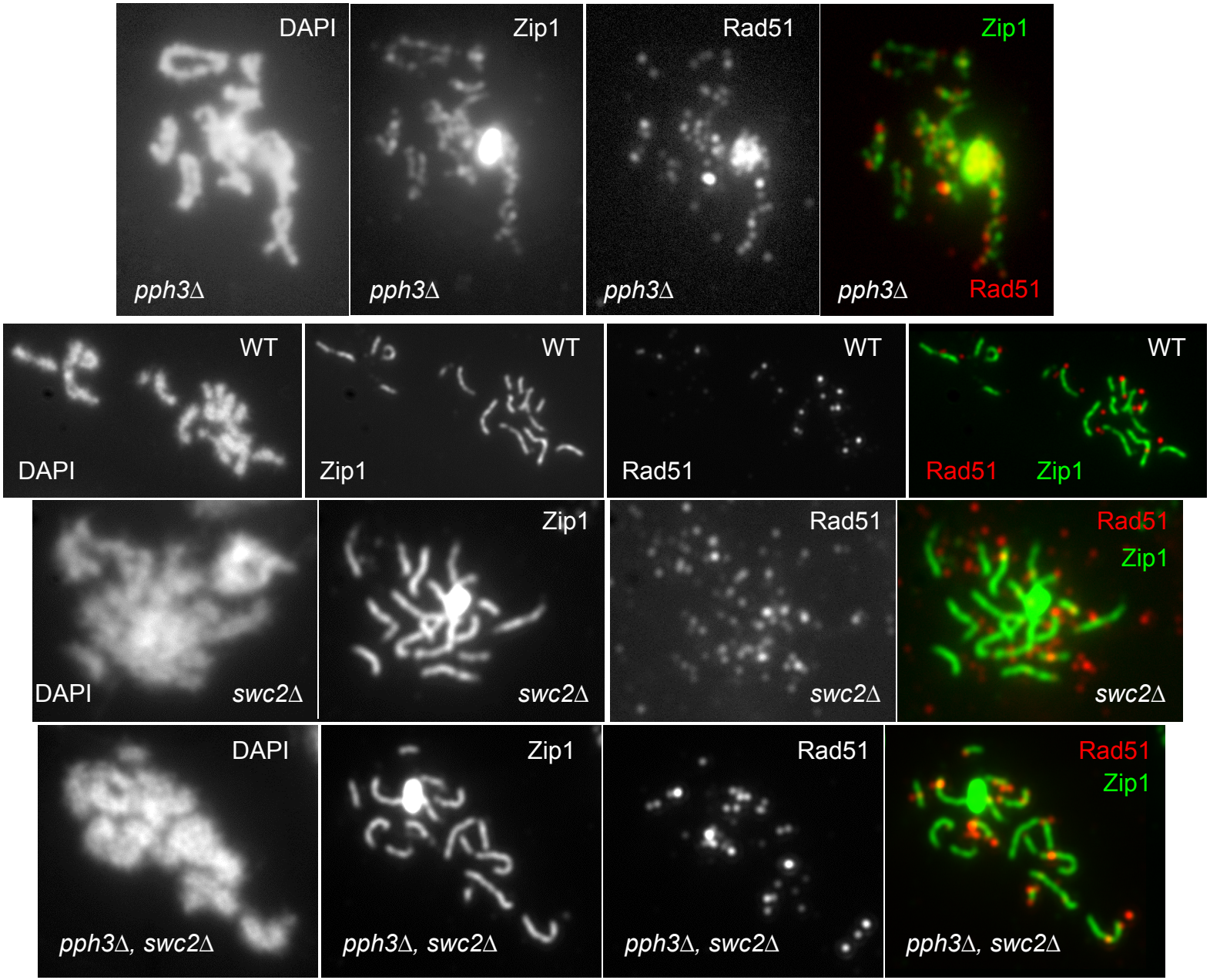

Fig 20B The synapsis defect of *pph3*Δ mutant is alleviated by the deletion of *SWC2,* but not of *HTZ1*, *LDB7* and *SWR1*

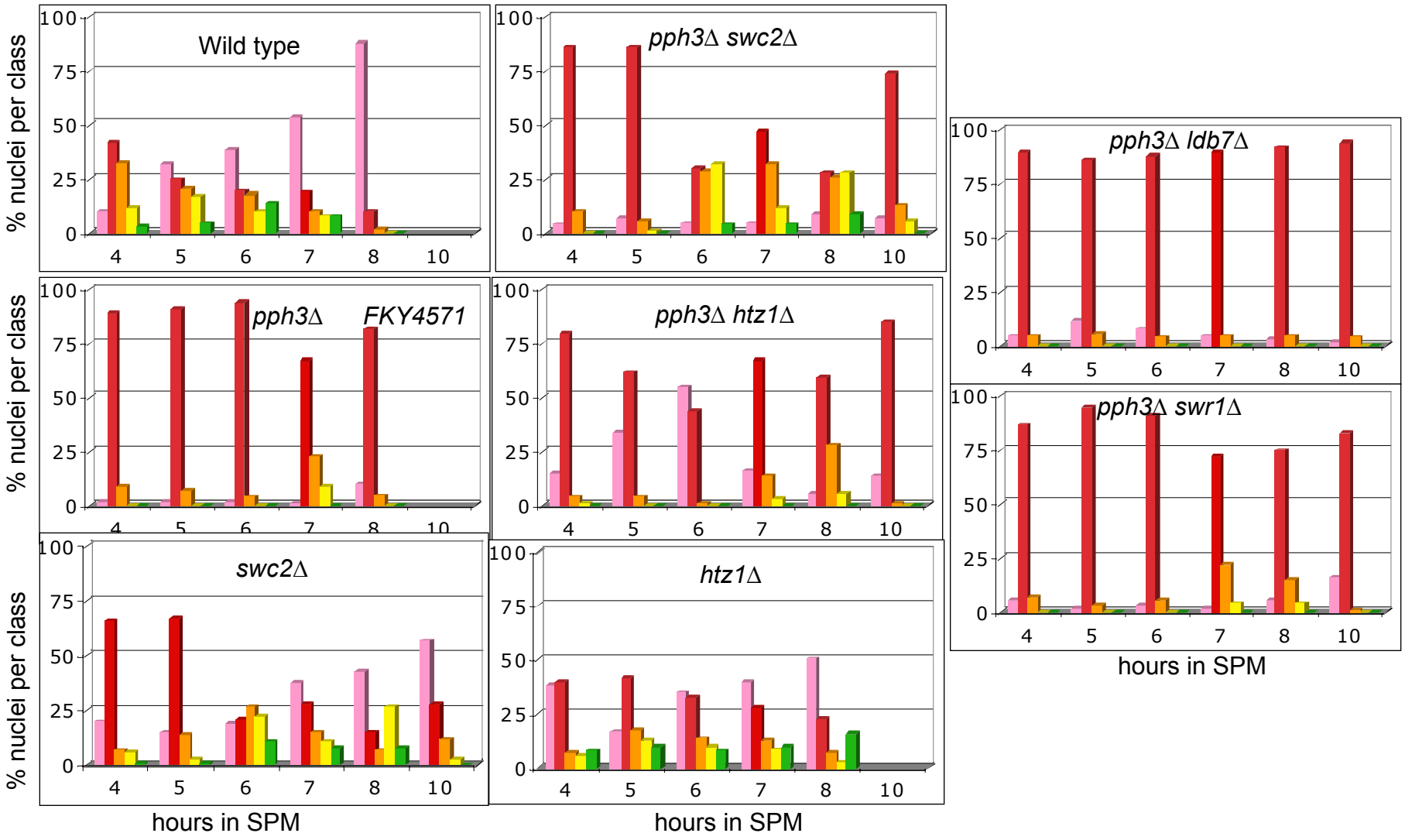

Fig 20C Deletion of *SWC2* , *HTZ1*, *LDB7* or *SWR1 reduced* Rad51 foci, but did not affect nuclear progression in the *pph3*Δ background

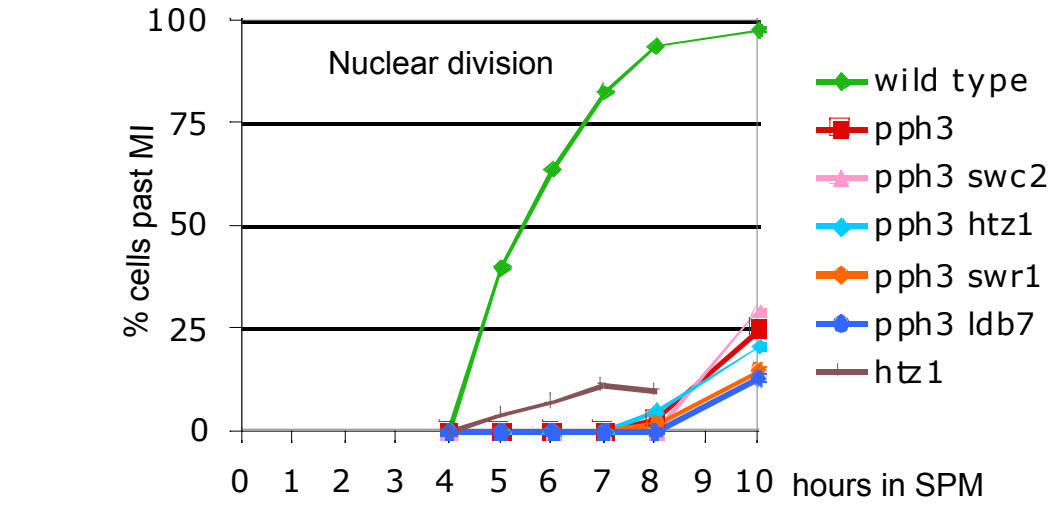

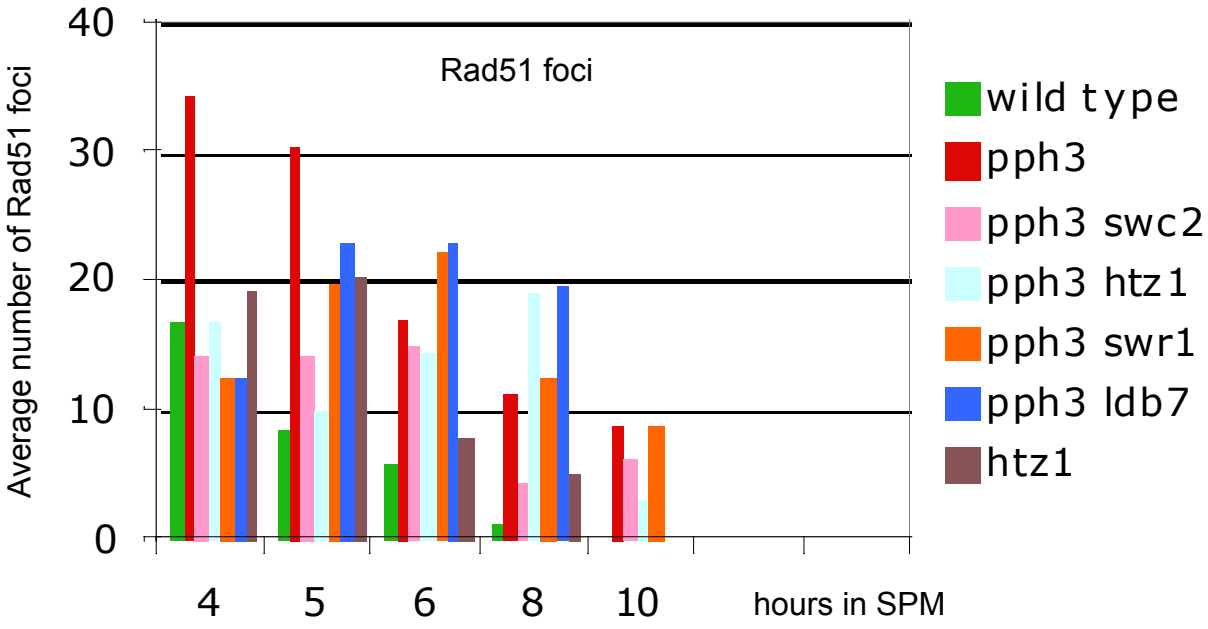

Fig 20D

Swc2 chromosomal binding sites overlap with those of Rec8, without showing any preference for centromeres.

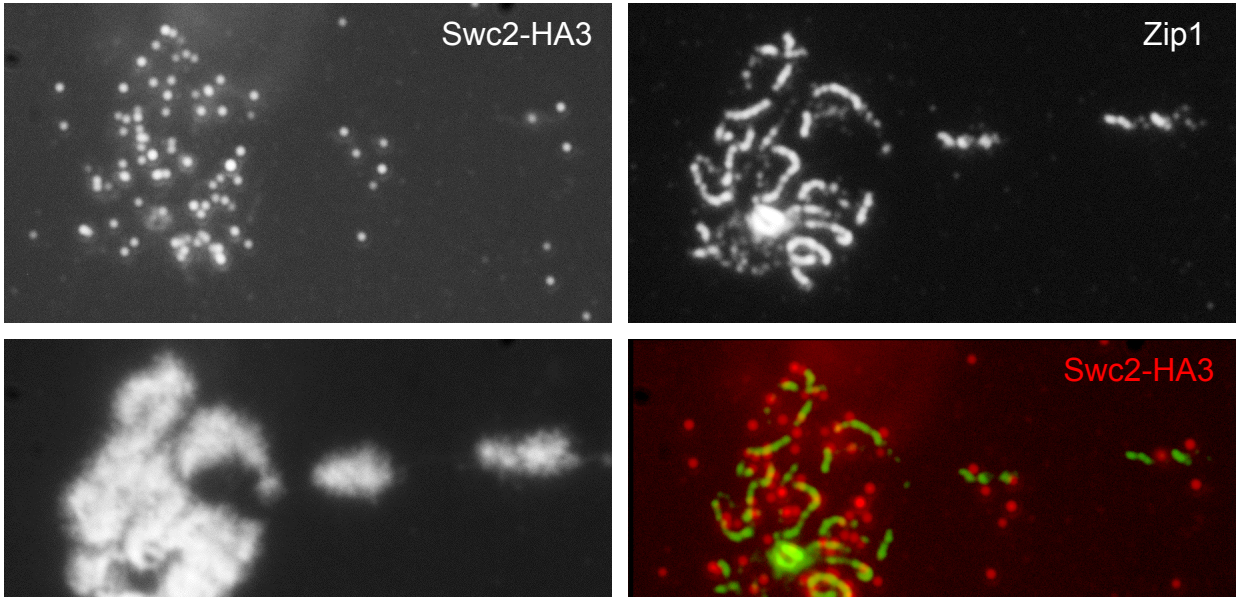

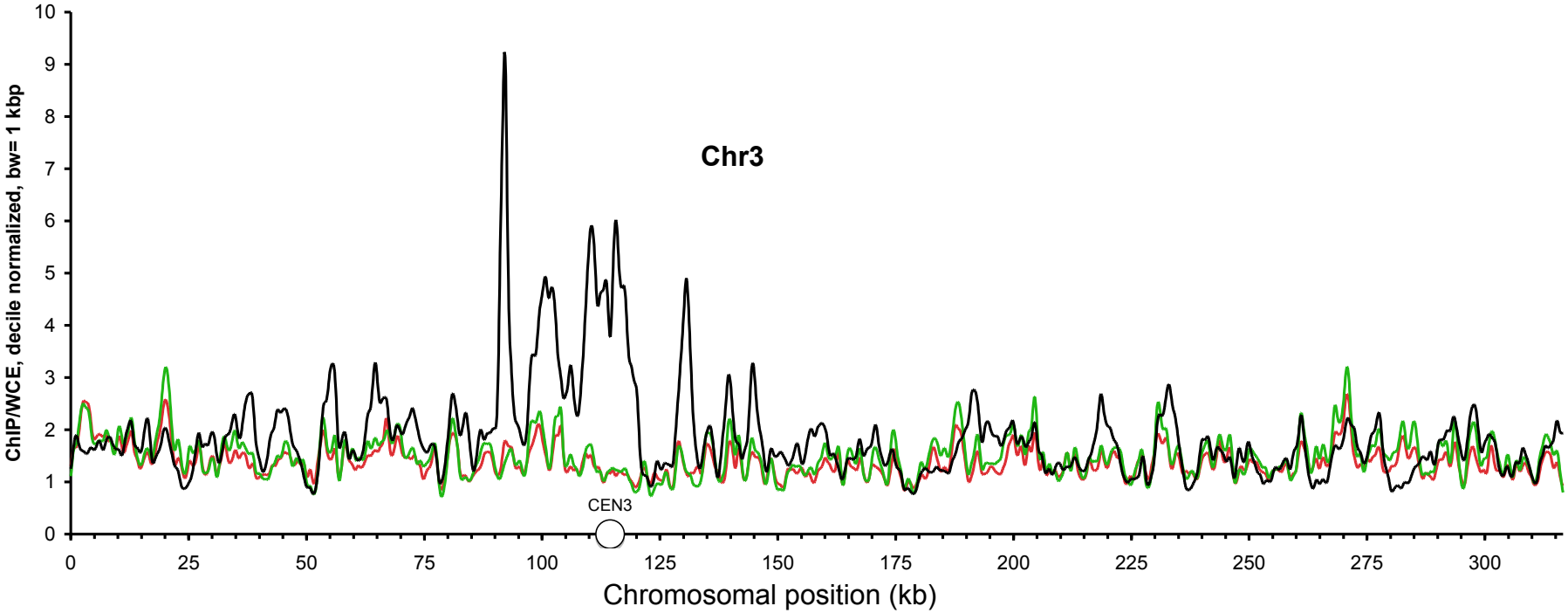

Fig 20E

Like Rec8, Swc2 sites on chromosomes do not overlap with DSB hotspots

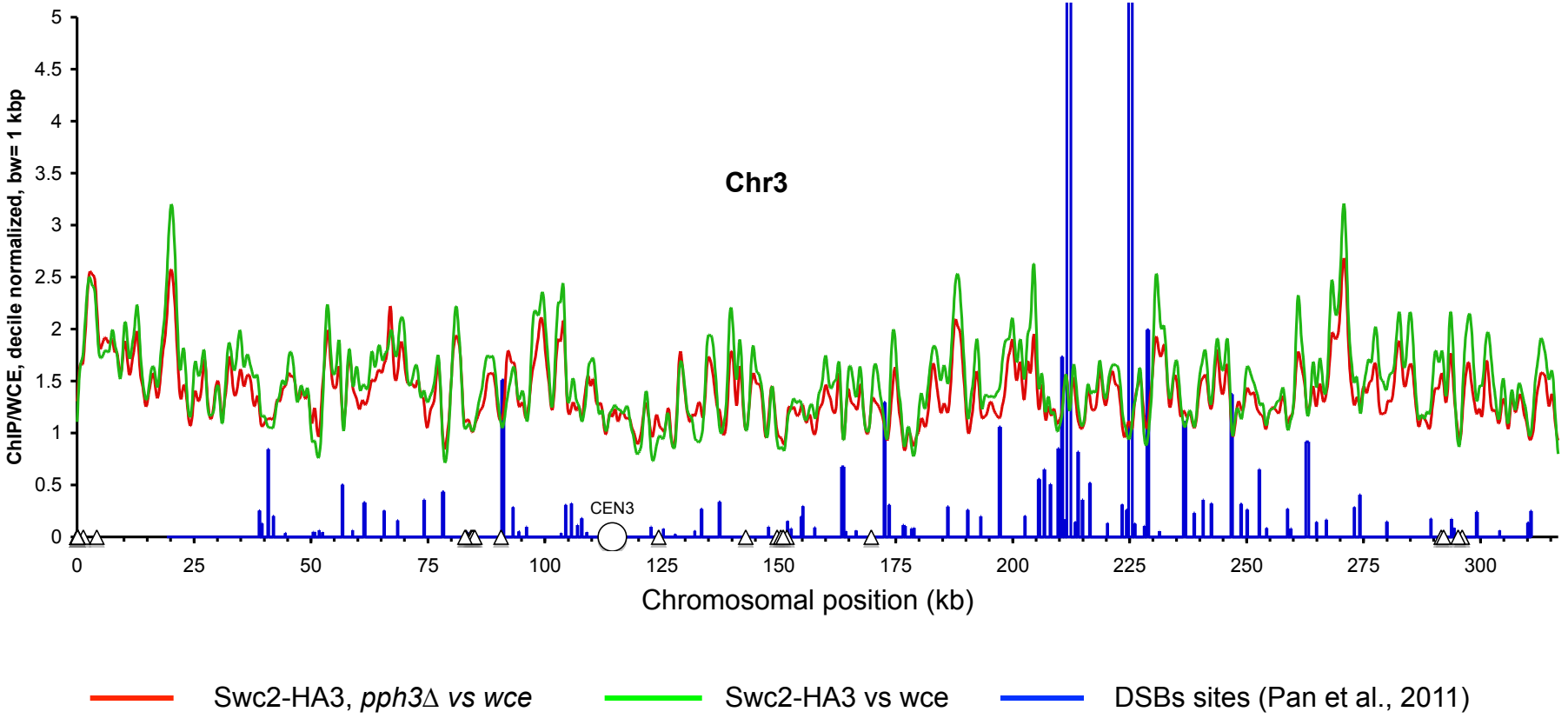

Fig 20F Swc2 binding along chromosomes is reduced in pph3Δ mutant.

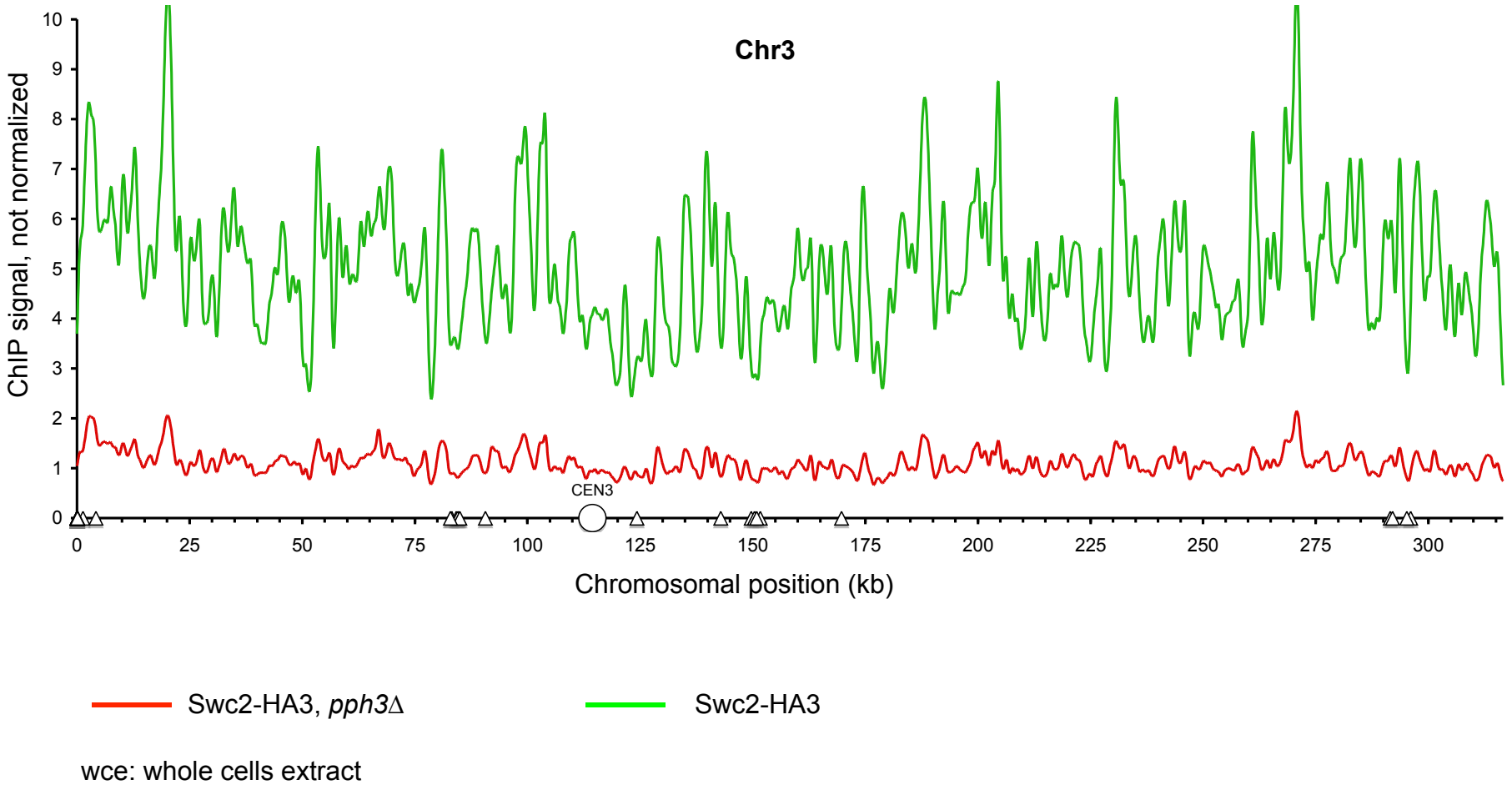

wce: whole cells extract

Fig 20G

Swc2 binding along chromosomes is reduced in pph3Δ mutant.

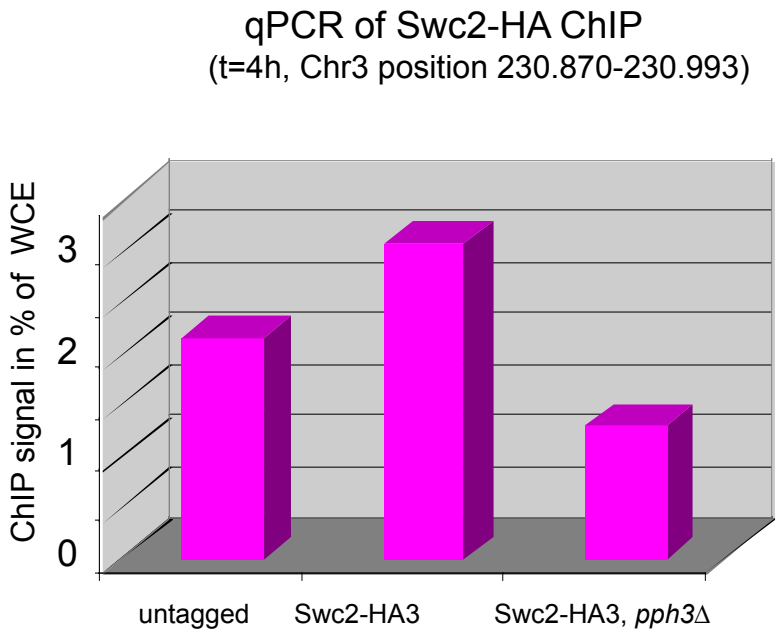

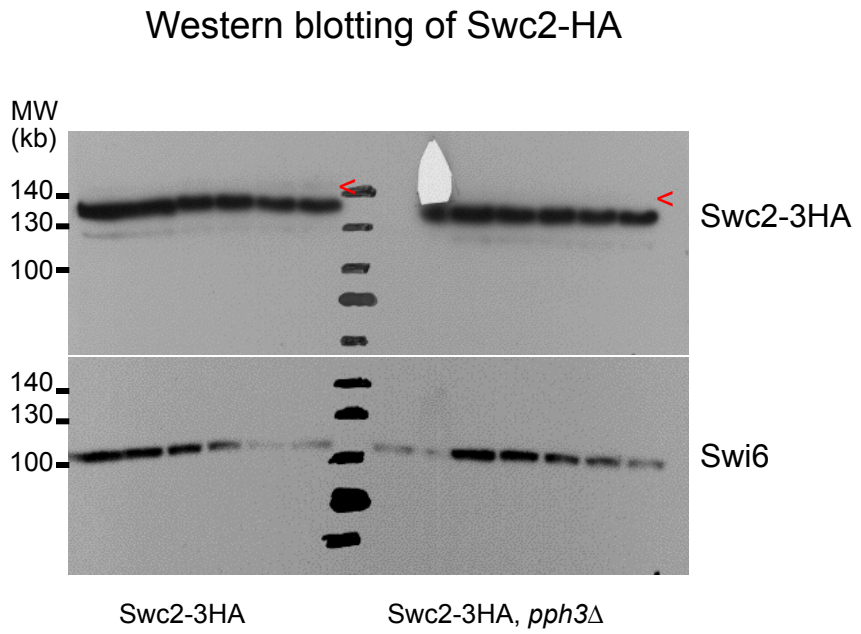

Fig 21A

Deletion of *PCH2* suppresses the synapsis defect of *pph3*Δ mutants

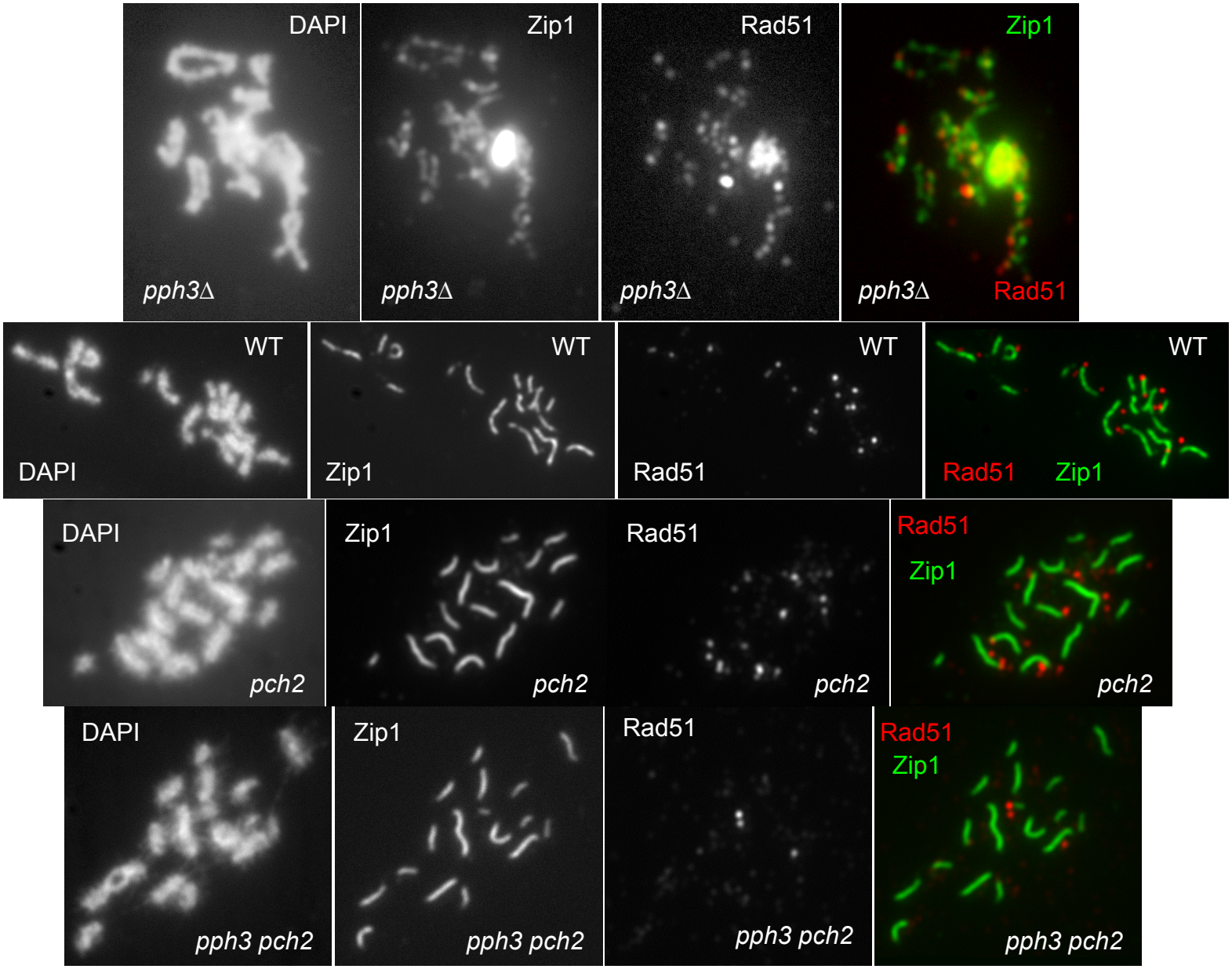

Fig 21B Synapsis hyper-accumulates in *pph3*Δ, *pch2*Δ double mutants, although with delay, while *dot1*Δ *does not suppress*

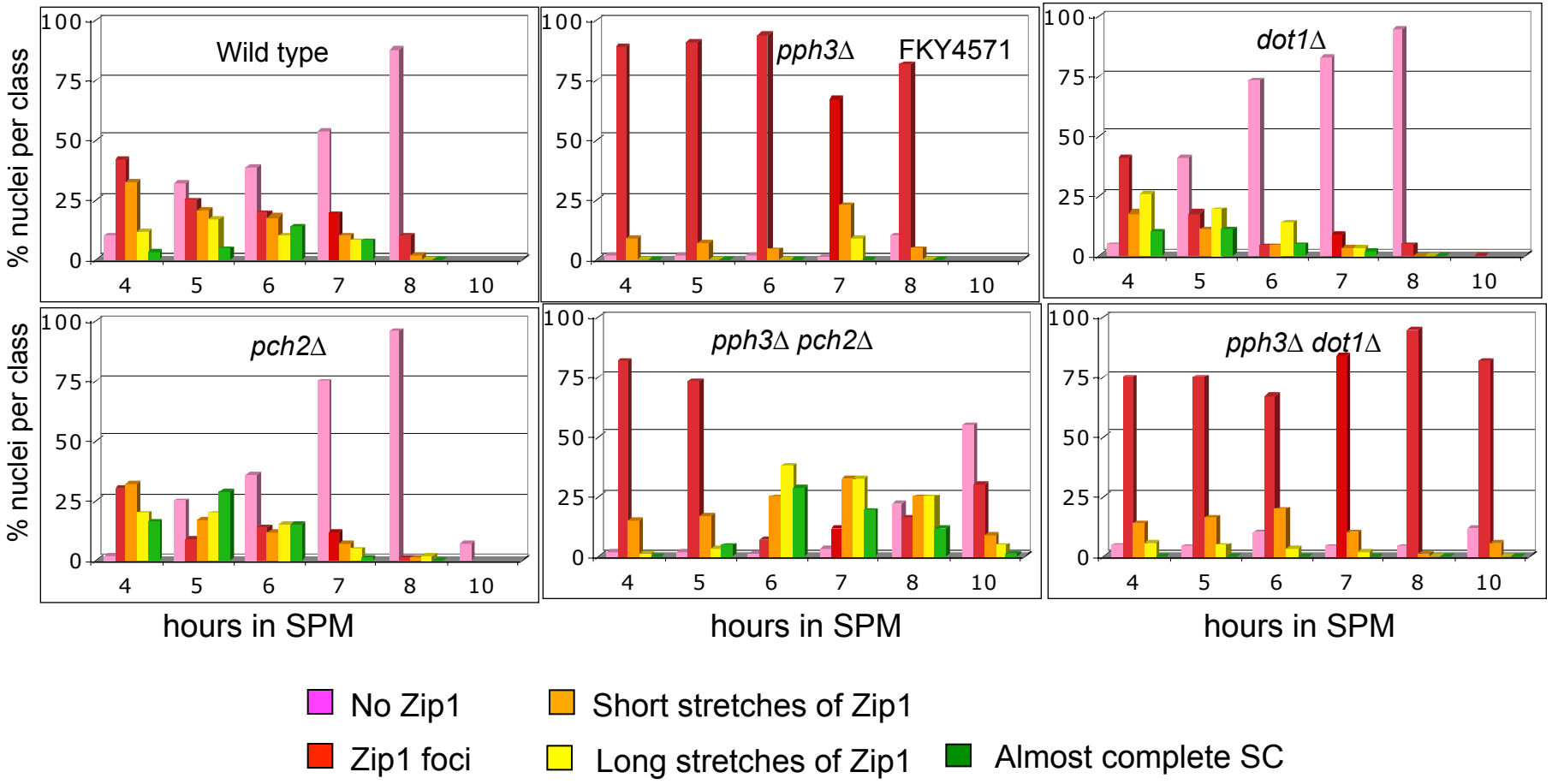

Fig 21C

Rad51 foci are reduced to wild type levels and meiotic progression is slightly advanced in *pph3*Δ cells in the absence of *PCH2.*

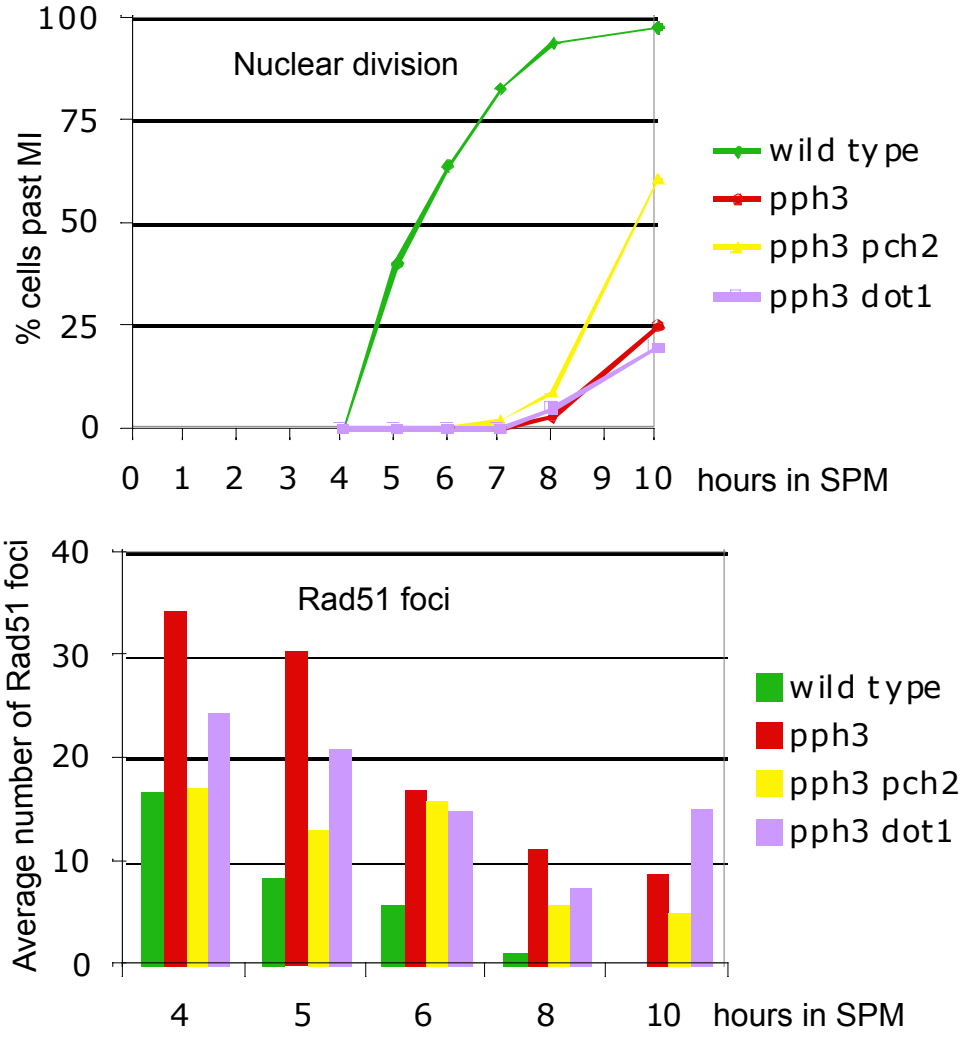

Fig 22A

Deletion of *FPR3* or *MEK1,* but not of *MEC1* alleviated the meiotic arrest of *pph3*Δ mutants.

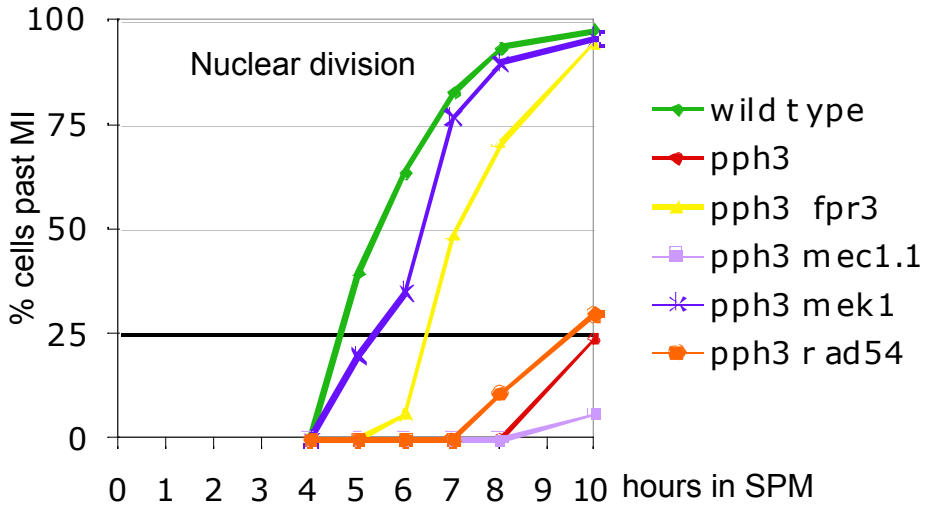

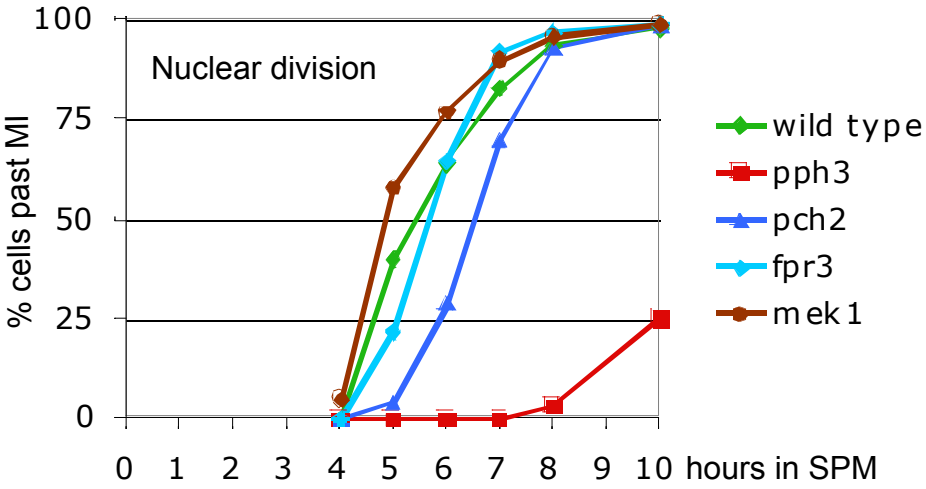

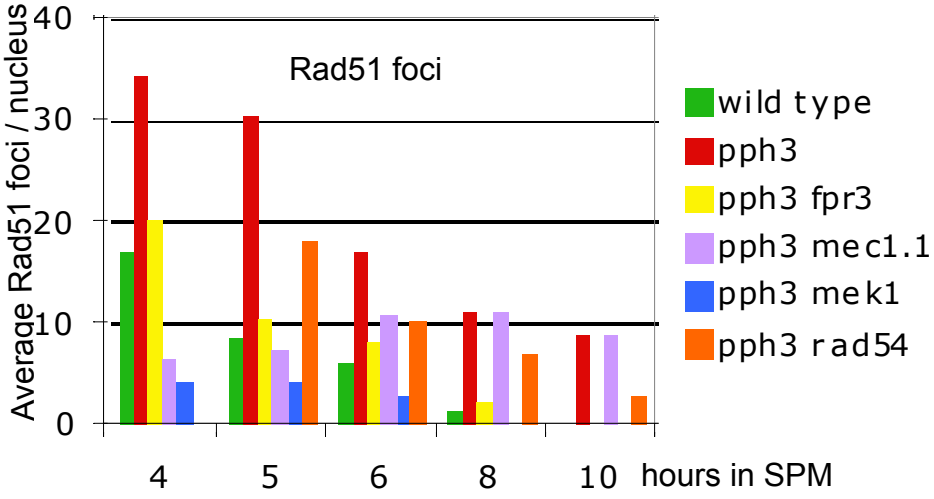

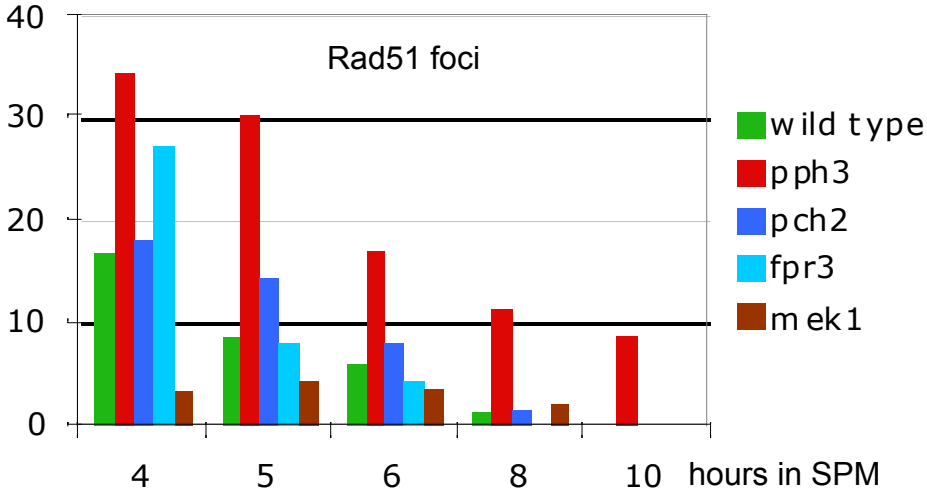

Fig. 22B

Only low levels of completely synapsed nuclei restored in *pph3Δ, fpr3Δ* double mutants.

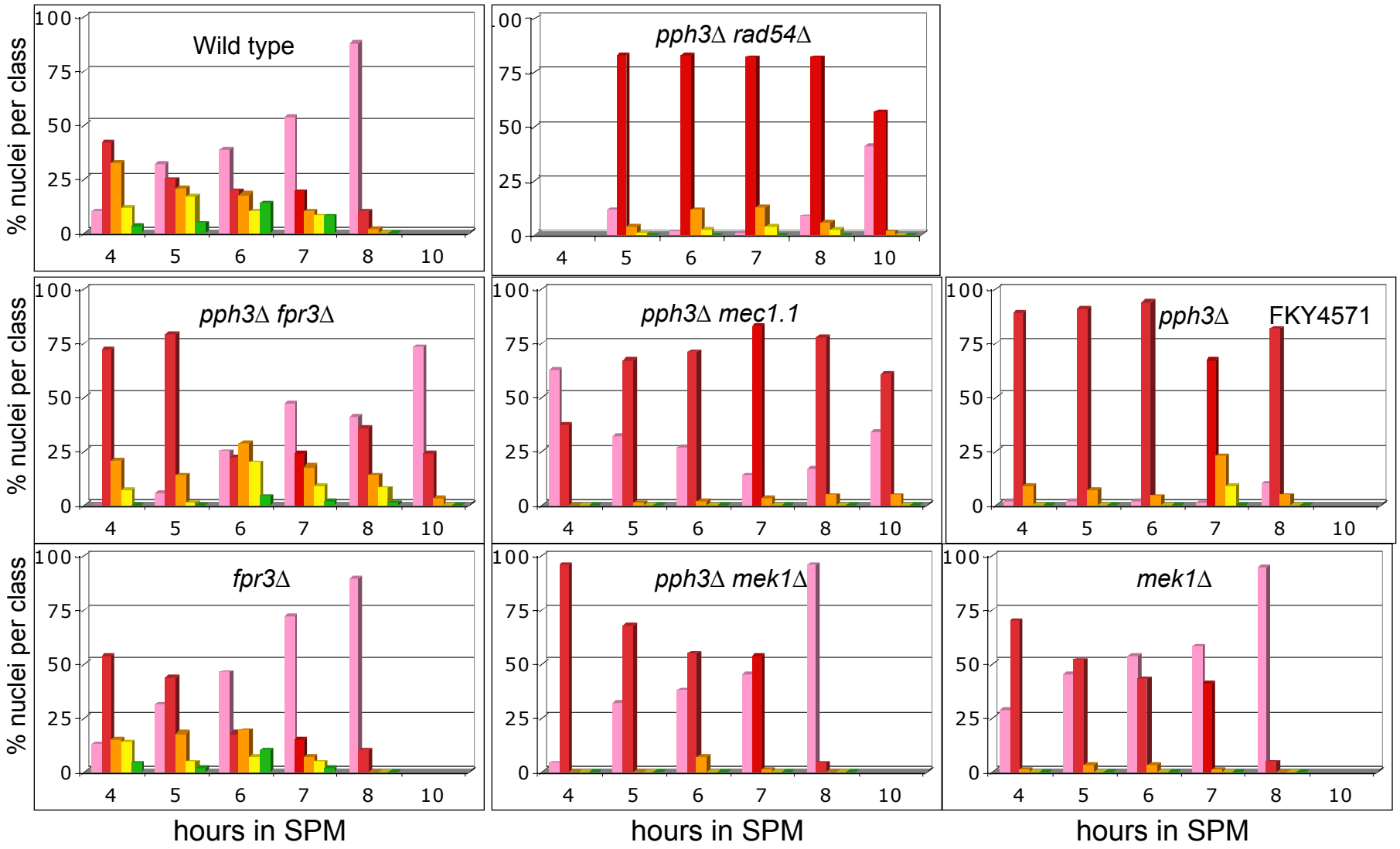

Fig. 23A Complete synapsis in *pph3Δ,pch2Δ,fpr3Δ* and *pph3Δ,swc2Δ,fpr3Δ* triple mutants.

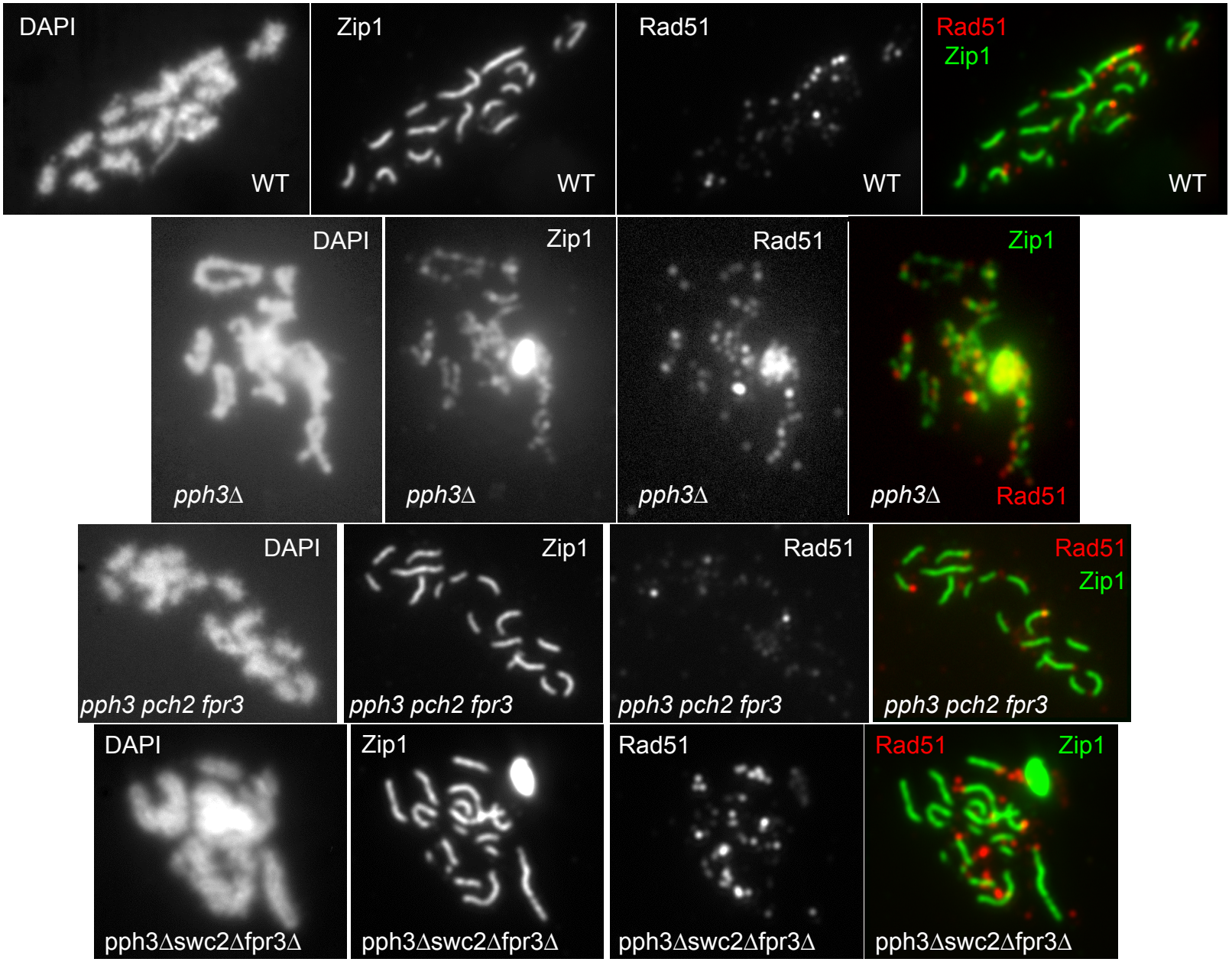

Fig. 23B *fpr3*Δ slightly decreases synapsis in both the *pph3*Δ,*swc2*Δ and the *pph3*Δ,*pch2*Δ backgrounds.

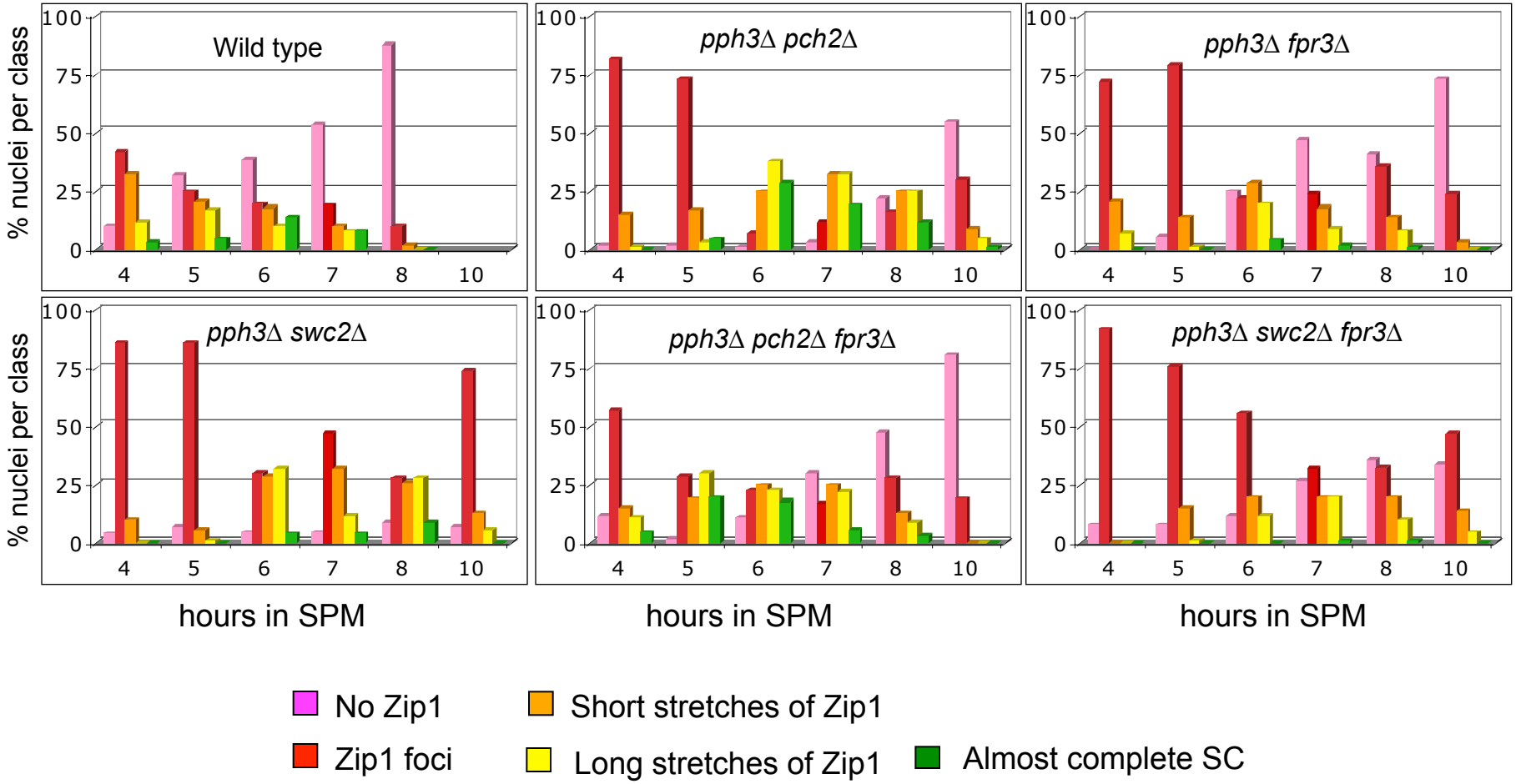

Fig. 23C Meiotic progression is advanced in *pph3*Δ, *pch2*Δ, *fpr3*Δ and *pph3*Δ, *swc2*Δ, *fpr3*Δ triple mutants, relative to the *FPR3* double mutants.

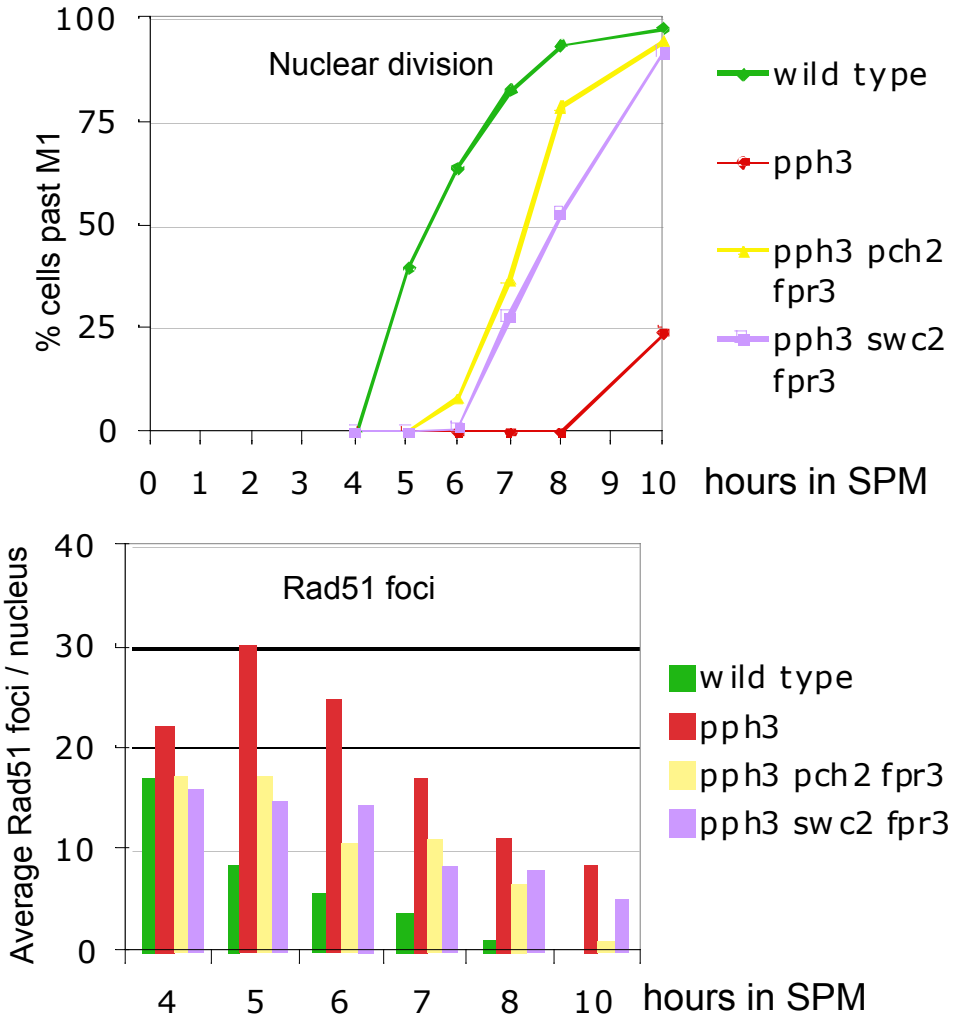

Fig. 23D

Pch2 and Fpr3 act redundantly to accumulate H2A-S129 phosphorylation in *pph3*Δ mutants.

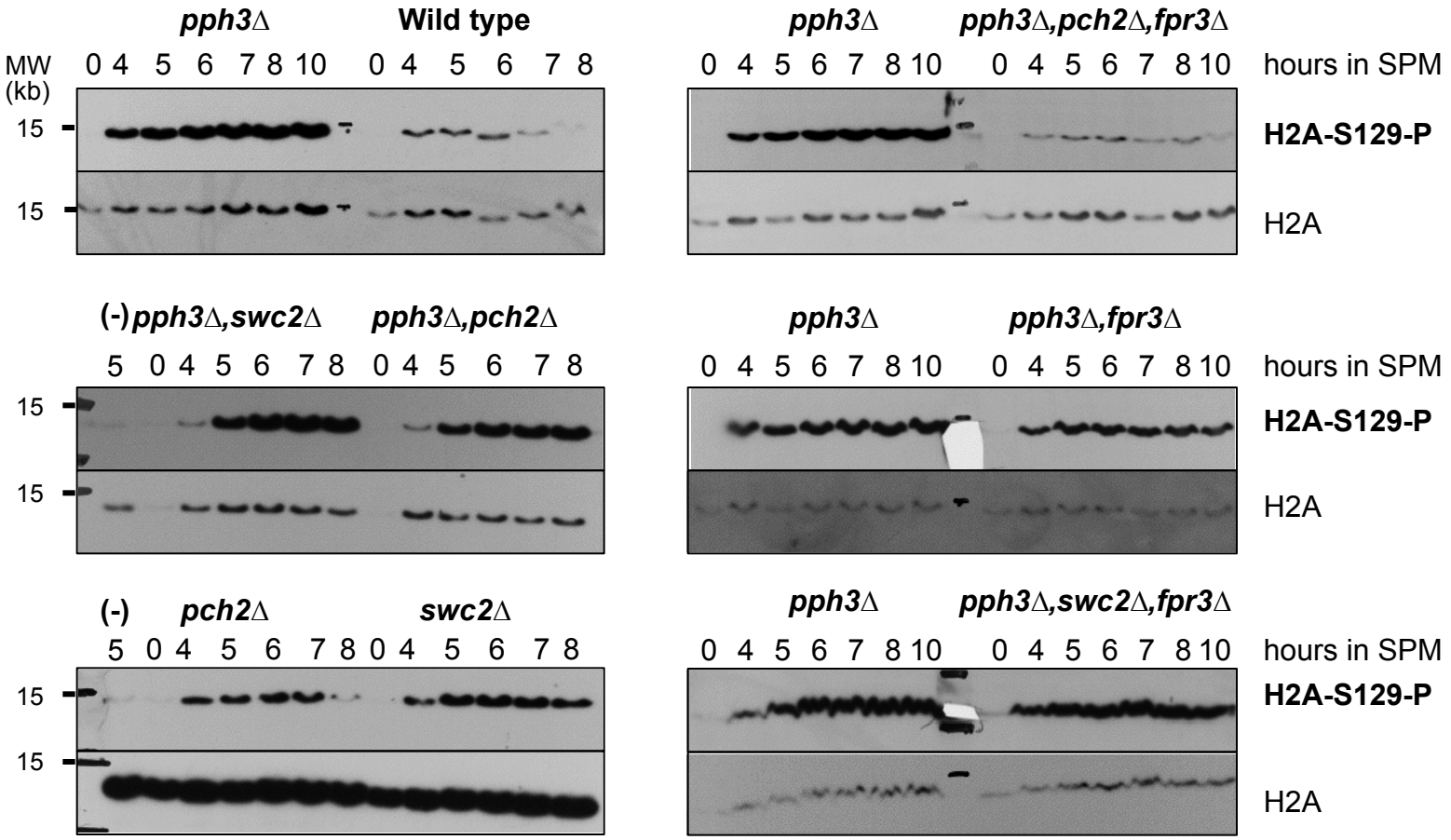

Fig: 24A

Maximum synapsis observed in *bre1Δ, rad6Δ, htb1,2-K123R* and *set1Δ, dot1Δ* double mutants.

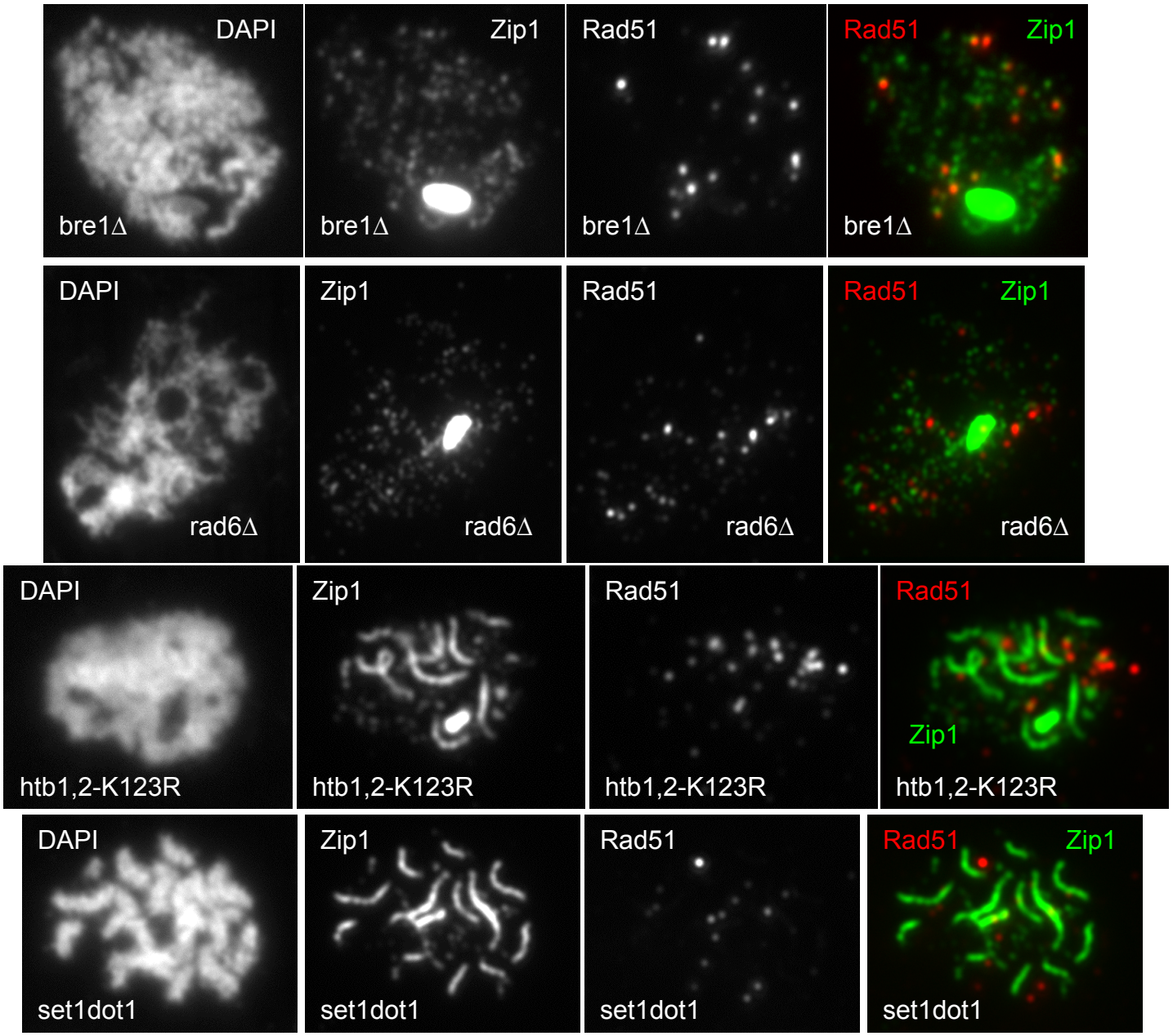

Fig: 24B

Synapsis is strongly reduced in htb1,2-K123R, but is only delayed in set1Δ, dot1Δ double mutants

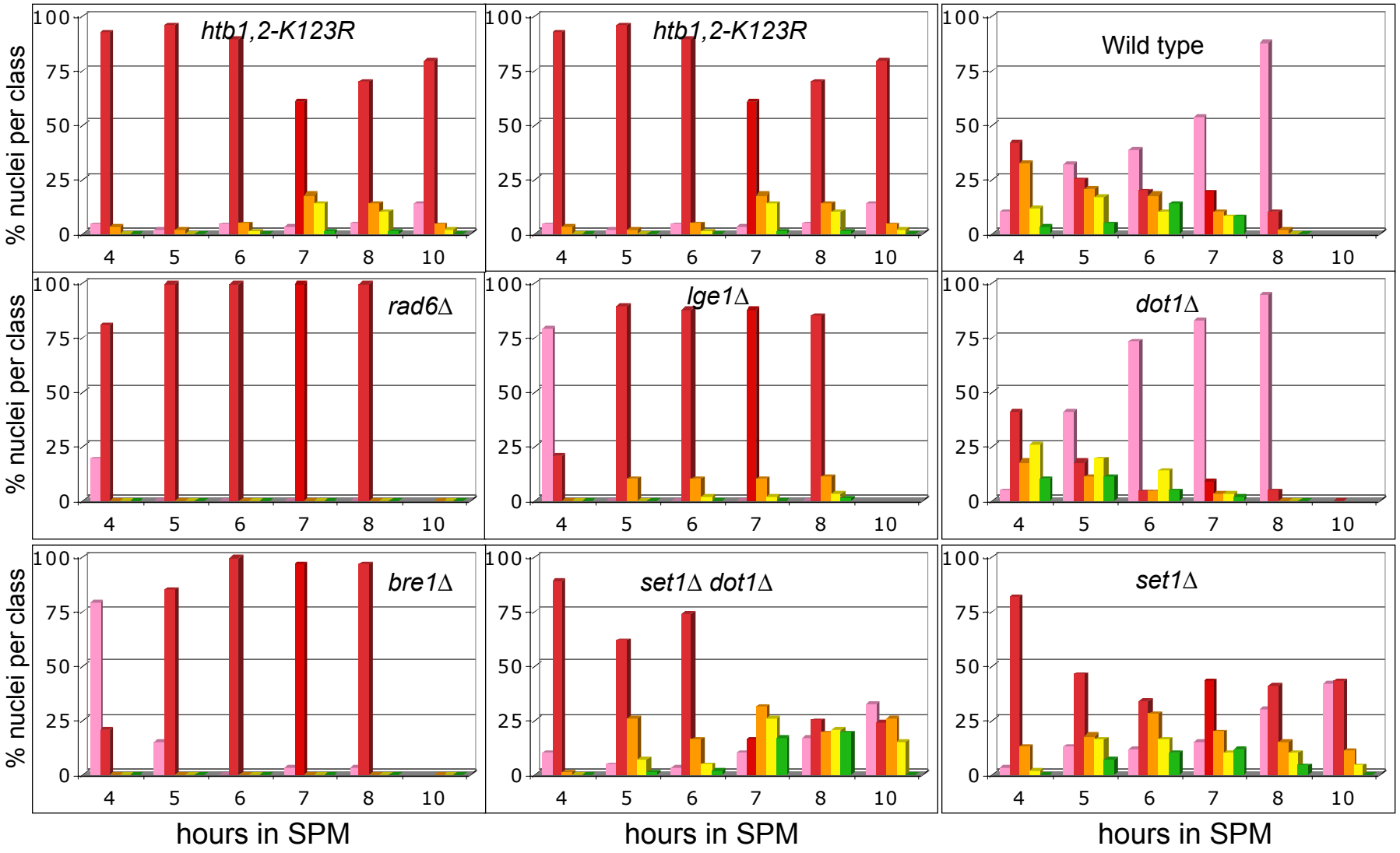

Fig: 24C Meiotic progression and Rad51 focus formation are delayed and reduced in *bre1Δ, H2B-K123R, lge1Δ, set1Δ* and *set1Δ, dot1Δ* double mutants.

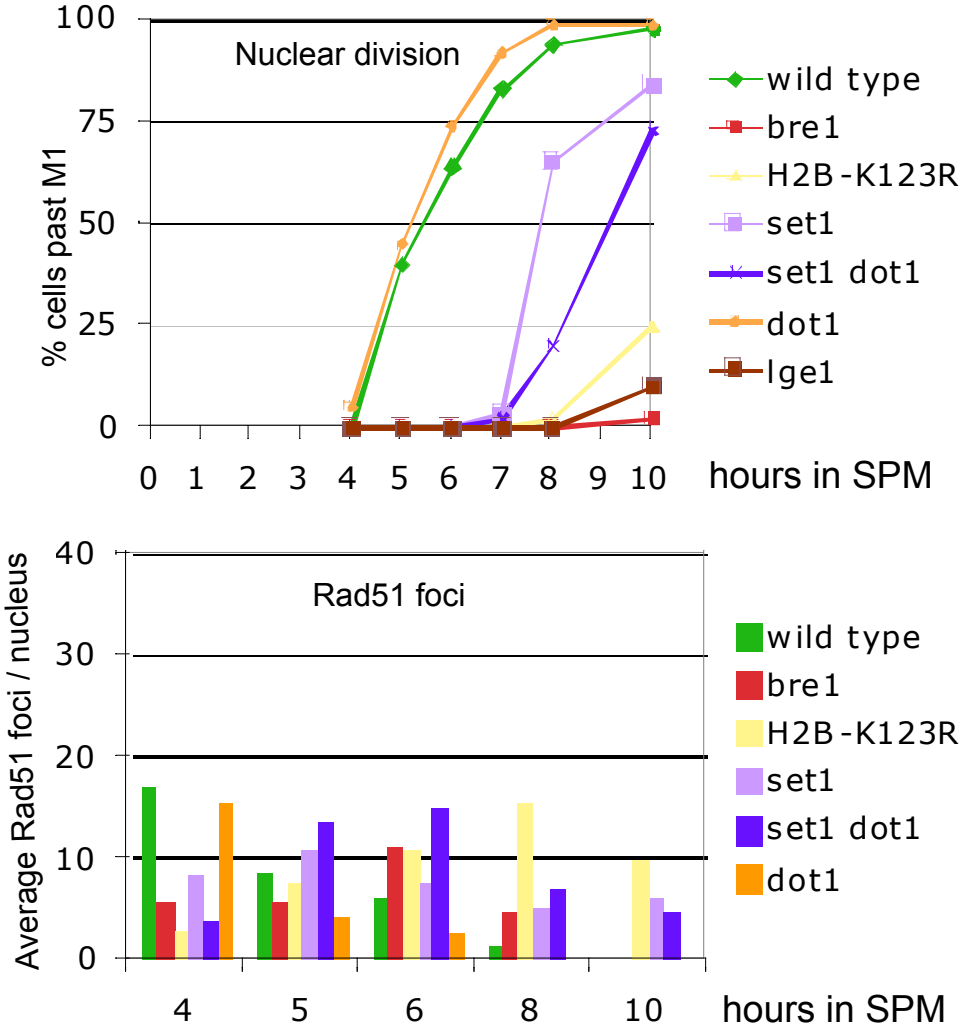

Fig: 25

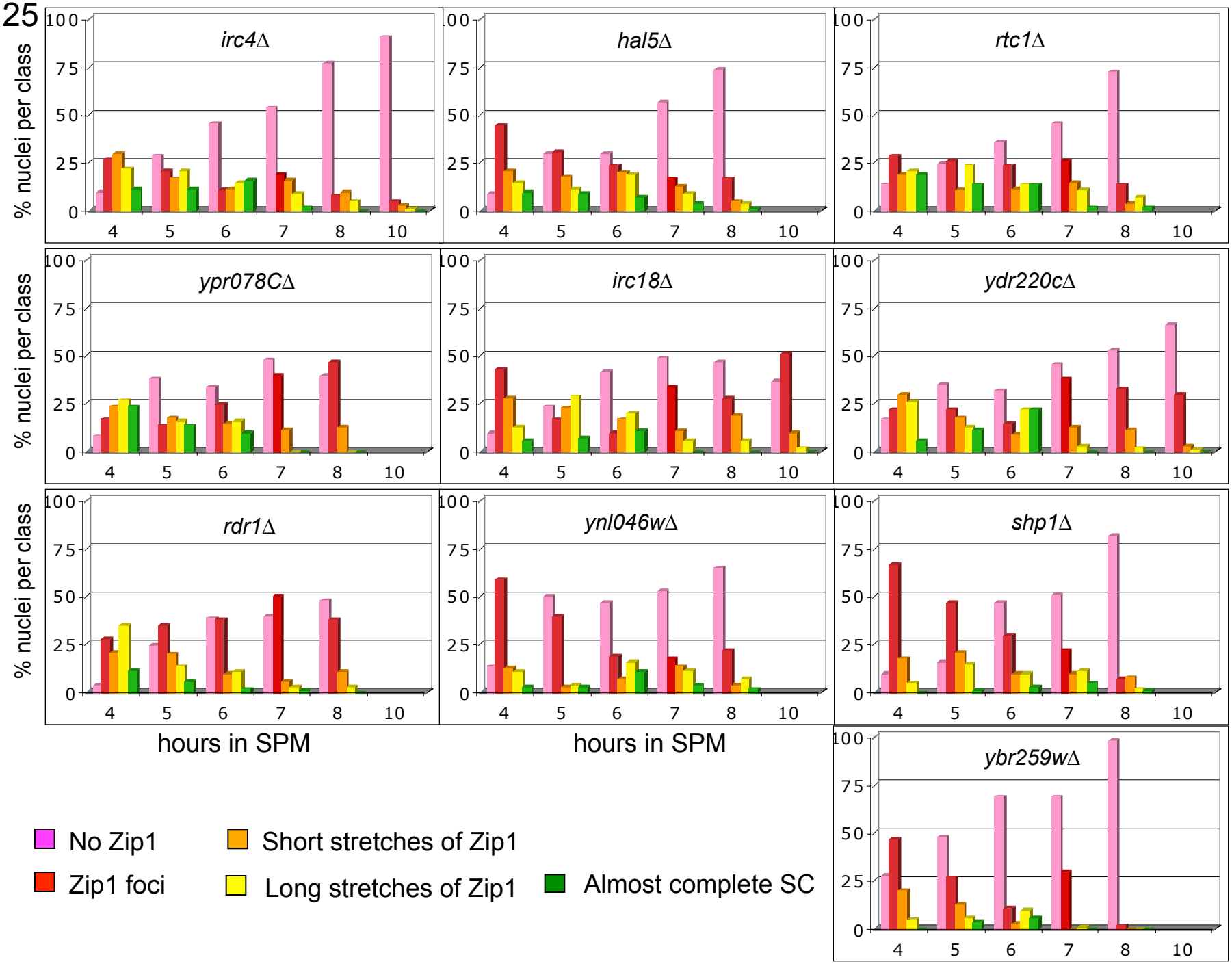
irc4Δ
hal5Δ
rtc1Δ
ypr078CΔ
irc18Δ
ydr220cΔ
rdr1Δ
ynl046wΔ
shp1Δ
ybr259wΔ
% nuclei per class
hours in SPM
No Zip1
Zip1 foci
Short stretches of Zip1
Long stretches of Zip1
Almost complete SC

Fig: 26

tma20Δ and *cts2Δ showed a decrease in synapsis*

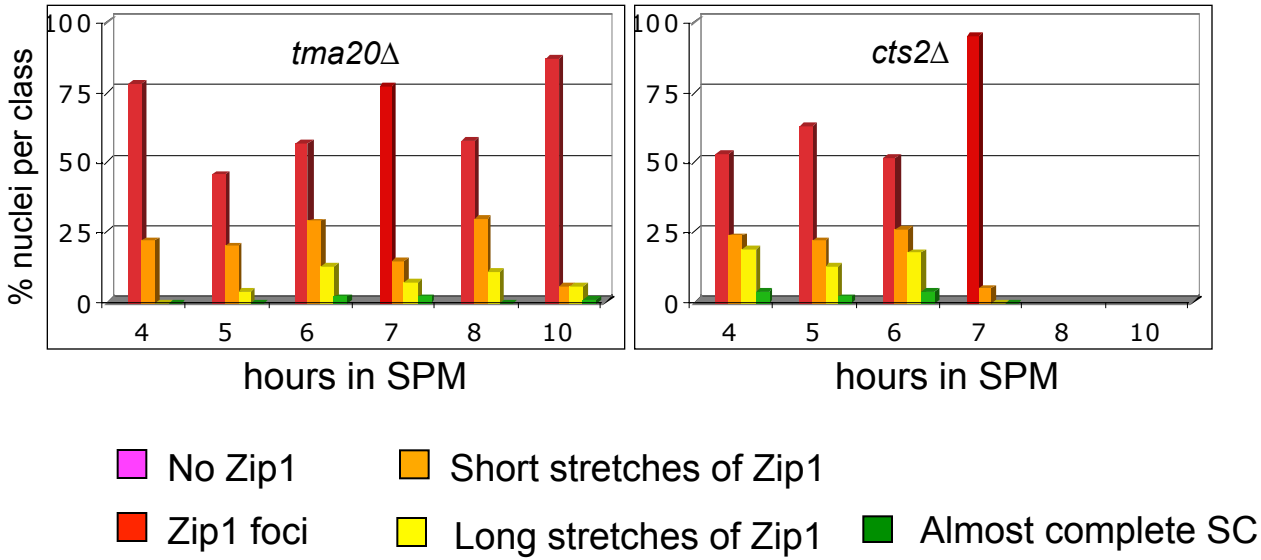

Fig: 27

*tma20*Δ and *shp1*Δ show a weak delay in meiotic progression

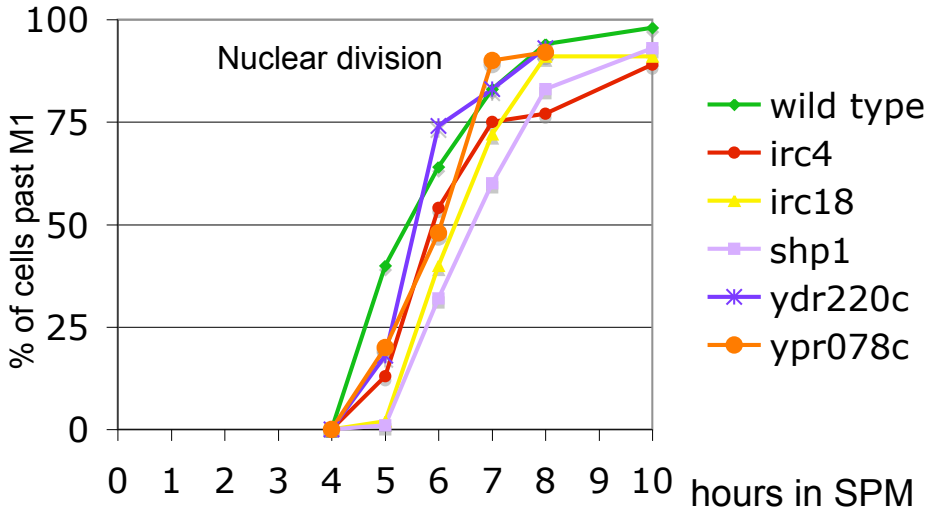

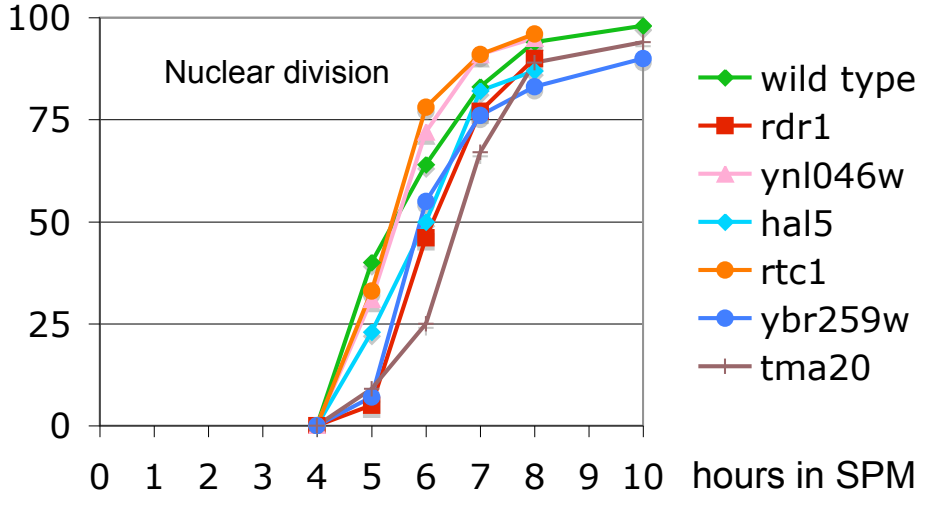

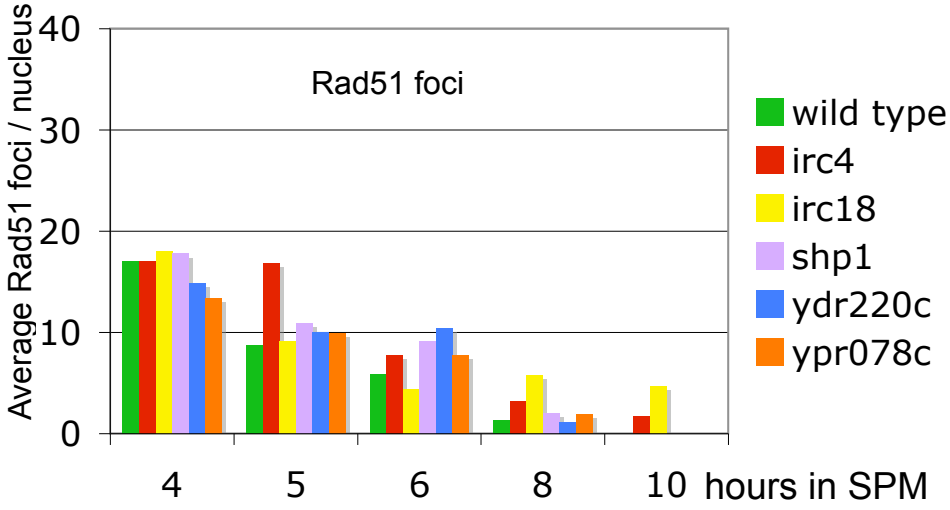

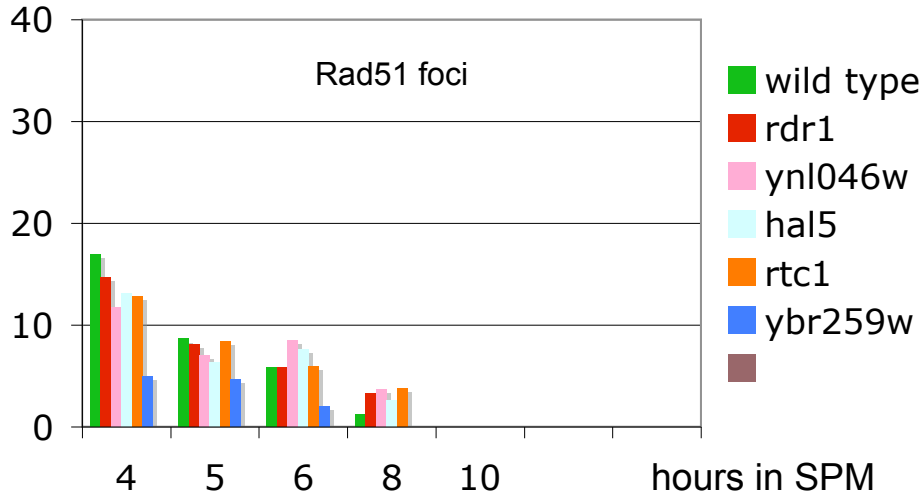

Fig: 28

Top2 foci numbers increase continuously during meiotic prophase

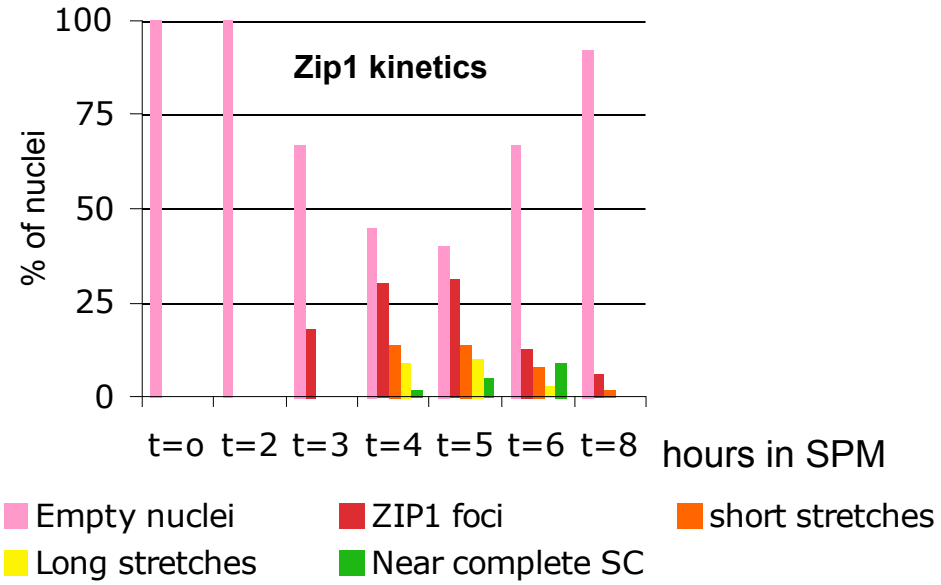

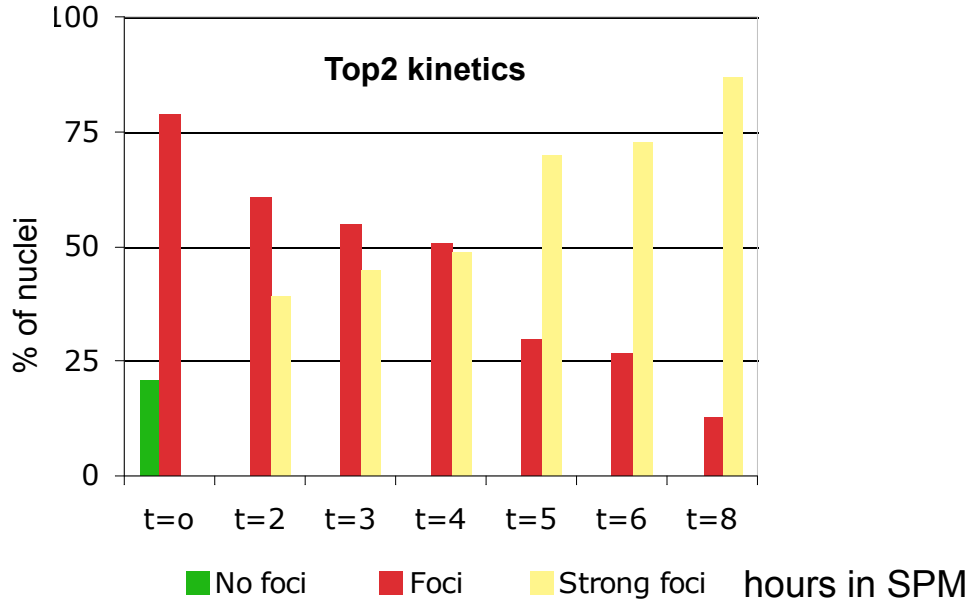

Fig: 29

Top2 does not colocalize with Zip1 or Rec8

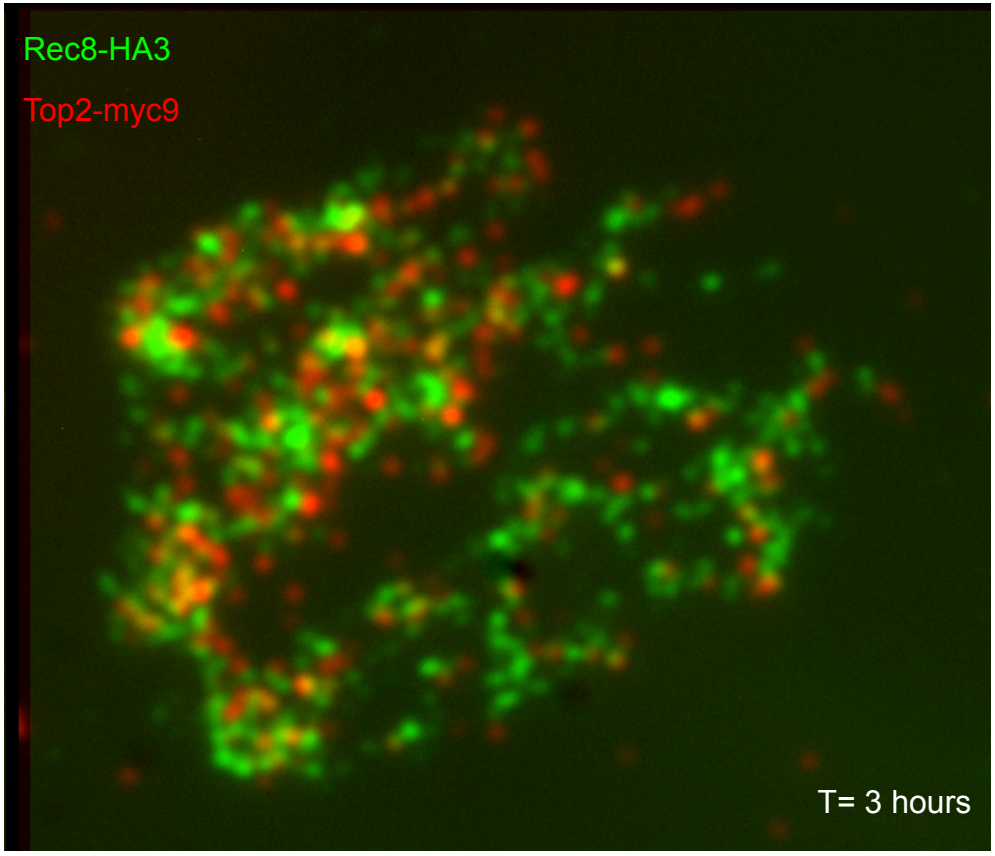

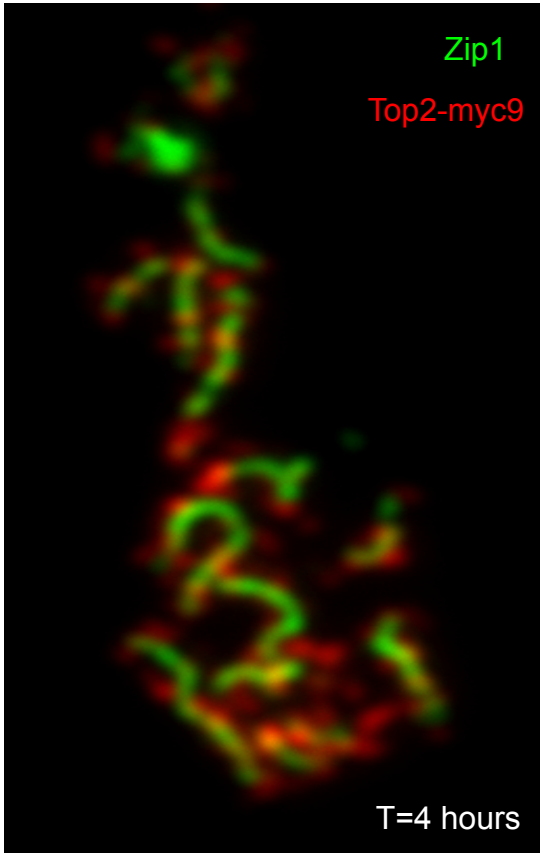

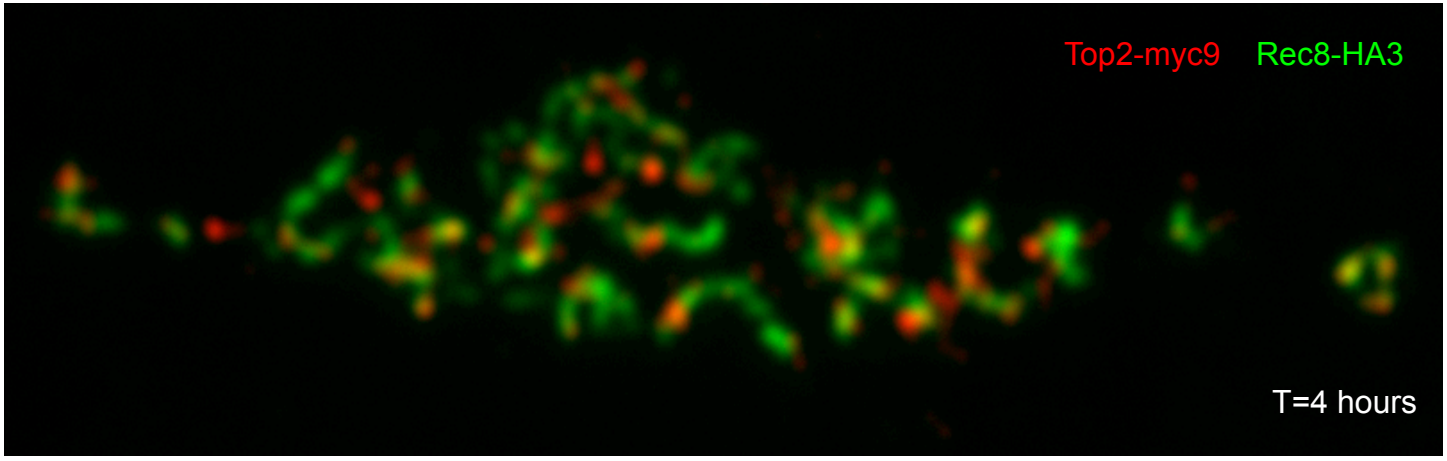

Fig: 30

Top2 colocalizes with many recombination hotspots

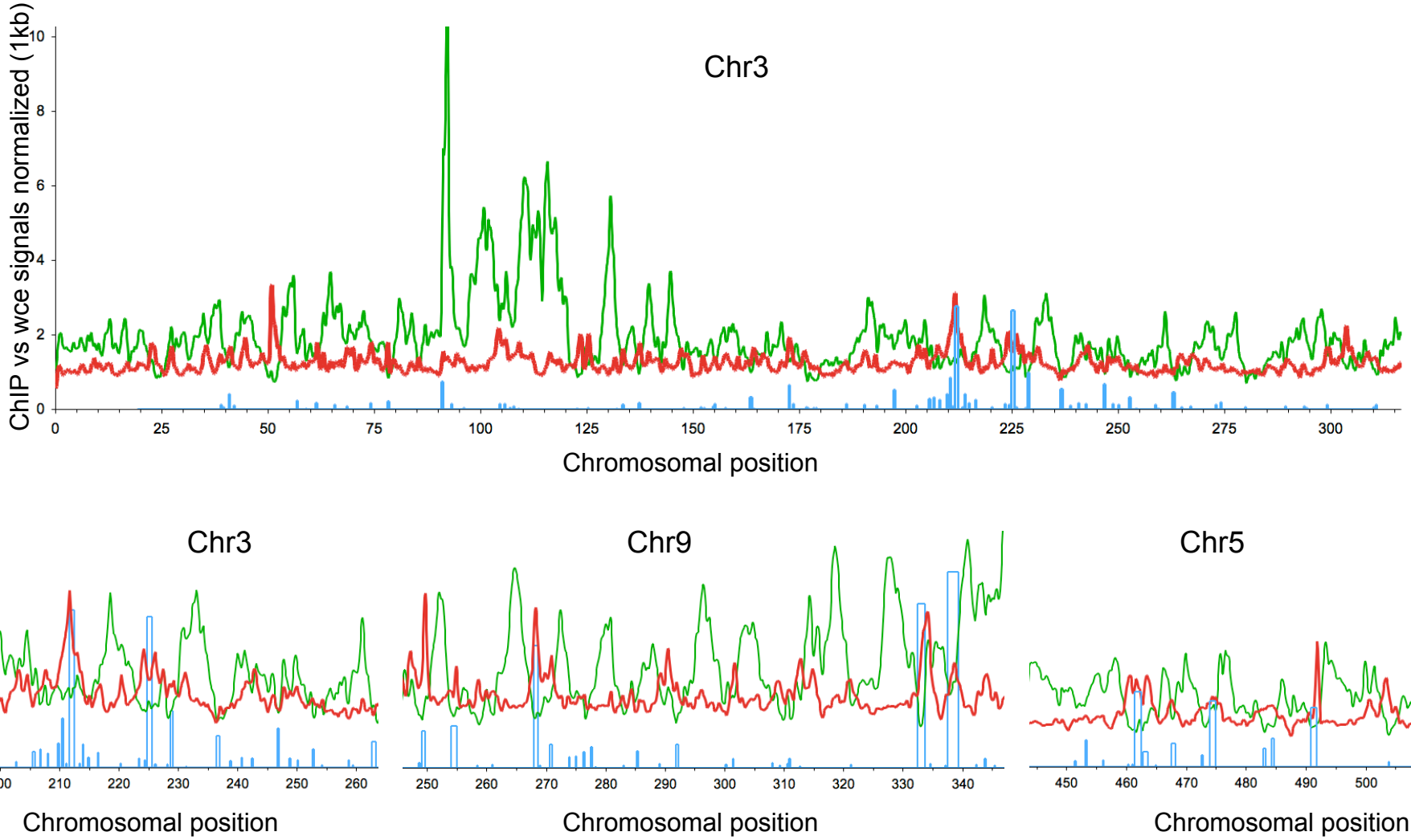

wce: whole cells extract